Passive Tomography to Image Stress Redistribution Prior to Failure on Berea Sandstone and Marcellus Shale for Caprock Integrity

Daniel Allan Sadtler

Thesis submitted to the faculty of Virginia Polytechnic Institute and State University in partial fulfillment of the requirements for the degree of

Masters of Science

In

Mining and Minerals Engineering

Erik C. Westman, Chairman

Mario G. Karfakis

Grant Brohmal

April 26, 2012

Blacksburg, VA 24061

Keywords: Carbon Sequestration, Caprock, Induced Seismicity, Tomography

Using Passive Tomography to Image Stress Redistribution Prior to Failure with Indentation Tests on Berea Sandstone and Marcellus Shale for Caprock Integrity

Daniel Allan Sadtler

Abstract

A recent concern is the cause and effect of global climate change. Many institutions give credit for these changes to the increased levels of greenhouse gases in the atmosphere, in particular the increase in the amount of carbon dioxide present. There is a growing interest in carbon capture and storage (CCS) as a means to reduce the global impact of CO_2 on the climate as a greenhouse gas. Carbon capture is the process of removing CO_2 from the atmosphere as well as preventing it from entering the atmosphere by means of exhaust. The captured carbon is stored underground in reservoirs. These reservoirs have the storage space to handle the volume of CO_2 injected as well as a caprock layer preventing the injection fluid from returning to the surface. Additionally, CO_2 can be used for enhanced oil recovery (EOR).

To monitor the injection sites used for the CO_2 storage or EOR process, the integrity of the caprock as well as the surrounding rock formations are the locations of interest. Knowing when a joint or a fracture is going to slip is necessary to prevent major failures within geologic strata. It is necessary to prevent these slips from occurring to retain the integrity of the caprock, which is keeping the fluid within the reservoirs.

Passive acoustic emissions monitoring was used to determine how effectively failure locations could be located in three unique tests. Coupled with double difference tomography, the failure of a Berea Sandstone sample and Marcellus Shale sample were calculated to determine how well the stress redistribution within the sample could be mapped using the recorded data. For the main indenter tests two samples were tested, a piece of Berea Sandstone and a piece of Marcellus Shale. The secondary test was a transform shear test using sandstone, and the third test for caprock upheaval test attempted to recreate the failure of caprock due to injection pressure. For all tests, the samples were monitored using acoustic emissions software until failure or it was deduced that the test would not produce failure.

The secondary tests did not progress through the data analysis as far as the indentation tests, however valuable information was gathered from these tests. The shear test demonstrated the

effectiveness of the passive acoustic emissions monitoring system to record shear failure. This test provides confidence in this technology to record and located events that are not occurring in compression. The caprock upheaval tests were not successful in causing failure in the caprock, however during the testing the passive acoustic emissions monitoring system was able record and locate events that occurred within the sample around the boundary on the reservoir. At the reservoir boundaries there was evidence of fluid flowing through the reservoir, and the events align with these locations. This positive result shows that the monitoring system is able to locate events induced by fluid injection.

The results of these tests provide confidence in the passive acoustic emissions monitoring system to record accurate data for the caprock integrity monitoring. The tomograms created from the recorded data accurately imaged the areas of interest within the rock samples. From these results, passive acoustic emissions monitoring systems coupled with double difference tomography has proven capable of monitoring homogeneous samples within a laboratory environment. With further testing, this technology could possibly be a viable option for monitoring carbon sequestration sites.

Acknowledgement

I would like to take this opportunity to thank my family and all of the faculty and staff of the Virginia Tech Mining and Minerals department for all of the assistance they provided during my research. Without your support, this research would not have gone as smoothly as it did. Thanks to my advisor Dr. Erik Westman for giving me the opportunity to pursue this research and for all of the assistance along the way. I would like to thank Dr. Mario Karfakis for his input during the design stages, and providing witty relief at the most opportune times. I would like to thank Jim Waddell for his continued support with testing in the lab, and helping redesign many of the samples as testing progressed. I would like to thank the main office staff for finding around the office tasks to accomplish when the research was becoming too much. A special thanks to Grant Brohmal for being on my committee and providing his input of the project. Finally I would like to thank NETL-RUA for supporting me and my research for the past year and a half.

Table of Contents

List of Figures

Chapter 1 – Introduction

A common interest in research and public concern today is the cause and effect of global climate change. Many institutions give credit for these changes to the increased levels of greenhouse gases in the atmosphere, in particular, the increase in the amount of carbon dioxide present. Fossil fuels such as petroleum products and coal are burned to create electricity for powering everyday devices. A byproduct of this combustion reaction creating the electricity to fuel our world is carbon dioxide. With the increased industrialization of world nations the amount of carbon dioxide being produced is continuing to rise, furthering the awareness of the general public of the effect carbon dioxide has on the climate. With the increased public awareness, there has been an increasing surge to find a solution to this problem.

The natural ecosystem of the earth takes carbon dioxide out of the air through plant growth, but the levels of carbon dioxide being released now are too high for the natural system to handle. Aside from switching to non-emission energy sources which would not release carbon dioxide into the atmosphere, a means to reduce the amount of carbon dioxide actively in the atmosphere is needed. A method to achieve this is carbon sequestration. Carbon sequestration is a process which takes liquid carbon dioxide and stores it underground in a location that will not allow the CO_2 to return to the atmosphere. For this process to work, it is necessary to find the proper geologic formations able to seal the material in place as well as handle a large volume of the highly pressurized material. To seal this material in place, a layer of impermeable rock referred to as caprock is required.

By pumping fluid into underground areas, material will be displaced, stresses will be altered and the sequestered carbon will react with surrounding rocks and reservoir fluids, possibly altering the integrity of the reservoir and caprock. To monitor the integrity of the underground reservoirs, a system can be put in place to record data that will give insight into what is taking place beneath the surface. Ideally, such a monitoring system will be able to determine whether the surrounding rock is fracturing due to the injection processes, including fault reactivation, and void caving. Most importantly, the monitoring system will need to be able to tell if the caprock is failing, allowing the carbon dioxide to migrate outside of the reservoir. For injection projects such as carbon sequestration, the monitoring process will take place for hundreds of years after the injection process has been completed, to make sure the CO_2 has not begun to escape the reservoir. Due to this long monitoring time, it is necessary for a system to be inexpensive, and easy to manage with minimal maintenance. For sites to remain functional for a prolonged period of time, a system capable of automated monitoring would be preferred so that onsite visits are not always required to retrieve records. Using an induced seismicity monitoring system for these underground injection sites could be a viable option.

Recording induced seismicity (at the field scale) or acoustic emissions (at the laboratory scale) is a technique involving recording arrival times of elastic waves at sensor stations as they propagate through a material. When a rock fails, energy is released in the form of elastic waves, also referred to as acoustic emissions or induced seismicity. These waves propagate through the surrounding medium. An acoustic monitoring system consists of geophones set up in different locations across a site. Different sensor setups, also called sensor arrays, will have different degrees of coverage. Three hundred sixty degrees of coverage is ideal, however at sites as deep as carbon sequestration sites it will be difficult to achieve this level of accuracy with a sensor array. The sensor arrays are able to record wave data in the monitoring system as the sound waves propagate through the ground and reach the sensors. The triggering mechanism in acoustic monitoring systems requires numerous sensors to register the same event so that background noise is not recorded instead of actual events.

Based on arrival times recorded by the acoustic monitoring system, a location for the source of the event can be found by back calculating a central origination point. Source locations are then used to develop a velocity model of the monitoring site, called tomography. This technique of processing provides locations of interest that could be inspected further to see if there was seal failure. In addition to the use of tomography, a technique called double difference tomography has the ability to increase the accuracy of the results. Double difference tomography uses surrounding event locations, within a certain radius, to recalculate each event location as well as the velocity model for the entire region. This recalculation technique provides updated information for each of the subsequent event relocations.

The scope of this project is to determine the effectiveness of using acoustic emissions recorded during laboratory rock failures combined with the double difference tomography method to accurately map stress redistribution prior to failure in a laboratory sample. Using two types of rock, Berea Sandstone and Marcellus Shale, failure was induced in samples that were being actively monitored by sensors attached to the walls of the sample. Berea sandstone was used because it is the industry standard for sequestration media. Marcellus Shale was used because it provides a good representation of an impermeable caprock. The information provided by this project gives valuable insight into how well the event relocation and double difference tomography method are able to map the stress changes prior to failure of the sample. By comparing the event locations and relocations to the failed samples tested in lab, a confirmation of the calculated data to the actual failure gives an excellent way of authenticating the data. With favorable results for the laboratory tests, field testing of sequestration sites can be initiated to monitor the caprock layer or layers holding the carbon dioxide in place.

Chapter 2 – Literature Review

In today's world, climate change is at the forefront of many conversations about the future. There are many theories as to what is causing the changing climate, but it is commonly accepted that the changes are due to greenhouse gases. It has been determined that of all the gases responsible for the changing climate, carbon dioxide (CO_2) accounts for about 64 percent(Bachu and Adams 2003).

Since the industrial revolution began in nineteenth century, human beings have been releasing more CO_2 into the air than ever before in history. The levels of CO_2 through history have been found by analyzing the amount of CO_2 that is trapped in samples from the icecaps. A number of these studies for CO_2 concentration in ice were performed on core samples of Antarctic ice. As snow turns to ice, air from the atmosphere gets trapped in the bubbles within the ice. These air bubbles can be tested to determine how much CO_2 there was at the time of formation. The results of this study show that around 1900 the CO_2 levels reached a level they had not exceeded over the previous six centuries (Raynaud and Barnola 1985).

With CO_2 levels rising and more countries becoming industrialized, CO_2 production is not going to be reduced in the foreseeable future; therefore, a way to prevent it from being released to the atmosphere is necessary to reduce the impact on the planet. Carbon sequestration is a method that is being pursued to store CO_2 under the surface of the earth, in attempts to reduce the level of CO_2 that is being released into the atmosphere. When locating a desired sequestration site, the caprock of the underground reservoir is important. The CO_2 needs to be trapped indefinitely or leak slowly enough so that no harm is caused by the CO_2 levels in the surrounding areas. The integrity of the caprock is important because it is the primary trapping mechanism, besides dissolution, for these underground reservoirs.

Section 2.1 - Carbon Capture and Sequestration

2.1.1 - Background

There is a growing interest in carbon capture and storage (CCS) as a means to reduce the global impact of CO_2 on the climate as a greenhouse gas. Carbon capture is the process of removing CO_2 from the atmosphere as well as preventing it from entering the atmosphere by means of exhaust. Countries with major manufacturing capabilities are consequently the leaders in CO_2 producing nations. Figure 2.1 shows the breakdown of the world's estimated CO_2 production.

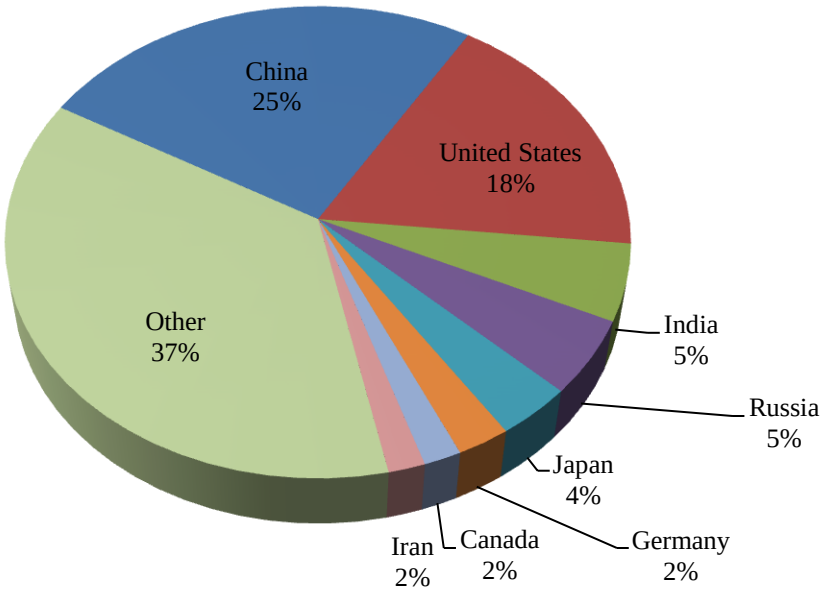

Figure 2.1: 2009 estimation of world CO_2 production.

China is the world leader in producing CO_2 with the United States second with annual production of 7,700 million metric tons and 5,400 million metric tons, respectively, in 2009. In 2009, the global emission of CO_2 was 30,300 million metric tons (EIA 2009). With China's ever growing economic expansion, these levels will continue to rise.

In coal fired power plants, the flue gas, or exhaust, contains 10 to 12 percent CO_2 and flue gas from natural gas combined cycle plants contains only 3-6 percent CO_2. This CO_2 must first be separated and then condensed for storage. Capture of CO_2 from exhaust is currently accomplished by using amine absorbers and cryogenic coolers. This method of carbon capture currently costs $150 per ton of carbon. If this technology for CO_2 capture were added to an electricity generation process, it would increase the cost of electricity by 2.5 cents/kWh to 4 cents/kWh, making it impracticable from an economic stand point. There are other forms of carbon capture which are being researched including absorption (chemical and physical), adsorption (physical and chemical), low-temperature distillation, gas separation membranes, mineralization and biomineralization (DOE). These new processes are anticipated solutions to lowering the costs of carbon capture so that the additional cost to power production is outweighed by the environmental gain.

The captured carbon is then stored underground in a process known as carbon sequestration. Carbon sequestration is defined in *Science* as the transferring of atmospheric CO_2 into long-lived pools and storing it securely so it is not immediately reemitted (Lal 2004). CO_2 can be captured in either the gaseous or supercritical phase, but generally CO_2 is stored underground in the supercritical phase to

reduce volume. To remove the CO_2 from the flue gas, the temperature of the exhaust must be cooled to between –56.6 and 31 degrees Celsius. The vapor pressures of CO_2 at these temperatures are 5 and 74 atm, respectively (Finley 2003). The pressure of the supercritical fluid generally reaches levels over 68 atm during injection. For the carbon to remain in its supercritical state, the formations used for injecting must be greater than 1000 feet below the surface (Sminchak and Gupta). The areas used for sequestration are either empty voids or locations that the pressurized CO_2 can displace whatever material is present. Adding additional pressure to these storage areas will contribute to additional stress in the surrounding rock formation. Over time, the CO_2 may eventually dissolve into ground water or may be trapped in the form of carbonate minerals (Sundquist and Geological Survey (U.S.) 2008).

2.1.2 - Formations for Storage

Since the CO_2 being sequestered needs to stay underground, only select locations underground will work for storage. A sizable reservoir is required, which has the capacity to store high quantities of CO_2. The reservoir must have an impermeable layer above it that prevents the CO_2 from ascending to the surface, since CO_2 is less dense than water in its supercritical state. Reservoirs must have sound and relatively un-fractured boundaries so that the sequestered CO_2 does not leak out of the reservoir. Also, the reservoir needs to be in a stable area for the CO_2 that is under high pressure to remain in place without losing its containment, and leaking out into the surrounding geologic formations due to ground movement. Because of these requirements, there are only certain types of geologic formations that are feasible for carbon sequestration: active and depleted oil and gas reservoirs, deep brine formations including saline formations, and deep coal seams, including coal-bed methane formations (Dave Reichle 1999). Figure 1.2 demonstrates how these formations may be situated.

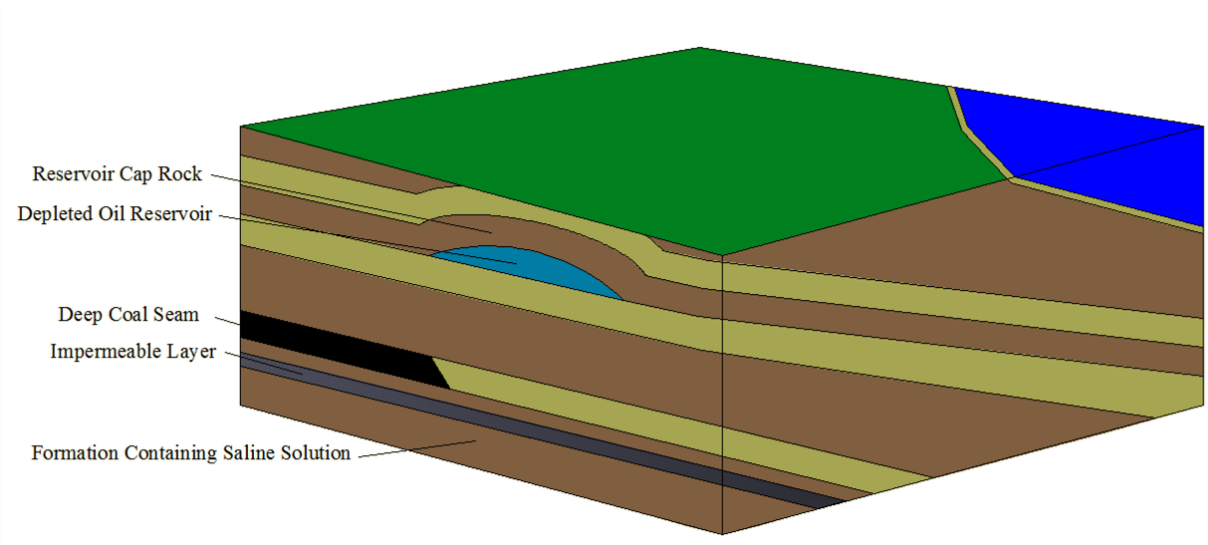

Figure 2.2: Examples of possible formations for carbon sequestration use.

Active and depleted oil reservoirs are viable options for CO_2 storage because of the natural structure. Oil reservoirs form from buried plant life such as algae being exposed to high heat and pressure. For this process to take place there needs to be sturdy caprock in place or the pressure on the biomaterial would dissipate. These reservoirs are appealing for sequestration because their formation is already in the shape of storage wells, the cap of the reserve is known to have been a good seal before exploration, and CO_2 injection can be used to increase the fuel recovery, offsetting the price. The knowledge and experience from many years of working with oil reservoirs provides confidence in using these formations to store CO_2. However, these reservoirs have a down side to consider as well. The storage capacity of these wells is minimal, approximately 142,250 million metric tons, and the number of available locations for this process is limited (NETL 2010). There are still some reservoirs that must be depleted before they can be used to store CO_2, so time is required before these locations can be used. Also, the caprock of these reservoirs has been punctured during exploration and production, so the integrity has been reduced.

Brine formations are locations that can store CO_2 in the pore space within the host rock. Sequestration in deep saline formations is achieved through the use of three mechanisms. These mechanisms include displacement of the insitu fluids by the CO_2, dissolution of CO_2 into the fluids, and chemical reaction of CO_2 with minerals present in the formation to form stable, solid compounds like carbonates (Herzog 2001). The saline formations that are capable of storing the CO_2 on average have salinity greater than 10,000 parts per million, making them impractical for use as future drinking water reservoirs (Friedmann 2007). These formations are the most abundant and appear to be the ideal areas for storage of large quantities of CO_2 because of the vast size. However, currently there is not enough information about these formations to determine their effectiveness. The saline formations in the United States are estimated to be able to hold between 1,652,550 and 20,213,050 million metric tons of CO_2 over a large area (NETL 2010). CO_2 injected in deep saline aquifers could take thousands to millions of years to migrate to the surface due to extremely low flow rates encountered in these formations (Damen, Faaij et al. 2006). The disadvantages of saline formations, as stated before, is that there is little known about them, such as how effective the trapping mechanism will be, or what characterizes a formation that will be effective for storage (Sundquist and Geological Survey (U.S.) 2008).

Deep coal seams, coal bed methane reservoirs and unminable coal seams naturally hold gases within their formations. Through natural processes, undisturbed coal beds have the potential to hold in methane gas due to impermeable material which does not allow the gases to rise. This would provide a natural caprock formation where carbon can be pumped into and dispersed throughout the entire seam. Another advantage for coal bed usage is that many of these seams, currently considered unminable are

adjacent to large power plants, so the cost to transport the CO_2 would be minimal. To be considered unminable, a seam needs to be too deep for economic removal, or the conditions too volatile for safe working conditions. With the world's growing need of fossil fuels however, it could prove to be a poor decision to pump CO_2 into areas that may need to be mined in the future (Sundquist and Geological Survey (U.S.) 2008). Not only is it rash to render these resources unusable, there is no way to be certain what seams will remain unminable. With increased demands, and new technologies, once uneconomical deposits may become profitable. With the limitations on what seams are available for the CO_2 to be stored in, the storage capacity of these formations is estimated between 59,460 and 117,810 million metric tons (NETL 2010).

2.1.3 - Dangers of Carbon Dioxide Storage

With the storage of CO_2 underground, there are dangers this process could impose on the surrounding area that are important to understand. If these issues are not taken into consideration when deciding on a storage location, the carbon sequestration projects could cause more harm than good. The dangers of CO_2 storage underground can be divided into five categories: CO_2 leakage, CH_4 leakage, ground movement, displacement of brine and seismicity.

When storing CO_2 in oil reservoirs, there is great potential for CH_4 to be present due to build-up from hydrocarbons previously in the reservoir. CO_2 and CH_4 leakage have similar dangers to their surroundings with only a slight variance between effects. CH_4 will migrate toward the surface at a much higher rate than the supercritical CO_2. As these gases rise, they pose a lethal threat of accumulating in the basement of structures and, being colorless, the inhabitants would be unaware of their presents. Humans as well as most animals will suffocate when exposed to CO_2 levels greater than 20-30%. Since CO_2 is denser than air in its gaseous state, the topography of the surrounding area is important to consider.

The gas can be trapped in low lying areas if it is not allowed to disperse, such as in lake beds and valleys (Damen, Faaij et al. 2006). However, atmospheric dispersion modeling indicates that small, isolated leaks in the range of 0.1 to 100 grams per square meter, per day will quickly disperse under typical topographic conditions and wind velocities, without posing a lethal threat (Ph 2004). CO_2 leakage also poses a threat to plant life if the concentration of CO_2 it too high. Though it is known that plant leaves convert CO_2 into oxygen, tree roots need to absorb oxygen directly. When the levels of CO_2 in the soil are too high, it interferes with nutrient intake, choking the tree to death (Sorey, Evans et al. 1998).

The injection of CO_2 in aquifers will cause saline groundwater to be displaced. This could cause undesirable effects such as an increase in salinity of sweet water reservoirs, which is used for drinking water and irrigation. Also a rise of the water table would negatively impact land quality and usage. Depending on the area of injection, a rise in the water table could bring the water to the surface, removing access to the land for agricultural purposes. Also, if CO_2 gets into the drinking water it could follow the

water, flowing into buildings where it would become concentrated in the pipes, possibly leaking out into living area. The movements of brine caused by injected CO_2 as well as all the dangers this movement could entail, remain uncertain (Benson, Hepple et al. 2002).Contamination of drinking water with CO_2 can cause metals or chemicals to leach out of surrounding rock which would cause the water to acidify. This would be very costly if the affected aquifer is used by a large number of people. Once an aquifer is contaminated, it will in all likelihood remain this way (Price, Mckone et al.).

By pumping CO_2 underground, pressures are being added to rock formations that naturally are not at that level. This added pressure can cause upheaval and subduction of the land above it. If upheaval were to occur, damage to structures above the injection site would ensue. Also if there is upheaval, the integrity of the caprock will most likely have been compromised due to the movement of the earth. Upheaval should not be a problem during CO_2 storage however, as long as the maximum storage pressure is kept below the geostatic pressure. Subsidence can occur due to chemical reaction between the CO_2 dissolved in brine and the reservoir rock. This reaction could cause the reservoir caprock to dissolve and the weight of the overburden to become too much, leading to the collapse of the reservoir. Reservoirs containing carbonate rocks, and even more so with carbonate caprock, pose a greater threat for subsidence due to the tendency of CO_2 to dissolve carbonates (Damen, Faaij et al. 2006).

Seismicity is a result of changing stresses in a rock formation exceeding the strength of the weakest joint in the surrounding rock. As large amounts of CO_2 are pumped into the reservoirs, the fluid pressure increases the pore pressure, which can cause seismic events to occur. These events are called induced seismicity. If there is a fault in the caprock, the increased pressure could allow the rock to slip, giving the CO_2 a path to follow out of the reservoir and up into uncontained area(Rutqvist and Tsang 2002). If the scenario is correct, the induced seismicity can also trigger slip faults, commonly known as earthquakes or earth tremors. Depending on the location of the injection site, movement of the earth could cause a great deal of structural damage on the surface.

Sections 2.2 - Sequestration

2.2.1 - Caprock Integrity

As has been explained in previous sections, the caprock is the key structure for trapping and maintaining a seal of the sequestered CO_2. If this structure fails, there is no barrier to keep the CO_2 from migrating to the surface and returning to the atmosphere. Due to the great importance of this mechanism, it is important to understand how the caprock can be affected by the sequestration process. Caprock integrity issues include exploration and production drill holes, naturally present cracks in the caprock and cracks formed during the sequestration process.

During the exploration process, wells are drilled into areas to determine where the oil reservoir is located. After the initial discovery, the well is used to pump out the hydrocarbon until the well stops producing. At this point, if going deeper with the current well is not an option, other wells are drilled to lower points of the reservoir so that all of the oil can be removed. Where the well holes breached the caprock, a plug needs to be secured before any CO_2 storage can begin. Without this plug the CO_2 could migrate to this opening and rise toward the surface. This is a similar situation for deep coal beds. The exploration process to determine if these coal beds are unminable would fracture the caprock of these deposits. With depth and seam thickness most likely being the limiting factor in minability of the seam, it would be exceedingly hard to have the drill holes effectively plugged. Another problem that could arise with the caprock integrity involves the record keeping of the persons who drilled on the property. Some seams have been pursued by numerous companies, resulting in many exploratory drill holes in the seam. If all of these drill holes have not been properly sealed or documented, when the CO_2 is pumped into the ground it will only remain there until it migrates to these uncapped holes.

2.2.2 – Stresses in Rock

Rocks have formed over many millions of years by mechanisms working within the earth that compress, move, and alter rock formations over time. When working with and shaping rocks while they are in place, these unseen stresses must be taken into account. To understand how these stresses affect a rock mass, the failure of rock has been studied, and theories have been generated to model the effect of stress in rock.

To understand the affects stress cause, knowing how stress, a tensor, differs from other quantities is necessary. The commonly understood quantities such as temperature and velocity are scalar and vector quantities, respectively. A scalar quantity is described completely by one value, which is its magnitude. A vector is described by two values, its magnitude and direction. A vector has components in the x, y and z axes to specify the direction and magnitude. A tensor has, in addition to magnitude and direction, a plane under consideration component (Hudson 2005). This gives tensors a distinct difference from scalar and vector quantities, which must be taken into account when calculating rock stresses.

In rock, as well as other material, the stress can be represented at a point as three normal stresses acting perpendicular to the faces of a small cube and three shear stress components acting along the faces. The three normal stresses are represented by $(\sigma_x, \sigma_y, \sigma_z)$, and the shear components are represented by $(\sigma_{xy}, \sigma_{yz}, \sigma_{xz})$ The principle stresses, referred to as σ_1, σ_2 and σ_3, are the major, intermediate and minor stresses which are acting on the rock. Figure 2.3 shows the orientation of the stress components.

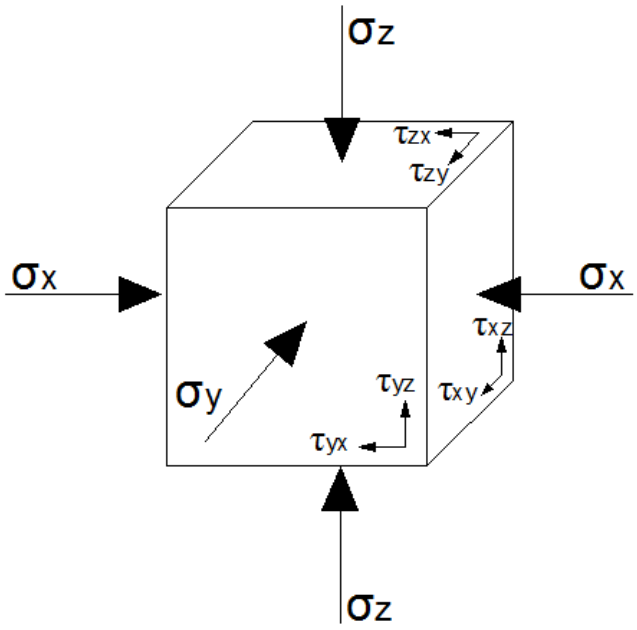

Figure 2.3: Stress components on an element.

There are a number of different forms of stress which act on rock in different orientations among these are tectonic, gravitational, induced and thermal stresses. Tectonic stress is a stress that is caused by tectonic plate movement on the earth's surface, stretching and compressing the rock. The gravitational stress is caused by the weight of the material above pressing down on the underlying material. Induced stress is the stress in the rock after some form of engineering has been applied to the rock. Knowing this stress will give the information necessary to compare the effects the engineering solution has on the surrounding rock. Finally, thermal stress is caused by the change in temperature of rock, as it expands and contracts (Hudson, Cornet et al. 2003). These stresses each act upon rock in different ways, but they all give each rock formation a unique stress profile.

2.2.3 - Failure Criterion

There are a number of failure criteria which are used to determine how much stress a particular rock is able to handle before failure. In particular, the Mohr-Coulomb failure criterion, Hoek-Brown failure criterion, and Griffith Crack Theory are failure predicting tools that can be used to determine stress properties of rock.

The Mohr-Coulomb strength criterion is based on the idea that the strength of a rock is made up of a constant cohesion and frictional resistance with varying normal force. It is limited in its effectiveness because it does not provide good results for rock with joints aligned with maximum principle stress, usually an orientation between 80 and 90 degrees (Paşamehmetoğlu 1993). The equation for Mohr-Coulomb failure criteria is:

(1) $$|\tau| = C + \sigma_n tan\emptyset$$

Where τ is the shear strength, C is the cohesion, σ_n is the normal stress acting on the plane, and $\emptyset$ is the angle of internal friction (J 2000). Another form of the criteria which is true at the point of failure is,

(2) $$|\tau| = \frac{1}{2}(\sigma_1 - \sigma_3)sin2\beta$$

where σ_1 is the major principle stress, σ_3 is the minor principle stress and β is orientation of the critical plane of failure (Engelder). When there is a change in the pore pressure causing a slip in a joint, the Mohr-Coulomb criterion, showing the mechanism behind the slip, can be written:

(3) $$\tau = \mu(S_n - P_p)$$

where τ is the shear stress on the fault, μ is the coefficient of friction, S_n is the normal stress and P_p is the pore pressure. Thus, by raising the pore pressure, the effective normal pressure,$(S_n - P_p)$, of the fault is reduced (Zoback and Zinke 2002).

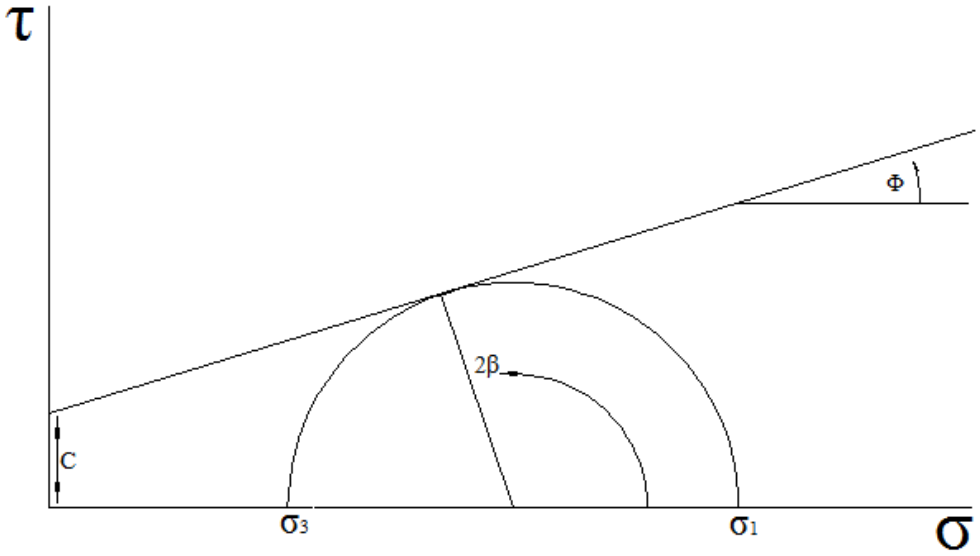

Figure 2.4: Mohr Circle Diagram with equation variables labeled.

The Mohr-Coulomb failure envelope can be obtained by plotting multiple Mohr circles and connecting a line through the tangent of the circles. Figure 2.4 shows a complete Mohr's circle with major components labeled. The failure envelope represents the dividing line between where the rock is expected to be stable and not stable. The stable area is below the failure envelope, and the unstable area is above the envelope. The τ intercept is the value of cohesion. A disadvantage to this failure criterion is that in real-world applications, the rocks tend to fail before the envelope is reached leaving error in the exact location of the failure envelope. Actual envelopes for rock is typically not linear, but is represented that way in this model.

The Hoek-Brown failure criterion is another empirical method that is designed to determine the failure properties of brittle rock. This model works well with intact rocks and rocks with many joints. The Hoek-Brown equation is:

$$\sigma_1 = \sigma_3 + \sigma_c \left(m \frac{\sigma_3}{\sigma_c} + s \right)^{0.5} \quad (4)$$

where, σ_1 is the major principal stress, σ_3 is the minor principle stress, σ_c is the uni-axial compressive strength of intact rock, m is a material constant that varies depending on the interfaces ranging from a value of 7 to 17, and s is a material constant that varies with each rock sample, with a value of 1.0 for intact rock (Hoek, Carranza-Torres et al. 2002). When the Hoek-Brown criterion is computed with the major and minor principle stresses equal to each other, the uniaxial tensile strength is equal to the bi-axial tensile strength for brittle rock.

After the Hoek-Brown failure criterion became widely used, it was necessary to adjust the original formula to include "disturbed" and "undisturbed" rocks so the results would be more accurate. The formula was adjusted so that instead of using the Rock Mass Rating to determine the material constant, the Geological Strength Index was used. With the new GSI, a new variable was added to the equation, the power of 0.5 was replaced with the variable a. Using the new GSI values, the s and a are then recalculated with the rock integrity accounted for.

The Griffith Crack Theory is a method that determines how rocks will crack under stress based on conditions of tensile and compressive stress. As the rocks are subjected to stress around the crack, the joint is subject to slipping. This means the confining pressure needs to increase if the sliding were to be stopped (Twiss and Moores 1973). The Griffith equation is:

$$G = \frac{\pi \sigma^2 a}{E} \quad (5)$$

where G is the elastic energy per unit area of crack surface, σ is the stress acting on the crack, a is the length of the crack and E is Young's modulus (Wei 2010). The failure envelope for the Griffith crack theory is similar to the Mohr-Coulomb failure envelope, but instead of being linear, the Griffith envelope is quadratic.

2.2.4 – Modes of Failure

Fractures in the caprock, whether naturally occurring or stress-induced, must be understood before a reservoir can be determined to be acceptable for CO_2 storage. As CO_2 is pumped into the reservoir, the pore pressure begins to increase, reducing the shear strength of the joints in the rock. A different perspective of this is that as CO_2 is injected, the fluid enters into pre-existing micro fractures in the rock, resulting in the normal stress being supported by the fluid. The fluid has no shear strength the frictional resistance to sliding is lowered by an amount equivalent to the pressure of the fluid (Suckale

2010). Once the frictional resistance is exceeded by the shear stress on the joint, the rock will slip. Since the Earth's crust is generally supporting very high stress levels, it is often close to failure (Deichmann and Evans 2010). This means that even the slightest disturbance from added pore pressure or removal of pressure in an area with existing fractures is capable of causing a slip, decreasing the integrity of the caprock.

Removal of hydrocarbons also can lead to fractures in the cap rock. As the pressure is removed from the reservoir from material being depleted, the caprock is under tensile stress. Due to the removal of the media which was acting as a support, the stresses become unbalanced and the weight of the overburden is distributed across the span (Hasegawa, Wetmiller et al. 1989). Once the weight becomes too much, the caprock will fail into the reservoir, leaving it unusable as a storage reservoir. These failures have already occurred in some of the depleted reservoirs, so the estimates of the current and future storage locations could be lower than expected due to the failure of the caprocks. Figure 2.5 shows different caprock conditions non conducive to successful CO_2 storage.

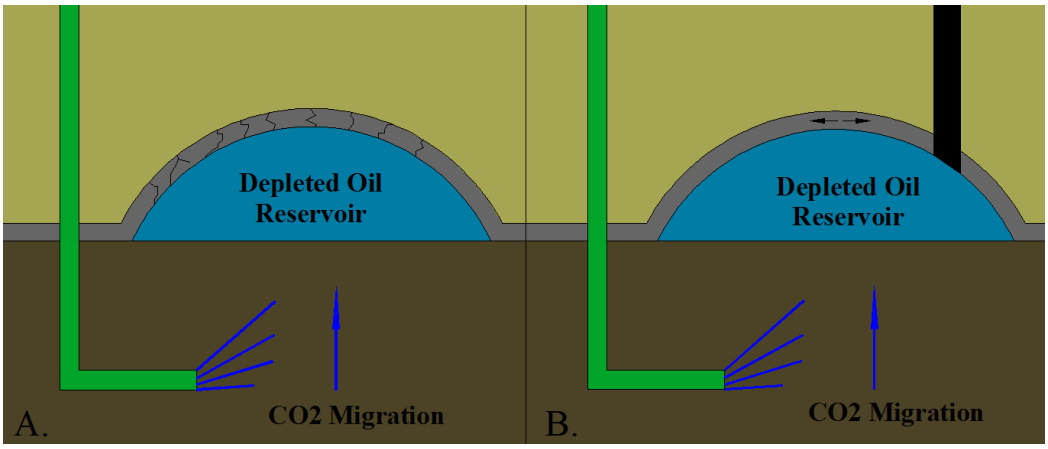

Figure 2.5: This diagram shows depleted oil reservoirs with caprock failures non conducive to CO_2 storage. Side A. shows fractured caprock due to increased pore pressure and side B. demonstrates a reservoir in tensile stress and with a bore hole in the cap rock.

Over pressurizing the reservoir is another problem that needs to be monitored to keep the integrity of the caprock sound. If caution is not used while filling the reservoirs, pressure could build up to the point that the caprock is compromised by the collapse of formations below. Finally, when looking for caprock that will be able to withstand long term storage, the reaction between the sequestered material and the caprock must be taken into consideration. Since the injection of CO_2 can cause the dissolution of carbonate rocks, it is important that the impermeable layer is not of this type. Otherwise, as the CO_2 remains in the reservoir, it will slowly cause the caprock to erode due to the precents of HCO_3 until it becomes too weak to hold up the overburden or the seal breaks, allowing the CO_2 to migrate freely towards the surface. If the seal was to break, the CO_2 would continue to expand these vents in a manner similar to the piping process of embankments.

In sandstone there are two broad classifications of failure modes subdivided into categories. Each category describes a specific form of failure that is achieved depending on the loading of material and the environment in which the material is located. The three motions that create these categories are compaction, dilation and shear. The classifications are:

- Deformation Bands
    - Shear deformation bands
        - Isochoric shear bands
        - Compactive shear bands
        - Dilatant shear bands
    - Volumetric deformation bands
        - Compaction bands
        - Dilation bands
- Sharp Discontinuities
    - Fractures with predominantly shearing/slip surfaces
    - Discontinuities with predominantly volumetric deformation
        - Joints (dilatant/opening fractures)
        - Pressure solution surfaces (compaction/closing fractures)

(Aydina, Borjab et al. 2006)

The first mode, which is compaction, is accomplished when the stresses acting on the material cause material to be compressed perpendicular to the shear. The second mode, dilation is when the stresses on the material are acting in opposite direction, pulling the material apart. These two can always be classified as volumetric deformation because the actions caused by the stresses create a change in volume, whether it is an increase in volume due to separation or a decrease in volume due to compaction. Shear is when two stresses are acting parallel or tangential along the same plane. The stresses causing strain can be acting in the same direction at different magnitudes, or in opposite directions, along the same plane. Shear deformation has two volumetric possibilities as well as an isochoric option. Shear can occur causing the material to either expand or compressed based on the orientation of the stresses. Isochoric shear occurs when the slip has no effect on the volume

Rock, when loaded in a column such as a pile or indenter, creates a specific type of failure known as Hertzian Cone Crack. This form of failure is used in rock fragmentation processes such as modern day tunneling and drilling. As pressure is applied to the surface of the indenter, the load is applied to the rock directly beneath indenter. The stresses applied to the rock propagate through the rock, compacting the rock directly beneath and creating a crack through the rock starting at the edges of the indenter and

extending into the sample. The angle from the horizontal to the crack is considered the angle of the Hertzian cone cracks (Kocer and Collins 1998). For a typical loading cycle, there are four stages:

(I) closure of microcracks,

(II) linear elastic deformauon,

(III) stable crack growth,

(IV) unstable crack propagation

During stage one, the indenter settles into place, closing any micro fractures and emitting minimal acoustic emissions. During stage two, the rock begins to deform, compacting the rock beneath the indenter. As this process continues, the loading cycle reaches stage three where the crack begins to grow steadily. During these two stages, the rock beneath the indenter begins to form into a wedge which begins to channel the load within the rock to a smaller area of influence. A graphic analysis of the formation of the wedge can be found in Figure 2.6. During stage three, the acoustic emissions per unit time increase rapidly. At stage four, the cracks continue to form, ultimately inducing failure of the rock. On a sample that is of the dimensions show in Figure 6, diameter of 19 mm and height of 22mm, the wedge created under compression is located underneath the punch, and the crack formation is located along the boundary of the tensile and compressive failure areas (Cook, Hood et al. 1984).

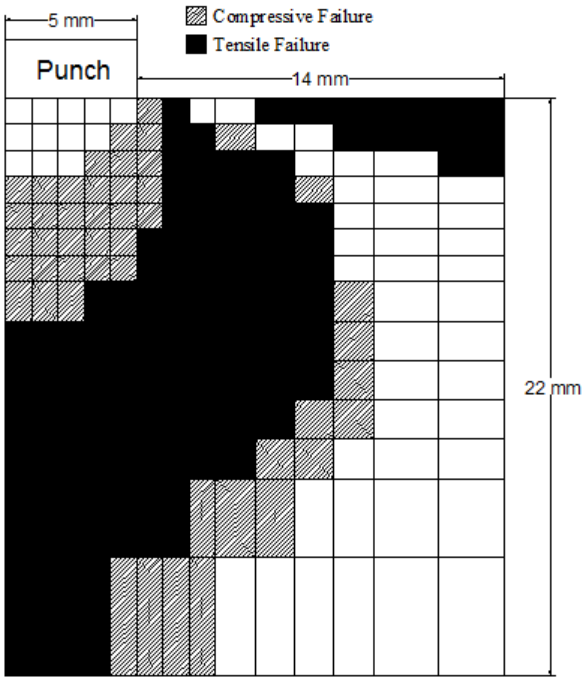

Figure 2.6: Plot of the stresses acting beneath an indenter (Modeled after Cook, Hook et al 1984).

Section 2.3 – Induced Seismicity Monitoring

Since caprock cannot be seen from the surface during the lifespan of the CO_2 storage process, the integrity of the caprock as well as the surrounding rock formations must be monitored from a distance.

Knowing when a joint or a fracture is going to slip is necessary to preventing major failures within rock formations. When monitoring an active joint it is to be able to determine at what point the shearing starts. Once the movement starts, alterations to injection can be implemented to stop the movement (Moradian, Ballivy et al. 2010).

2.3.1 – Seismic Waves

As rock fails, energy is released into its surroundings in the form of movement, and energy waves. These failures can be caused by sudden release of built up strain, as well as a change in the stress field due to excavation or explosive detonation. If the movement is significant, this type of seismic activity is referred to as an earthquake. Seismic waves can also be produced from induced seismicity from increased pore pressure.

To measure the amount of energy released from an earthquake, the Richter scale is referred to for a numeric value. The Richter scale is a logarithmic base ten scale representing the magnitude of the energy released. When the equation for calculating magnitude was made in 1942, the scale was set based on the data available (Gutenberg and Richter 1955). With new technologies, lower emission events are registering, with Richter values in the negatives.

There are two forms of seismic waves, compressional and shear waves. The particle motion for compressional waves, also referred to as P waves, consist of alternation condensation and rarefaction in the same direction of the wave propagation. This motion will propagate through fluid, however the magnitude may decrease. The particle motion for shear waves, also referred to as S waves, is always perpendicular to the direction of wave propagation, when traveling through elastic solid. S waves do not propagate through fluid (Hamada 2004).

2.3.2 – Tomography

As the rock fractures, acoustic waves are emitted from the rocks and can be detected by sensors. Acoustic tests are a way to monitor these events as the failures take place deep underground, providing a form of warning when there is movement below. Tomography is a tool that uses waves to model entities based on arrival times of waves passing through them. The origins of tomography can be traced back to the discovery of the X-ray in 1895 by Wilhelm Conrad Roentgen. It was not until 1930, however, that stratigraphy was developed which paved the way for modern tomography. Again in 1972, another step forward in technology provided the components for Godfrey Houndsfield to develop computed tomography, marking a new era in mapping using waves (Medical). Modern technology allows doctors to use X-Rays to map the internal workings of the human body. Using the same key principles of tomography, scientists can locate stress concentration within a rock formation using pressure waves (Westman 2003). This form of tomography has come to be known as seismic tomography. When

seismic tomography is used in monitoring a site, the arrival times of waves to sensors set up on the property are used to determine where these waves originated (Zhang and Thurber 2003). When seismic tomography is being used to map a site, there is a source, such as a bar being struck by a hammer, that sends waves into the earth which are then reflected back up to the sensors. Knowing where the sources originated, the anomalies within the earth can be recorded (NIOSH 1997). Tomography provides a visual representation of the geology beneath the surface of the earth, allowing for imaging of the subsurface without causing damage.

The same principle can be applied to locate events when passive sensors record different arrival times for the same seismic event. Though the source's location is unknown, the locations of the sensors recording the waves are known. Since waves travel in the path of least resistance, a line representing the travel path can be drawn from each sensor. A representation of this can be found in Figure 2.7.

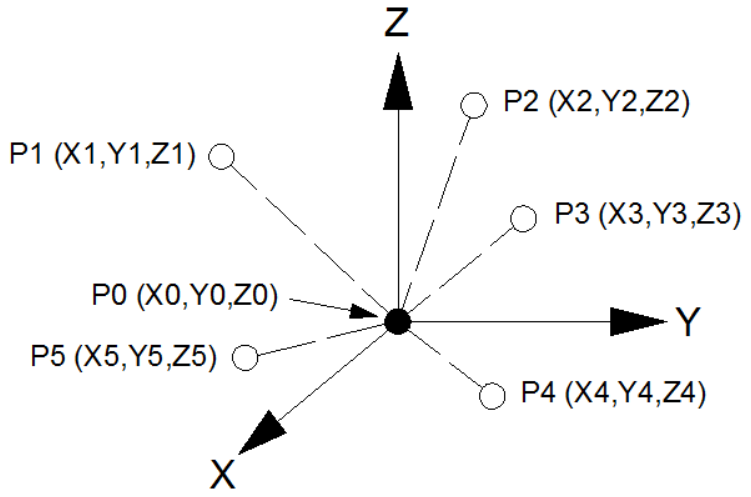

Figure 2.7: Coordinate points for a seismic event, and the sensor orientation affiliated. Modeled after (Hardy, Mowrey et al. 1981).

This figure corresponds with the equation:

$$(X_i - X_o)^2 + (Y_i - Y_o)^2 + (Z_i + Z_o)^2 = V_i{}^2(T_i - T_o)^2 \quad (6)$$

where $X_i,\ Y_i,\ Z_i$ are the geophone coordinates, $X_o,\ Y_o,\ Z_o$ are the source coordinates, V_i is the velocity of the waves, T_i is the arrival time of the wave, and T_o is the true origin time. An equation can be written for each of the sensor locations, with a total of four unknowns. This means data from four stations are necessary to solve for all four unknowns. Due to error in sensor locations as well as arrival times, at least five sensors should be used (Hardy, Mowrey et al. 1981).

2.3.3 – Double Difference Tomography

Traditionally, tomography uses only the difference between calculated and observed travel times for seismic waves from seismic events to stations, the residual, to adjust a velocity model. Double difference tomography is a method of performing tomography that, in addition to minimizing residuals between calculated and observed travel times, also minimizes the travel time residuals between two similarly located events. The equation for the double difference, dr_k^{ij}, is given as

$$dr_k^{ij} = (T_k^i - T_k^j)^{obs} - (T_k^i - T_k^j)^{cal} \quad (7)$$

where T_k^i and T_k^j are the travel times from events i and j to a station k. Seismic waves emanating from event hypocenters located close to one another should propagate along a nearly identical path. Minimizing the travel time residuals of two events forces them onto a similar travel path, improving the precision of relocated events (Zhang, Subhash et al. 2003). The double difference method adds better accuracy to the velocity structure, with each additional event that is used in the calculation (Hirose, Nakajima et al. 2008).

2.3.4 – Seismic Monitoring Equipment

Seismic monitoring equipment captures seismic waves using specially installed geophone arrays. There are three companies that provide short term monitoring systems suitable for mining operations. These companies are ESG based in Canada, ISS from South Africa and CSIR from South Africa. Short term monitoring systems have between 6 and 16 channels, are usually based on uniaxial geophones and have a one day installation time frame. These systems include a sufficient number of sensors to cover a volume of rock 125 million cubic meters (Turner 2005). The ESG monitoring system contains a 24 bit digital microseismic recorder, called the Paladin, capable of recording data as a standalone unit or as part of a multi-station system (Solutions 2012). The Paladin system is a web based system that can be accessed remotely and provides real-time monitoring (Elliot 2008). This seismic monitoring system is used in deep mines to monitor rock bursts and other seismic events. The receivers used by these systems are considered passive, because the source of the event created by the seismic events does not come from sensors themselves. Instead of pulsing a signal, the sensors are stations that wait for a signal to pass through them and record the wave information.

For the monitoring equipment to register the wave arrival, the signals must be received from geophones, or accelerometers that are installed on site. These sensors, also referred to as receivers, vibrate at the same frequency as the wave, as the seismic wave propagates through the surrounding rock as well as the sensor. Two main types of geophones are uniaxial and triaxial. Uniaxial geophones only measure the ground movement perpendicular to the face of the sensor, while a tiraxial sensor can measure in all three directions. A geophone contains a magnet with a cylindrical coil of wire being held in place

by leaf springs. As the ground vibration passes through the sensor, the coiled wire vibrates at the same frequency as the ground vibration, passing back and forth across the central magnet. This movement creates a voltage that is passed through the data wire to the monitoring system, where it is recorded (Barzili 2000).

Sensor coverage is an important part of installing a monitoring system. Placing as many receivers as possible across an area of interest will produce the greatest results. However, with having sensors only at one elevation does not provide a strong grid for confidence in results. When one seismic event occurs, the wave travels away from the source to the receiver directly. The next event occurs in a slightly different location causing the ray path to the same sensor stations to vary slightly. When these paths cross, more confidence is placed in the area that the ray paths intersected, since multiple events have passed through the same area. Having geophones at different elevations rather than on a level surface will create a larger grid with greater confidence, rather than having high confidence centralized in a small section of the coverage area.

Chapter 3 - Passive Tomography to Image Stress Redistribution Prior to Failure on Berea Sandstone and Marcellus Shale for Caprock Integrity

Section 3.1 – Introduction & Background

A recent concern is the cause and effect of global climate change. Many institutions give credit for these changes to the increased levels of greenhouse gases in the atmosphere, in particular the increase in the amount of carbon dioxide present. Fossil fuels such as petroleum products and coal are burned to create energy for powering everyday devices. A byproduct of this combustion reaction is carbon dioxide. With the increased industrialization of developing and developed nations the amount of carbon dioxide being produced is continuing to rise, furthering the awareness of the general public of the effect carbon dioxide has on the climate. With the increased public awareness, there has been an increasing surge to find a solution to this problem.

There is a growing interest in carbon capture and storage (CCS) as a means to reduce the global impact of CO_2 on the climate as a greenhouse gas. Carbon capture is the process of removing CO_2 from the atmosphere as well as preventing it from entering the atmosphere by means of exhaust. The captured carbon is stored underground in reservoirs. These reservoirs have the storage space to handle the volume of CO_2 injected as well as a caprock layer preventing the injection fluid from returning to the surface. Additionally, CO_2 can be used for enhanced oil recovery (EOR). The methods

Since caprock cannot be seen from the surface during the lifespan of the CO_2 storage or EOR process, the integrity of the caprock as well as the surrounding rock formations must be remotely monitored from a distance. Knowing when a joint or a fracture is going to slip is necessary to prevent major failures within geologic strata. It is necessary to prevent these slips from occurring to retain the integrity of the caprock, keeping the fluid within the reservoirs. When monitoring an active joint it is imperative to be able to determine at what point the shearing starts. Once the movement starts, alterations to injection can be implemented to stop the movement (Moradian, Ballivy et al. 2010).

3.1.1 - Seismic Waves

As rock fails, energy is released into its surroundings in the form of movement, and elastic waves. These failures can be caused by sudden release of built up strain, as well as a change in the stress field due to excavation or explosive detonation. If the movement is significant, this type of seismic activity is referred to as an earthquake. Seismic waves can also be produced from induced seismicity from increased pore pressure.

To measure the amount of energy released from an earthquake, the Richter scale is referred to. The Richter scale is a base ten logarithmic scale representing the magnitude of the energy released. When the equation for calculating magnitude was developed in 1942, the scale was set based on the data

available (Gutenberg and Richter 1955). With new technologies, lower magnitude events are registering, resulting in Richter values less than zero.

There are two forms of seismic waves, compressional and shear. The particle motion for compressional waves, also referred to as P waves, consists of alternating condensation and rarefaction in the same direction of the wave propagation. This motion will propagate through fluid. The particle motion for shear waves, also referred to as S waves, is always perpendicular to the direction of wave propagation, when traveling through an elastic solid. S waves do not propagate through fluid (Hamada 2004).

3.1.2 - Tomography

As the rock fractures, acoustic waves are emitted from the rocks and can be detected by sensors. Tomography is a tool that uses waves to model entities based on arrival times of waves passing through them. The origins of tomography can be traced back to the discovery of the X-ray in 1895 by Wilhelm Conrad Roentgen. In 1972, another step forward in technology provided the components for Godfrey Houndsfield to develop computed tomography, marking a new era in mapping using waves (Medical). Modern technology allows doctors to use X-Rays to map the internal workings of the human body. Using the same key principles of tomography, scientists can locate stress concentration within a rock formation using pressure waves (Westman 2003). This form of tomography is known as seismic tomography. When seismic tomography is used in monitoring a site, the travel times of waves to sensors set up on the property are used to determine where these waves originated (Zhang and Thurber 2003). When seismic tomography is used to map a site, there is a source, such as a bar being struck by a hammer, that sends waves into the earth which are then reflected up to the sensors. Knowing where the sources originated, the anomalies within the earth can be mapped (NIOSH 1997). Tomography provides a visual representation of the geology beneath the surface of the earth, allowing for imaging of the subsurface without causing damage.

The same principle can be applied to locate events when passive sensors record different arrival times for the same seismic event. Though the source's location is unknown, the locations of the sensors recording the waves are known. Since the first arrivals travel in the path of highest velocity, a line representing the travel path can be drawn from each sensor. A representation of this is shown in Figure 3.1.

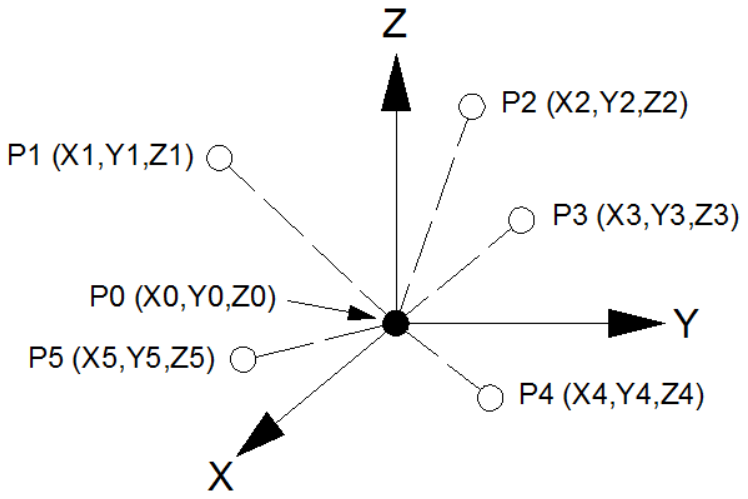

Figure 3.1: Coordinate points for a seismic event (P0), and the affiliated sensor orientation (P1-P4).

This figure corresponds with the equation:

(1) $$(X_i - X_o)^2 + (Y_i - Y_o)^2 + (Z_i + Z_o)^2 = {V_i}^2(T_i - T_o)^2$$

where $X_i,\ Y_i,\ Z_i$ are the geophone coordinates, $X_o,\ Y_o,\ Z_o$ are the source coordinates, V_i is the velocity of the waves, T_i is the arrival time of the wave, and T_o is the true origin time. An equation can be written for each of the sensor locations, with a total of four unknowns. This means data from four stations are necessary to solve for all four unknowns. Due to error in sensor locations as well as arrival times, at least five sensors should be used (Hardy, Mowrey et al. 1981).

3.1.3 - Double Difference Tomography

Traditionally, seismic tomography uses only the difference between calculated and observed travel times for seismic waves from seismic events to stations, the residual, to adjust a velocity model. Double difference tomography is a method of performing tomography that, in addition to minimizing residuals between calculated and observed travel times, also minimizes the travel time residuals between two similarly located events. The equation for the double difference, dr_k^{ij}, is given as

(2) $$dr_k^{ij} = (T_k^i - T_k^j)^{obs} - (T_k^i - T_k^j)^{cal}$$

where T_k^i and T_k^j are the travel times from events i and j to a station k. Seismic waves emanating from event hypocenters located close to one another should propagate along nearly identical paths. Minimizing the travel time residuals due to two events forces them onto a similar travel path, improving the precision of relocated events and the velocity model (Zhang, Subhash et al. 2003). The double difference method adds better precision to the velocity structure with each additional event that is used in the calculation (Hirose, Nakajima et al. 2008).

3.1.4 - Seismic Monitoring Equipment

Seismic monitoring equipment captures seismic waves using site specific geophone arrays. There are three primary companies that provide monitoring systems suitable for mining operations. These companies are ESG based in Canada, ISS from South Africa and CSIR from South Africa. Short term monitoring systems have between 6 and 16 channels, are usually based on uniaxial geophones and have a one day installation time frame. These systems include a sufficient number of sensors to cover a volume of rock of 125 million cubic meters (Turner 2005). The ESG monitoring system contains a 24-bit digital microseismic recorder, called the Paladin, capable of recording data as a standalone unit or as part of a multi-station system (Solutions 2012). The Paladin system is a web-based system that can be accessed remotely and provides real-time monitoring (Elliot 2008). This seismic monitoring system is used in deep mines to monitor rock bursts and other seismic events. The receivers used by these systems are considered passive, because the source of the event created by the seismic events does not come from sensors themselves. Instead of emitting a signal, the sensors are stations that wait for a signal to arrive and then they record the wave information.

For the monitoring equipment to register the wave arrival, the signals must be received from geophones, or accelerometers that are installed on site. These sensors, also referred to as receivers, vibrate at the same frequency as the wave as the seismic wave propagates through the surrounding rock as well as the sensor. Two main types of geophones are uniaxial and triaxial. Uniaxial geophones only measure the ground movement perpendicular to the face of the sensor, while a triaxial sensor can measure in three orthogonal directions. A geophone contains a magnet with a cylindrical coil of wire being held in place by leaf springs. As the ground vibration passes through the sensor, the coiled wire vibrates at the same frequency as the ground vibration, passing back and forth across the central magnet. This movement creates a voltage that is passed through the data wire to the monitoring system, where it is recorded (Barzili 2000).

Sensor coverage is an important part of installing a monitoring system. Placing as many receivers as possible across an area of interest will produce the best results. However, having sensors only at one elevation does not provide a strong arrangement for confidence in results. When one seismic event occurs, the wave travels away from the source to the receiver directly. The next event occurs in a slightly different location causing the ray path to the same sensor stations to vary slightly. When these paths cross, more confidence is placed in the area that the ray paths intersected, since multiple events have passed through the same area. Having geophones at different elevations rather than on one level will create a larger volume with greater confidence, rather than having high confidence centralized in a small section of the coverage area.

3.1.5 – Punch Loading of Rock Samples

Rock, when loaded in a column such as a pile or indenter, creates a specific type of failure known as a Hertzian cone crack. This form of failure is used in rock fragmentation processes such as tunneling and drilling. As pressure is applied to the surface of the flat circular punch, the load is applied to the rock directly beneath it. The stresses applied to the rock propagate through the rock, compacting the rock directly beneath and creating a crack through the rock starting at the edges of the punch and extending into the sample. The angle from the horizontal to the crack is considered the angle of the Hertzian cone cracks (Kocer and Collins 1998). For a typical loading cycle, there are four stages:

(I) closure of microcracks,

(II) linear elastic deformation,

(III) stable crack growth,

(IV) unstable crack propagation

During stage one, the indenter settles into place, closing any micro fractures and emitting minimal acoustic emissions. During stage two, the rock begins to deform, compacting the rock beneath the indenter. As this process continues, the loading cycle reaches stage three where the crack begins to grow steadily. During these two stages, the rock beneath the indenter begins to form into a wedge which begins to channel the load within the rock to a smaller area of influence. A numerical model of the formation of the wedge can be found in Figure 3.2. The model shown in Figure 3.2 was created to model stage IV. During stage three, the acoustic emissions per unit time increase rapidly. At stage four, the cracks continue to form, ultimately inducing failure of the rock. On a sample that is of the dimensions show in Figure 3.2, diameter of 19 mm and height of 22mm, the wedge created under compression is located underneath the punch, and the crack formation is located along the boundary of the tensile and compressive failure areas (Cook, Hood et al. 1984).

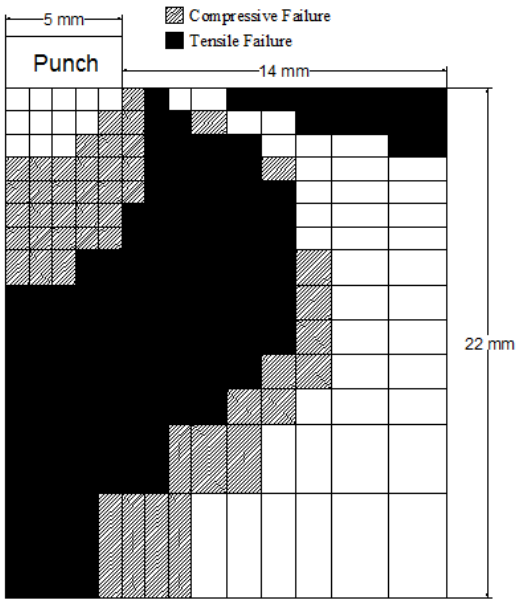

Figure 3.2: Plot of the stresses acting beneath an indenter during stage IV of testing, in an unconfined sample (Modeled after Cook, Hook et al 1984).

In a 2005 publication, Michael Murphy reported results of an active tomography test completed using an indenter and a piece of Berea Sandstone. One side of the sample had passive sensors attached to record the waves passing through the sample. The opposite side of the sample had active sources attached which sent pulses through the sample. The sample was loaded until failure using an indenter while the active sources pulsed acoustic waves through the sample, and the passive sensors recorded the data. The tomogram created from the results of this test can be found in Figure 3.3.

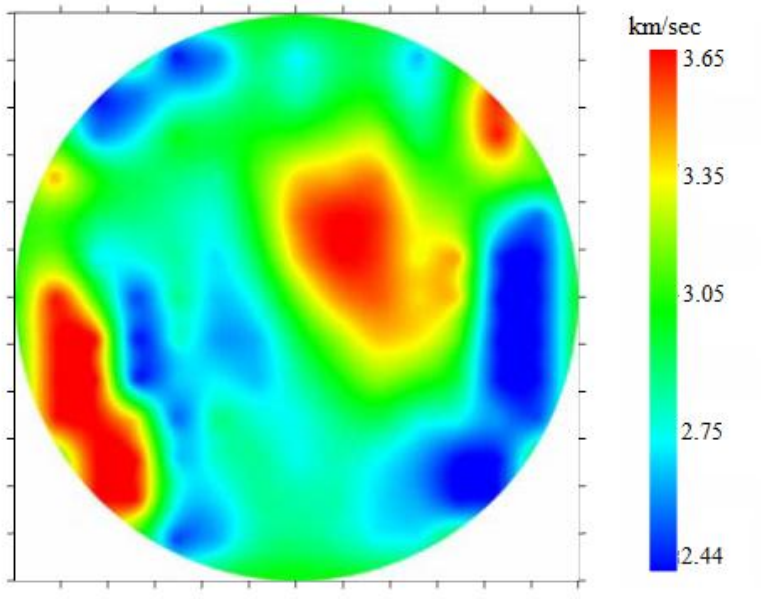

Figure 3.3: Tomogram created using data obtained from active tomography of an indentation test of Berea Sandstone (Murphy 2005)

This tomogram was created using the data collected just prior to failure of the sample at 114.2 MPa. On the right side of the tomogram there is a concentration of high velocity which corresponds with the indenter location. As stress was added to the sample, the active tomography was able to monitor this area effectively. Since the area of high velocity was located beneath the indenter, where compression took place, the result of the active tomography was accepted as successful.

Section 3.2 - Sample Preparation

In preparation for testing, samples of Berea Sandstone and Marcellus Shale were prepared. Berea Sandstone was used for a test sample because it is an industry standard for testing for petroleum engineering. The homogeneousness is a characteristic of the Berea Sandstone that makes it desirable for testing. Marcellus Shale was used for a test sample because shale could possibly be a caprock layer which would require monitoring at a carbon sequestration site. Also, the discovery of a large natural gas deposit within the Marcellus Shale makes any information about the Marcellus Shale sample pertinent to future research.

The Berea Sandstone sample had a diferent preparation procedure since the samples provided came in 343 mm x 343 mm x 152 mm blocks, whereas the Marcellus Shale sample acquired was taken from a core drill sample. Using a coring bit, a sample was cut out of the sandstone blocks with a height of 152 mm and diameter of 152 mm. Once the sample was cored, the top and bottom faces were checked to determine if they were parallel. If the faces were found to not be parallel, the sample was placed in a grinder and the faces were ground down so the faces were parallel within 0.1mm. Once the vertical axis of the sample was perpendicular to the top and bottom faces, the sample was dried in an oven and heated at 75 degrees Celsius.

The Marcellus sample was received already in cylindrical form. For this test, an 88 millimeter diameter and 74 millimeter tall sample of Marcellus Shale from a test drill in West Virginia was used. The core number was 7996, from Merc 1 Box 110, at a depth between 2,284.71 meters and 2,284.87 meters. Using a rock saw, the faces were cut to smooth planes which were perpendicular to the vertical axis. Utilizing the grinder, these planes were made parallel to one another, creating a sample that had a flat surface for even distribution of the load from the press. To preserve the bonds between the layers of the shale, the Marcellus Shale sample was not dried in the oven, rather was allowed to air dry over the weekend. The concern over the drying of the sample was that the rapid removal of moisture would cause the sample to lose strength along the foliation.

The next step for both samples was to mark sensor locations and make the pads for the sensor attachment. The Berea Sandstone sample and the Marcellus Shale sample had different sensor locations due to the size of the samples limiting the number of sensors that could fit. The Berea Sandstone samples

had fifteen sensors attached, divided into three rows of five. The Marcellus Shale sample had fourteen sensors attached, divided into two rows of seven. A diagram of the prepared samples with sensor locations shown can be found in Figure 3.4.

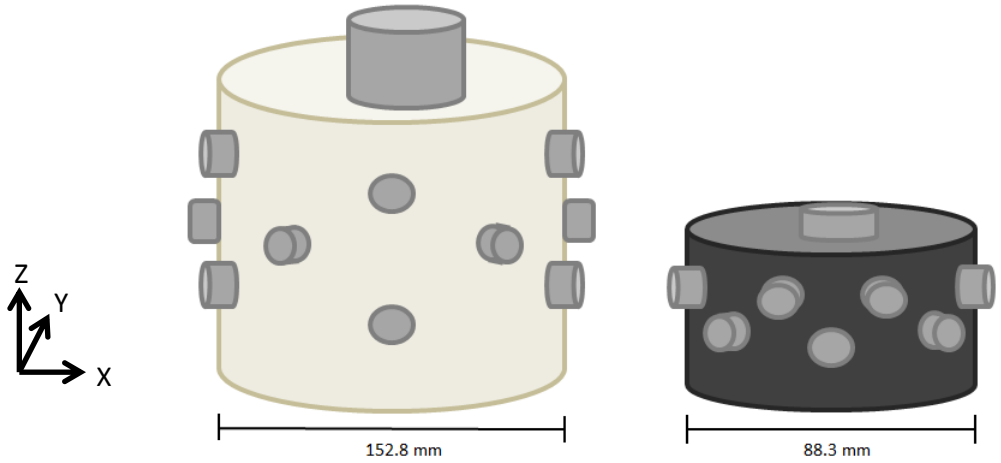

Figure 3.4: Berea Sandstone and Marcellus Shale samples with sensors locations.

To mark the locations of the sensors, a band was placed around the sample using masking tape. With a pencil, the upper edge of the band on each sensor level was marked on the sample. The Berea Sandstone sample was marked 30 mm, 70 mm and 110 mm for the top surface of the sample. The Marcellus Shale was marked 64 mm and 38 mm from the top of the sample. The next step was marking the location of each individual sensor around the sample. For the Berea Sandstone sample the sensor was located every 72 degrees about the Z axis, and for the Marcellus Shale sample, sensors were located every 51.4 degrees about the Z axis.

Once the sensor locations were marked on the sample, it was necessary to create a flat surface to attach the sensors. To do this, a grinding stone was used. The flat areas, or pads, provided a greater surface area of the sensor to be in contact with the sample to receive the acoustic emissions. Once the pads had been ground down, the band was put back onto the sample and the sensor centroids were once again marked on the sample. After grinding the precise sensor locations were remarked. Before attaching the sensors, the sensor pads were labeled corresponding to the sensor number that was placed in that location so that when the sample is attached to the ESG Hyperion system, there is no confusion between what sensor is attached to which channel. Pictures of the equipment used to fabricate the Berea Sandstone and Marcellus Shale samples can be found in Appendix A.

Just prior to sensor attachment each sensor was tested to make sure there was a signal being registered on the ESG Hyperion system. This was done by placing the sensor on a counter top, or other solid surface, on a drop of oil. An object such as a wrench was then tapped against the surface of the counter. If the sensor worked, the ESG software would register that the sensor had been triggered. This

was repeated three times for each sensor to ensure that the sensor was reading correctly. In this test the counter top was used to represent a medium that could carry elastic waves and the oil acted as a couplant between the sensor and the table top that would allow the waves to pass thorough without losing energy.

For attachment to the samples, cyanoacrylate (superglue) was used. Superglue was used for two reasons. Firstly, when dry, superglue has an impedance that is similar to rock. This allows the waves to pass though the superglue without influencing the arrival times detected by the receivers. Secondly, using a readily available solvent, the superglue can be removed from the sensors without any harm, and the sensors can be reused within 24 hours of the completion of the previous test. This allowed quick turnaround in testing.

When attaching the sensors, the location of the channel attachment was of utmost importance. The connector on the sensor protrudes from the side of the sensor, while the connection on the wire is too stiff to bend for about 10 mm. Working with smaller samples such as these, the orientation of the connectors needs to be in the direction of the recording apparatus so that the wires do not get caught up in any moving parts of the press.

The next step in preparing the sample was to mark the location of the steel indenter. Two perpendicular diameters were drawn on the sample. The punch was placed tangent to the intersection with its diameter lined up with the sample diameter. The outside of the indenter is then traced on the surface of the sample. Tracing the indenter is a precautionary measure in case during transport to the rock press the indenter is moved, there is visual outline that will show at what position the indenter must be placed. The result of this layout makes the indenter focus the pressure into a specific area to induce failure rather than spreading the load across the entire top surface of the sample. By having the indenter completely on one side of the sample, the sensors on the side of the diameter opposite the indenter will record waves that have traveled through intact and undisturbed rock. This loading style was used to have asymmetric loading resulting in a preferential zone of failure. The tomography results shoud clearly display the off-center stress redistribution. As shown in Figure 3.5, the indenter is located closer to the edge of the sample on one side compared to the other.

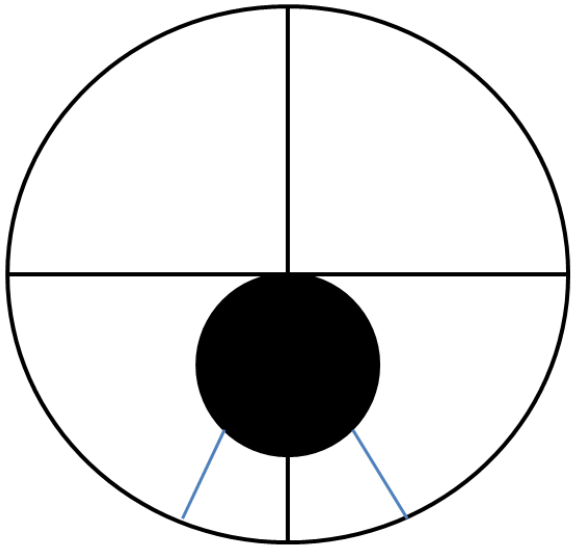

Figure 3.5: Indenter location with area of expected failure indicated between two blue lines.

The sample is expected to fail in the area between the blue lines because the cracks from the failure will reach the free face fastest in this area. Though an exact location cannot be forecast, the expected zone of failure provides a location to focus observations. A completed sample of Berea sandstone can be seen in Figure 3.5.

Figure 3.6: A prepared sample of Berea Sandstone with sensors attached and indenter in desired location

The final step for preparing the sample is to ensure that the sample is properly placed in the rock press and the sensors connected. For this test a 100kip MTS 810 testing system, was used along with an

ESG Solutions 16 channel acoustic emissions monitoring system. The orientation of the sample in the rock press is important because the indenter needs to receive even loading from the rock press or the load concentration will be eccentric. To accomplish this, the indenter must be centered beneath the pressing surface, causing the sample to be off center on the platform. This caused an issue with the safety shields around the sample not closing completely; however, it was necessary to have the sample properly loaded. To ensure safety to the operator and equipment, a second shield was installed.

Section 3.3 - System Preparation and Data Acquisition

Upon completion of the sample preparation, data collection began. To ensure accurate data collection, a number of steps were taken. Since separate machines were used for loading and data acquisition, programming and calibration were key components to accurate data collection. Two tutorials, one for the MTS 810 Materials Test System rock press and the other for the ESG Solutions Acoustic Emissions machine, were completed after running these tests, both of which can be found in Appendix C and D, respectively. Both pieces of equipment are displayed in Figure 3.7.

Figure 3.7: Side A is the MTS 810 Material Test System. Side B is the ESG Solutions Hyperion system.

Prior to loading the sample, a program was created to control the MTS Rock Press in the manner necessary for these tests. Using the built-in programming software, based on Labview code, a procedure was developed to load the sample at a constant rate with the option to pause and restart the system if there were any problems. The code can be seen in Figure 3.8.

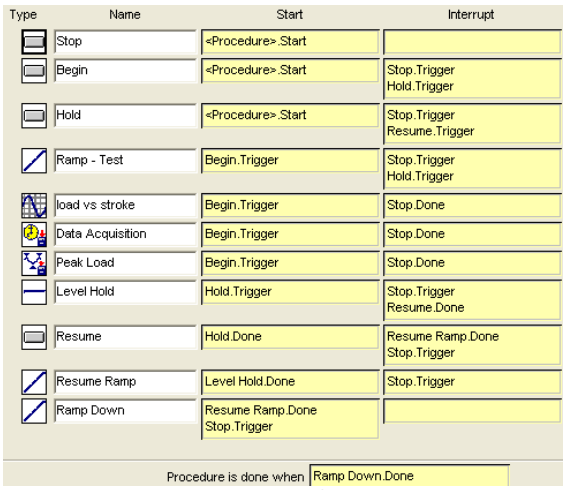

Figure 3.8: Procedure code for MTS rock press.

The sample was loaded at a constant deformation of 6.35e-5 mm per second. This loading rate was calculated so that the sample would fail after approximately six hours based on the compressive strength of Berea Sandstone. A long test duration was desired to allow as many distinct events to be recorded as possible. Also by pressing the "Begin" button, the program begins to record the load in pound force over time, the peak load, and a real time load vs. time plot. The press continues to load until either the "Hold" or the "Stop" button is selected. The "Hold" button pauses the loading process in case of an emergency, and will resume at the same loading rate when pressed again. The "Stop" button stops the loading process and returns the platform to its original position so that it is simpler to remove the sample, post failure.

The ESG Solutions Hyperion system is not programmed in the same manner as the MTS rock press. The key component that is necessary for data recording and processing is the sensor file. This file contains the location of the sensors in reference to the sample itself. The program uses whichever values are input into the software as the exact point in space that the wave reading was taken. Inconsistencies with coordinate planes and origin location while inputting sensor locations will create invalid results.

Prior to the data acquisition step, the rock press and acoustic emission machines have to be calibrated individually and to one another. Between these two machines, time was the common variable collected. Due to this, it is necessary to synchronize the times between the two systems prior to starting the test. This provides a common timeline that does not need to be adjusted during the data processing portion. To calibrate the MTS rock press, the displacement value as well as the load value must be zeroed prior to the test initializing so that the recorded values of force and displacement begin at zero.

To calibrate the ESG Hyperion system, the sensors were tested to make sure each one was recording data. This was accomplished by tapping directly underneath each sensor, in increasing order by channel number, around the entire sample. Based on the active readings on the ESG system monitor, the recorded data for each channel is displayed by sensor number. If the sensor was triggered by the test tap,

then the sensor was considered active and functioning. The tap test was used to zero the system once the sample was prepared, but before the sample fails to ensure all sensors are still in contact with the sample. Also, based on previous tests, it was determined that the valve that controls the hydraulics on the MTS rock press, called a servo-valve, adjusted so rapidly that it created enough background noise during the test to trigger events. To prevent unnecessary background noise, a sensor was attached to the servo-valve for monitoring purposes. While the hydraulics were on, the sensor registered noise, so the threshold value, in mV, was increased until the sensor attached to the servo-valve no longer registered activity. The threshold level was set to 325 mV throughout the entire test. Once the equipment was calibrated and testing procedures set, the sample was seated in the rock press so that the press was making contact with the indenter.

The first step in data acquisition was to make sure that both systems were running the proper programs for data collection. The MTS code was then run, starting the constant deformation rate applied to the sample. As the rock press continued to load, the ESG acoustic emissions machine automatically recorded any event that triggered more than five sensors. Once the sample failed, the press was allowed to run for approximately five minutes longer so that data could be recorded representing events post failure. Upon completion, the ESG Hyperion system was shut down completely, and the channel wires were disconnected from the sensors. This procedure ensured that no events were recorded due to vibration made during disassembly.

The final step in the data acquisition was to determine the P and S wave arrival times for each of the samples. The P and S wave velocities are needed for processing the data collected in these tests, which can be calculated from the arrival times. To do this, a core sample was taken of each failed Berea Sandstone sample, in the non-fractured area, and the Marcellus Shale sample was used as is. The test cores were placed in the P and S wave apparatus. The elastic wave velocities for each sample were recorded. Upon completing the data acquisition, the first step was to determine the velocities of the P and S waves which travelled through each sample. These values were calculated by taking the overall length of each sample and dividing it by the time it took for the wave to travel the length of the sample, commonly referred to as wave arrival time. Once these values were determined and confirmed with previously published sources, the values were used as the P and S wave velocities for event locations.

Section 3.4 - Event Location

The raw data collected from samples provided the information necessary to locate the recorded events within the sample. From this information, a velocity model mapping the areas of high and low velocities can be created using tomography. Based on the actual failure locations of the rock samples compared to these velocity models will determine how accurately tomography can map insitu failure events.

Within the ESG software there is a program called SeisTree. This program allows the user to create processors to map the location of events based on certain parameters. The processor used for event location for the Berea Sandstone sample is shown in Figure 3.9.

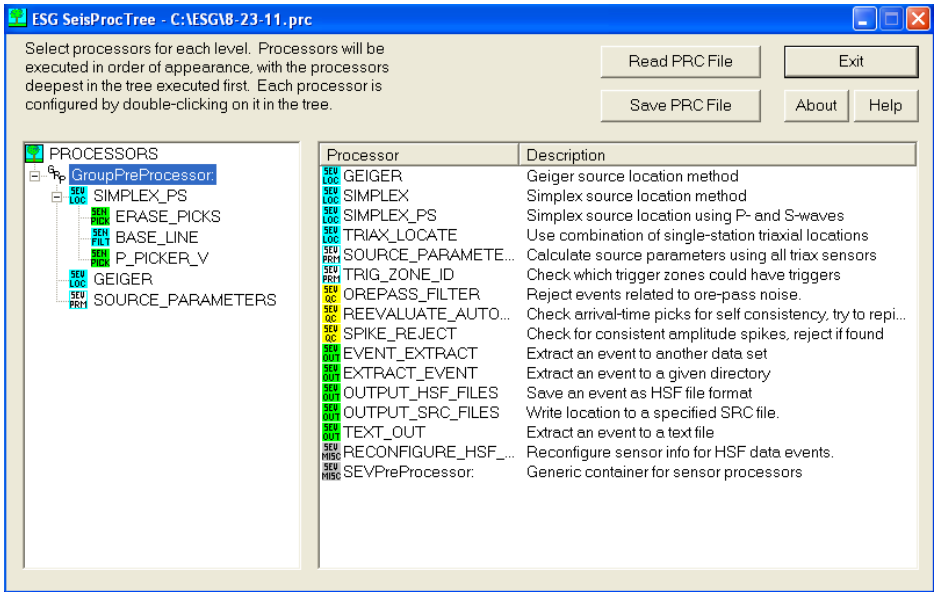

Figure 3.9: The processor used to locate events in the Berea Sandstone and Marcellus Shale samples.

Within the SeisTree program there are options for different filters, arrival time pickers and other actions that are useful for processing the data. The P_Picker arrival time picker in cooperation with the Geiger arrival time picker were used based on recommendations from ESG Solutions to filter and locate the events most effectively. The P_Picker was used as an initial filter for the data, while the Geiger processor processed the data to tighter standards and confined the located events to with the boundaries of the sample. The P_Picker processor has sub processors, which can be seen in Figure 5.3.1, called Erase_All, Base_Line and PV_Picker. Erase_All erases all previous picks before new ones are picked. This prevents left over events from previous processing runs from contaminating the results based on the most recent settings. Base_Line allows the users to filter out a certain frequency of the background noise, in this case the 60 Hz produced by the overhead lights in the testing room. The PV_Picker is the function that picks the arrival times of the p waves in the recorded data. The Geiger processor is set to select only the data that is within the confines of the sample boundaries. The event locations sometimes are created outside of the sample due to incorrect P wave picking by the sensor, or background noise being mistaken as actual events. This confining step removes the erroneous results from the final data file. The P wave velocity used for the Berea Sandstone and the Marcellus Shale was 2.8 km/s and 2.3 km/s, respectively.

Another check that was used to determine that the correct P and S wave velocities were being assigned involved zeroing the event locations to the initial taps around each sensor. Once the events were located from running the processor, the locations of the first recorded events were compared to the

location of the sensors. This extra step ensured that the calculated data and the values previously reported were accurate for these particular samples.

Running the processors creates two files. The Source file, or SRC, which includes event locations and the Quality Data Base file, or QDB, which includes the arrival times of each pick. These files were combined into a spreadsheet for input into code written in MatLab. The MatLab code took the event location, sensors location and arrival time data and output four new files: events.dat, station.dat, tt.dat and phase.dat. The events.dat and station.dat contain the locations of the recorded event and sensors in latitude and longitude location. This coordinate system is needed for input into TomoDD. The tt.dat file converted the provided arrival times into travel times. The phase.dat file combined this information into one summary file.

The next step was to input the phase.dat and station.dat files into PH2DT. PH2DT is a program that creates the necessary files for running TomoDD. A number of parameters were set before processing in PH2DT. To determine which events were used to relocate another event, an epicentral separation of 25 mm was set between events. This setting prevented any events further than the set distance to be used to adjust the location of a specific event. The max number of surrounding events used was set to 10, so that if there was a tight cluster of events, only the closest events would be used. The output file for PH2DT was dt.ct.

Prior to running TomoDD a MOD file was written. The MOD file is the starting point for the velocity model. The velocity model is a grid created by individual nodes, encompassing the coordinates that contain the sample. The MOD file contains the background velocity for each node, for the entire velocity model. For the Berea Sandstone sample a uniform background velocity of 2.3 km/sec was used and for the Marcellus Shale sample a uniform background velocity of 2.8 km/sec was used.

Once the MOD file is created, TomoDD was run. The files that were input into TomoDD were the MOD file, dt.ct, phase.dat, tt.dat, station.dat, events.dat, and the input file for TomoDD. Examples of these files can be found in Appendix A. The TomoDD input file sets the name of the output files for the new velocity model, original locations of events and the relocation of events files. In the output file for the velocity model, a derivative weight sum (DWS) value is added, which provides a confidence value for the results based on the number of raypaths in each voxel. Upon processing the data through TomoDD, the new locations of events are more precise due to the use of double difference tomography.

Once TomoDD has finished running, there are certain values which need to be checked before the velocity model can be considered reasonable. A condition number is reported for each iteration as TomoDD Runs. A value of over 20 is desired, and a range of up to 80 is considered acceptable for this value at the final iteration. If the resulting value is not in the desired range, the damping values used in

the tomoDD input file were adjusted. The damping value changes the weighted amount each event is given in the relocation calculation and velocity model creation.

Section 3.5 - Results and Discussion

3.5.1 - Recorded Data

The MTS rock press recorded the data for each sample's deformation throughout the test along with the load being applied to the sample. The Marcellus Shale sample and Berea Sandstone sample were each loaded using an indenter. The Marcellus Shale sample used a one inch diameter indenter and the Berea Sandstone sample used a two inch diameter indenter due to the relative size of the samples. Using the area of the indenter and the load applied to the sample, the stress applied to the sample was calculated. The strain was calculated for each sample by using the deformation recorded by the MTS equipment and dividing it by the initial length of each sample.

The Berea Sandstone is a porous rock, approximately 15 percent pore space. This void space provides area within the rock that must be compressed before the full strength of the rock is reached. When the Berea Sandstone fails it is gradual, since it is not a brittle material. This provides two distinct regions on the stress vs. strain curve that show linear elastic deformation, during the majority of the test, and plastic deformation when approaching failure. The Marcellus Shale is a brittle and impermeable rock that naturally has foliation. Since the Marcellus Shale is impermeable, there is little void space within the rock that needs to be closed. The foliation causes the sample to be strong perpendicular to the foliation plane, however parallel to the foliation the sample is must weaker. As the sample is loaded perpendicular to the plane of the foliation, the material beneath the indenter is being compressed. As this is occurring, the material is bending away from the point of loading. This applies a tensile stress to the sample perpendicular to the foliation plane. When the Marcellus Shale fails it is sudden to the brittle nature of the rock, so there is no zone of plastic deformation as in the Berea Sandstone. Figure 3.10 show the stress strain curve for both the Berea Sandstone and the Marcellus Shale.

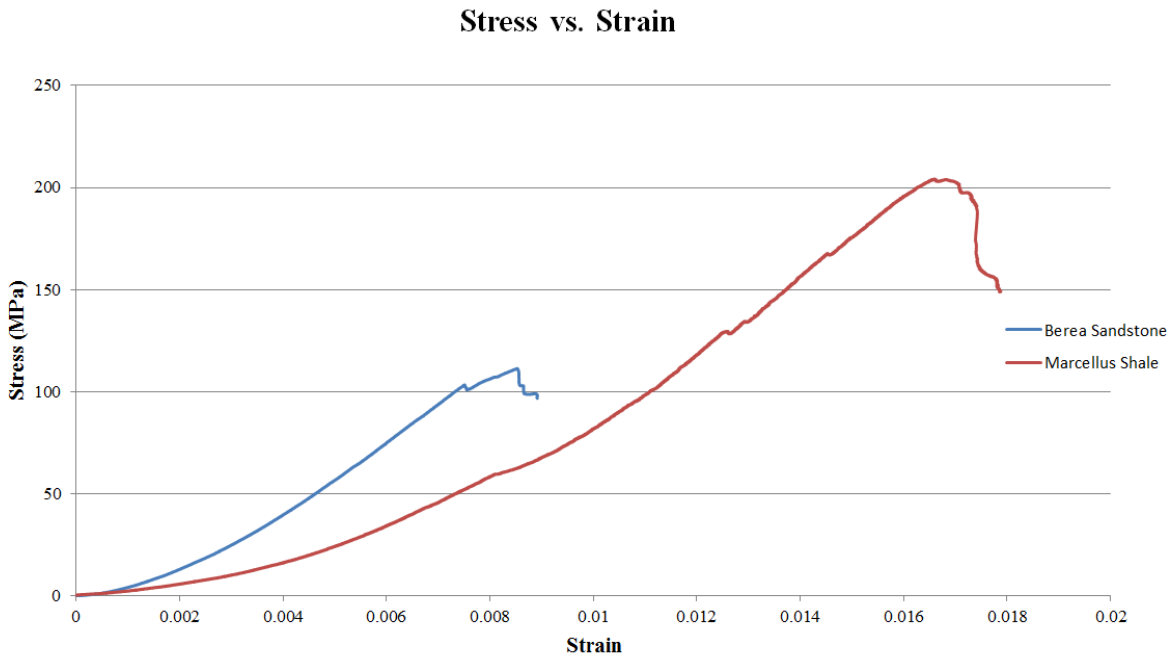

Figure 3.10: The stress vs. strain curve for the Berea Sandstone sample and Marcellus Shale sample.

To analyze the data from each sample in smaller segments, the data for each sample was divided into three regimes based on the stress vs. strain curves. Due to the different rock properties, each curve was divided differently. The Berea Sandstone curve was divided based on what type of deformation was occurring and the Marcellus Shale curve was divide based on event frequency and relation of the curve to failure. For the Berea Sandstone sample, the first regime was the part of the test that showed linear, elastic deformation. Regime number two includes when the sample begins to approach failure and the stress vs strain curve shows plastic deformation. Regime three includes the data at failure and post failure. For the Marcellus Shale sample, the first regime encapsulated the loading time frame that there were an infrequent number of events. Regime two starts when the event frequency begins to increase and ends prior to failure. The third regime includes the data from failure and post failure.

For the Berea Sandstone sample the boundary between regimes one and two is located at 91 percent of the ultimate stress and the boundary between regime two and three is located at 98 percent of the ultimate stress. The boundary between the first and second regimes for the Marcellus Shale sample is located at 86 percent of the ultimate stress, and the boundary between regime two and three is located at 99 percent ultimate stress. The stress vs. strain curves for the Berea Sandstone and Marcellus Shale samples can be found in Figure 11 and 12, respectively.

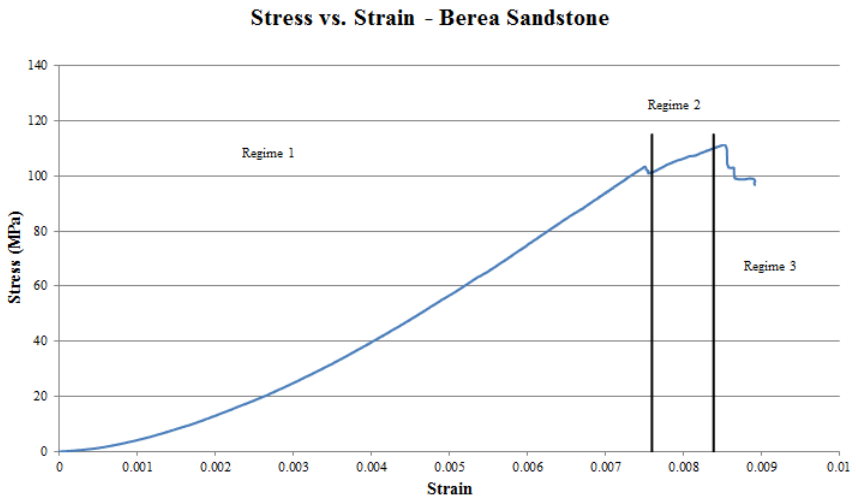

Figure 3.11: The stress vs strain curve for Berea Sandstone sample divided into regimes.

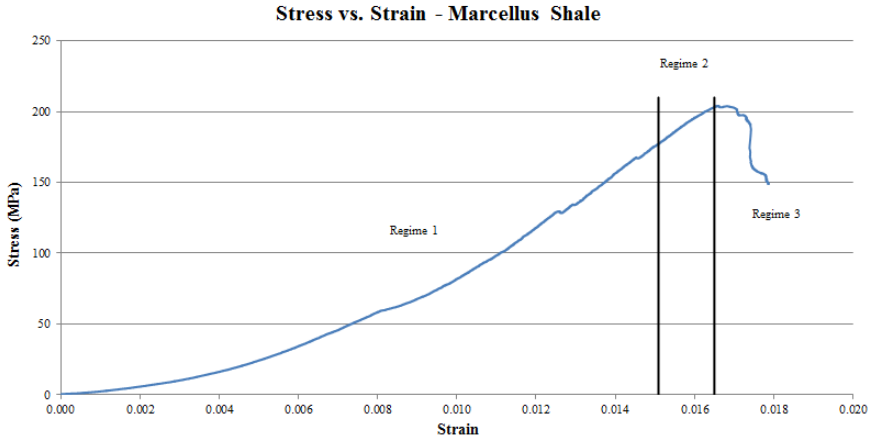

Figure 3.12: The stress vs strain curve for Marcellus Shale divided into regimes.

Along with the MTS rock press, the acoustic emissions equipment recorded the arrival time of waves, and recorded the time each event was detected. This data provided the means to compare the number of located events with the load applied to the sample. Figure 3.13 and 3.14 shows the event frequency plotted on the same time line as the load applied to both the Berea Sandstone sample and the Marcellus Shale sample, respectively.

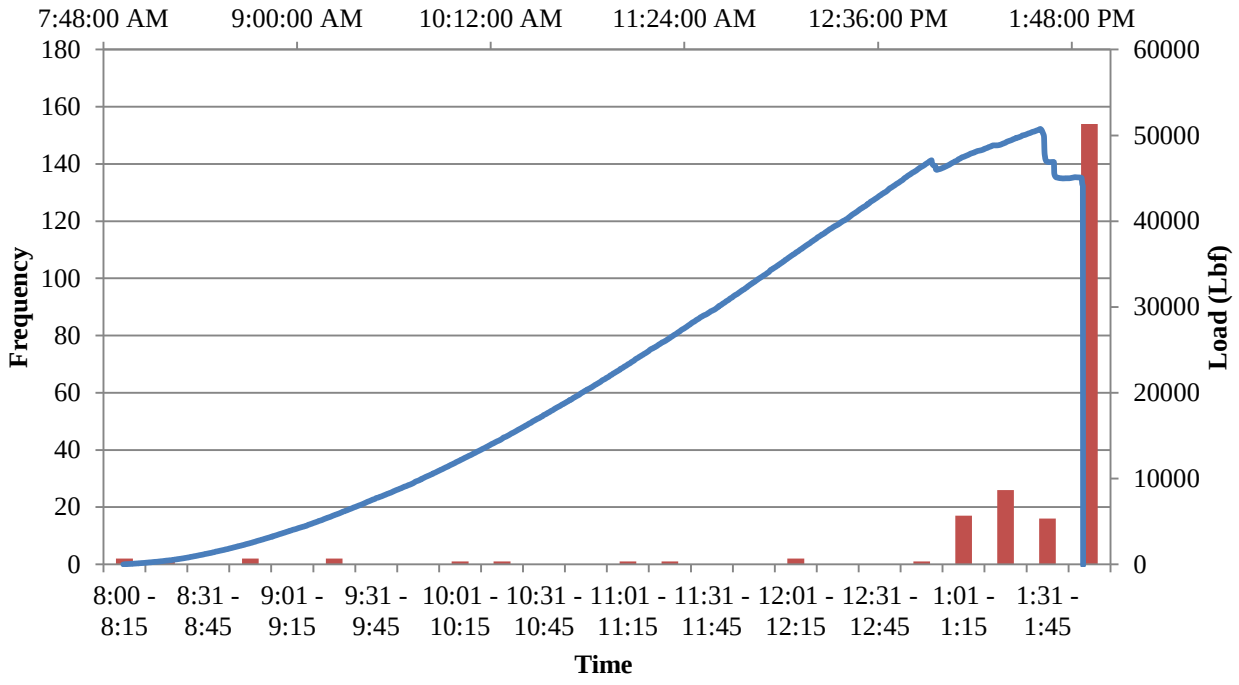

Figure 3.13: The load vs time plot and event frequency vs. time plot for the Berea Sandstone indenter test.

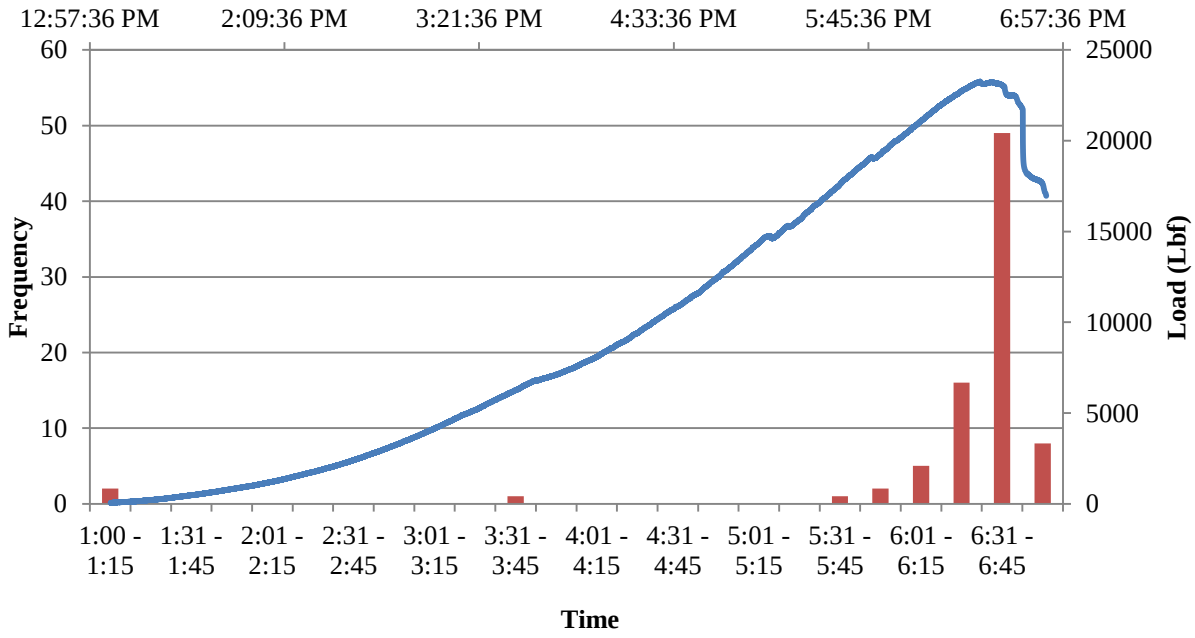

Figure 3.14: The load vs time plot and event frequency vs. time plot for the Marcellus Shale indenter test.

The Marcellus Shale plot shows a peak applied load of 23,253 lbf. The first regime is defined in this plot between the start of the test and 86 percent of the ultimate load. In this regime the load curve shows that the load being applied to the sample deviates from a constant linear elastic load. These slips

represent the indenter seating itself in the sample, closing micro-fractures in the sample. In regime two, between 86 percent and 99 percent of the ultimate load, the load begins to gradually reduce as the sample approaches failure. During this regime, the cracks being created by the indenter in the sample are expanding. In the final regime, the sample fails and the load on the sample reduces. The pressure being applied to the sample by the indenter exceeded the strength of the cracks and the sample ultimately failed and could not take any more load.

The number of acoustic events from the Marcellus Shale sample test varied between the three regimes. The first regime contained 9 recorded events, regime two had 32 recorded events, and regime three had 44. The number of events coincides with the expected behavior of the sample. The first regime had fewer events while the micro fractures were closing since no significant failures were occurring. In the time leading up to the failure of the sample, the amount of acoustic emissions increased as the cracks began to grow. As the sample failed, the highest number of events were recorded due to the movement, and redistribution of stress.

The Berea plot shows a peak applied load of 50,755 lbf. In this plot, the first regime is defined by the start of the test and the point at which the curve begins to decrease in slope at 90 percent of the ultimate load. In this regime the load curve shows a constant linear elastic load until there is a slip at which point the slope of the curve begins to decrease. In regime two, between 90 percent and 98 percent ultimate load, the load begins to gradually reduce as the sample approaches failure. During this time frame, the cracks being created by the indenter in the sample are expanding. In the final regime, the sample fails and the load on the sample reduces. The pressure being applied to the sample by the indenter exceeded the strength of the cracks and the sample ultimately failed and could not take any more load.

The number of acoustic events from the Berea Sandstone sample test varied between the three regimes. The first regime contained 14 recorded events, regime two had 45 recorded events, and regime three had 168. The number of events coincides with the expected behavior of the sample. However, unlike the Marcellus Shale sample, the Berea sample had 74 percent of the events during or post failure while the Marcellus sample had only 52 percent occur in the same regime.

Plots showing the travel time vs source-receiver separation distance for the Berea Sandstone and Marcellus Shale samples can be found in Figure 3.15 and 3.16 respectively. These plots show the travel time for each located event as well as the distance that the wave had to travel to reach the sensor. The inverse of the slope represents the velocity of the waves propagating through the sample. For the Berea Sandstone sample, the data recorded from the events was scattered with a number of extreme values which shifted the average velocity to an unreasonably high value. Rather than using the average of this data to determine the velocity of the sample, the median velocity was used which was 2.7 km/sec. This value was 0.4 km/sec higher than the background velocity originally used in the double difference

tomography created velocity model, however due to the number of events used to adjust the velocity model, the results reflect the velocities accurately. For the Marcellus shale sample, the data had a reasonable distribution around the average velocity line, located at 2.75 km/sec. The original background velocity for the Marcellus Shale sample was 2.8 km/sec. This sample did not have as many events to adjust the model as the Berea Sandstone sample, so the close average velocity to the original background velocity instills greater confidence in the velocity model, than there would be otherwise.

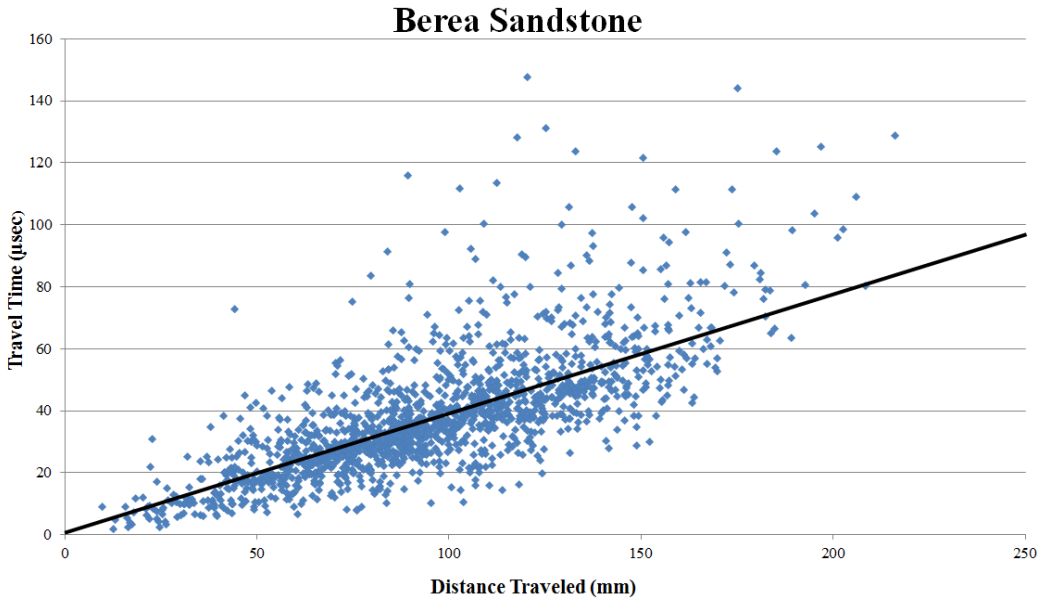

Figure 3.15: Travel time vs. distance traveled plot for the Berea Sandstone sample.

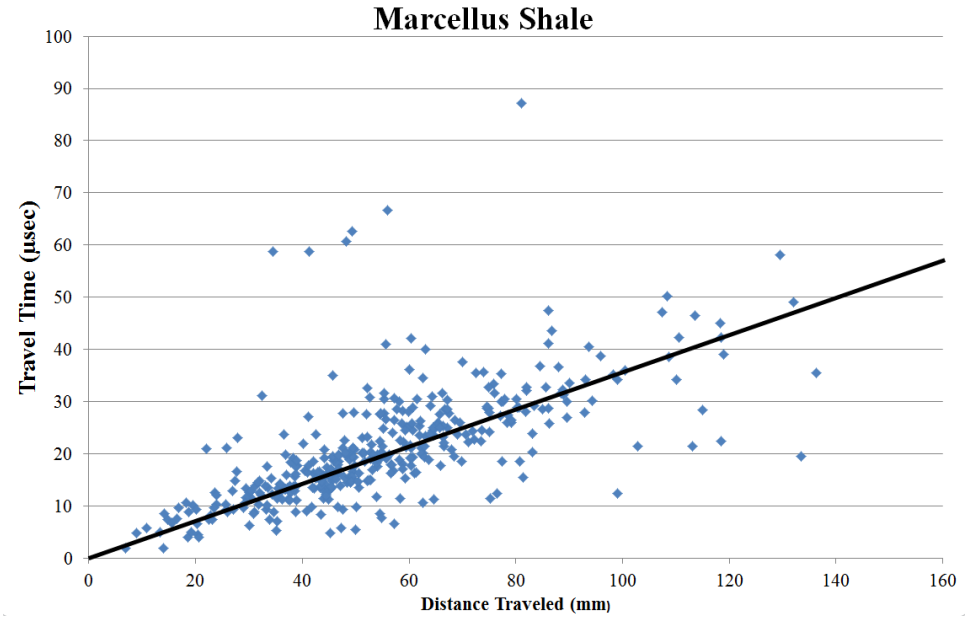

Figure 3.16: Travel time vs. distance traveled plot for the Marcellus Shale sample.

3.5.2 - Berea Sandstone Sample

Test Comparisons

A test performed in 2005, loaded a 152 mm diameter sample of Berea Sandstone in the same manner with a 51 mm indenter. The results from this test provided a stress strain curve of the Berea Sandstone sample that had similar results to the current test. Figure 3.17 shows the stress strain curves for the the two Berea Sandstone samples. The data for the Murphy indenter plot was retrieved from the 2005 thesis (Murphy 2005). The Murphy stress vs strain curve has one distinct peak where the sample fails at 117.3 Mpa and a strain of 0.0073. The 2011 Berea Sandstone indenter test has a slip which occurs at a strain value of 0.0075 and stress of 103.67 MPa. The strain of this first slip coincides with the failure of Murphy's indenter test, however, the 2011 test continued to hold until ultimate failure at a stress of 111.4 MPa and a strain of 0.0085. The slope of the 2011 indenter test stress vs. strain curve is more linear than the Murphy test until the point of failure. The similarity of these two tests validates the loading data from the MTS rock press since both shows a failure at the same point. Each stone sample has its own characteristics, accounting for the differences between the stress vs. strain curves.

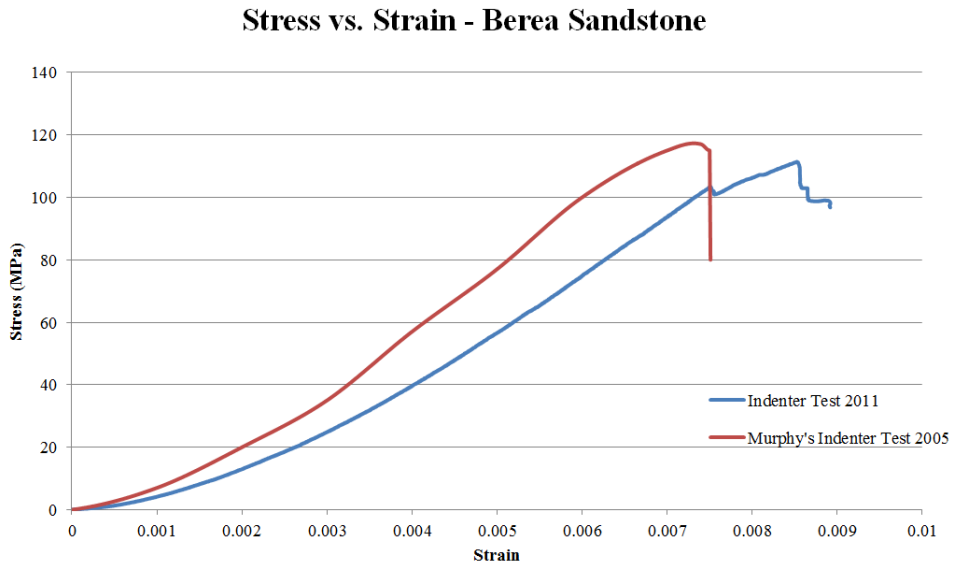

Figure 3.17: The stress vs. strain curve for Murphy's 2005 indenter test as well as the stress vs strain curve for the test completed in 2011.

Event Locations

Using the arrival time data recorded by the sensors during the tests, the events were located for the Berea Sandstone sample. The results for the initial locations of the Berea Sandstone sample can be found in Figure 3.18, side A. Using these source locations, the data was run through TomoDD, a double difference tomography program. Based on the locations of surrounding events, each event location was

adjusted. The original and relocated events can be found in Figure 3.18, side B. Images of the event locations in the XZ and YZ planes can be found in Appendix A.

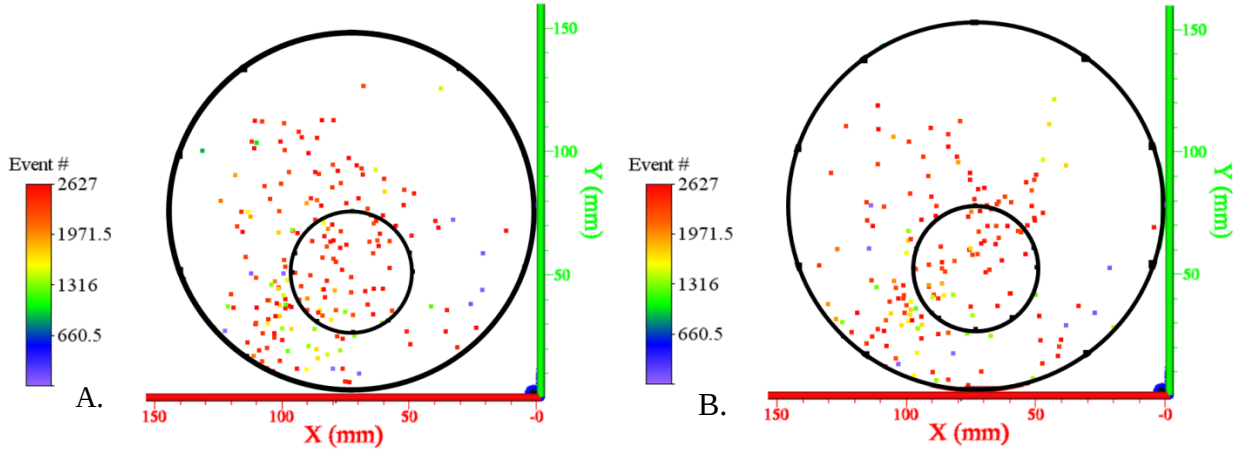

Figure 3.18: Event locations for the Berea Sandstone sample. Multicolored nodes are events. Side A contains the original locations from ESG software, Side B. contains relocated events after running through TomoDD.

In the original event location plot, there are more events located, with high density clusters beneath the indenter and another around 110 mm in the x direction and 20 mm in the y direction. Beneath the indenter the majority of the events in the original locations occur during stages III and IV of testing. There are few events located outside of the sample boundaries in the initial data.

The relocated events, side B of Figure 3.18, show fewer events, but they are located in tighter clusters. Beneath the indenter the events occurring at the end of the test are located in a close vicinity to each other, and there is a dense cluster of events on the edge of the indenter closes to the center of the sample. Also, in the area the wedge is created, events taking place in the beginning of the test are more prevalent than in the original data. In the relocated events plot, there are more events that are not within the sample boundaries. The events around 110 mm in the x direction and 20 mm in the y direction are more densely clustered after the relocation processing. When compared to the original data plot, there are more events clustered near the indenter's edge.

The events relocations correlate well with the failure locations on the Berea Sandstone sample. Figure 3.16 shows the fractured sample. The events located beneath the indenter are the result of the sandstone beneath the indenter compressing into a wedge. As the stress on the sample increases, the material beneath the indenter begins to compact, and the stress is focused into a point at the tip of the wedge. As the stress continues to increase, the wedge presses further into the sample. Eventually, the wedge causes the surrounding rock to fail in tension, allowing the affected rock to fall away. In the relocated events plot, the cluster of events beneath the indenter corresponds with the interface between the wedge and the intact sandstone sample. The events are located at a depth that correlates with the base of

the wedge, where the stress would be focused. The cluster of events located at 110 mm in the x direction and 30 mm in the y direction also line up with the failure of the Berea Sandstone test sample. Though there is not a dense cluster of events at 50 mm in the x direction and 30 mm in the y direction, there are a significant number that are in the vicinity of the failure on the right side of the sample. The accuracy of the event locations compared with the actual failure location on the test sample shows that the event location technique can effectively locate the source of the events, using passive sensors.

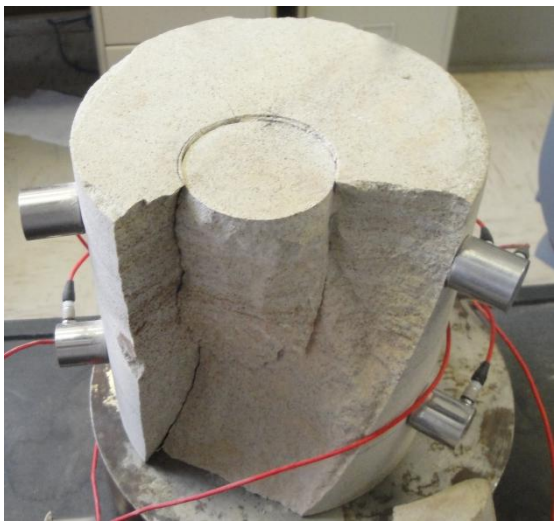

Figure 3.19:Failed sample of Berea Sandstone after indenter test was concluded.

Berea Sandstone Velocity Model

Calculating tomograms for each regime of the Berea Sandstone test with TomoDD separately provided a velocity model for each stage of the test. Using a uniform background velocity of 2.3 km/sec, which was determined using a P and S wave testing machine, the velocity models were calculated using the events in each regime. In areas through which no ray paths traveled, the velocity model remained 2.3 km/sec. Due to the lack of ray path coverage in certain locations, the areas had a DWS value of zero at the conclusion of processing. To remove these low confidence values from the results, all nodes of the velocity model that had a DWS value of zero were removed when viewing the results. Each velocity model was created with dimensions of 160 mm in the x and y plane and 150 mm in the z plane. These dimensions were used to include the entire sample which had a height of 152 mm and a diameter 152 mm.

Certain areas of interest within the sample were monitored to take note of the velocity change during loading. The locations of interest for the Berea Sandstone sample were beneath the indenter at the point of the wedge, beneath the wedge, 30 mm from the surface of the sample in the left and right most fracture, and a final point in the left most fracture plane at a depth of 50 mm. These points were chosen to determine if the sample had reacted to the indenter loading in the sample manner as depicted in Cook's results in Figure 3.2.

Cook's results shows that at the tip of the wedge there should be an area of compressive failure. In a region of compressive failure, such as the wedge in the indenter test, the rock is under stress and the material will be more compact than the surrounding rock. This compact material has less pore space and a higher modulus, allowing seismic waves to propagate through the rock more quickly than unstressed rock. The calculated velocities of waves that pass through these areas are expected to be higher than the surrounding, less compact rock. To display the velocity models for the Berea Sandstone sample created in TomoDD, an orthogonal image of each regime was plotted in the 3-D modeling software Voxler 3. To create the orthogonal image, the inverse distance method was used with a search radius of 30 mm. The orthogonal images are slices taken across the sample showing the velocity distribution.

Figures 3.20, 3.21 and 3.22 show the orthogonal images of the velocities for the Berea Sandstone sample at a depth of 45 mm for each of the three regimes. This depth corresponds to the depth on the sample at which the tip of the wedge was located at the time of failure. The velocity location that was considered on this orthogonal image was located at 85 mm in the x direction and 60 mm in the y direction. This point was chosen because it is within the wedge and was expected to have distinct velocity change across all three regimes. In regime one the velocity was 2.75 km/sec, regime two had a velocity of 3.2 km/sec and the velocity in regime three was 2.5 km/sec. With a background velocity of 2.3 km/sec, in each of the three regimes there was an increase in velocity. In regime one, the velocity increase to 2.75 km/sec due to the increasing compaction taking place beneath the indenter. The velocity peaked just prior to failure in regime two when the sample was beginning to deform due to the stresses being applied. Once the sample failed the velocity dropped to 2.5 km/sec which is still higher than the original velocity of the sample due to compaction.

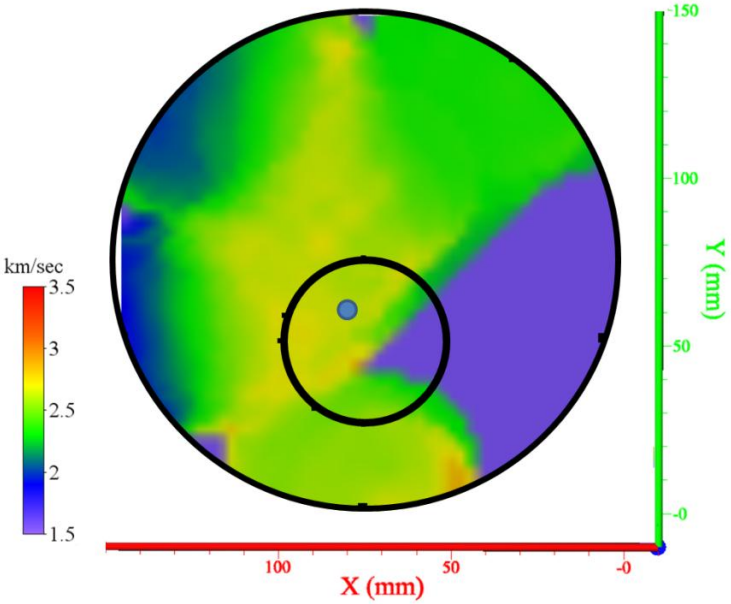

Figure 3.20: Orthogonal image for the first regime of the Berea Sandstone sample. Point of interest located at 85 mm in the x direction and 60 mm in the y direction, at a depth of 45 mm represented by blue point.

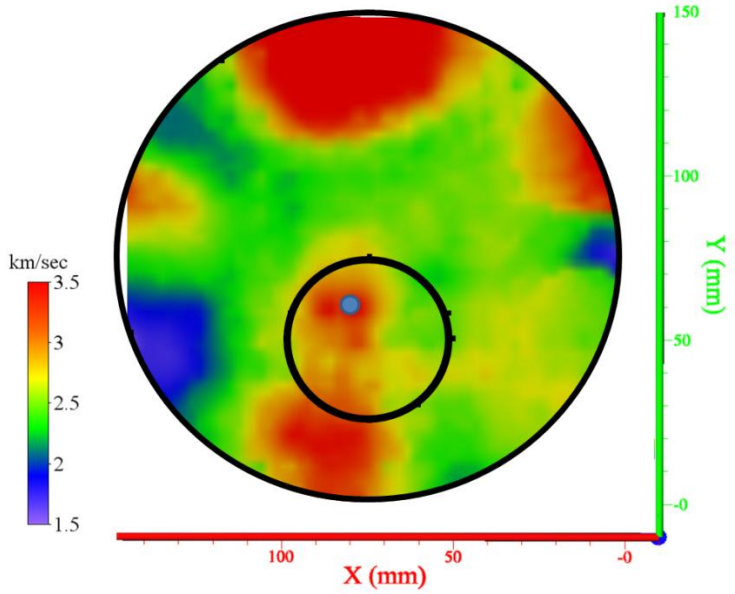

Figure 3.21: Orthogonal image for the second regime of the Berea Sandstone sample. Point of interest located at 85 mm in the x direction and 60 mm in the y direction, at a depth of 45 mm represented by blue point.

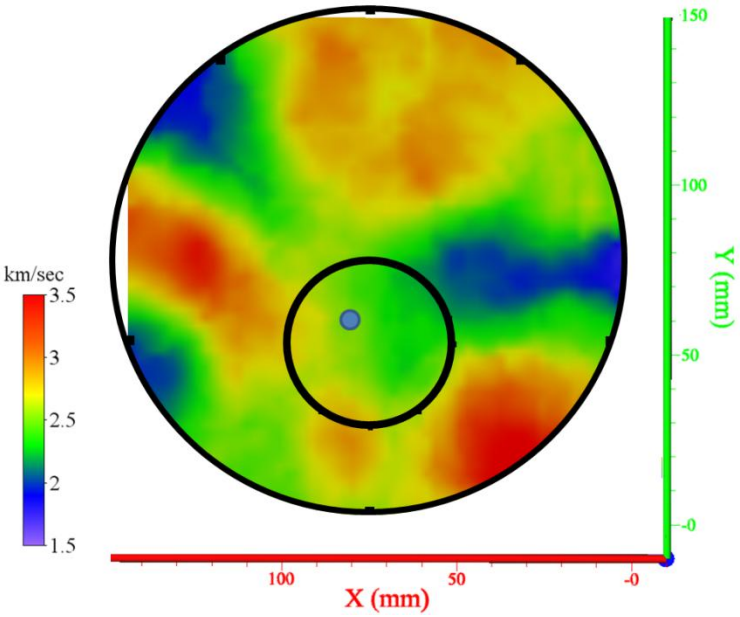

Figure 3.22: Orthogonal image for the third regime of the Berea Sandstone sample. Point of interest located at 85 mm in the x direction and 60 mm in the y direction, at a depth of 45 mm represented by blue point.

From the first regime to the third regime, the passive sensors were able to record events emitted by the rock during testing. These results were successfully used to create a velocity model for the sample that in multiple instances was able to accurately depict the area under stress in the sample. In a compressive zone beneath the indenter, this method was able to accurately image how the sample theorized to behave in previous tests, as well as locate areas of high velocity corresponding to failure locations on the actual sample.

Cook's results also show a tensile zone that forms beneath the wedge as the test progresses. In a region of tensile failure, such as the area beneath the wedge in the indenter test, the stresses on the rock are causing the rock to dilate rather than compress. Seismic waves propagate through the dialted rock at a slower rate than they would through more compressed rock. The calculated velocities of waves that pass through these areas are expected to be lower than the surrounding, intact rock. The orthogonal images in the zone expected to show tensile failure were plotted.

Figures 3.23, 3.24 and 3.25 show the orthogonal images of the velocities for the Berea Sandstone sample at a depth of 85 mm for each of the three regimes. This depth correlates to the depth on the sample below the tip on the wedge at which a tensile failure zone was expected to be present based on Cook's results. The point that was monitored on this orthogonal image was located at 90 mm in the x direction and 30 mm in the y direction. This location was chosen because it is below the wedge and it is in the expected tensile area. In regime one the velocity was 2.6 km/sec, regime two had a velocity of 2.2 km/sec and the velocity in regime three returned to 2.3 km/sec. With a background velocity of 2.3 km/sec, regime one and two showed a change in velocity and regime three returned to the original velocity. In regime one, the velocity increased to 2.6 km/sec due to the increasing compaction taking place beneath the indenter. As the wedge began to form, the stress distribution became more focused by the tip of the wedge, and this region began experience tensile stresses. The velocity was at its lowest just prior to failure in regime two when the sample was near failure due to the stresses being applied. Once the sample failed the velocity returned to 2.3 km/sec.

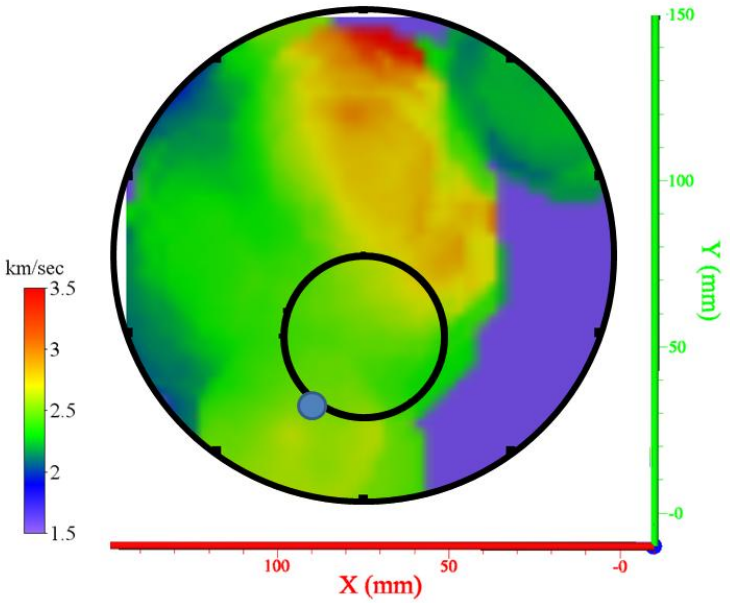

Figure 3.23: Orthogonal image for the first regime of the Berea Sandstone sample. Point of interest located at 90 mm in the x direction and 30 mm in the y direction, at a depth of 85 mm represented by blue point.

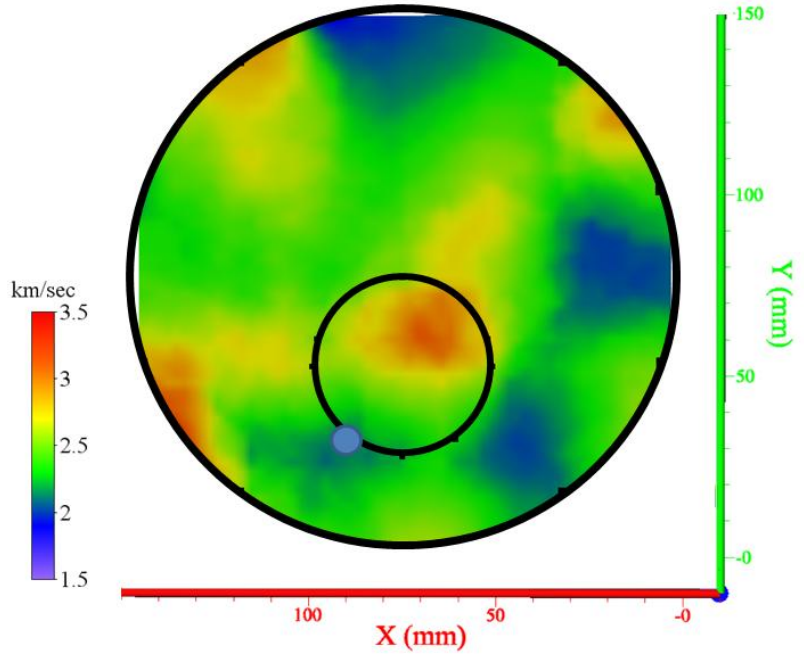

Figure 3.24: Orthogonal image for the second regime of the Berea Sandstone sample. Point of interest located at 90 mm in the x direction and 30 mm in the y direction, at a depth of 85 mm represented by blue point.

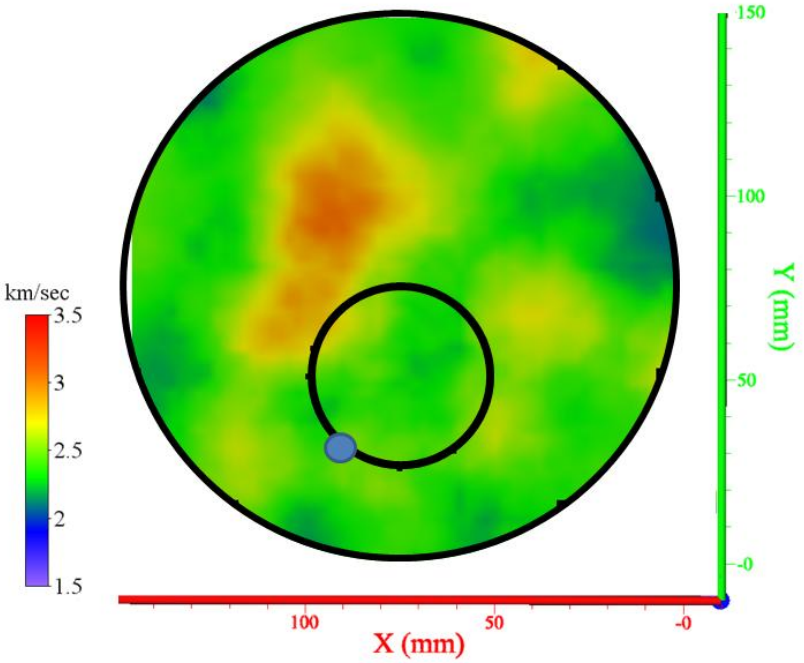

Figure 3.25: Orthogonal image for the third regime of the Berea Sandstone sample. Point of interest located at 90 mm in the x direction and 30 mm in the y direction, at a depth of 85 mm represented by blue point.

A vertical orthogonal image was also taken of the Berea Sandstone sample, intersecting through the high velocity zone beneath the indenter. Figure 3.26 shows the vertical slice with the blue circles located beneath the indenter at high velocity area and beneath the wedge in the low velocity zone.

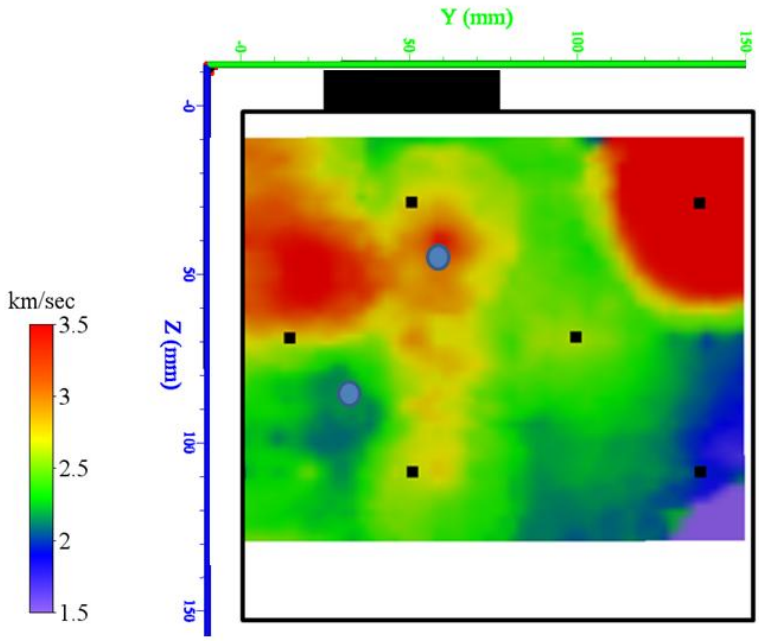

Figure 3.26: Orthogonal image of Berea Sandstone sample in regime two with blue circles representing points of interest.

In all three regimes, the passive sensors were able to record events emitted by the rock during testing. These results were successfully used to create a velocity model for the sample that in multiple instances was able to accurately depict the area under stress in the sample. In a tensile zone beneath the wedge, this method was able to accurately image how the sample has been theroized to behave in previous work.

The five monitored positions within the sample were plotted to compare the change in velocity as the stress on the sample increased until failure. Figure 3.27 shows the strain vs stress curve for the Berea Sandstone sample as well as the velocity progression for all five points of interest. The orthogonal images for the three interest points not discussed in this section can be found in Appendix A.

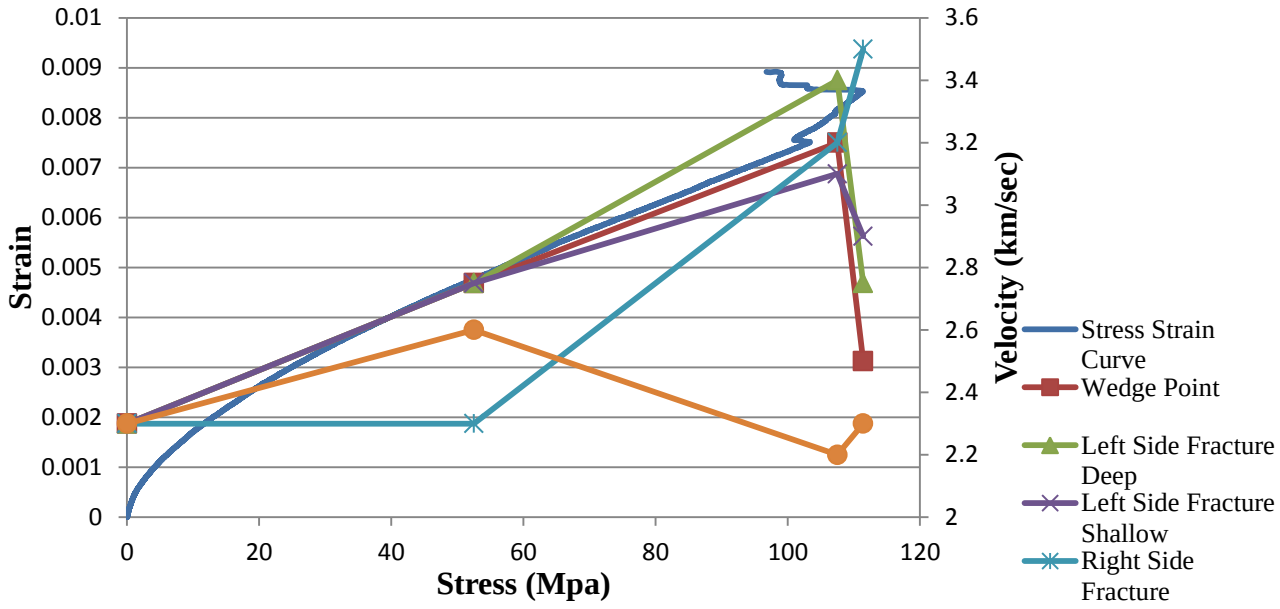

Figure 3.27: Strain vs stress curve for the Berea Sandstone plotted with the velocities of different points of interest within the sample plotted against the stress applied to the sample.

As the stress increases on the sample, the velocity of the wave propagation through the fracture on the left side of the sample and at the wedge point increased. When the sample failed the velocities in these regions fell back toward the original velocity of 2.3 km/sec. The fracture on the right side of the sample behaved differently; the velocity remained high, even as the sample failed. The tensile zone beneath the wedge initially had an increased velocity, but as the stress continued to increase, the velocity dropped back down below the original velocity before returning to the starting velocity once the stress was released.

In the area of compaction, such as the wedge and the left fracture, the velocities increased as expected. In the tensile area under the wedge, the velocity fell as expected. These positive results show that the data collected by passive sensors is sufficient to accurately determine wave propagation through a sample of Berea Sandstone to image velocity change due to stress redistribution. The locations of the five points of interest corresponding with the velocity vs. stress plot can be found in Figure 3.28, as they would appear on Cook's model.

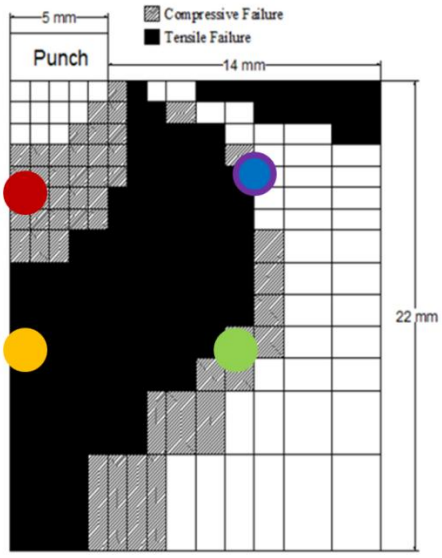

Figure 3.28: Points of interest used to create velocity vs. stress plot.

In Figure 3.28 the red dot corresponds with the high velocity zone located beneath the indenter. The orange circle corresponds with the low velocity zone beneath the wedge. The green circle corresponds with the deep fracture on the right side of the sample. The blue and purple circle corresponds with the fracture on the right and left side of the sample at a shallow depth.

3.5.3 - Marcellus Shale Sample

Event Locations

Using the arrival time data recorded by the sensors during the tests, the events were located for The Marcellus Shale sample. The results for the initial locations of the Marcellus Shale sample can be found in Figure 3.29, side A. Using these source locations, the data was run through TomoDD. The relocated events can be found in Figure 3.29, side B. Images of the event locations in the XZ and YZ planes can be found in Appendix A.

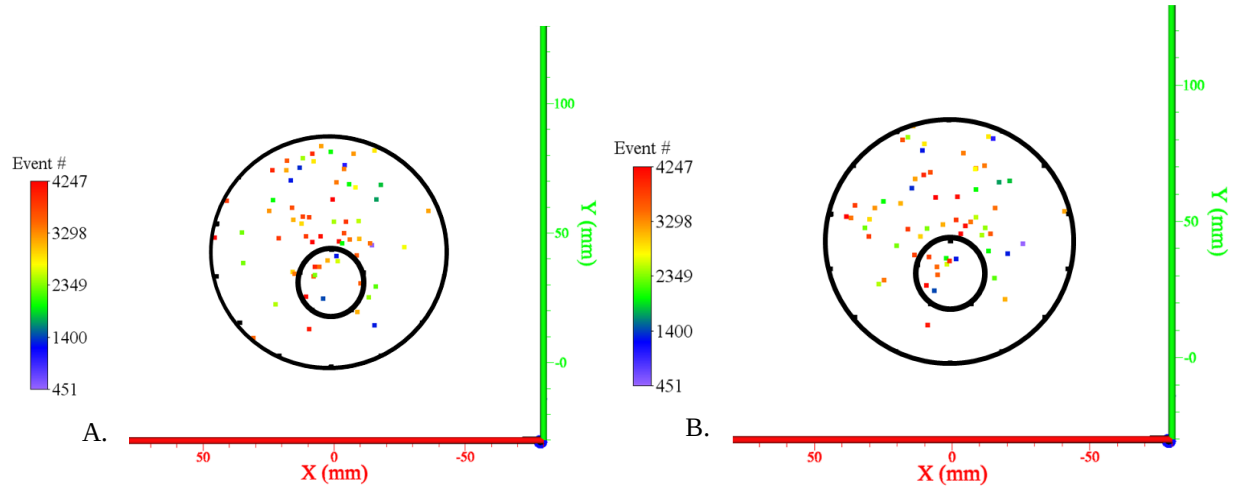

Figure 3.29: Event locations for the Marcellus Shale sample. Multicolored nodes are events, outer ring of black nodes are sensors and inner ring of black nodes is the indenter. Side A contains the original locations from ESG software, Side B. contains relocated events after running through TomoDD.

In Figure 3.29 side A shows the original events located by the ESG software, side B shows the relocated events once the acoustic data was processed using TomoDDThe colored nodes are the event locations, with purple representing the lowest event number and red the highest. In the original event plot, the events are located towards the center of the sample, with the majority of the events falling between -20 mm and 20 mm on the X axis. A number of events were located outside of the sample boundaries due to anomalies of the locating software. In the Z direction, the events are spread out along the full depth of the sample as well as a few located beyond the sample boundaries.

The relocated events, side B of Figure 3.29, are fewer and more spaced out. Rather than a dense population of events located in the center of the sample, the events are spread out through the sample, between -30 mm and 40 mm on the X axis. The located events take place through all stages of the test providing data to adjust the velocity models.

The event relocations correspond with the failure locations on the Marcellus Shale sample used in testing. Figure 3.30 shows the fractured sample, after the sample failed due to the deformation from the indenter. The events located in the top portion of the sample, above 40 mm in the y direction, are located in the area where the shale broke off along existing foliation. The events located beneath the indenter in are the result of the shale compressing beneath the indenter. As the stress on the sample increases, the material beneath the indenter becomes more compact, the stress is disperse throughout the sample. As the stress continues to increase, the sample began to exfoliate due to the tensile stress. In the relocated events plot, the events located on the top half of the sample are in the area that the sample failed. In Figure 3.30 the top half of the sample has a failure zone where the rock broke apart along existing

foliation. Also, in the relocated events, there are more events located to the right of the indenter, which I s continuation of the failure zone above the indenter.

Figure 3.30: Failed sample of Marcellus Shale after indenter test was concluded.

Marcellus Sandstone Velocity Model

As in the Berea Sandstone test, the Marcellus Shale data was run through TomoDD in three different regimes. Using a background velocity of 2.8 km/sec, which was determined using a P and S wave testing machine, the velocity models were adjusted by the events in each regime. Due to the lack of events in certain locations, a DWS value of zero was assigned to the data in these areas. To remove the low confidence values from the results, all nodes of the velocity model that had a DWS value of zero were removed from the orthogonal image plots. Each velocity model was created with dimensions of 160 mm in the x and y plane and 120 mm in the z plane. These dimensions were used to encapsulate the entire sample which had a height of 734 mm and a diameter 89 mm.

Between all three regimes, certain areas of interest within the sample were monitored to take note of the velocity change during loading. The locations of interest for the Marcellus Shale sample were beneath the indenter, where a wedge was assumed to be forming, beneath where the wedge would be located, and in zone of initial failure. These points were chosen to determine if the sample had reacted to the indenter loading in the same manner as depicted in Cook's model in Figure 3.2.

As in the Berea Sandstone sample, the Marcellus Shale sample was expected to behave in the same manner, a compact wedge, causing tensile and compressive failure regions. To display the velocity models for the Marcellus Shale sample created in TomoDD, a tomogram of each regime was plotted in 3-D modeling software. The tomogram was created, with the same settings as with the Berea Sandstone sample.

Figures 3.31, 3.32 and 3.33 show the orthogonal images of the velocities for the Marcellus Shale sample at a depth of 30 mm for each of the three regimes. This depth correlates to the depth on the sample at where the wedge would most like be created during loading. Two points of interest were monitored at this depth, a low velocity zone in the northern section of the sample, 30 mm in the x direction and 80 mm in the y direction, as well as the area beneath the wedge, located at 0 mm in the x direction and 30 mm in the y direction. These points were chosen because across all three regimes, a change in velocity can be noted, and the failure in the upper region of the sample was different than in the Berea Sample. The locations of interest are noted with blue circles in the following figures.

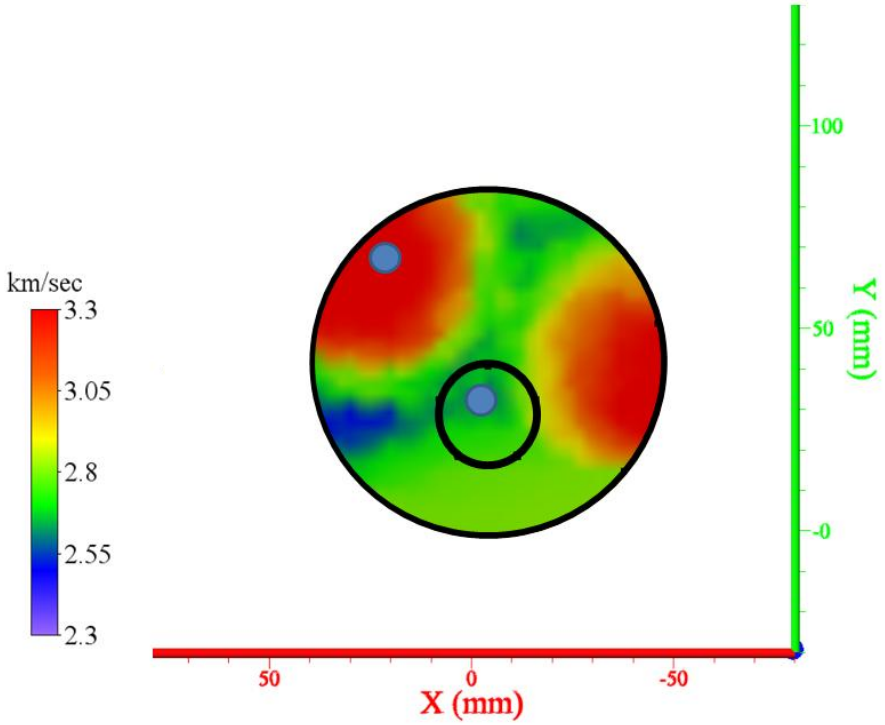

Figure 3.31: Orthogonal image for the first regime of the Marcellus Shale sample. Points of interest: 30 mm in the x direction and 80 mm in the y direction, and 0 mm in the x direction and 30 mm in the y direction, both at a depth of 30 mm represented by blue points.

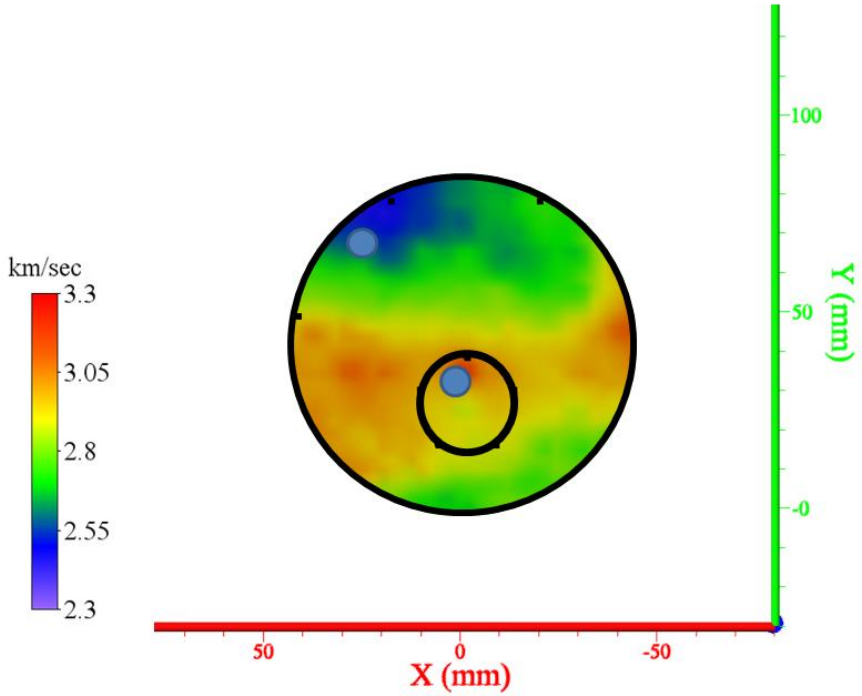

Figure 3.32: Orthogonal image for the second regime of the Marcellus Shale sample. Points of interest: 30 mm in the x direction and 80 mm in the y direction, and 0 mm in the x direction and 30 mm in the y direction, both at a depth of 30 mm represented by blue points.

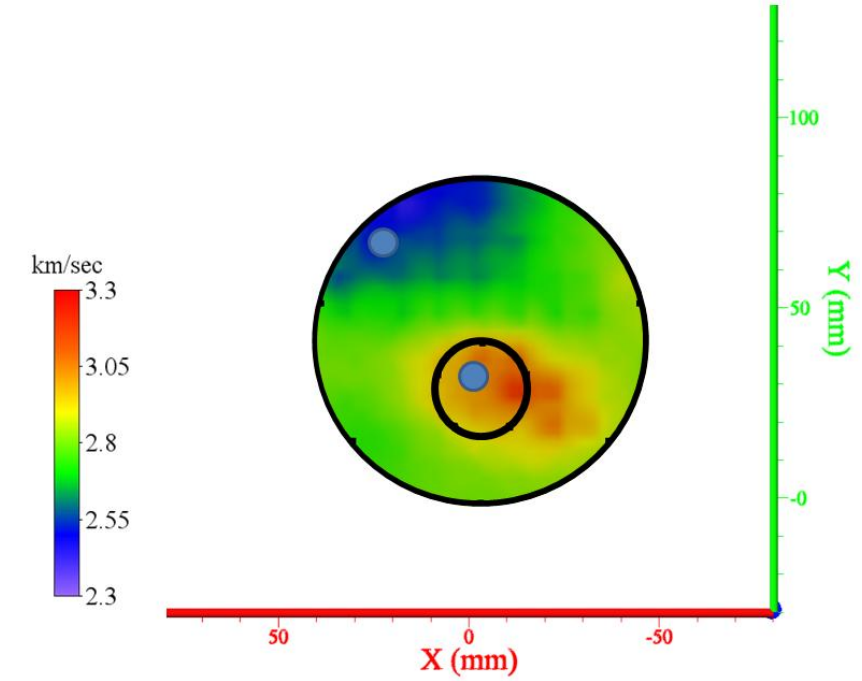

Figure 3.33: Orthogonal image for the third regime of the Marcellus Shale sample. Points of interest: 30 mm in the x direction and 80 mm in the y direction, and 0 mm in the x direction and 30 mm in the y direction, both at a depth of 30 mm represented by blue points.

A vertical orthogonal image was also taken of the Marcellus Shale sample, intersecting through the high velocity zone beneath the indenter. Figure 3.34 shows the vertical slice with the blue circles located beneath the indenter at high velocity area, beneath the wedge in the low velocity zone, as well as in the low velocity zone away from the indenter.

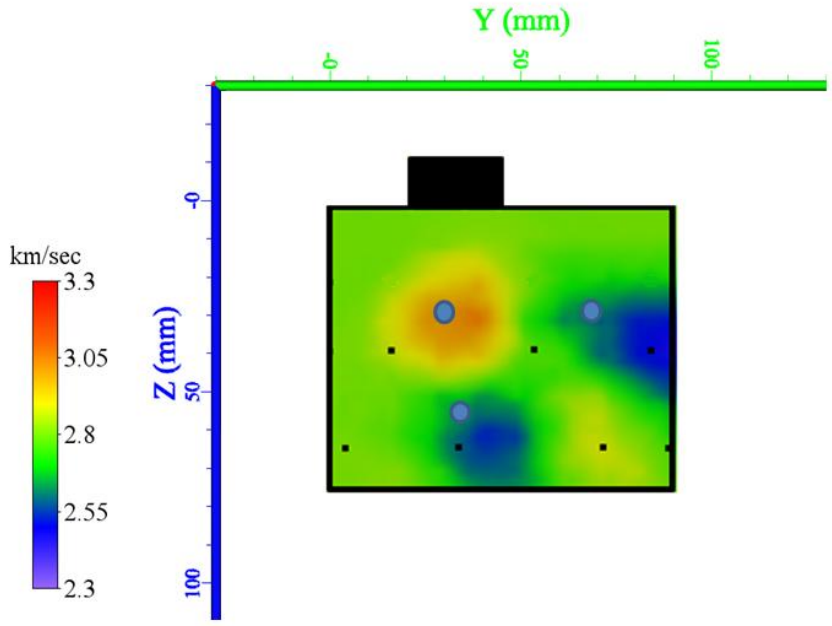

Figure 3.34: Orthogonal image of Marcellus Shale sample in regime three with blue circles representing points of interest.

For the area beneath the indenter where the wedge was expected to form, regime one had a velocity of 2.8 km/sec, regime two had a velocity of 3.1 km/sec and the velocity in regime three returned to 3.15 km/sec. With an initial velocity of 2.8 km/sec, the velocities in this region increased until the sample failed. In regime one, the velocity remained the same as the stress increased on the sample. The velocity increased in regime two as the sample approach failure. At the end of the test, the velocity was at its highest value of 3.15 km/sec. This high velocity as the end of the test is believe to be caused because when the sample ultimately failed it was not beneath the indenter as was the case with the Berea Sandstone. The Marcellus Shale failed in an area away from the wedge compaction zone as defined in Cook's model. Since no defined wedge was noticed on the Marcellus Sample, the wedge likely did not develop enough to cause failure, rather the stresses working on the sample exceeded the strength of the foliation which caused failure.

The failure area above the indenter on the sampe was another point of interest on the Marcellus Shale sample, due to the uniqueness of the failure. Rather than shearing off as the Berea Sandstone had, in this particular area the Marcellus Shale popped and then remained seated on the sample, held on only by the friction between surfaces. In regime one the velocity in this area increased to 3.3 km/sec, then fell

to 2.5 km/sec where it remained through failure. This low velocity region shows that as the stress increased on the sample, the seismic waves traveling through the failure area were moving at a slower rate. The tensile failure in this area shows that the rock was being forced apart by the stresses being applied. Rather than failing due to the wedge being forced through the material, as was the case with the Berea Sandstone sample, the Marcellus Shale failed due to the tensile strength being exceeded.

The three monitored positions within the sample were plotted to compare the change in velocity as the stress on the sample increased until failure. Figure 3.35 shows the strain vs. stress curve for the Marcellus Shale sample as well as the velocity progression for the three locations of interest. The tomograms for the location below the assumed wedge not discussed in this section can be found in Appendix A. As the stress increases on the sample, the velocity of the wave propagation beneath the expected wedge showed lower velocities than 20 mm above, beneath the indenter. When the sample failed the velocities in the regions outside of the expected wedge fell below the original velocity of 2.8 km/sec. However, the area beneath the indenter remained above the original velocity once the maximum stress had been applied. The tensile zone beneath the wedge initially decreases velocity, unlike the Berea Sandstone sample which initially increased, and then rebounded before ultimately falling once the ultimate stress was reached.

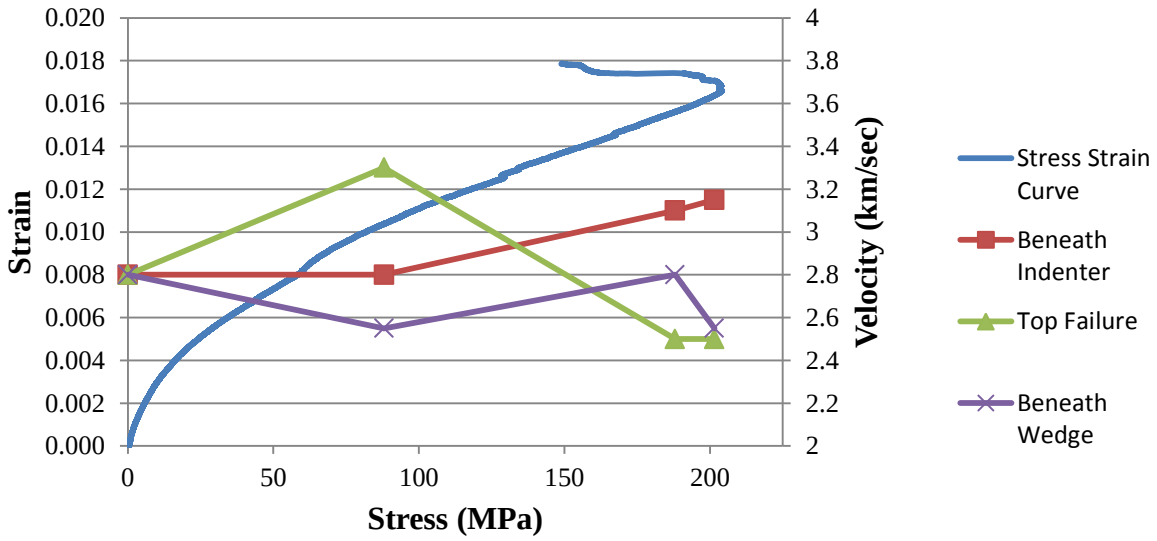

Figure 3.35: Strain vs. stress curve for the Marcellus Shale plotted with the velocities of different points of interest within the sample plotted against the stress applied to the sample.

In the area of compaction, the velocity increased as expected, but did not drop as the sample failed. This reaction demonstrates how the more brittle Marcellus Shale reacted differently than the less brittle Berea Sandstone. In the tensile area under the wedge, the velocity fell as expected. These results show that even though the sample failed in a different manner than anticipated, the passive acoustic emission array was able to record accurate data. The locations of the five points of interest

corresponding with the velocity vs. stress plot can be found in Figure 3.36, as they would appear on Cook's model.

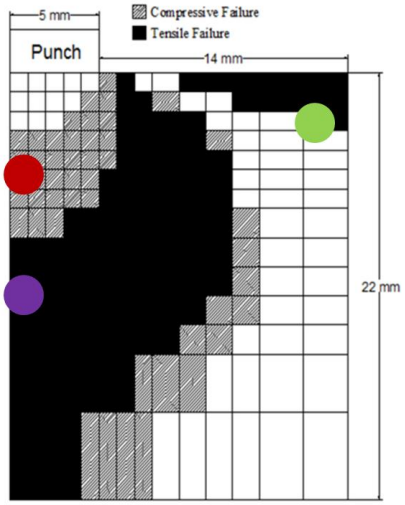

Figure 3.36: Points of interest used to create velocity vs. stress plot.

In Figure 3.34 the red dot corresponds with the high velocity zone located beneath the indenter. The purple circle corresponds with the low velocity zone beneath the wedge. The green circle corresponds with the low velocity zone on the away from the indenter.

3.6 - Conclusions

Two samples, one Berea Sandstone and Marcellus Shale, were loaded until failure using an indenter to focus the loading. While loading was taking place, the samples were monitored for acoustic emissions using a 16-channel acoustic monitoring system. The collected data then processed resulting in a velocity model for each sample, as well as more precisely located events using double difference tomography. The results from running double difference tomography were investigated and compared to the failure of the samples. Upon inspection of the tomograms created from the velocity models, conclusions were drawn about the tests.

From the collected data from the Berea Sandstone and Marcellus Shale indentation tests the following conclusions were made:

- The passive acoustic emissions system was able to record data throughout the test which provided accurate results for processing.
- Due to different rock characteristics the samples failed differently. The Berea Sandstone failed due to the compaction of material into a wedge, forcing the rock apart. The Marcellus Shale failed due to tensile stresses exceeding the strength of the lamination.
- In regions of expected failure by compaction, as forecasted by Cook's model, there was evidence of velocity increase as stress increased, until failure at which point the velocity decreased.

- In regions of expected failure in tension, as forecasted by Cook's theory, there was evidence that as the stress on the sample increased, the velocity initially decreased. Then as failure approached, the velocity began to fall.

The positive result of the passive monitoring system in the laboratory setting provides confidence in this method for monitoring sequestration projects in the future. The relocated events had a more pronounced cluster in areas of actual failure when compared to the original event locations. Using surrounding events to adjust the original location for each event created a more accurate representation of where subsequent failure took place. The regions of compressive failure and tensile failure had distinct differences when located in the tomograms. The successful separation of the velocity zones, during multiple regimes of loading, promotes confidence in the success of forecasting failures in Berea Sandstone and Marcellus Shale.

Chapter 3 References

Barzili, A. (2000). Improving a Geophone to Produce an Affordable, Broadband Seismometer. Mechanical Engineering, Standford. **PhD**.

Cook, N. G. W., M. Hood, et al. (1984). "Observations of crack growth in hard rock loaded by an indenter." International Journal of Rock Mechanics and Mining Sciences & Geomechanics Abstracts **21**(2): 97-107.

Elliot, A. (2008). "Mining Ground Support." Retrieved March 5, 2012, from http://www.mining-technology.com/features/feature2017/.

Gutenberg, B. and C. F. Richter (1955). "Magnitude and Energy of Earthquakes." Nature **176**(4486): 795-795.

Hamada, G., M. (2004). "Reservoir Fluids Identification Using Vp/Vs Ratio." Oil & Gas Science and Technology - Rev. IFP **59**(6): 649-654.

Hardy, R. H., G. L. Mowrey, et al. (1981). A microseismic study of an underground natural gas storage reservoir, American Gas Association.

Hirose, F., J. Nakajima, et al. (2008). "Three-dimensional seismic velocity structure and configuration of the Philippine Sea slab in southwestern Japan estimated by double-difference tomography." J. Geophys. Res. **113**.

Ishida, T. (2001). "Acoustic Emission Monitoring of Hydraulic Fracturing in Laboratory and Field." Construction and Building Matrerials **15.5-6**: 283-295.

Kocer, C. and R. E. Collins (1998). "Angle of Hertzian Cone Cracks." Journal of the American Ceramic Society **81**(7): 1736-1742.

Medical, S. "Computed Tomography Its History and Technology." Retrieved March 5, 2012, from http://www.medical.siemens.com/siemens/zh_CN/gg_ct_FBAs/files/brochures/CT_History_and_Technology.pdf.

Moradian, Z. A., G. Ballivy, et al. (2010). "Evaluating damage during shear tests of rock joints using acoustic emissions." International Journal of Rock Mechanics and Mining Sciences **47**(4): 590-598.

Murphy, M. M. (2005). Defining stress changes ahead of a tunnel face and design of a data acquisition system. VPI & SU Mining and Minerals Engineering M S 2005. Blacksburg, Va., University Libraries, Virginia Polytechnic Institute and State University,.

NIOSH (1997). Use of Seismic Tomography To Identify Geologic Hazards in Underground Mines. NIOSH.

Solutions, E. (2012). "Paladin 24-bit Digital Microsesmic Recorder." Retrieved March 5, 2012, from https://www.esgsolutions.com/english/view.asp?x=782.

Turner, M. (2005). "Management of Seismicity using Portable Seismic Systems." Australian Centre for Geomechanics – Course on Advance Geomechanics in Underground Mines.

Westman, E. C. (2003). Use of tomography for inference of stress redistribution in rock. Industry Applications Conference, 2003. 38th IAS Annual Meeting. Conference Record. 1649

Zhang, H. and C. H. Thurber (2003). "Double-Difference Tomography: The Method and Its Application to the Hayward Fault, California." Bulletin of the Seismological Society of America **93**(5): 1875-1889.

Zhang, H. W., G. Subhash, et al. (2003). "Mechanical behavior of bulk (ZrHf)TiCuNiAl amorphous alloys." Scripta Materialia **49**(5): 447-452.

Chapter 4 – Secondary Testing

Section 4.1 –Caprock and Shear Failure Test Introduction

Failure in shear is a mode of failure that can occur during carbon sequestration. As the pore pressure increases, the normal stress holding joints in place is weakened and the joints slip. When these slippages occur in the impermeable layer, there is a pathway for the compressed fluid to seep into. As the pressure in these cracks increased, the host rock begins to fracture, expanding the size of the cracks. Once a crack such as this propagates to the outer edge of the impermeable layer above a reservoir, the pressure within the reservoir will force the fluid out through the crack. This leakage will continue as the system attempts to reach equilibrium with the surrounding environment.

Since failure events in the impermeable layer will occur in formations within the earth, a method of monitoring that can survey beneath the surface of the earth is necessary. Monitoring for these types of events can be accomplished using acoustic emission equipment and double difference tomography. Acoustic emissions equipment has the ability to record seismic activity created by rock movement based on the arrival time of the propagated waves to different sensors stations. The seismic activity is then used to create a velocity model to map the region that provides an image of what is taking place below the surface.

Two tests were designed to test different types of failure in rock induced by two different means: slipping and upheaval. One test was designed to create failure by shear only. The second test was created to monitor the failure as fluid was injected into a reservoir, pressurizing the surrounding rock until failure was induced. These two methods required samples to be created unique to each failure mode.

For the shear failure test, a sample was created to imitate failure at a transform fault boundary with two plates moving in opposite directions. Applying a load, in opposite directions, to two slabs of rock attached by a weak bridge of intact rock, will cause the rock to fail in tension due to a lower tensile strength in Berea Sandstone compared to its compressive strength. The data collected from this test will determine whether or not the acoustic emissions equipment is able to locate events that are created only by shear failure.

For the caprock upheaval test, multiple samples were created, each adjusted from previous test results. With the goal of inducing caprock failure by increasing the pore pressure from injection fluid, a sample was created that had a Berea Sandstone reservoir encased in concrete, with a caprock layer directly over top of the reservoir. As the fluid injection progressed, the pressure on the caprock increased, theoretically causing the rock to upheave. The resulting failure of the caprock is in tension.

Section 4.2 – Shear Failure Sample

4.2.1 – Sample Preparation, Testing and Analysis

The shear sample was created out of a solid block of the Berea Sandstone which had dimensions of 342 mm x 165 mm x 152 mm. Due to size constraints, the length of the sample was trimmed to eleven inches so that the sample could stand vertically in the rock press with two steel platens on each end. A rock saw with an eight inch radius saw blade was used to make the cut. The design for the sample called for the block to be sliced down the middle length wise, leaving a two inch section of intact rock in the center, holding the two halves together. Since the rock saw blade would be unable to leave a straight face along the center bridge, a concrete saw with a 356 mm radius blade was used. Since the saw was hand held, care was taken to make sure the cut was not too deep and the face remained straight on both ends two inch bridge. To further weaken the bridge, three 6.35 mm drill holes were drilled on a line between the two slices. A completed sample is shown in Figure 4.1.

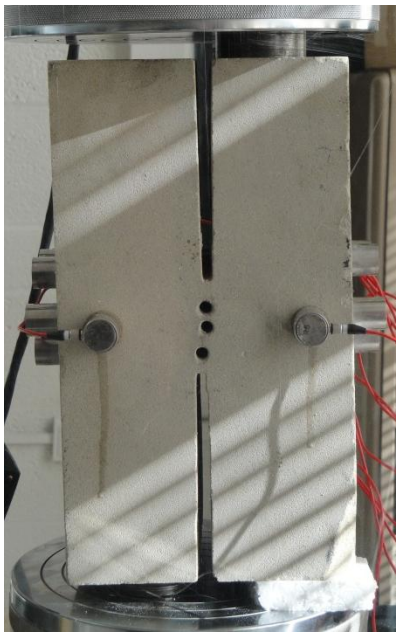

Figure 4.1: Shear failure test with sensors attached

Fourteen sensors were attached to the sample. Each face parallel to the slice had five sensors attached. The sensors on each face were attached in the same pattern with two sensors, an inch above the midpoint of the sample, and two an inch below the midpoint. These sensors were attached one and a half and three inches from the back edge of the sample. The fifth sensor was attached on the midline of the sample, four and a half inches from the back edge. The remaining four sensors were attached to the faces that were split on the mid line, one inch from the outside edge. These locations were picked because they provided 360 degrees of coverage around the expected failure area, making them enough to the event locations to pick up strong wave signals from the failure.

Prior to beginning the test, the sensors were tested to ensure each one was functioning correctly. This was accomplished by tapping directly underneath each sensor, in order by channel number, around the entire sample. The taps were done using a screwdriver. Based on the active readings on the ESG acoustic emissions monitoring system, the recorded data for each channel is displayed by channel sensor number. If the sensor was triggered by the test tap, then the sensor was considered active and functioning. The tap test will be used to zero the machine once the test has been completed in the data processing stage; however, the taps needed be done before the test began to ensure all sensors were still be in contact with the sample.

To load the sample in a manner that would replicate the movement of a transform fault, stresses being applied in opposite directions, steel platens were used. Two platens per side of the sample were placed as close to the vertical cuts as possible, while maintaining full contact with the sample. Figure 4.1 shows the platens on top of the right section and at the bottom of the left section. This setup created equal pressure to each side of the sample applied by the platens. Once the stress being applied exceeded the shear strength of the Berea Sandstone, the sample failed in shear. While the sample is being loaded, the ESG acoustic emissions monitoring system recorded any seismic activity within the sample.

Once the data was collected it was then processed using the ESG software. Using the built in program SeisTree, a processor was created that used a P wave velocity of 2.8 km/sec to calculate the event locations. This velocity was used based on previous studies done on Berea Sandstone samples, and the calibration of the initial test taps. With a P wave velocity of 2.8 km/sec, the located events from the test taps were in the vicinity of the sensor locations.

4.2.2 – Results

The desired goal of this shear test was to determine if events could be located by the use of acoustic emissions equipment when a rock failed in shear. As Figure 4.2 shows, the sample failed in shear, then began to separate due to lack of confining stress. Without confining stress to keep the sample together, the acoustic emissions resonated from the initial failure, but there was not subsequent slippage to produce more events. The failure occurred in the bridge of the sample, as was the design, and the fracture connected the two slices created by the saw cuts. As can be seen in Figure 4.2, the fracture followed the weakened path through the drilled holes. The two pieces of sandstone stayed in place on the rock press platform due to the relief of pressure post failure.

Figure 4.2: Failed shear test sample.

Due to the restrictions of the press, only one platform could be moved at a time while applying load to the sample. This created a tilting movement on the sample as the test progressed. A progression of the sample failure can be found in Appendix B.

After the collected acoustic data was processed, the event locations were plotted in a 3-D rendering software. The event locations are represented in Figure 4.3. The events are colored in sequential order by occurrence with the purple to yellow on the color scale representing the initial tap tests. The cyan nodes represented on the image are the actual sensor locations as entered into the ESG software. The black nodes and connecting lines represent the outside border of the sample. In the image, on side B of Figure 4.3, the bridge is visible in the center for a point of comparison to the real world sample shown in Figure 4.1. All of the test taps were not located by the software however the majority of the test tap locations, the light green and yellow events, are in close proximity to the sensors location.

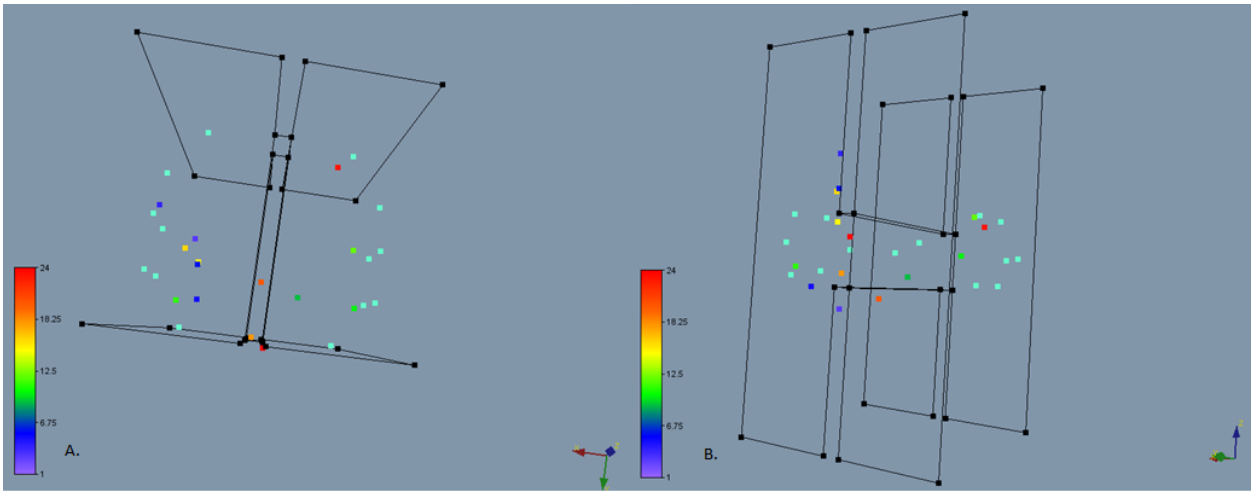

Figure 4.3: Side A. shows a top view of the shear test sample with events located. Side B. shows an askew view of the shear test sample with events located

A total of 14 events were located using the ESG software, eight of which were tap tests and 6 of which were actual event. Of these six events, there were two located inside the bridge, one in close proximity to the bridge and the remaining events occurred within the solid sandstone. The events that took place during failure are represented by the red and orange nodes in Figure 4.3. The red and orange nodes, events 18, 20, and 24 in the source file, are located at the front of the sample within the boundary of the bridge. Without the added adjustment of running the double difference tomography software TomoDD, the events were located in close proximity to the bridge showing the accuracy of the event location, since the event locations coincide with the failure shown in Figure 4.1.

4.2.3 – Discussion and Conclusion

Based on the results of the data processing, the use of tomography was able to record data from a shear failure accurately. The location of the events coinciding with the failure that is visually captured on camera shows that the locating software was able to produce reasonable results. However, the lack of events is a point of concern. Without confining stress on the sample, causing the sample to resettle and slip more than on the initial failure, the test does not provide a large enough data pool to determine that shear failure will always be located correctly. A sample with a similar design that also has a confining pressure applied is more likely to provide more events due to increased contact between the rock surfaces. If the sample is held together after the initial failure, the surfaces would grind together, similar to the movements of a transform fault.

Another point of concern with the result of this test is that the accurately located events are found close to the front face of the sample. Even though the sample failed along the bridge through the whole depth of the sample, the located events were not found except near the face. This could be due to how the rock failed, only creating acoustic emissions at the front of the sample. However, this could also be due to the manner in which the sample was loaded in the press. Since one platform of the press stays static, and the other platform was adjusted by hydraulics, the sample began to tilt slightly as the test progressed. This motion could have caused the sample to fail in a manner focusing the stresses on the bridge near the front of the sample.

Based on the results of this test, it can be concluded that shear failure can be recorded and located accurately through the use of acoustic emissions software. However, the minimal number of events at the point of failure does not provide the necessary confidence that this test could be repeated with the same results.

Section 4.3 – Caprock Upheaval Sample

4.3.1 – Sample Preparation and Testing

The caprock upheaval test was designed to test the failure of the caprock of a reservoir from over pressurization. As the reservoir is injected with fluid, the pressure builds, possibly causing the failure of the caprock. While the sample was being pressurized with injection fluid, acoustic emission sensors monitored the sample for any acoustic events.

The main structure on the caprock upheaval test samples was created out of a Berea Sandstone block, and Portland cement. The first step to creating the sample was to cut a block of Berea Sandstone into the dimensions of 165 mm x 165 mm x 152 mm. The sandstone reservoir was dual coated in a concrete sealer called, UGL Drylok, on all sides except for the top. This sealer prevented the fluid from escaping from the reservoir except through the top of the sample so that the pressure build up was directed on the caprock. Each of the six samples created had these initial steps in common. However, based on experimental results, the process for each subsequent sample changed.

The first two samples were made in the same manner, incased in two inches of concrete all the way around the sample. This was accomplished by creating a form that had inside dimensions of 266 mm x 266 mm x 355 mm. To keep the bottom of the sample elevated so that the concrete could fill in beneath the sample, nine, two inch screws were placed, tip up, centered in the base of the form as shown in Figure 4.4. The screws were put through a metal screen so that any lateral movement by the sandstone reservoir would not knock over the screws. Prior to filling the form, the water proofing sealer was applied to the plywood walls so that the form would not absorb the moisture, and could be reused. Once the sealer had dried, a line was drawn on the form to where the top level of the concrete should be poured.

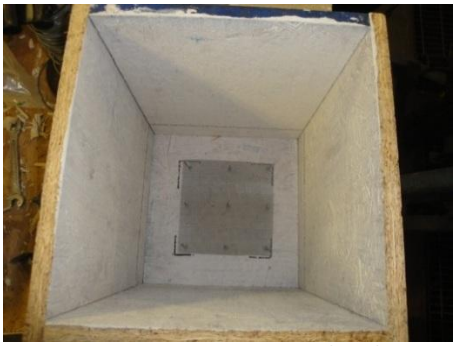

Figure 4.4: Screws in the base of the form to elevate the reservoir for concrete casting

The Portland cement was mixed one part to two parts manufacturers' sand until the consistency was wet enough to fill crevices and make air bubble removal easier. The bottom two inches were poured into the form, then the sandstone reservoir was placed on top of the screws. To prevent the sandstone from shifting while the sides were being poured, pouring alternated between faces that were directly across from each other. The concrete layer was necessary to reinforce the contact between the sealer and the

sandstone reservoir to prevent separation during injection. Once the concrete level reached the top of the reservoir, two pieces of nylon screen were placed in the caprock concrete approximately two inches apart. These pieces of screen were intended to act as fault lines in the caprock, weakening the bond of the concrete. Having the weakened areas in the caprock gave an expected area of failure to monitor.

The third and fourth samples were prepared in similar fashion. Sample three was created with a one inch caprock layer, while the fourth sample was created with a half inch caprock layer. Based on the results of the first four tests, a new approach was taken for sample five. Instead of pouring the caprock last, the caprock was poured first. To do this, four pieces of rubber were cut and attached to the top of the sandstone reservoir using duct tape. A half-inch layer of caprock was created using the same mixture of Portland cement and Manufacturers' sand as the other samples. The fault lines were created in the same fashion as previous samples with one piece of screen per artificial fault. A picture of this method can be found in Figure 4.5.

Figure 4.5: Form made of rubber for fifth and sixth sample to pour caprock first.

Once the concrete set for one day, the rubber form was taken off of the sample, and a coat of sealer was applied to the whole sandstone reservoir and extended to the top of the caprock layer. Once two coats of sealer were applied to the sample and had dried, the sample was placed in the plywood form and encased in the same Portland cement and sand mixture as previous samples.

The sixth sample was made in the same fashion as the fifth with the addition of two more pieces of nylon screen in the faults. Rather than having one piece of screen acting as the fault, two pieces of screen were placed back to back, allowing the concrete to bond through the fault, but not as strongly as with a single piece of screen. Also, the injection sleeve was attached to the sample prior to any concrete being pour. This was done to ensure that the injection sleeve was secured to the sandstone, not only to the surrounding concrete.

The sample was allowed to dry for more than three days, at which point the form was removed. The next step was to install an injection sleeve. The injection sleeve used for these tests was a one foot long piece of 16 mm CPVC. CPVC was chosen because of its durability and the ease of finding

connection fittings. The injection tube was installed on the side of the sample, three inches from the bottle and located in the center of the face, side to side. To install the injection tube, three masonry bits were used. The initial hole was drilled by a 16 mm drill bit to within half an inch of the center of the sample, approximately 121 mm deep. To attach the injection sleeve to the stone, a two-hour epoxy was used. To give enough room for the injection sleeve and epoxy within the hole, a wider hole was necessary. To accomplish this a 19 mm drill bit was used to widen the hole to a depth of 95 mm. Prior to inserting the sleeve, the dust was cleaned out of the drill hole using compressed air. The epoxy was then applied to the side of the injection tube and was worked down the drill hole between the sleeve and the rock. Once the epoxy hardened, a 9.5 mm bit was extended the injection hole an additional inch, to a total depth from the surface of the sample of 146 mm. Again, the injection hole was cleared out by compressed air before continuing. The final hole was drilled after the injection tube was attached so that any epoxy that may have leaked below the sleeve would be cleaned out of the injection area. A diagram of the initial sample design can be found in Appendix B.

Once the concrete had completely cured, the sensors were attached to the sample using superglue. If the concrete was too rough to attach the sensor to the surface of the sample, a grinding stone was used to make a pad. For these tests, a variation of sensor locations was used due to losing a sensor to malfunction. The initial layout for sensors can be found in Appendix B. Each vertical face had three sensors that alternated between three and four inches from the top of the sample. This pattern was extended around the sample. The first two tests had four sensors on the caprock surface, one in each corner two inches in from each face. Once one of the sensors stopped working after test two, the sensor orientation of the caprock surface was adjusted. The orientation of the sensors can be found in Figure 4.6.

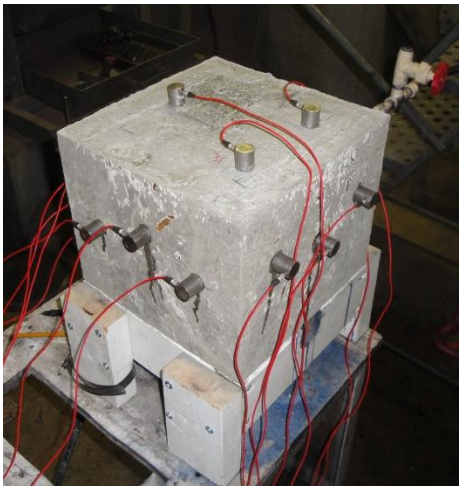

Figure 4.6: Caprock sample with sensors attached.

For injection, a vessel was needed that could store a significant amount of fluid for testing, as well as handle up to 120 psi supplied by the lab's air compressor. Based on these specifications, a steel tank was equipped with an air regulator that could hook into an air compressor, a tank level indicator tube

for fluid level monitoring, as well as a discharge valve at the bottom of the tank. An additional air pressure gauge was added to the top of the tank to double check the pressure inside of the tank. The pressure tank can be found in in Appendix B.

To connect the tank to the sample, a rubber tube was attached to the base of the tank. This tube was connected to a piece of the CPVC pipe with a fluid release valve. This valve was installed to provide a way to bleed the air bubbles out of the line prior to injection. The CPVC piece was then attached to the injection sleeve with cement. Prior to testing, the tank was pressurized and the line connected to the sample was closed to test the seals on the tank.

Prior to starting the testing, the tank was filled with water to be used as the injection fluid. Water was chosen because it was readily available, and once the tests were failing in the desired manner, the water would be easily replaced with a more viscous fluid, such as oil. A dye was then added to the fluid. The dye would act as a tracer to mark inside the sample where the fluid permeated during the test. For the first test, red food coloring was used, but upon completion of the test the dye was switched to a Navy, Procion MX Dye that would contrast the sandstone better, and would not be filtered by the sandstone as easily. A stand was created to elevate the sample off of the table to keep the fluid leaking from the surface of the sample from pooling on the table surface and reabsorbing into the concrete. The stand, shown in Figure 4.7, also provided a means to see what was happening to the underside of the sample during injection.

With the sensors attached to the ESG acoustic emissions machine, the sensors were once again tested by tapping below the sensors on the sample surface to help to zero the equipment settings during processing. Without pressure on the tank, the fluid in the tank was released and allowed to gravity feed to the sample. With the fluid release valve open, the air in the line was bled until the flow of fluid through the valve was uninterrupted, at which point the valve was closed. If the air was not bled from the line, the sample tube would be air-locked, and the fluid would not begin to be injected until the air in the tube had been displaced. Any events that took place while the line was bled were noted in the data journal.

To begin the test, the pressure on the tank was increased to twenty psi where it remained for twenty minutes. The pressure was increased by twenty psi every twenty minutes until the regulator was completely open, normally around 120 psi. One hundred twenty psi was the maximum the supplied compressor would reach, however, the maximum pressure being applied would fluctuate between 100 psi and 120 psi due to compressor settings. This approach was used to simulate gradual addition of fluid into the system, until the ultimate pressure was reached. Once the regulator was completely opened, the test was run until the water in the tank was gone, or the water level did not change for two hours. The test ran between 5 and 72 hours depending on the sample.

Once the samples were done being tested, a core of the concrete encasing the sample was taken and run through the P and S wave machine for analysis. The values returned were then used for testing for locating seismic events in the ESG software. Also, the samples were cut into quarters, from the top face down the length of the sample. From the cross sections, the concentration of dye could be observed, representing the movement of water during injection. Based on what was observed, the sample preparation was adjusted as needed.

4.3.2 – Results

For tests one through six, the same testing procedures were used until the test was deemed complete and data collection ceased. In none of the six tests did the caprock upheave and fail. In the first three tests, fluid was not seen coming out of the artificial fractures. Instead, in the first three tests, the fluid leaked out of the concrete on the vertical faces. Where the fluid did leak out of the top of the sample, the relief points were located outside of the region that was directly over the reservoir. The fourth test was deemed unusable due to a tank rupture five hours into testing. The tank failed when a hose come loose from the tank, covering the sample in dye, preventing any data to be collected as to where the dye was beaching the sample surface. The fifth and sixth tests provided promising results, with fluid reaching the surface of the sample through the artificial faults. Figure 4.7 shows the fluid escaping through the artificial fault during the fifth test.

Figure 4.7: Dyed fluid escaping through artificial fault in a caprock sample.

In Figure 4.7, the dye can be seen escaping and pooling on the surface of the sample. The slightly raised area of the sample is where the cap rock was precast and hardened before the rest of the concrete was poured. The sealer comes to the top of the caprock on this sample. The fluid escaped the reservoir within the sample and followed the walls of the reservoir to the surface of the sample. This can be seen by the concentration of dye on the surface. Though this build-up could be from the run off of the fluid escaping from the artificial faults, there were air bubbles noted coming from the same area as the concentrated dye. This fluid migration was confirmed when the sample was cut open and the

concentration of dye was found to be on the inside and outside of the sealed reservoir wall. The cross section images of all six tests can be found in Appendix B.

Using the ESG software, the events recorded during testing were located. A P-wave velocity of 2.3 km/sec was set for the processor to locate events based on the proximity of the initial tap tests to the actual sensor locations. The results of the processing are presented in Figure 4.8 in a 3-D rendering on the model. The black nodes that are conneced by black lines in the shape of the node are the outline of the caprock sample. The injection tube is represented by the black cylinder on the left side of the sample, and the black nodes that are not connected on the faces of the cube are the sensor locations. The multicolored nodes represent the located events within the sample. The located events for the other caprock samples can be found in Appendix B.

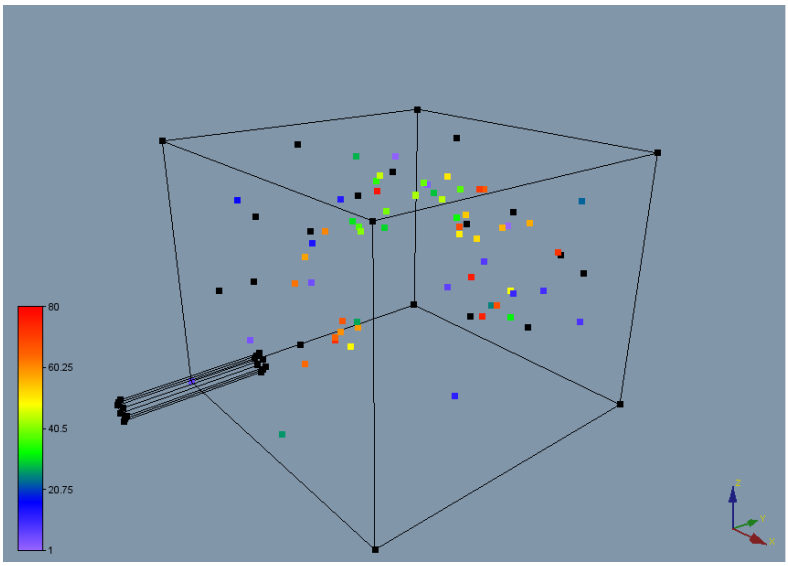

Figure 4.8: 3-D rendering of caprock sample for test number five.

4.3.3 – Discussion and Conclusion

The results of this test show a correlation between the seismic event locations and the visual evidence provided by the dyed fluid post injection. Within the sample, there are clusters of events that are located in the proximity of the reservoir layer and the injection tube. Both of these areas had concentrations of the navy dye. These areas had seismic activity due to the pressure build up within the reservoir. As the pressure begins to build within the sample, the fluid is forced away from the injection area to the walls of the reservoir. Once the fluid reached the reservoir walls, it hits the impermeable sealer layer and the fluid level began to rise to the surface of the sample. At the top of the reservoir, the fluid again ran into the caprock layer, and begsn to press against the concrete creating seismic events. The cluster of green nodes at the surface of the sample corresponds with the level at which these events occurred.

As the sample continued to be pressurized, the pressure began to push outward in all directions causing the events depicted in red and orange. The cluster of events that occurred around the injection sleeve was most likely due to the pressure of the reservoir exceeding the strength of the rock and epoxy around the injection tube.

Along all boundaries with sealer as well as along the division between the caprock layer and the top of the reservoir, which has no sealer, the navy dye was present. Because of this concentration, it is evident that the fluid moved through the sample away from the injection area, and came in contact with the sealer barrier before adjusting its path. The buildup of dye along the bottom of the reservoir, but not in the concrete on the other side of the seal, shows that the fluid rebounded off of the sealer and ascended to the surface of the sample. Also, the area around the injection tube had a buildup of dye as well.

Though there are numerous events that support this pattern of fluid flow, there are other observations of note to consider. The concentration of fluid along the bottom layer of the sample leads to the expectation of seismic activity as well, but there were no events recorded in that area. Also, there were very few events recorded in the center of the reservoir where the fluid passed through, as the reservoir pressurized. Finally, in some cases, the navy dye is located outside of the sealer, between the concrete and the sandstone. This could be due to leakage of the fluid through the sealer as the pressure increases, or the fluid is finding a path out of the reservoir and is following the sealer layer around the sample.

A major point of concern with this sample is that the caprock never failed in the manner expected. There was no evidence of upheaval to the caprock layer, visually or seismically. Due to this, it appears evident from these results that the pressures created in this test were not great enough to cause the caprock to shift. Testing the effect of higher pressures on the caprock could be a possible direction to testing tomography's ability to monitor caprock failure. However, a more likely course would be to test a different mode of failure in the caprock. If none of the samples were able to create events within the caprock layer, this particular test is not yet set up to create seismic activity in the caprock.

Chapter 5 – Summary of Results and Conclusions

Section 5.1 – Results and Conclusions

Passive acoustic emissions monitoring was used to determine how effectively failure locations could be located in a three unique tests. Coupled with double difference tomography, the failure of a Berea Sandstone sample and Marcellus Shale sample were calculated to determine how well the stress redistribution within the sample could be mapped using the recorded data. For the main indenter tests two samples were tested. One, a 153 mm diameter by 153 mm tall sample of Berea Sandstone was connected to 15 sensors monitoring the sample, and the second, an 88 mm diameter by 74 mm tall Marcellus Shale sample with 14 sensors monitoring the sample were tested. The transform shear test had 14 sensors monitoring the sample, while the caprock upheaval test had variable number of sensors monitoring, 15 or 16. For all tests, the samples were monitored until failure or it was deduced that the test would not produce failure.

The data recorded from the indenter tests was used to develop a velocity model for both the Berea Sandstone and the Marcellus Shale. The initial event locations calculated by the 16 channel ESG Hyperion acoustic monitoring system were located in the correct vicinity of the sample failure. However, after relocation using double different tomography, the event locations correlated more readily to the failure planes on the sample. The velocity models were divided into three regimes to separate the stress distribution of the sample between linear elastic deformation, plastic deformation and events at and post failure. Orthogonal images were created from the velocity models made using double difference tomography.

On both the Berea Sandstone sample and the Marcellus Shale sample, the tomograms displayed the velocities at certain locations of interest. On the Berea Sandstone sample, the locations of interest beneath the indenter, as well as beneath the wedge created by loading, behaved according to the model presented by Cook on how failure occurs beneath the punch. As the stress increased on the sample, an area of high velocity formed beneath the indenter that would have compressive failure, and a zone of low velocity formed beneath the wedge in a zone of tensile failure. For the Marcellus Shale sample, the orthogonal images based on the velocity model showed the same results beneath the indenter and beneath the wedge; however the sample did not fail the same way as the Berea Sandstone Sample. The Marcellus Shale sample had a low velocity zone which occurred away from the indenter on the sample where the sample initially failed. The Marcellus Shale sample did not have a distinct wedge that formed prior to failure like the Berea Sandstone sample. Due to this, it is believed that the sample exfoliated before the wedge had the opportunity to cause ultimate failure.

The secondary tests did not progress through the data analysis as far as the indentation tests, however valuable information was gathered from these tests. The shear test demonstrated the

effectiveness of the passive acoustic emissions monitoring system to record shear failure. Also, the event location software built into the ESG Hyperion system successfully located the locations of the events within the region of failure. This test provides confidence in this technology to record and located events that are not occurring in compression. The caprock upheaval tests were not successful in causing failure in the caprock, however during the testing the passive acoustic emissions monitoring system was able record and locate events that occurred within the sample around the boundary of the reservoir. At the reservoir boundaries there was evidence of fluid flowing through the reservoir, and the events align with these locations. This positive result shows that the monitoring system is able to locate events induced by fluid injection, which will be helpful with carbon sequestration projects.

The results of these tests provide confidence in the passive acoustic emissions monitoring system to record accurate data for the caprock integrity monitoring. The velocity models that were created from the recorded data using double difference tomography accurately mapped the areas of interest within the rock samples. From these results, passive acoustic emissions monitoring systems coupled with double difference tomography has proven capable of monitoring uniform samples within a laboratory environment. With further testing, this technology could possibly be a viable option for monitoring carbon sequestration sites.

Section 5.2 – Possible Sources of Error

In laboratory testing there are possible sources of error which must be taken into account when discussing the final results. Two of the major sources of error noted during testing were the possibility of over filtering the acoustic emissions, and the error involved in placing the sensors in the appropriate locations. The possibility of over filtering of the acoustic emissions was necessary to reduce the amount of background noise created by the servo-valve. Without setting a threshold value to block out the servo-value, too many false readings would have been recorded, possibly covering up results. Having more, actual events would have created a stronger velocity model. However, having incorrect events would have incorrectly influenced the velocity model as well. Though the impact of the final results is believed to be minimal, there are a few acoustic events that could have been missed.

The possibility of sensors not being located in the correct location impacts data analysis on all levels. If the sensors were not installed on the sample precisely, the sensor locations input in the monitoring equipment will incorrectly represent the locations of the receivers for calculation. With incorrect sensor locations the events will be initially located in the incorrect location, affecting the relocation later. Also, if the events are located in the wrong location, the velocities calculated for each event will be incorrect as well. If the velocities are incorrect, the velocity model will be mistakenly calculated as well.

Section 5.2 – Future Work

There are a number of possible steps to continue research into the effectiveness of passive seismic monitoring systems coupled with double difference tomography in monitoring underground injection sites. Field testing is a possible next step in the process. With the positive results found in the laboratory, it is important to determine how this method reacts in a real word environment. However, factors that do not appear in the laboratory environment could cause the sensors readings to be erroneous. Both samples used in the laboratory were homogenous samples of their representative rock type. The geology of an injection site will differ from this because there will be multiple striation layers causing waves to refract at the boundaries. Different sensor orientation in the field could catch reflected waves differently than in the lab, so the geology's effect on the sensors will be a factor that needs to be tested.

In the laboratory, additional testing with the passive monitoring system and double difference tomography would provide greater confidence in this process. Two samples are recommended to be tested: another indenter test with multiple layers, and a sample that will produce caprock failure. The new indentation test sample should contain a reservoir layer, a caprock layer and an overburden layer. This test will help determine if a passive acoustic monitoring system can record and determine accurate locations of events in a sample with a geologic layout similar to where sequestration or enhances oil recovery will occur. The results from this test would also show how well double difference tomography could differential between the boundary layers within the sample. The caprock failure sample would further the secondary testing upheaval test to determine if the passive acoustic monitoring system would be successful monitoring and locating caprock failure.

With the knowledge gained from performing these tests, a move toward a probabilistic approach to forecasting future induced seismicity needs to be made. The positive results represented by the tomograms accurately representing stress redistribution shows that the areas of future seismic events can be forecast. The likelihood of future seismic events as well as failure is related to the subsequent changes to the velocities of the mapped area. By monitoring the areas of changing velocities, failure zones can be forecast and adjustments can be made to the injection to prevent further failure.

References

Aydina, A., R. I. Borjab, et al. (2006). "Geological and Mathematical Framework for Failure Modes in Granular Rock." Journal of Structural Geology: 83-98.

Bachu, S. and J. J. Adams (2003). "Sequestration of CO2 in geological media in response to climate change: capacity of deep saline aquifers to sequester CO2 in solution." Energy Conservation and Management **44**(20): 3151-3175.

Barzili, A. (2000). Improving a Geophone to Produce an Affordable, Broadband Seismometer. Mechanical Engineering, Standford. **PhD**.

Benson, S. M., R. Hepple, et al. (2002). "Lessons Learned from Natural and Industrial Analogues for Storage of Carbon Dioxide in Deep Geological Formations." Earth Sciences Division, E.O Larence Berkley National Laboratory, Berkley: 135.

Cook, N. G. W., M. Hood, et al. (1984). "Observations of crack growth in hard rock loaded by an indenter." International Journal of Rock Mechanics and Mining Sciences & Geomechanics Abstracts **21**(2): 97-107.

Damen, K., A. Faaij, et al. (2006). "Health, Safety and Environmental Risks of Underground Co₂ Storage – Overview of Mechanisms and Current Knowledge." Climatic Change **74**(1): 289-318.

Dave Reichle, e. a. (1999). CARBON SEQUESTRATION RESEARCH AND DEVELOPMENT. DOE.

Deichmann, N. and K. F. Evans (2010). Injection-Induced Seismicity: Placing the Problem in Perspective. European Seismological Commission 32nd General Assembly. Montpellier, France.

DOE DOE - Fossil Energy: Office of Fossil Energy Home Page. DOE.

EIA (2009). U.S. Energy Information Administratrion - EIA - Independent Statistics and Analysis.

Elliot, A. (2008). "Mining Ground Support." Retrieved March 5, 2012, from http://www.mining-technology.com/features/feature2017/.

Engelder, D. T. "Lect. 13. - Coulomb Failure Criterion." from http://www.geosc.psu.edu/~jte2/geosc465/notes465.html.

Finley, R. (2003). Assessment of Geological Carbon Sequestration Options in the Illinois Basin.

Friedmann, S. J. (2007). "Geological Carbon Dioxide Sequestration." Elements **3**(3): 179-184.

Gutenberg, B. and C. F. Richter (1955). "Magnitude and Energy of Earthquakes." Nature **176**(4486): 795-795.

Hamada, G., M. (2004). "Reservoir Fluids Identification Using Vp/Vs Ratio." Oil & Gas Science and Technology - Rev. IFP **59**(6): 649-654.

Hardy, R. H., G. L. Mowrey, et al. (1981). A microseismic study of an underground natural gas storage reservoir, American Gas Association.

Hasegawa, H. S., R. J. Wetmiller, et al. (1989). "Induced seismicity in mines in Canada—An overview." Pure and Applied Geophysics **129**(3): 423-453.

Herzog, H. J. (2001). "What Future for Carbon Capture and Sequestration." Environmental Science & Technology **35**(7): 148 A - 153A.

Hirose, F., J. Nakajima, et al. (2008). "Three-dimensional seismic velocity structure and configuration of the Philippine Sea slab in southwestern Japan estimated by double-difference tomography." J. Geophys. Res. **113**.

Hoek, E., C. Carranza-Torres, et al. (2002). Hoek-Brown failure criterion. Proc. NARMS-TAC Conference.

Hudson, J. A. (2005). Engineering Rock Mechanics: An Intoduction to the Principles. Oxford, Elsevier Ltd.

Hudson, J. A., F. H. Cornet, et al. (2003). "ISRM SuggestedMethod s for rock stress estimation—Part 1:

Strategy for rock stress estimation." International Journal of Rock Mechanics and Mining Sciences **40**: 991-998.

J, Z. (2000). "Applicability of Mohr–Coulomb and Hoek–Brown strength criteria to the dynamic strength of brittle rock." International Journal of Rock Mechanics and Mining Sciences **37**(7): 1115-1121.

Kocer, C. and R. E. Collins (1998). "Angle of Hertzian Cone Cracks." Journal of the American Ceramic Society **81**(7): 1736-1742.

Lal, R. (2004). "Soil Carbon Sequestration Impacts on Global Climate Change and Food Security." Science **304**(5677): 1623-1627.

Medical, S. "Computed Tomography Its History and Technology." Retrieved March 5, 2012, from http://www.medical.siemens.com/siemens/zh_CN/gg_ct_FBAs/files/brochures/CT_History_and_Technology.pdf.

Moradian, Z. A., G. Ballivy, et al. (2010). "Evaluating damage during shear tests of rock joints using acoustic emissions." International Journal of Rock Mechanics and Mining Sciences **47**(4): 590-598.

Murphy, M. M. (2005). Defining stress changes ahead of a tunnel face and design of a data acquisition system. VPI & SU Mining and Minerals Engineering M S 2005. Blacksburg, Va., University Libraries, Virginia Polytechnic Institute and State University,.

NETL (2010). "2010 Carbon Sequestration Atlas of the United States and Canada." (3) **156-158**.

NIOSH (1997). Use of Seismic Tomography To Identify Geologic Hazards in Underground Mines. NIOSH.

Paşamehmetoğlu, A. G. (1993). Assessment and Prevention of Failure Phenomena in Rock Engineering. Netherlands, A.A. Balkema Publishers.

Ph, R. N. (2004). "Risk Assessment Workshop." Victoria: 458.

Price, P. N., T. E. Mckone, et al. "Carbon Sequestration Risks and Risk Management." Lawrence Berkely National Laboratory.

Raynaud, D. and J. M. Barnola (1985). "An Antarctic ice core reveals atmospheric CO2 variations over the past few centuries." Nature **315**(6017): 309-311.

Rutqvist, J. and C.-F. Tsang (2002). "A Study of Caprock Hydromechanical Changes Associated with CO 2 -injection into a Brine Formation." Environmental Geology **42.2-3**: 296-305.

Sminchak, J. and N. Gupta "Issues Related to Seismic Activity Induced by the Injection of CO2 in Deep Saline Aquifers." National Energy Technology Laboratory.

Solutions, E. (2012). "Paladin 24-bit Digital Microsesmic Recorder." Retrieved March 5, 2012, from https://www.esgsolutions.com/english/view.asp?x=782.

Sorey, M. L., W. C. Evans, et al. (1998). "Carbon dioxide and helium emissions from a reservoir of magmatic gas beneath Mammoth Mountain, California." J. Geophys. Res. **103**(B7): 15303-15323.

Suckale, J. (2010). "Moderate-to-large seismicity induced by hydrocarbon production." The Leading Edge **29**(3): 310-319.

Sundquist, E. T. and Geological Survey (U.S.) (2008). Carbon sequestration to mitigate climate change. Fact sheet 2008-3097. Reston, Va., U.S. Dept. of the Interior, U.S. Geological Survey,**:** 4 p. digital, PDF file.

Turner, M. (2005). "Management of Seismicity using Portable Seismic Systems." Australian Centre for Geomechanics – Course on Advance Geomechanics in Underground Mines.

Twiss, R. J. and E. M. Moores (1973). Structural Geology. U.S.A, W. H. Freeman and Company.

Wei, R. P. (2010). Fracture Mechanics - Integration of Mechanics, Material Science, and Chemistry. U.S.A, Cambridge University Press.

Westman, E. C. (2003). Use of tomography for inference of stress redistribution in rock. Industry Applications Conference, 2003. 38th IAS Annual Meeting. Conference Record of the.

Zhang, H. and C. H. Thurber (2003). "Double-Difference Tomography: The Method and Its Application to the Hayward Fault, California." Bulletin of the Seismological Society of America **93**(5): 1875-1889.

Zhang, H. W., G. Subhash, et al. (2003). "Mechanical behavior of bulk (ZrHf)TiCuNiAl amorphous alloys." Scripta Materialia **49**(5): 447-452.

Zoback, M. D. and J. C. Zinke (2002). "Production-induced Normal Faulting in the Valhall and Ekofisk Oil Fields." Pure and Applied Geophysics **159**(1): 403-420.

Appendix A – Indenter Test Results

Appendix A will have information that is relevant to the understanding of the results of the primary indenter experiments. The preparation equipment used to make the samples as well as additional images of the Berea Sandstone and Marcellus Shale Samples will be documented. The orthogonal images for both samples will be documented as well.

Figure A-1: Stone drill press used to cut Berea Sandstone samples

Figure A-2: Stone grinder, used to smooth the faces of the Marcellus Shale sample.

Figure A-3: Stone saw used to prepare core samples.

Figure A-4: Stone saw with 8 inch blade used to cut Marcellus Shale and Berea Sandstone samples.

Figure A-5: P and S wave testing equipment to determine background velocity of each sample.

TomoDD input file for Berea Sandstone

```
* add uniform noise to absolute data 0.2*(rand()-0.5).
* the maximum noise is 100 ms.
* use the CC data constructed from absoulte data without noise
* RELOC.INP:
*--- input file selection
* cross correlation diff times:
*dt.cc.noise4

*
*catalog P diff times:
dt.ct
*
* event file:
events.dat
*
* station file:
station.dat
*
*--- output file selection
* original locations:
Berea627.loc
* relocations:
Berea627.reloc
* station information:
Berea627_syn.sta
* residual information:
Berea627_syn.res
* source paramater information:
*hypo3VDD.src

*Output velocity
Berea627.vel
*absolute data
tt.dat
*--- data type selection:
* IDAT:  0 = synthetics; 1= cross corr; 2= catalog; 3= cross & cat
* IPHA: 1= P; 2= S; 3= P&S
* DIST:max dist [km] between cluster centroid and station
* IDAT   IPHA   DIST
   2     1     200
*
*--- event clustering:
* OBSCC:    min # of obs/pair for crosstime data (0= no clustering)
* OBSCT:    min # of obs/pair for network data (0= no clustering)
* OBSCC  OBSCT  CC_format
  0      0       2
*
*--- solution control:
* ISTART:                 1 = from single source; 2 = from network sources
* ISOLV:  1 = SVD, 2=lsqr
* NSET:                   number of sets of iteration with specifications following
*  ISTART  ISOLV  NSET weight1 weight weight3 air_depth
   2        2     10     20     20    20        0
* i3D delt1 ndip iskip scale1 scale2 iusep iuses iuseq
  2    0    9     1     0.2   0.2    1     1    0
* invdel ifixl xfac   tlim     nitpb(1) nitpb(2) stepl
   1      0    1.3   0.002     10        10      0.2
* lat_Orig lon_Orig Z_Orig iorig rota
  0.00001      0.00001                  0     1      0
*
*--- data weighting and re-weighting:
* NITER:                  last iteration to used the following weights
* WTCCP, WTCCS:                   weight cross P, S
* WTCTP, WTCTS:                   weight catalog P, S
* WRCC, WRCT:                     residual threshold in sec for cross, catalog data
* WDCC, WDCT:                     max dist [km] between cross, catalog linked pairs
* DAMP:                           damping (for lsqr only)
```

```
*      ---  CROSS DATA ----- ----CATALOG DATA ----
* NITER WTCCP WTCCS WRCC WDCC WTCTP WTCTS WRCT WDCT WTCD DAMP JOINT THRES
  5      0.01  0.01 -9    -9  0.1   0.08   -9   -9  10    800   1   3
  5      0.01  0.01 -9    -9  0.1   0.08   -9   -9  10    300   0   3
  5      0.01  0.01 -9    -9  0.1   0.08    8   -9  10    200   1   3
  5      0.01  0.01 -9    -9  0.1   0.08    8   -9  10    150   0   3
  5      0.01  0.01 -9    -9  1.0   0.08    6   -9  10    100   1   3
  5      0.01  0.01 -9    -9  1.0   0.8     6   -9  10     75   0   3
  5      0.01  0.01 -9    -9  1.0   0.8     6   10  10     50   1   3
  5      0.01  0.01 -9    -9  1.0   0.8     6   10  10     25   0   3
  5      0.01  0.01 -9    -9  1.0   0.8     6   10  10     15   1   3
  10     0.01  0.01 -9    -9  1.0   0.8     6   10  10     10   0   3
*
*--- event selection:
* CID:      cluster to be relocated (0 = all)
* ID:       cuspids of event to be relocated (8 per line)
* CID
   0
* ID
```

MOD.dat file for Berea Sandstone used in TomoDD

```
1.0 21 21 21
-4999. -999 -10 0 10 20 30 40 50 60 70 80 90 100 110 120 130 140 150 999. 5000.
-4999. -999 -10 0 10 20 30 40 50 60 70 80 90 100 110 120 130 140 150 999. 5000.
-4999. -999 -10 0 10 20 30 40 50 60 70 80 90 95 100 110 120 130 150 999. 5000.
 2.30 2.30 2.30 2.30 2.30 2.30 2.30 2.30 2.30 2.30 2.30 2.30 2.30 2.30 2.30 2.30 2.30 2.30 2.30 2.30 2.30
 2.30 2.30 2.30 2.30 2.30 2.30 2.30 2.30 2.30 2.30 2.30 2.30 2.30 2.30 2.30 2.30 2.30 2.30 2.30 2.30 2.30
 2.30 2.30 2.30 2.30 2.30 2.30 2.30 2.30 2.30 2.30 2.30 2.30 2.30 2.30 2.30 2.30 2.30 2.30 2.30 2.30 2.30
 2.30 2.30 2.30 2.30 2.30 2.30 2.30 2.30 2.30 2.30 2.30 2.30 2.30 2.30 2.30 2.30 2.30 2.30 2.30 2.30 2.30
 2.30 2.30 2.30 2.30 2.30 2.30 2.30 2.30 2.30 2.30 2.30 2.30 2.30 2.30 2.30 2.30 2.30 2.30 2.30 2.30 2.30
 2.30 2.30 2.30 2.30 2.30 2.30 2.30 2.30 2.30 2.30 2.30 2.30 2.30 2.30 2.30 2.30 2.30 2.30 2.30 2.30 2.30
 2.30 2.30 2.30 2.30 2.30 2.30 2.30 2.30 2.30 2.30 2.30 2.30 2.30 2.30 2.30 2.30 2.30 2.30 2.30 2.30 2.30
 2.30 2.30 2.30 2.30 2.30 2.30 2.30 2.30 2.30 2.30 2.30 2.30 2.30 2.30 2.30 2.30 2.30 2.30 2.30 2.30 2.30
 2.30 2.30 2.30 2.30 2.30 2.30 2.30 2.30 2.30 2.30 2.30 2.30 2.30 2.30 2.30 2.30 2.30 2.30 2.30 2.30 2.30
 2.30 2.30 2.30 2.30 2.30 2.30 2.30 2.30 2.30 2.30 2.30 2.30 2.30 2.30 2.30 2.30 2.30 2.30 2.30 2.30 2.30
 2.30 2.30 2.30 2.30 2.30 2.30 2.30 2.30 2.30 2.30 2.30 2.30 2.30 2.30 2.30 2.30 2.30 2.30 2.30 2.30 2.30
 2.30 2.30 2.30 2.30 2.30 2.30 2.30 2.30 2.30 2.30 2.30 2.30 2.30 2.30 2.30 2.30 2.30 2.30 2.30 2.30 2.30
 2.30 2.30 2.30 2.30 2.30 2.30 2.30 2.30 2.30 2.30 2.30 2.30 2.30 2.30 2.30 2.30 2.30 2.30 2.30 2.30 2.30
 2.30 2.30 2.30 2.30 2.30 2.30 2.30 2.30 2.30 2.30 2.30 2.30 2.30 2.30 2.30 2.30 2.30 2.30 2.30 2.30 2.30
 2.30 2.30 2.30 2.30 2.30 2.30 2.30 2.30 2.30 2.30 2.30 2.30 2.30 2.30 2.30 2.30 2.30 2.30 2.30 2.30 2.30
 2.30 2.30 2.30 2.30 2.30 2.30 2.30 2.30 2.30 2.30 2.30 2.30 2.30 2.30 2.30 2.30 2.30 2.30 2.30 2.30 2.30
 2.30 2.30 2.30 2.30 2.30 2.30 2.30 2.30 2.30 2.30 2.30 2.30 2.30 2.30 2.30 2.30 2.30 2.30 2.30 2.30 2.30
 2.30 2.30 2.30 2.30 2.30 2.30 2.30 2.30 2.30 2.30 2.30 2.30 2.30 2.30 2.30 2.30 2.30 2.30 2.30 2.30 2.30
 2.30 2.30 2.30 2.30 2.30 2.30 2.30 2.30 2.30 2.30 2.30 2.30 2.30 2.30 2.30 2.30 2.30 2.30 2.30 2.30 2.30
 2.30 2.30 2.30 2.30 2.30 2.30 2.30 2.30 2.30 2.30 2.30 2.30 2.30 2.30 2.30 2.30 2.30 2.30 2.30 2.30 2.30
 2.30 2.30 2.30 2.30 2.30 2.30 2.30 2.30 2.30 2.30 2.30 2.30 2.30 2.30 2.30 2.30 2.30 2.30 2.30 2.30 2.30
 2.30 2.30 2.30 2.30 2.30 2.30 2.30 2.30 2.30 2.30 2.30 2.30 2.30 2.30 2.30 2.30 2.30 2.30 2.30 2.30 2.30
 2.30 2.30 2.30 2.30 2.30 2.30 2.30 2.30 2.30 2.30 2.30 2.30 2.30 2.30 2.30 2.30 2.30 2.30 2.30 2.30 2.30
 2.30 2.30 2.30 2.30 2.30 2.30 2.30 2.30 2.30 2.30 2.30 2.30 2.30 2.30 2.30 2.30 2.30 2.30 2.30 2.30 2.30
 2.30 2.30 2.30 2.30 2.30 2.30 2.30 2.30 2.30 2.30 2.30 2.30 2.30 2.30 2.30 2.30 2.30 2.30 2.30 2.30 2.30
 2.30 2.30 2.30 2.30 2.30 2.30 2.30 2.30 2.30 2.30 2.30 2.30 2.30 2.30 2.30 2.30 2.30 2.30 2.30 2.30 2.30
 2.30 2.30 2.30 2.30 2.30 2.30 2.30 2.30 2.30 2.30 2.30 2.30 2.30 2.30 2.30 2.30 2.30 2.30 2.30 2.30 2.30
 2.30 2.30 2.30 2.30 2.30 2.30 2.30 2.30 2.30 2.30 2.30 2.30 2.30 2.30 2.30 2.30 2.30 2.30 2.30 2.30 2.30
 2.30 2.30 2.30 2.30 2.30 2.30 2.30 2.30 2.30 2.30 2.30 2.30 2.30 2.30 2.30 2.30 2.30 2.30 2.30 2.30 2.30
 2.30 2.30 2.30 2.30 2.30 2.30 2.30 2.30 2.30 2.30 2.30 2.30 2.30 2.30 2.30 2.30 2.30 2.30 2.30 2.30 2.30
 2.30 2.30 2.30 2.30 2.30 2.30 2.30 2.30 2.30 2.30 2.30 2.30 2.30 2.30 2.30 2.30 2.30 2.30 2.30 2.30 2.30
 2.30 2.30 2.30 2.30 2.30 2.30 2.30 2.30 2.30 2.30 2.30 2.30 2.30 2.30 2.30 2.30 2.30 2.30 2.30 2.30 2.30
 2.30 2.30 2.30 2.30 2.30 2.30 2.30 2.30 2.30 2.30 2.30 2.30 2.30 2.30 2.30 2.30 2.30 2.30 2.30 2.30 2.30
 2.30 2.30 2.30 2.30 2.30 2.30 2.30 2.30 2.30 2.30 2.30 2.30 2.30 2.30 2.30 2.30 2.30 2.30 2.30 2.30 2.30
 2.30 2.30 2.30 2.30 2.30 2.30 2.30 2.30 2.30 2.30 2.30 2.30 2.30 2.30 2.30 2.30 2.30 2.30 2.30 2.30 2.30
 2.30 2.30 2.30 2.30 2.30 2.30 2.30 2.30 2.30 2.30 2.30 2.30 2.30 2.30 2.30 2.30 2.30 2.30 2.30 2.30 2.30
 2.30 2.30 2.30 2.30 2.30 2.30 2.30 2.30 2.30 2.30 2.30 2.30 2.30 2.30 2.30 2.30 2.30 2.30 2.30 2.30 2.30
 2.30 2.30 2.30 2.30 2.30 2.30 2.30 2.30 2.30 2.30 2.30 2.30 2.30 2.30 2.30 2.30 2.30 2.30 2.30 2.30 2.30
 2.30 2.30 2.30 2.30 2.30 2.30 2.30 2.30 2.30 2.30 2.30 2.30 2.30 2.30 2.30 2.30 2.30 2.30 2.30 2.30 2.30
 2.30 2.30 2.30 2.30 2.30 2.30 2.30 2.30 2.30 2.30 2.30 2.30 2.30 2.30 2.30 2.30 2.30 2.30 2.30 2.30 2.30
 2.30 2.30 2.30 2.30 2.30 2.30 2.30 2.30 2.30 2.30 2.30 2.30 2.30 2.30 2.30 2.30 2.30 2.30 2.30 2.30 2.30
 2.30 2.30 2.30 2.30 2.30 2.30 2.30 2.30 2.30 2.30 2.30 2.30 2.30 2.30 2.30 2.30 2.30 2.30 2.30 2.30 2.30
 2.30 2.30 2.30 2.30 2.30 2.30 2.30 2.30 2.30 2.30 2.30 2.30 2.30 2.30 2.30 2.30 2.30 2.30 2.30 2.30 2.30
 2.30 2.30 2.30 2.30 2.30 2.30 2.30 2.30 2.30 2.30 2.30 2.30 2.30 2.30 2.30 2.30 2.30 2.30 2.30 2.30 2.30
 2.30 2.30 2.30 2.30 2.30 2.30 2.30 2.30 2.30 2.30 2.30 2.30 2.30 2.30 2.30 2.30 2.30 2.30 2.30 2.30 2.30
```

2.30 2.30 2.30 2.30 2.30 2.30 2.30 2.30 2.30 2.30 2.30 2.30 2.30 2.30 2.30 2.30 2.30 2.30 2.30 2.30 2.30
2.30 2.30 2.30 2.30 2.30 2.30 2.30 2.30 2.30 2.30 2.30 2.30 2.30 2.30 2.30 2.30 2.30 2.30 2.30 2.30 2.30
2.30 2.30 2.30 2.30 2.30 2.30 2.30 2.30 2.30 2.30 2.30 2.30 2.30 2.30 2.30 2.30 2.30 2.30 2.30 2.30 2.30
2.30 2.30 2.30 2.30 2.30 2.30 2.30 2.30 2.30 2.30 2.30 2.30 2.30 2.30 2.30 2.30 2.30 2.30 2.30 2.30 2.30
2.30 2.30 2.30 2.30 2.30 2.30 2.30 2.30 2.30 2.30 2.30 2.30 2.30 2.30 2.30 2.30 2.30 2.30 2.30 2.30 2.30
2.30 2.30 2.30 2.30 2.30 2.30 2.30 2.30 2.30 2.30 2.30 2.30 2.30 2.30 2.30 2.30 2.30 2.30 2.30 2.30 2.30
2.30 2.30 2.30 2.30 2.30 2.30 2.30 2.30 2.30 2.30 2.30 2.30 2.30 2.30 2.30 2.30 2.30 2.30 2.30 2.30 2.30
2.30 2.30 2.30 2.30 2.30 2.30 2.30 2.30 2.30 2.30 2.30 2.30 2.30 2.30 2.30 2.30 2.30 2.30 2.30 2.30 2.30
2.30 2.30 2.30 2.30 2.30 2.30 2.30 2.30 2.30 2.30 2.30 2.30 2.30 2.30 2.30 2.30 2.30 2.30 2.30 2.30 2.30
2.30 2.30 2.30 2.30 2.30 2.30 2.30 2.30 2.30 2.30 2.30 2.30 2.30 2.30 2.30 2.30 2.30 2.30 2.30 2.30 2.30
2.30 2.30 2.30 2.30 2.30 2.30 2.30 2.30 2.30 2.30 2.30 2.30 2.30 2.30 2.30 2.30 2.30 2.30 2.30 2.30 2.30
2.30 2.30 2.30 2.30 2.30 2.30 2.30 2.30 2.30 2.30 2.30 2.30 2.30 2.30 2.30 2.30 2.30 2.30 2.30 2.30 2.30
2.30 2.30 2.30 2.30 2.30 2.30 2.30 2.30 2.30 2.30 2.30 2.30 2.30 2.30 2.30 2.30 2.30 2.30 2.30 2.30 2.30
2.30 2.30 2.30 2.30 2.30 2.30 2.30 2.30 2.30 2.30 2.30 2.30 2.30 2.30 2.30 2.30 2.30 2.30 2.30 2.30 2.30
2.30 2.30 2.30 2.30 2.30 2.30 2.30 2.30 2.30 2.30 2.30 2.30 2.30 2.30 2.30 2.30 2.30 2.30 2.30 2.30 2.30
2.30 2.30 2.30 2.30 2.30 2.30 2.30 2.30 2.30 2.30 2.30 2.30 2.30 2.30 2.30 2.30 2.30 2.30 2.30 2.30 2.30
2.30 2.30 2.30 2.30 2.30 2.30 2.30 2.30 2.30 2.30 2.30 2.30 2.30 2.30 2.30 2.30 2.30 2.30 2.30 2.30 2.30
2.30 2.30 2.30 2.30 2.30 2.30 2.30 2.30 2.30 2.30 2.30 2.30 2.30 2.30 2.30 2.30 2.30 2.30 2.30 2.30 2.30
2.30 2.30 2.30 2.30 2.30 2.30 2.30 2.30 2.30 2.30 2.30 2.30 2.30 2.30 2.30 2.30 2.30 2.30 2.30 2.30 2.30
2.30 2.30 2.30 2.30 2.30 2.30 2.30 2.30 2.30 2.30 2.30 2.30 2.30 2.30 2.30 2.30 2.30 2.30 2.30 2.30 2.30
2.30 2.30 2.30 2.30 2.30 2.30 2.30 2.30 2.30 2.30 2.30 2.30 2.30 2.30 2.30 2.30 2.30 2.30 2.30 2.30 2.30
2.30 2.30 2.30 2.30 2.30 2.30 2.30 2.30 2.30 2.30 2.30 2.30 2.30 2.30 2.30 2.30 2.30 2.30 2.30 2.30 2.30
2.30 2.30 2.30 2.30 2.30 2.30 2.30 2.30 2.30 2.30 2.30 2.30 2.30 2.30 2.30 2.30 2.30 2.30 2.30 2.30 2.30
2.30 2.30 2.30 2.30 2.30 2.30 2.30 2.30 2.30 2.30 2.30 2.30 2.30 2.30 2.30 2.30 2.30 2.30 2.30 2.30 2.30
2.30 2.30 2.30 2.30 2.30 2.30 2.30 2.30 2.30 2.30 2.30 2.30 2.30 2.30 2.30 2.30 2.30 2.30 2.30 2.30 2.30
2.30 2.30 2.30 2.30 2.30 2.30 2.30 2.30 2.30 2.30 2.30 2.30 2.30 2.30 2.30 2.30 2.30 2.30 2.30 2.30 2.30
2.30 2.30 2.30 2.30 2.30 2.30 2.30 2.30 2.30 2.30 2.30 2.30 2.30 2.30 2.30 2.30 2.30 2.30 2.30 2.30 2.30
2.30 2.30 2.30 2.30 2.30 2.30 2.30 2.30 2.30 2.30 2.30 2.30 2.30 2.30 2.30 2.30 2.30 2.30 2.30 2.30 2.30
2.30 2.30 2.30 2.30 2.30 2.30 2.30 2.30 2.30 2.30 2.30 2.30 2.30 2.30 2.30 2.30 2.30 2.30 2.30 2.30 2.30
2.30 2.30 2.30 2.30 2.30 2.30 2.30 2.30 2.30 2.30 2.30 2.30 2.30 2.30 2.30 2.30 2.30 2.30 2.30 2.30 2.30
2.30 2.30 2.30 2.30 2.30 2.30 2.30 2.30 2.30 2.30 2.30 2.30 2.30 2.30 2.30 2.30 2.30 2.30 2.30 2.30 2.30
2.30 2.30 2.30 2.30 2.30 2.30 2.30 2.30 2.30 2.30 2.30 2.30 2.30 2.30 2.30 2.30 2.30 2.30 2.30 2.30 2.30
2.30 2.30 2.30 2.30 2.30 2.30 2.30 2.30 2.30 2.30 2.30 2.30 2.30 2.30 2.30 2.30 2.30 2.30 2.30 2.30 2.30
2.30 2.30 2.30 2.30 2.30 2.30 2.30 2.30 2.30 2.30 2.30 2.30 2.30 2.30 2.30 2.30 2.30 2.30 2.30 2.30 2.30
2.30 2.30 2.30 2.30 2.30 2.30 2.30 2.30 2.30 2.30 2.30 2.30 2.30 2.30 2.30 2.30 2.30 2.30 2.30 2.30 2.30
2.30 2.30 2.30 2.30 2.30 2.30 2.30 2.30 2.30 2.30 2.30 2.30 2.30 2.30 2.30 2.30 2.30 2.30 2.30 2.30 2.30
2.30 2.30 2.30 2.30 2.30 2.30 2.30 2.30 2.30 2.30 2.30 2.30 2.30 2.30 2.30 2.30 2.30 2.30 2.30 2.30 2.30
2.30 2.30 2.30 2.30 2.30 2.30 2.30 2.30 2.30 2.30 2.30 2.30 2.30 2.30 2.30 2.30 2.30 2.30 2.30 2.30 2.30
2.30 2.30 2.30 2.30 2.30 2.30 2.30 2.30 2.30 2.30 2.30 2.30 2.30 2.30 2.30 2.30 2.30 2.30 2.30 2.30 2.30
2.30 2.30 2.30 2.30 2.30 2.30 2.30 2.30 2.30 2.30 2.30 2.30 2.30 2.30 2.30 2.30 2.30 2.30 2.30 2.30 2.30
2.30 2.30 2.30 2.30 2.30 2.30 2.30 2.30 2.30 2.30 2.30 2.30 2.30 2.30 2.30 2.30 2.30 2.30 2.30 2.30 2.30
2.30 2.30 2.30 2.30 2.30 2.30 2.30 2.30 2.30 2.30 2.30 2.30 2.30 2.30 2.30 2.30 2.30 2.30 2.30 2.30 2.30
2.30 2.30 2.30 2.30 2.30 2.30 2.30 2.30 2.30 2.30 2.30 2.30 2.30 2.30 2.30 2.30 2.30 2.30 2.30 2.30 2.30
2.30 2.30 2.30 2.30 2.30 2.30 2.30 2.30 2.30 2.30 2.30 2.30 2.30 2.30 2.30 2.30 2.30 2.30 2.30 2.30 2.30
2.30 2.30 2.30 2.30 2.30 2.30 2.30 2.30 2.30 2.30 2.30 2.30 2.30 2.30 2.30 2.30 2.30 2.30 2.30 2.30 2.30
2.30 2.30 2.30 2.30 2.30 2.30 2.30 2.30 2.30 2.30 2.30 2.30 2.30 2.30 2.30 2.30 2.30 2.30 2.30 2.30 2.30
2.30 2.30 2.30 2.30 2.30 2.30 2.30 2.30 2.30 2.30 2.30 2.30 2.30 2.30 2.30 2.30 2.30 2.30 2.30 2.30 2.30
2.30 2.30 2.30 2.30 2.30 2.30 2.30 2.30 2.30 2.30 2.30 2.30 2.30 2.30 2.30 2.30 2.30 2.30 2.30 2.30 2.30
2.30 2.30 2.30 2.30 2.30 2.30 2.30 2.30 2.30 2.30 2.30 2.30 2.30 2.30 2.30 2.30 2.30 2.30 2.30 2.30 2.30
2.30 2.30 2.30 2.30 2.30 2.30 2.30 2.30 2.30 2.30 2.30 2.30 2.30 2.30 2.30 2.30 2.30 2.30 2.30 2.30 2.30
2.30 2.30 2.30 2.30 2.30 2.30 2.30 2.30 2.30 2.30 2.30 2.30 2.30 2.30 2.30 2.30 2.30 2.30 2.30 2.30 2.30
2.30 2.30 2.30 2.30 2.30 2.30 2.30 2.30 2.30 2.30 2.30 2.30 2.30 2.30 2.30 2.30 2.30 2.30 2.30 2.30 2.30
2.30 2.30 2.30 2.30 2.30 2.30 2.30 2.30 2.30 2.30 2.30 2.30 2.30 2.30 2.30 2.30 2.30 2.30 2.30 2.30 2.30
2.30 2.30 2.30 2.30 2.30 2.30 2.30 2.30 2.30 2.30 2.30 2.30 2.30 2.30 2.30 2.30 2.30 2.30 2.30 2.30 2.30
2.30 2.30 2.30 2.30 2.30 2.30 2.30 2.30 2.30 2.30 2.30 2.30 2.30 2.30 2.30 2.30 2.30 2.30 2.30 2.30 2.30
2.30 2.30 2.30 2.30 2.30 2.30 2.30 2.30 2.30 2.30 2.30 2.30 2.30 2.30 2.30 2.30 2.30 2.30 2.30 2.30 2.30
2.30 2.30 2.30 2.30 2.30 2.30 2.30 2.30 2.30 2.30 2.30 2.30 2.30 2.30 2.30 2.30 2.30 2.30 2.30 2.30 2.30
2.30 2.30 2.30 2.30 2.30 2.30 2.30 2.30 2.30 2.30 2.30 2.30 2.30 2.30 2.30 2.30 2.30 2.30 2.30 2.30 2.30
2.30 2.30 2.30 2.30 2.30 2.30 2.30 2.30 2.30 2.30 2.30 2.30 2.30 2.30 2.30 2.30 2.30 2.30 2.30 2.30 2.30
2.30 2.30 2.30 2.30 2.30 2.30 2.30 2.30 2.30 2.30 2.30 2.30 2.30 2.30 2.30 2.30 2.30 2.30 2.30 2.30 2.30
2.30 2.30 2.30 2.30 2.30 2.30 2.30 2.30 2.30 2.30 2.30 2.30 2.30 2.30 2.30 2.30 2.30 2.30 2.30 2.30 2.30
2.30 2.30 2.30 2.30 2.30 2.30 2.30 2.30 2.30 2.30 2.30 2.30 2.30 2.30 2.30 2.30 2.30 2.30 2.30 2.30 2.30
2.30 2.30 2.30 2.30 2.30 2.30 2.30 2.30 2.30 2.30 2.30 2.30 2.30 2.30 2.30 2.30 2.30 2.30 2.30 2.30 2.30
2.30 2.30 2.30 2.30 2.30 2.30 2.30 2.30 2.30 2.30 2.30 2.30 2.30 2.30 2.30 2.30 2.30 2.30 2.30 2.30 2.30
2.30 2.30 2.30 2.30 2.30 2.30 2.30 2.30 2.30 2.30 2.30 2.30 2.30 2.30 2.30 2.30 2.30 2.30 2.30 2.30 2.30
2.30 2.30 2.30 2.30 2.30 2.30 2.30 2.30 2.30 2.30 2.30 2.30 2.30 2.30 2.30 2.30 2.30 2.30 2.30 2.30 2.30
2.30 2.30 2.30 2.30 2.30 2.30 2.30 2.30 2.30 2.30 2.30 2.30 2.30 2.30 2.30 2.30 2.30 2.30 2.30 2.30 2.30
2.30 2.30 2.30 2.30 2.30 2.30 2.30 2.30 2.30 2.30 2.30 2.30 2.30 2.30 2.30 2.30 2.30 2.30 2.30 2.30 2.30
2.30 2.30 2.30 2.30 2.30 2.30 2.30 2.30 2.30 2.30 2.30 2.30 2.30 2.30 2.30 2.30 2.30 2.30 2.30 2.30 2.30
2.30 2.30 2.30 2.30 2.30 2.30 2.30 2.30 2.30 2.30 2.30 2.30 2.30 2.30 2.30 2.30 2.30 2.30 2.30 2.30 2.30

2.30 2.30 2.30 2.30 2.30 2.30 2.30 2.30 2.30 2.30 2.30 2.30 2.30 2.30 2.30 2.30 2.30 2.30 2.30 2.30 2.30
2.30 2.30 2.30 2.30 2.30 2.30 2.30 2.30 2.30 2.30 2.30 2.30 2.30 2.30 2.30 2.30 2.30 2.30 2.30 2.30 2.30
2.30 2.30 2.30 2.30 2.30 2.30 2.30 2.30 2.30 2.30 2.30 2.30 2.30 2.30 2.30 2.30 2.30 2.30 2.30 2.30 2.30
2.30 2.30 2.30 2.30 2.30 2.30 2.30 2.30 2.30 2.30 2.30 2.30 2.30 2.30 2.30 2.30 2.30 2.30 2.30 2.30 2.30
2.30 2.30 2.30 2.30 2.30 2.30 2.30 2.30 2.30 2.30 2.30 2.30 2.30 2.30 2.30 2.30 2.30 2.30 2.30 2.30 2.30
2.30 2.30 2.30 2.30 2.30 2.30 2.30 2.30 2.30 2.30 2.30 2.30 2.30 2.30 2.30 2.30 2.30 2.30 2.30 2.30 2.30
2.30 2.30 2.30 2.30 2.30 2.30 2.30 2.30 2.30 2.30 2.30 2.30 2.30 2.30 2.30 2.30 2.30 2.30 2.30 2.30 2.30
2.30 2.30 2.30 2.30 2.30 2.30 2.30 2.30 2.30 2.30 2.30 2.30 2.30 2.30 2.30 2.30 2.30 2.30 2.30 2.30 2.30
2.30 2.30 2.30 2.30 2.30 2.30 2.30 2.30 2.30 2.30 2.30 2.30 2.30 2.30 2.30 2.30 2.30 2.30 2.30 2.30 2.30
2.30 2.30 2.30 2.30 2.30 2.30 2.30 2.30 2.30 2.30 2.30 2.30 2.30 2.30 2.30 2.30 2.30 2.30 2.30 2.30 2.30
2.30 2.30 2.30 2.30 2.30 2.30 2.30 2.30 2.30 2.30 2.30 2.30 2.30 2.30 2.30 2.30 2.30 2.30 2.30 2.30 2.30
2.30 2.30 2.30 2.30 2.30 2.30 2.30 2.30 2.30 2.30 2.30 2.30 2.30 2.30 2.30 2.30 2.30 2.30 2.30 2.30 2.30
2.30 2.30 2.30 2.30 2.30 2.30 2.30 2.30 2.30 2.30 2.30 2.30 2.30 2.30 2.30 2.30 2.30 2.30 2.30 2.30 2.30
2.30 2.30 2.30 2.30 2.30 2.30 2.30 2.30 2.30 2.30 2.30 2.30 2.30 2.30 2.30 2.30 2.30 2.30 2.30 2.30 2.30
2.30 2.30 2.30 2.30 2.30 2.30 2.30 2.30 2.30 2.30 2.30 2.30 2.30 2.30 2.30 2.30 2.30 2.30 2.30 2.30 2.30
2.30 2.30 2.30 2.30 2.30 2.30 2.30 2.30 2.30 2.30 2.30 2.30 2.30 2.30 2.30 2.30 2.30 2.30 2.30 2.30 2.30
2.30 2.30 2.30 2.30 2.30 2.30 2.30 2.30 2.30 2.30 2.30 2.30 2.30 2.30 2.30 2.30 2.30 2.30 2.30 2.30 2.30
2.30 2.30 2.30 2.30 2.30 2.30 2.30 2.30 2.30 2.30 2.30 2.30 2.30 2.30 2.30 2.30 2.30 2.30 2.30 2.30 2.30
2.30 2.30 2.30 2.30 2.30 2.30 2.30 2.30 2.30 2.30 2.30 2.30 2.30 2.30 2.30 2.30 2.30 2.30 2.30 2.30 2.30
2.30 2.30 2.30 2.30 2.30 2.30 2.30 2.30 2.30 2.30 2.30 2.30 2.30 2.30 2.30 2.30 2.30 2.30 2.30 2.30 2.30
2.30 2.30 2.30 2.30 2.30 2.30 2.30 2.30 2.30 2.30 2.30 2.30 2.30 2.30 2.30 2.30 2.30 2.30 2.30 2.30 2.30
2.30 2.30 2.30 2.30 2.30 2.30 2.30 2.30 2.30 2.30 2.30 2.30 2.30 2.30 2.30 2.30 2.30 2.30 2.30 2.30 2.30
2.30 2.30 2.30 2.30 2.30 2.30 2.30 2.30 2.30 2.30 2.30 2.30 2.30 2.30 2.30 2.30 2.30 2.30 2.30 2.30 2.30
2.30 2.30 2.30 2.30 2.30 2.30 2.30 2.30 2.30 2.30 2.30 2.30 2.30 2.30 2.30 2.30 2.30 2.30 2.30 2.30 2.30
2.30 2.30 2.30 2.30 2.30 2.30 2.30 2.30 2.30 2.30 2.30 2.30 2.30 2.30 2.30 2.30 2.30 2.30 2.30 2.30 2.30
2.30 2.30 2.30 2.30 2.30 2.30 2.30 2.30 2.30 2.30 2.30 2.30 2.30 2.30 2.30 2.30 2.30 2.30 2.30 2.30 2.30
2.30 2.30 2.30 2.30 2.30 2.30 2.30 2.30 2.30 2.30 2.30 2.30 2.30 2.30 2.30 2.30 2.30 2.30 2.30 2.30 2.30
2.30 2.30 2.30 2.30 2.30 2.30 2.30 2.30 2.30 2.30 2.30 2.30 2.30 2.30 2.30 2.30 2.30 2.30 2.30 2.30 2.30
2.30 2.30 2.30 2.30 2.30 2.30 2.30 2.30 2.30 2.30 2.30 2.30 2.30 2.30 2.30 2.30 2.30 2.30 2.30 2.30 2.30
2.30 2.30 2.30 2.30 2.30 2.30 2.30 2.30 2.30 2.30 2.30 2.30 2.30 2.30 2.30 2.30 2.30 2.30 2.30 2.30 2.30
2.30 2.30 2.30 2.30 2.30 2.30 2.30 2.30 2.30 2.30 2.30 2.30 2.30 2.30 2.30 2.30 2.30 2.30 2.30 2.30 2.30
2.30 2.30 2.30 2.30 2.30 2.30 2.30 2.30 2.30 2.30 2.30 2.30 2.30 2.30 2.30 2.30 2.30 2.30 2.30 2.30 2.30
2.30 2.30 2.30 2.30 2.30 2.30 2.30 2.30 2.30 2.30 2.30 2.30 2.30 2.30 2.30 2.30 2.30 2.30 2.30 2.30 2.30
2.30 2.30 2.30 2.30 2.30 2.30 2.30 2.30 2.30 2.30 2.30 2.30 2.30 2.30 2.30 2.30 2.30 2.30 2.30 2.30 2.30
2.30 2.30 2.30 2.30 2.30 2.30 2.30 2.30 2.30 2.30 2.30 2.30 2.30 2.30 2.30 2.30 2.30 2.30 2.30 2.30 2.30
2.30 2.30 2.30 2.30 2.30 2.30 2.30 2.30 2.30 2.30 2.30 2.30 2.30 2.30 2.30 2.30 2.30 2.30 2.30 2.30 2.30
2.30 2.30 2.30 2.30 2.30 2.30 2.30 2.30 2.30 2.30 2.30 2.30 2.30 2.30 2.30 2.30 2.30 2.30 2.30 2.30 2.30
2.30 2.30 2.30 2.30 2.30 2.30 2.30 2.30 2.30 2.30 2.30 2.30 2.30 2.30 2.30 2.30 2.30 2.30 2.30 2.30 2.30
2.30 2.30 2.30 2.30 2.30 2.30 2.30 2.30 2.30 2.30 2.30 2.30 2.30 2.30 2.30 2.30 2.30 2.30 2.30 2.30 2.30
2.30 2.30 2.30 2.30 2.30 2.30 2.30 2.30 2.30 2.30 2.30 2.30 2.30 2.30 2.30 2.30 2.30 2.30 2.30 2.30 2.30
2.30 2.30 2.30 2.30 2.30 2.30 2.30 2.30 2.30 2.30 2.30 2.30 2.30 2.30 2.30 2.30 2.30 2.30 2.30 2.30 2.30
2.30 2.30 2.30 2.30 2.30 2.30 2.30 2.30 2.30 2.30 2.30 2.30 2.30 2.30 2.30 2.30 2.30 2.30 2.30 2.30 2.30
2.30 2.30 2.30 2.30 2.30 2.30 2.30 2.30 2.30 2.30 2.30 2.30 2.30 2.30 2.30 2.30 2.30 2.30 2.30 2.30 2.30
2.30 2.30 2.30 2.30 2.30 2.30 2.30 2.30 2.30 2.30 2.30 2.30 2.30 2.30 2.30 2.30 2.30 2.30 2.30 2.30 2.30
2.30 2.30 2.30 2.30 2.30 2.30 2.30 2.30 2.30 2.30 2.30 2.30 2.30 2.30 2.30 2.30 2.30 2.30 2.30 2.30 2.30
2.30 2.30 2.30 2.30 2.30 2.30 2.30 2.30 2.30 2.30 2.30 2.30 2.30 2.30 2.30 2.30 2.30 2.30 2.30 2.30 2.30
2.30 2.30 2.30 2.30 2.30 2.30 2.30 2.30 2.30 2.30 2.30 2.30 2.30 2.30 2.30 2.30 2.30 2.30 2.30 2.30 2.30
2.30 2.30 2.30 2.30 2.30 2.30 2.30 2.30 2.30 2.30 2.30 2.30 2.30 2.30 2.30 2.30 2.30 2.30 2.30 2.30 2.30
2.30 2.30 2.30 2.30 2.30 2.30 2.30 2.30 2.30 2.30 2.30 2.30 2.30 2.30 2.30 2.30 2.30 2.30 2.30 2.30 2.30
2.30 2.30 2.30 2.30 2.30 2.30 2.30 2.30 2.30 2.30 2.30 2.30 2.30 2.30 2.30 2.30 2.30 2.30 2.30 2.30 2.30
2.30 2.30 2.30 2.30 2.30 2.30 2.30 2.30 2.30 2.30 2.30 2.30 2.30 2.30 2.30 2.30 2.30 2.30 2.30 2.30 2.30
2.30 2.30 2.30 2.30 2.30 2.30 2.30 2.30 2.30 2.30 2.30 2.30 2.30 2.30 2.30 2.30 2.30 2.30 2.30 2.30 2.30
2.30 2.30 2.30 2.30 2.30 2.30 2.30 2.30 2.30 2.30 2.30 2.30 2.30 2.30 2.30 2.30 2.30 2.30 2.30 2.30 2.30
2.30 2.30 2.30 2.30 2.30 2.30 2.30 2.30 2.30 2.30 2.30 2.30 2.30 2.30 2.30 2.30 2.30 2.30 2.30 2.30 2.30
2.30 2.30 2.30 2.30 2.30 2.30 2.30 2.30 2.30 2.30 2.30 2.30 2.30 2.30 2.30 2.30 2.30 2.30 2.30 2.30 2.30
2.30 2.30 2.30 2.30 2.30 2.30 2.30 2.30 2.30 2.30 2.30 2.30 2.30 2.30 2.30 2.30 2.30 2.30 2.30 2.30 2.30
2.30 2.30 2.30 2.30 2.30 2.30 2.30 2.30 2.30 2.30 2.30 2.30 2.30 2.30 2.30 2.30 2.30 2.30 2.30 2.30 2.30
2.30 2.30 2.30 2.30 2.30 2.30 2.30 2.30 2.30 2.30 2.30 2.30 2.30 2.30 2.30 2.30 2.30 2.30 2.30 2.30 2.30
2.30 2.30 2.30 2.30 2.30 2.30 2.30 2.30 2.30 2.30 2.30 2.30 2.30 2.30 2.30 2.30 2.30 2.30 2.30 2.30 2.30
2.30 2.30 2.30 2.30 2.30 2.30 2.30 2.30 2.30 2.30 2.30 2.30 2.30 2.30 2.30 2.30 2.30 2.30 2.30 2.30 2.30
2.30 2.30 2.30 2.30 2.30 2.30 2.30 2.30 2.30 2.30 2.30 2.30 2.30 2.30 2.30 2.30 2.30 2.30 2.30 2.30 2.30
2.30 2.30 2.30 2.30 2.30 2.30 2.30 2.30 2.30 2.30 2.30 2.30 2.30 2.30 2.30 2.30 2.30 2.30 2.30 2.30 2.30
2.30 2.30 2.30 2.30 2.30 2.30 2.30 2.30 2.30 2.30 2.30 2.30 2.30 2.30 2.30 2.30 2.30 2.30 2.30 2.30 2.30
2.30 2.30 2.30 2.30 2.30 2.30 2.30 2.30 2.30 2.30 2.30 2.30 2.30 2.30 2.30 2.30 2.30 2.30 2.30 2.30 2.30
2.30 2.30 2.30 2.30 2.30 2.30 2.30 2.30 2.30 2.30 2.30 2.30 2.30 2.30 2.30 2.30 2.30 2.30 2.30 2.30 2.30
2.30 2.30 2.30 2.30 2.30 2.30 2.30 2.30 2.30 2.30 2.30 2.30 2.30 2.30 2.30 2.30 2.30 2.30 2.30 2.30 2.30
2.30 2.30 2.30 2.30 2.30 2.30 2.30 2.30 2.30 2.30 2.30 2.30 2.30 2.30 2.30 2.30 2.30 2.30 2.30 2.30 2.30
2.30 2.30 2.30 2.30 2.30 2.30 2.30 2.30 2.30 2.30 2.30 2.30 2.30 2.30 2.30 2.30 2.30 2.30 2.30 2.30 2.30
2.30 2.30 2.30 2.30 2.30 2.30 2.30 2.30 2.30 2.30 2.30 2.30 2.30 2.30 2.30 2.30 2.30 2.30 2.30 2.30 2.30
2.30 2.30 2.30 2.30 2.30 2.30 2.30 2.30 2.30 2.30 2.30 2.30 2.30 2.30 2.30 2.30 2.30 2.30 2.30 2.30 2.30

2.30 2.30 2.30 2.30 2.30 2.30 2.30 2.30 2.30 2.30 2.30 2.30 2.30 2.30 2.30 2.30 2.30 2.30 2.30 2.30 2.30
2.30 2.30 2.30 2.30 2.30 2.30 2.30 2.30 2.30 2.30 2.30 2.30 2.30 2.30 2.30 2.30 2.30 2.30 2.30 2.30 2.30
2.30 2.30 2.30 2.30 2.30 2.30 2.30 2.30 2.30 2.30 2.30 2.30 2.30 2.30 2.30 2.30 2.30 2.30 2.30 2.30 2.30
2.30 2.30 2.30 2.30 2.30 2.30 2.30 2.30 2.30 2.30 2.30 2.30 2.30 2.30 2.30 2.30 2.30 2.30 2.30 2.30 2.30
2.30 2.30 2.30 2.30 2.30 2.30 2.30 2.30 2.30 2.30 2.30 2.30 2.30 2.30 2.30 2.30 2.30 2.30 2.30 2.30 2.30
2.30 2.30 2.30 2.30 2.30 2.30 2.30 2.30 2.30 2.30 2.30 2.30 2.30 2.30 2.30 2.30 2.30 2.30 2.30 2.30 2.30
2.30 2.30 2.30 2.30 2.30 2.30 2.30 2.30 2.30 2.30 2.30 2.30 2.30 2.30 2.30 2.30 2.30 2.30 2.30 2.30 2.30
2.30 2.30 2.30 2.30 2.30 2.30 2.30 2.30 2.30 2.30 2.30 2.30 2.30 2.30 2.30 2.30 2.30 2.30 2.30 2.30 2.30
2.30 2.30 2.30 2.30 2.30 2.30 2.30 2.30 2.30 2.30 2.30 2.30 2.30 2.30 2.30 2.30 2.30 2.30 2.30 2.30 2.30
2.30 2.30 2.30 2.30 2.30 2.30 2.30 2.30 2.30 2.30 2.30 2.30 2.30 2.30 2.30 2.30 2.30 2.30 2.30 2.30 2.30
2.30 2.30 2.30 2.30 2.30 2.30 2.30 2.30 2.30 2.30 2.30 2.30 2.30 2.30 2.30 2.30 2.30 2.30 2.30 2.30 2.30
2.30 2.30 2.30 2.30 2.30 2.30 2.30 2.30 2.30 2.30 2.30 2.30 2.30 2.30 2.30 2.30 2.30 2.30 2.30 2.30 2.30
2.30 2.30 2.30 2.30 2.30 2.30 2.30 2.30 2.30 2.30 2.30 2.30 2.30 2.30 2.30 2.30 2.30 2.30 2.30 2.30 2.30
2.30 2.30 2.30 2.30 2.30 2.30 2.30 2.30 2.30 2.30 2.30 2.30 2.30 2.30 2.30 2.30 2.30 2.30 2.30 2.30 2.30
2.30 2.30 2.30 2.30 2.30 2.30 2.30 2.30 2.30 2.30 2.30 2.30 2.30 2.30 2.30 2.30 2.30 2.30 2.30 2.30 2.30
2.30 2.30 2.30 2.30 2.30 2.30 2.30 2.30 2.30 2.30 2.30 2.30 2.30 2.30 2.30 2.30 2.30 2.30 2.30 2.30 2.30
2.30 2.30 2.30 2.30 2.30 2.30 2.30 2.30 2.30 2.30 2.30 2.30 2.30 2.30 2.30 2.30 2.30 2.30 2.30 2.30 2.30
2.30 2.30 2.30 2.30 2.30 2.30 2.30 2.30 2.30 2.30 2.30 2.30 2.30 2.30 2.30 2.30 2.30 2.30 2.30 2.30 2.30
2.30 2.30 2.30 2.30 2.30 2.30 2.30 2.30 2.30 2.30 2.30 2.30 2.30 2.30 2.30 2.30 2.30 2.30 2.30 2.30 2.30
2.30 2.30 2.30 2.30 2.30 2.30 2.30 2.30 2.30 2.30 2.30 2.30 2.30 2.30 2.30 2.30 2.30 2.30 2.30 2.30 2.30
2.30 2.30 2.30 2.30 2.30 2.30 2.30 2.30 2.30 2.30 2.30 2.30 2.30 2.30 2.30 2.30 2.30 2.30 2.30 2.30 2.30
2.30 2.30 2.30 2.30 2.30 2.30 2.30 2.30 2.30 2.30 2.30 2.30 2.30 2.30 2.30 2.30 2.30 2.30 2.30 2.30 2.30
2.30 2.30 2.30 2.30 2.30 2.30 2.30 2.30 2.30 2.30 2.30 2.30 2.30 2.30 2.30 2.30 2.30 2.30 2.30 2.30 2.30
2.30 2.30 2.30 2.30 2.30 2.30 2.30 2.30 2.30 2.30 2.30 2.30 2.30 2.30 2.30 2.30 2.30 2.30 2.30 2.30 2.30
2.30 2.30 2.30 2.30 2.30 2.30 2.30 2.30 2.30 2.30 2.30 2.30 2.30 2.30 2.30 2.30 2.30 2.30 2.30 2.30 2.30
2.30 2.30 2.30 2.30 2.30 2.30 2.30 2.30 2.30 2.30 2.30 2.30 2.30 2.30 2.30 2.30 2.30 2.30 2.30 2.30 2.30
2.30 2.30 2.30 2.30 2.30 2.30 2.30 2.30 2.30 2.30 2.30 2.30 2.30 2.30 2.30 2.30 2.30 2.30 2.30 2.30 2.30
2.30 2.30 2.30 2.30 2.30 2.30 2.30 2.30 2.30 2.30 2.30 2.30 2.30 2.30 2.30 2.30 2.30 2.30 2.30 2.30 2.30
2.30 2.30 2.30 2.30 2.30 2.30 2.30 2.30 2.30 2.30 2.30 2.30 2.30 2.30 2.30 2.30 2.30 2.30 2.30 2.30 2.30
2.30 2.30 2.30 2.30 2.30 2.30 2.30 2.30 2.30 2.30 2.30 2.30 2.30 2.30 2.30 2.30 2.30 2.30 2.30 2.30 2.30
2.30 2.30 2.30 2.30 2.30 2.30 2.30 2.30 2.30 2.30 2.30 2.30 2.30 2.30 2.30 2.30 2.30 2.30 2.30 2.30 2.30
2.30 2.30 2.30 2.30 2.30 2.30 2.30 2.30 2.30 2.30 2.30 2.30 2.30 2.30 2.30 2.30 2.30 2.30 2.30 2.30 2.30
2.30 2.30 2.30 2.30 2.30 2.30 2.30 2.30 2.30 2.30 2.30 2.30 2.30 2.30 2.30 2.30 2.30 2.30 2.30 2.30 2.30
2.30 2.30 2.30 2.30 2.30 2.30 2.30 2.30 2.30 2.30 2.30 2.30 2.30 2.30 2.30 2.30 2.30 2.30 2.30 2.30 2.30
2.30 2.30 2.30 2.30 2.30 2.30 2.30 2.30 2.30 2.30 2.30 2.30 2.30 2.30 2.30 2.30 2.30 2.30 2.30 2.30 2.30
2.30 2.30 2.30 2.30 2.30 2.30 2.30 2.30 2.30 2.30 2.30 2.30 2.30 2.30 2.30 2.30 2.30 2.30 2.30 2.30 2.30
2.30 2.30 2.30 2.30 2.30 2.30 2.30 2.30 2.30 2.30 2.30 2.30 2.30 2.30 2.30 2.30 2.30 2.30 2.30 2.30 2.30
2.30 2.30 2.30 2.30 2.30 2.30 2.30 2.30 2.30 2.30 2.30 2.30 2.30 2.30 2.30 2.30 2.30 2.30 2.30 2.30 2.30
2.30 2.30 2.30 2.30 2.30 2.30 2.30 2.30 2.30 2.30 2.30 2.30 2.30 2.30 2.30 2.30 2.30 2.30 2.30 2.30 2.30
2.30 2.30 2.30 2.30 2.30 2.30 2.30 2.30 2.30 2.30 2.30 2.30 2.30 2.30 2.30 2.30 2.30 2.30 2.30 2.30 2.30
2.30 2.30 2.30 2.30 2.30 2.30 2.30 2.30 2.30 2.30 2.30 2.30 2.30 2.30 2.30 2.30 2.30 2.30 2.30 2.30 2.30
2.30 2.30 2.30 2.30 2.30 2.30 2.30 2.30 2.30 2.30 2.30 2.30 2.30 2.30 2.30 2.30 2.30 2.30 2.30 2.30 2.30
2.30 2.30 2.30 2.30 2.30 2.30 2.30 2.30 2.30 2.30 2.30 2.30 2.30 2.30 2.30 2.30 2.30 2.30 2.30 2.30 2.30
2.30 2.30 2.30 2.30 2.30 2.30 2.30 2.30 2.30 2.30 2.30 2.30 2.30 2.30 2.30 2.30 2.30 2.30 2.30 2.30 2.30
2.30 2.30 2.30 2.30 2.30 2.30 2.30 2.30 2.30 2.30 2.30 2.30 2.30 2.30 2.30 2.30 2.30 2.30 2.30 2.30 2.30
2.30 2.30 2.30 2.30 2.30 2.30 2.30 2.30 2.30 2.30 2.30 2.30 2.30 2.30 2.30 2.30 2.30 2.30 2.30 2.30 2.30
2.30 2.30 2.30 2.30 2.30 2.30 2.30 2.30 2.30 2.30 2.30 2.30 2.30 2.30 2.30 2.30 2.30 2.30 2.30 2.30 2.30
2.30 2.30 2.30 2.30 2.30 2.30 2.30 2.30 2.30 2.30 2.30 2.30 2.30 2.30 2.30 2.30 2.30 2.30 2.30 2.30 2.30
2.30 2.30 2.30 2.30 2.30 2.30 2.30 2.30 2.30 2.30 2.30 2.30 2.30 2.30 2.30 2.30 2.30 2.30 2.30 2.30 2.30
2.30 2.30 2.30 2.30 2.30 2.30 2.30 2.30 2.30 2.30 2.30 2.30 2.30 2.30 2.30 2.30 2.30 2.30 2.30 2.30 2.30
2.30 2.30 2.30 2.30 2.30 2.30 2.30 2.30 2.30 2.30 2.30 2.30 2.30 2.30 2.30 2.30 2.30 2.30 2.30 2.30 2.30
2.30 2.30 2.30 2.30 2.30 2.30 2.30 2.30 2.30 2.30 2.30 2.30 2.30 2.30 2.30 2.30 2.30 2.30 2.30 2.30 2.30
2.30 2.30 2.30 2.30 2.30 2.30 2.30 2.30 2.30 2.30 2.30 2.30 2.30 2.30 2.30 2.30 2.30 2.30 2.30 2.30 2.30
2.30 2.30 2.30 2.30 2.30 2.30 2.30 2.30 2.30 2.30 2.30 2.30 2.30 2.30 2.30 2.30 2.30 2.30 2.30 2.30 2.30
2.30 2.30 2.30 2.30 2.30 2.30 2.30 2.30 2.30 2.30 2.30 2.30 2.30 2.30 2.30 2.30 2.30 2.30 2.30 2.30 2.30
2.30 2.30 2.30 2.30 2.30 2.30 2.30 2.30 2.30 2.30 2.30 2.30 2.30 2.30 2.30 2.30 2.30 2.30 2.30 2.30 2.30
2.30 2.30 2.30 2.30 2.30 2.30 2.30 2.30 2.30 2.30 2.30 2.30 2.30 2.30 2.30 2.30 2.30 2.30 2.30 2.30 2.30
2.30 2.30 2.30 2.30 2.30 2.30 2.30 2.30 2.30 2.30 2.30 2.30 2.30 2.30 2.30 2.30 2.30 2.30 2.30 2.30 2.30
2.30 2.30 2.30 2.30 2.30 2.30 2.30 2.30 2.30 2.30 2.30 2.30 2.30 2.30 2.30 2.30 2.30 2.30 2.30 2.30 2.30
2.30 2.30 2.30 2.30 2.30 2.30 2.30 2.30 2.30 2.30 2.30 2.30 2.30 2.30 2.30 2.30 2.30 2.30 2.30 2.30 2.30
2.30 2.30 2.30 2.30 2.30 2.30 2.30 2.30 2.30 2.30 2.30 2.30 2.30 2.30 2.30 2.30 2.30 2.30 2.30 2.30 2.30
2.30 2.30 2.30 2.30 2.30 2.30 2.30 2.30 2.30 2.30 2.30 2.30 2.30 2.30 2.30 2.30 2.30 2.30 2.30 2.30 2.30
2.30 2.30 2.30 2.30 2.30 2.30 2.30 2.30 2.30 2.30 2.30 2.30 2.30 2.30 2.30 2.30 2.30 2.30 2.30 2.30 2.30
2.30 2.30 2.30 2.30 2.30 2.30 2.30 2.30 2.30 2.30 2.30 2.30 2.30 2.30 2.30 2.30 2.30 2.30 2.30 2.30 2.30
2.30 2.30 2.30 2.30 2.30 2.30 2.30 2.30 2.30 2.30 2.30 2.30 2.30 2.30 2.30 2.30 2.30 2.30 2.30 2.30 2.30
2.30 2.30 2.30 2.30 2.30 2.30 2.30 2.30 2.30 2.30 2.30 2.30 2.30 2.30 2.30 2.30 2.30 2.30 2.30 2.30 2.30
2.30 2.30 2.30 2.30 2.30 2.30 2.30 2.30 2.30 2.30 2.30 2.30 2.30 2.30 2.30 2.30 2.30 2.30 2.30 2.30 2.30
2.30 2.30 2.30 2.30 2.30 2.30 2.30 2.30 2.30 2.30 2.30 2.30 2.30 2.30 2.30 2.30 2.30 2.30 2.30 2.30 2.30
2.30 2.30 2.30 2.30 2.30 2.30 2.30 2.30 2.30 2.30 2.30 2.30 2.30 2.30 2.30 2.30 2.30 2.30 2.30 2.30 2.30
2.30 2.30 2.30 2.30 2.30 2.30 2.30 2.30 2.30 2.30 2.30 2.30 2.30 2.30 2.30 2.30 2.30 2.30 2.30 2.30 2.30

2.30 2.30 2.30 2.30 2.30 2.30 2.30 2.30 2.30 2.30 2.30 2.30 2.30 2.30 2.30 2.30 2.30 2.30 2.30 2.30 2.30
2.30 2.30 2.30 2.30 2.30 2.30 2.30 2.30 2.30 2.30 2.30 2.30 2.30 2.30 2.30 2.30 2.30 2.30 2.30 2.30 2.30
2.30 2.30 2.30 2.30 2.30 2.30 2.30 2.30 2.30 2.30 2.30 2.30 2.30 2.30 2.30 2.30 2.30 2.30 2.30 2.30 2.30
2.30 2.30 2.30 2.30 2.30 2.30 2.30 2.30 2.30 2.30 2.30 2.30 2.30 2.30 2.30 2.30 2.30 2.30 2.30 2.30 2.30
2.30 2.30 2.30 2.30 2.30 2.30 2.30 2.30 2.30 2.30 2.30 2.30 2.30 2.30 2.30 2.30 2.30 2.30 2.30 2.30 2.30
2.30 2.30 2.30 2.30 2.30 2.30 2.30 2.30 2.30 2.30 2.30 2.30 2.30 2.30 2.30 2.30 2.30 2.30 2.30 2.30 2.30
2.30 2.30 2.30 2.30 2.30 2.30 2.30 2.30 2.30 2.30 2.30 2.30 2.30 2.30 2.30 2.30 2.30 2.30 2.30 2.30 2.30
2.30 2.30 2.30 2.30 2.30 2.30 2.30 2.30 2.30 2.30 2.30 2.30 2.30 2.30 2.30 2.30 2.30 2.30 2.30 2.30 2.30
2.30 2.30 2.30 2.30 2.30 2.30 2.30 2.30 2.30 2.30 2.30 2.30 2.30 2.30 2.30 2.30 2.30 2.30 2.30 2.30 2.30
2.30 2.30 2.30 2.30 2.30 2.30 2.30 2.30 2.30 2.30 2.30 2.30 2.30 2.30 2.30 2.30 2.30 2.30 2.30 2.30 2.30
2.30 2.30 2.30 2.30 2.30 2.30 2.30 2.30 2.30 2.30 2.30 2.30 2.30 2.30 2.30 2.30 2.30 2.30 2.30 2.30 2.30
2.30 2.30 2.30 2.30 2.30 2.30 2.30 2.30 2.30 2.30 2.30 2.30 2.30 2.30 2.30 2.30 2.30 2.30 2.30 2.30 2.30
2.30 2.30 2.30 2.30 2.30 2.30 2.30 2.30 2.30 2.30 2.30 2.30 2.30 2.30 2.30 2.30 2.30 2.30 2.30 2.30 2.30
2.30 2.30 2.30 2.30 2.30 2.30 2.30 2.30 2.30 2.30 2.30 2.30 2.30 2.30 2.30 2.30 2.30 2.30 2.30 2.30 2.30
2.30 2.30 2.30 2.30 2.30 2.30 2.30 2.30 2.30 2.30 2.30 2.30 2.30 2.30 2.30 2.30 2.30 2.30 2.30 2.30 2.30
2.30 2.30 2.30 2.30 2.30 2.30 2.30 2.30 2.30 2.30 2.30 2.30 2.30 2.30 2.30 2.30 2.30 2.30 2.30 2.30 2.30
2.30 2.30 2.30 2.30 2.30 2.30 2.30 2.30 2.30 2.30 2.30 2.30 2.30 2.30 2.30 2.30 2.30 2.30 2.30 2.30 2.30
2.30 2.30 2.30 2.30 2.30 2.30 2.30 2.30 2.30 2.30 2.30 2.30 2.30 2.30 2.30 2.30 2.30 2.30 2.30 2.30 2.30
2.30 2.30 2.30 2.30 2.30 2.30 2.30 2.30 2.30 2.30 2.30 2.30 2.30 2.30 2.30 2.30 2.30 2.30 2.30 2.30 2.30
2.30 2.30 2.30 2.30 2.30 2.30 2.30 2.30 2.30 2.30 2.30 2.30 2.30 2.30 2.30 2.30 2.30 2.30 2.30 2.30 2.30
2.30 2.30 2.30 2.30 2.30 2.30 2.30 2.30 2.30 2.30 2.30 2.30 2.30 2.30 2.30 2.30 2.30 2.30 2.30 2.30 2.30
2.30 2.30 2.30 2.30 2.30 2.30 2.30 2.30 2.30 2.30 2.30 2.30 2.30 2.30 2.30 2.30 2.30 2.30 2.30 2.30 2.30
2.30 2.30 2.30 2.30 2.30 2.30 2.30 2.30 2.30 2.30 2.30 2.30 2.30 2.30 2.30 2.30 2.30 2.30 2.30 2.30 2.30
2.30 2.30 2.30 2.30 2.30 2.30 2.30 2.30 2.30 2.30 2.30 2.30 2.30 2.30 2.30 2.30 2.30 2.30 2.30 2.30 2.30
2.30 2.30 2.30 2.30 2.30 2.30 2.30 2.30 2.30 2.30 2.30 2.30 2.30 2.30 2.30 2.30 2.30 2.30 2.30 2.30 2.30
2.30 2.30 2.30 2.30 2.30 2.30 2.30 2.30 2.30 2.30 2.30 2.30 2.30 2.30 2.30 2.30 2.30 2.30 2.30 2.30 2.30
2.30 2.30 2.30 2.30 2.30 2.30 2.30 2.30 2.30 2.30 2.30 2.30 2.30 2.30 2.30 2.30 2.30 2.30 2.30 2.30 2.30
2.30 2.30 2.30 2.30 2.30 2.30 2.30 2.30 2.30 2.30 2.30 2.30 2.30 2.30 2.30 2.30 2.30 2.30 2.30 2.30 2.30
2.30 2.30 2.30 2.30 2.30 2.30 2.30 2.30 2.30 2.30 2.30 2.30 2.30 2.30 2.30 2.30 2.30 2.30 2.30 2.30 2.30
2.30 2.30 2.30 2.30 2.30 2.30 2.30 2.30 2.30 2.30 2.30 2.30 2.30 2.30 2.30 2.30 2.30 2.30 2.30 2.30 2.30
2.30 2.30 2.30 2.30 2.30 2.30 2.30 2.30 2.30 2.30 2.30 2.30 2.30 2.30 2.30 2.30 2.30 2.30 2.30 2.30 2.30
2.30 2.30 2.30 2.30 2.30 2.30 2.30 2.30 2.30 2.30 2.30 2.30 2.30 2.30 2.30 2.30 2.30 2.30 2.30 2.30 2.30
2.30 2.30 2.30 2.30 2.30 2.30 2.30 2.30 2.30 2.30 2.30 2.30 2.30 2.30 2.30 2.30 2.30 2.30 2.30 2.30 2.30
2.30 2.30 2.30 2.30 2.30 2.30 2.30 2.30 2.30 2.30 2.30 2.30 2.30 2.30 2.30 2.30 2.30 2.30 2.30 2.30 2.30
2.30 2.30 2.30 2.30 2.30 2.30 2.30 2.30 2.30 2.30 2.30 2.30 2.30 2.30 2.30 2.30 2.30 2.30 2.30 2.30 2.30
2.30 2.30 2.30 2.30 2.30 2.30 2.30 2.30 2.30 2.30 2.30 2.30 2.30 2.30 2.30 2.30 2.30 2.30 2.30 2.30 2.30
2.30 2.30 2.30 2.30 2.30 2.30 2.30 2.30 2.30 2.30 2.30 2.30 2.30 2.30 2.30 2.30 2.30 2.30 2.30 2.30 2.30
2.30 2.30 2.30 2.30 2.30 2.30 2.30 2.30 2.30 2.30 2.30 2.30 2.30 2.30 2.30 2.30 2.30 2.30 2.30 2.30 2.30
2.30 2.30 2.30 2.30 2.30 2.30 2.30 2.30 2.30 2.30 2.30 2.30 2.30 2.30 2.30 2.30 2.30 2.30 2.30 2.30 2.30
2.30 2.30 2.30 2.30 2.30 2.30 2.30 2.30 2.30 2.30 2.30 2.30 2.30 2.30 2.30 2.30 2.30 2.30 2.30 2.30 2.30
2.30 2.30 2.30 2.30 2.30 2.30 2.30 2.30 2.30 2.30 2.30 2.30 2.30 2.30 2.30 2.30 2.30 2.30 2.30 2.30 2.30
2.30 2.30 2.30 2.30 2.30 2.30 2.30 2.30 2.30 2.30 2.30 2.30 2.30 2.30 2.30 2.30 2.30 2.30 2.30 2.30 2.30
2.30 2.30 2.30 2.30 2.30 2.30 2.30 2.30 2.30 2.30 2.30 2.30 2.30 2.30 2.30 2.30 2.30 2.30 2.30 2.30 2.30
2.30 2.30 2.30 2.30 2.30 2.30 2.30 2.30 2.30 2.30 2.30 2.30 2.30 2.30 2.30 2.30 2.30 2.30 2.30 2.30 2.30
2.30 2.30 2.30 2.30 2.30 2.30 2.30 2.30 2.30 2.30 2.30 2.30 2.30 2.30 2.30 2.30 2.30 2.30 2.30 2.30 2.30
2.30 2.30 2.30 2.30 2.30 2.30 2.30 2.30 2.30 2.30 2.30 2.30 2.30 2.30 2.30 2.30 2.30 2.30 2.30 2.30 2.30
2.30 2.30 2.30 2.30 2.30 2.30 2.30 2.30 2.30 2.30 2.30 2.30 2.30 2.30 2.30 2.30 2.30 2.30 2.30 2.30 2.30
2.30 2.30 2.30 2.30 2.30 2.30 2.30 2.30 2.30 2.30 2.30 2.30 2.30 2.30 2.30 2.30 2.30 2.30 2.30 2.30 2.30
2.30 2.30 2.30 2.30 2.30 2.30 2.30 2.30 2.30 2.30 2.30 2.30 2.30 2.30 2.30 2.30 2.30 2.30 2.30 2.30 2.30
2.30 2.30 2.30 2.30 2.30 2.30 2.30 2.30 2.30 2.30 2.30 2.30 2.30 2.30 2.30 2.30 2.30 2.30 2.30 2.30 2.30
2.30 2.30 2.30 2.30 2.30 2.30 2.30 2.30 2.30 2.30 2.30 2.30 2.30 2.30 2.30 2.30 2.30 2.30 2.30 2.30 2.30
2.30 2.30 2.30 2.30 2.30 2.30 2.30 2.30 2.30 2.30 2.30 2.30 2.30 2.30 2.30 2.30 2.30 2.30 2.30 2.30 2.30
2.30 2.30 2.30 2.30 2.30 2.30 2.30 2.30 2.30 2.30 2.30 2.30 2.30 2.30 2.30 2.30 2.30 2.30 2.30 2.30 2.30
2.30 2.30 2.30 2.30 2.30 2.30 2.30 2.30 2.30 2.30 2.30 2.30 2.30 2.30 2.30 2.30 2.30 2.30 2.30 2.30 2.30
2.30 2.30 2.30 2.30 2.30 2.30 2.30 2.30 2.30 2.30 2.30 2.30 2.30 2.30 2.30 2.30 2.30 2.30 2.30 2.30 2.30
2.30 2.30 2.30 2.30 2.30 2.30 2.30 2.30 2.30 2.30 2.30 2.30 2.30 2.30 2.30 2.30 2.30 2.30 2.30 2.30 2.30
2.30 2.30 2.30 2.30 2.30 2.30 2.30 2.30 2.30 2.30 2.30 2.30 2.30 2.30 2.30 2.30 2.30 2.30 2.30 2.30 2.30
2.30 2.30 2.30 2.30 2.30 2.30 2.30 2.30 2.30 2.30 2.30 2.30 2.30 2.30 2.30 2.30 2.30 2.30 2.30 2.30 2.30
2.30 2.30 2.30 2.30 2.30 2.30 2.30 2.30 2.30 2.30 2.30 2.30 2.30 2.30 2.30 2.30 2.30 2.30 2.30 2.30 2.30
2.30 2.30 2.30 2.30 2.30 2.30 2.30 2.30 2.30 2.30 2.30 2.30 2.30 2.30 2.30 2.30 2.30 2.30 2.30 2.30 2.30
2.30 2.30 2.30 2.30 2.30 2.30 2.30 2.30 2.30 2.30 2.30 2.30 2.30 2.30 2.30 2.30 2.30 2.30 2.30 2.30 2.30
2.30 2.30 2.30 2.30 2.30 2.30 2.30 2.30 2.30 2.30 2.30 2.30 2.30 2.30 2.30 2.30 2.30 2.30 2.30 2.30 2.30
2.30 2.30 2.30 2.30 2.30 2.30 2.30 2.30 2.30 2.30 2.30 2.30 2.30 2.30 2.30 2.30 2.30 2.30 2.30 2.30 2.30
2.30 2.30 2.30 2.30 2.30 2.30 2.30 2.30 2.30 2.30 2.30 2.30 2.30 2.30 2.30 2.30 2.30 2.30 2.30 2.30 2.30
2.30 2.30 2.30 2.30 2.30 2.30 2.30 2.30 2.30 2.30 2.30 2.30 2.30 2.30 2.30 2.30 2.30 2.30 2.30 2.30 2.30
2.30 2.30 2.30 2.30 2.30 2.30 2.30 2.30 2.30 2.30 2.30 2.30 2.30 2.30 2.30 2.30 2.30 2.30 2.30 2.30 2.30
2.30 2.30 2.30 2.30 2.30 2.30 2.30 2.30 2.30 2.30 2.30 2.30 2.30 2.30 2.30 2.30 2.30 2.30 2.30 2.30 2.30
2.30 2.30 2.30 2.30 2.30 2.30 2.30 2.30 2.30 2.30 2.30 2.30 2.30 2.30 2.30 2.30 2.30 2.30 2.30 2.30 2.30
2.30 2.30 2.30 2.30 2.30 2.30 2.30 2.30 2.30 2.30 2.30 2.30 2.30 2.30 2.30 2.30 2.30 2.30 2.30 2.30 2.30
2.30 2.30 2.30 2.30 2.30 2.30 2.30 2.30 2.30 2.30 2.30 2.30 2.30 2.30 2.30 2.30 2.30 2.30 2.30 2.30 2.30

2.30 2.30 2.30 2.30 2.30 2.30 2.30 2.30 2.30 2.30 2.30 2.30 2.30 2.30 2.30 2.30 2.30 2.30 2.30 2.30 2.30
2.30 2.30 2.30 2.30 2.30 2.30 2.30 2.30 2.30 2.30 2.30 2.30 2.30 2.30 2.30 2.30 2.30 2.30 2.30 2.30 2.30
2.30 2.30 2.30 2.30 2.30 2.30 2.30 2.30 2.30 2.30 2.30 2.30 2.30 2.30 2.30 2.30 2.30 2.30 2.30 2.30 2.30
2.30 2.30 2.30 2.30 2.30 2.30 2.30 2.30 2.30 2.30 2.30 2.30 2.30 2.30 2.30 2.30 2.30 2.30 2.30 2.30 2.30
2.30 2.30 2.30 2.30 2.30 2.30 2.30 2.30 2.30 2.30 2.30 2.30 2.30 2.30 2.30 2.30 2.30 2.30 2.30 2.30 2.30
2.30 2.30 2.30 2.30 2.30 2.30 2.30 2.30 2.30 2.30 2.30 2.30 2.30 2.30 2.30 2.30 2.30 2.30 2.30 2.30 2.30
2.30 2.30 2.30 2.30 2.30 2.30 2.30 2.30 2.30 2.30 2.30 2.30 2.30 2.30 2.30 2.30 2.30 2.30 2.30 2.30 2.30
2.30 2.30 2.30 2.30 2.30 2.30 2.30 2.30 2.30 2.30 2.30 2.30 2.30 2.30 2.30 2.30 2.30 2.30 2.30 2.30 2.30
2.30 2.30 2.30 2.30 2.30 2.30 2.30 2.30 2.30 2.30 2.30 2.30 2.30 2.30 2.30 2.30 2.30 2.30 2.30 2.30 2.30
2.30 2.30 2.30 2.30 2.30 2.30 2.30 2.30 2.30 2.30 2.30 2.30 2.30 2.30 2.30 2.30 2.30 2.30 2.30 2.30 2.30
2.30 2.30 2.30 2.30 2.30 2.30 2.30 2.30 2.30 2.30 2.30 2.30 2.30 2.30 2.30 2.30 2.30 2.30 2.30 2.30 2.30
2.30 2.30 2.30 2.30 2.30 2.30 2.30 2.30 2.30 2.30 2.30 2.30 2.30 2.30 2.30 2.30 2.30 2.30 2.30 2.30 2.30
2.30 2.30 2.30 2.30 2.30 2.30 2.30 2.30 2.30 2.30 2.30 2.30 2.30 2.30 2.30 2.30 2.30 2.30 2.30 2.30 2.30
2.30 2.30 2.30 2.30 2.30 2.30 2.30 2.30 2.30 2.30 2.30 2.30 2.30 2.30 2.30 2.30 2.30 2.30 2.30 2.30 2.30
2.30 2.30 2.30 2.30 2.30 2.30 2.30 2.30 2.30 2.30 2.30 2.30 2.30 2.30 2.30 2.30 2.30 2.30 2.30 2.30 2.30
2.30 2.30 2.30 2.30 2.30 2.30 2.30 2.30 2.30 2.30 2.30 2.30 2.30 2.30 2.30 2.30 2.30 2.30 2.30 2.30 2.30
2.30 2.30 2.30 2.30 2.30 2.30 2.30 2.30 2.30 2.30 2.30 2.30 2.30 2.30 2.30 2.30 2.30 2.30 2.30 2.30 2.30
2.30 2.30 2.30 2.30 2.30 2.30 2.30 2.30 2.30 2.30 2.30 2.30 2.30 2.30 2.30 2.30 2.30 2.30 2.30 2.30 2.30
2.30 2.30 2.30 2.30 2.30 2.30 2.30 2.30 2.30 2.30 2.30 2.30 2.30 2.30 2.30 2.30 2.30 2.30 2.30 2.30 2.30
2.30 2.30 2.30 2.30 2.30 2.30 2.30 2.30 2.30 2.30 2.30 2.30 2.30 2.30 2.30 2.30 2.30 2.30 2.30 2.30 2.30
2.30 2.30 2.30 2.30 2.30 2.30 2.30 2.30 2.30 2.30 2.30 2.30 2.30 2.30 2.30 2.30 2.30 2.30 2.30 2.30 2.30
2.30 2.30 2.30 2.30 2.30 2.30 2.30 2.30 2.30 2.30 2.30 2.30 2.30 2.30 2.30 2.30 2.30 2.30 2.30 2.30 2.30
2.30 2.30 2.30 2.30 2.30 2.30 2.30 2.30 2.30 2.30 2.30 2.30 2.30 2.30 2.30 2.30 2.30 2.30 2.30 2.30 2.30
2.30 2.30 2.30 2.30 2.30 2.30 2.30 2.30 2.30 2.30 2.30 2.30 2.30 2.30 2.30 2.30 2.30 2.30 2.30 2.30 2.30
2.30 2.30 2.30 2.30 2.30 2.30 2.30 2.30 2.30 2.30 2.30 2.30 2.30 2.30 2.30 2.30 2.30 2.30 2.30 2.30 2.30
2.30 2.30 2.30 2.30 2.30 2.30 2.30 2.30 2.30 2.30 2.30 2.30 2.30 2.30 2.30 2.30 2.30 2.30 2.30 2.30 2.30
2.30 2.30 2.30 2.30 2.30 2.30 2.30 2.30 2.30 2.30 2.30 2.30 2.30 2.30 2.30 2.30 2.30 2.30 2.30 2.30 2.30
2.30 2.30 2.30 2.30 2.30 2.30 2.30 2.30 2.30 2.30 2.30 2.30 2.30 2.30 2.30 2.30 2.30 2.30 2.30 2.30 2.30
2.30 2.30 2.30 2.30 2.30 2.30 2.30 2.30 2.30 2.30 2.30 2.30 2.30 2.30 2.30 2.30 2.30 2.30 2.30 2.30 2.30
2.30 2.30 2.30 2.30 2.30 2.30 2.30 2.30 2.30 2.30 2.30 2.30 2.30 2.30 2.30 2.30 2.30 2.30 2.30 2.30 2.30
2.30 2.30 2.30 2.30 2.30 2.30 2.30 2.30 2.30 2.30 2.30 2.30 2.30 2.30 2.30 2.30 2.30 2.30 2.30 2.30 2.30
2.30 2.30 2.30 2.30 2.30 2.30 2.30 2.30 2.30 2.30 2.30 2.30 2.30 2.30 2.30 2.30 2.30 2.30 2.30 2.30 2.30
2.30 2.30 2.30 2.30 2.30 2.30 2.30 2.30 2.30 2.30 2.30 2.30 2.30 2.30 2.30 2.30 2.30 2.30 2.30 2.30 2.30
2.30 2.30 2.30 2.30 2.30 2.30 2.30 2.30 2.30 2.30 2.30 2.30 2.30 2.30 2.30 2.30 2.30 2.30 2.30 2.30 2.30
2.30 2.30 2.30 2.30 2.30 2.30 2.30 2.30 2.30 2.30 2.30 2.30 2.30 2.30 2.30 2.30 2.30 2.30 2.30 2.30 2.30
2.30 2.30 2.30 2.30 2.30 2.30 2.30 2.30 2.30 2.30 2.30 2.30 2.30 2.30 2.30 2.30 2.30 2.30 2.30 2.30 2.30
2.30 2.30 2.30 2.30 2.30 2.30 2.30 2.30 2.30 2.30 2.30 2.30 2.30 2.30 2.30 2.30 2.30 2.30 2.30 2.30 2.30
2.30 2.30 2.30 2.30 2.30 2.30 2.30 2.30 2.30 2.30 2.30 2.30 2.30 2.30 2.30 2.30 2.30 2.30 2.30 2.30 2.30
2.30 2.30 2.30 2.30 2.30 2.30 2.30 2.30 2.30 2.30 2.30 2.30 2.30 2.30 2.30 2.30 2.30 2.30 2.30 2.30 2.30
2.30 2.30 2.30 2.30 2.30 2.30 2.30 2.30 2.30 2.30 2.30 2.30 2.30 2.30 2.30 2.30 2.30 2.30 2.30 2.30 2.30
2.30 2.30 2.30 2.30 2.30 2.30 2.30 2.30 2.30 2.30 2.30 2.30 2.30 2.30 2.30 2.30 2.30 2.30 2.30 2.30 2.30
2.30 2.30 2.30 2.30 2.30 2.30 2.30 2.30 2.30 2.30 2.30 2.30 2.30 2.30 2.30 2.30 2.30 2.30 2.30 2.30 2.30
2.30 2.30 2.30 2.30 2.30 2.30 2.30 2.30 2.30 2.30 2.30 2.30 2.30 2.30 2.30 2.30 2.30 2.30 2.30 2.30 2.30
2.30 2.30 2.30 2.30 2.30 2.30 2.30 2.30 2.30 2.30 2.30 2.30 2.30 2.30 2.30 2.30 2.30 2.30 2.30 2.30 2.30
2.30 2.30 2.30 2.30 2.30 2.30 2.30 2.30 2.30 2.30 2.30 2.30 2.30 2.30 2.30 2.30 2.30 2.30 2.30 2.30 2.30
2.30 2.30 2.30 2.30 2.30 2.30 2.30 2.30 2.30 2.30 2.30 2.30 2.30 2.30 2.30 2.30 2.30 2.30 2.30 2.30 2.30
2.30 2.30 2.30 2.30 2.30 2.30 2.30 2.30 2.30 2.30 2.30 2.30 2.30 2.30 2.30 2.30 2.30 2.30 2.30 2.30 2.30
2.30 2.30 2.30 2.30 2.30 2.30 2.30 2.30 2.30 2.30 2.30 2.30 2.30 2.30 2.30 2.30 2.30 2.30 2.30 2.30 2.30
2.30 2.30 2.30 2.30 2.30 2.30 2.30 2.30 2.30 2.30 2.30 2.30 2.30 2.30 2.30 2.30 2.30 2.30 2.30 2.30 2.30
2.30 2.30 2.30 2.30 2.30 2.30 2.30 2.30 2.30 2.30 2.30 2.30 2.30 2.30 2.30 2.30 2.30 2.30 2.30 2.30 2.30
2.30 2.30 2.30 2.30 2.30 2.30 2.30 2.30 2.30 2.30 2.30 2.30 2.30 2.30 2.30 2.30 2.30 2.30 2.30 2.30 2.30
2.30 2.30 2.30 2.30 2.30 2.30 2.30 2.30 2.30 2.30 2.30 2.30 2.30 2.30 2.30 2.30 2.30 2.30 2.30 2.30 2.30
2.30 2.30 2.30 2.30 2.30 2.30 2.30 2.30 2.30 2.30 2.30 2.30 2.30 2.30 2.30 2.30 2.30 2.30 2.30 2.30 2.30
2.30 2.30 2.30 2.30 2.30 2.30 2.30 2.30 2.30 2.30 2.30 2.30 2.30 2.30 2.30 2.30 2.30 2.30 2.30 2.30 2.30
2.30 2.30 2.30 2.30 2.30 2.30 2.30 2.30 2.30 2.30 2.30 2.30 2.30 2.30 2.30 2.30 2.30 2.30 2.30 2.30 2.30
2.30 2.30 2.30 2.30 2.30 2.30 2.30 2.30 2.30 2.30 2.30 2.30 2.30 2.30 2.30 2.30 2.30 2.30 2.30 2.30 2.30
2.30 2.30 2.30 2.30 2.30 2.30 2.30 2.30 2.30 2.30 2.30 2.30 2.30 2.30 2.30 2.30 2.30 2.30 2.30 2.30 2.30
2.30 2.30 2.30 2.30 2.30 2.30 2.30 2.30 2.30 2.30 2.30 2.30 2.30 2.30 2.30 2.30 2.30 2.30 2.30 2.30 2.30
2.30 2.30 2.30 2.30 2.30 2.30 2.30 2.30 2.30 2.30 2.30 2.30 2.30 2.30 2.30 2.30 2.30 2.30 2.30 2.30 2.30
2.30 2.30 2.30 2.30 2.30 2.30 2.30 2.30 2.30 2.30 2.30 2.30 2.30 2.30 2.30 2.30 2.30 2.30 2.30 2.30 2.30
2.30 2.30 2.30 2.30 2.30 2.30 2.30 2.30 2.30 2.30 2.30 2.30 2.30 2.30 2.30 2.30 2.30 2.30 2.30 2.30 2.30
2.30 2.30 2.30 2.30 2.30 2.30 2.30 2.30 2.30 2.30 2.30 2.30 2.30 2.30 2.30 2.30 2.30 2.30 2.30 2.30 2.30
2.30 2.30 2.30 2.30 2.30 2.30 2.30 2.30 2.30 2.30 2.30 2.30 2.30 2.30 2.30 2.30 2.30 2.30 2.30 2.30 2.30
2.30 2.30 2.30 2.30 2.30 2.30 2.30 2.30 2.30 2.30 2.30 2.30 2.30 2.30 2.30 2.30 2.30 2.30 2.30 2.30 2.30
2.30 2.30 2.30 2.30 2.30 2.30 2.30 2.30 2.30 2.30 2.30 2.30 2.30 2.30 2.30 2.30 2.30 2.30 2.30 2.30 2.30
2.30 2.30 2.30 2.30 2.30 2.30 2.30 2.30 2.30 2.30 2.30 2.30 2.30 2.30 2.30 2.30 2.30 2.30 2.30 2.30 2.30
2.30 2.30 2.30 2.30 2.30 2.30 2.30 2.30 2.30 2.30 2.30 2.30 2.30 2.30 2.30 2.30 2.30 2.30 2.30 2.30 2.30
2.30 2.30 2.30 2.30 2.30 2.30 2.30 2.30 2.30 2.30 2.30 2.30 2.30 2.30 2.30 2.30 2.30 2.30 2.30 2.30 2.30
2.30 2.30 2.30 2.30 2.30 2.30 2.30 2.30 2.30 2.30 2.30 2.30 2.30 2.30 2.30 2.30 2.30 2.30 2.30 2.30 2.30
2.30 2.30 2.30 2.30 2.30 2.30 2.30 2.30 2.30 2.30 2.30 2.30 2.30 2.30 2.30 2.30 2.30 2.30 2.30 2.30 2.30

2.30 2.30 2.30 2.30 2.30 2.30 2.30 2.30 2.30 2.30 2.30 2.30 2.30 2.30 2.30 2.30 2.30 2.30 2.30 2.30 2.30
2.30 2.30 2.30 2.30 2.30 2.30 2.30 2.30 2.30 2.30 2.30 2.30 2.30 2.30 2.30 2.30 2.30 2.30 2.30 2.30 2.30
2.30 2.30 2.30 2.30 2.30 2.30 2.30 2.30 2.30 2.30 2.30 2.30 2.30 2.30 2.30 2.30 2.30 2.30 2.30 2.30 2.30
2.30 2.30 2.30 2.30 2.30 2.30 2.30 2.30 2.30 2.30 2.30 2.30 2.30 2.30 2.30 2.30 2.30 2.30 2.30 2.30 2.30
2.30 2.30 2.30 2.30 2.30 2.30 2.30 2.30 2.30 2.30 2.30 2.30 2.30 2.30 2.30 2.30 2.30 2.30 2.30 2.30 2.30
2.30 2.30 2.30 2.30 2.30 2.30 2.30 2.30 2.30 2.30 2.30 2.30 2.30 2.30 2.30 2.30 2.30 2.30 2.30 2.30 2.30
2.30 2.30 2.30 2.30 2.30 2.30 2.30 2.30 2.30 2.30 2.30 2.30 2.30 2.30 2.30 2.30 2.30 2.30 2.30 2.30 2.30
2.30 2.30 2.30 2.30 2.30 2.30 2.30 2.30 2.30 2.30 2.30 2.30 2.30 2.30 2.30 2.30 2.30 2.30 2.30 2.30 2.30
2.30 2.30 2.30 2.30 2.30 2.30 2.30 2.30 2.30 2.30 2.30 2.30 2.30 2.30 2.30 2.30 2.30 2.30 2.30 2.30 2.30
2.30 2.30 2.30 2.30 2.30 2.30 2.30 2.30 2.30 2.30 2.30 2.30 2.30 2.30 2.30 2.30 2.30 2.30 2.30 2.30 2.30
2.30 2.30 2.30 2.30 2.30 2.30 2.30 2.30 2.30 2.30 2.30 2.30 2.30 2.30 2.30 2.30 2.30 2.30 2.30 2.30 2.30
2.30 2.30 2.30 2.30 2.30 2.30 2.30 2.30 2.30 2.30 2.30 2.30 2.30 2.30 2.30 2.30 2.30 2.30 2.30 2.30 2.30
2.30 2.30 2.30 2.30 2.30 2.30 2.30 2.30 2.30 2.30 2.30 2.30 2.30 2.30 2.30 2.30 2.30 2.30 2.30 2.30 2.30
2.30 2.30 2.30 2.30 2.30 2.30 2.30 2.30 2.30 2.30 2.30 2.30 2.30 2.30 2.30 2.30 2.30 2.30 2.30 2.30 2.30
2.30 2.30 2.30 2.30 2.30 2.30 2.30 2.30 2.30 2.30 2.30 2.30 2.30 2.30 2.30 2.30 2.30 2.30 2.30 2.30 2.30
2.30 2.30 2.30 2.30 2.30 2.30 2.30 2.30 2.30 2.30 2.30 2.30 2.30 2.30 2.30 2.30 2.30 2.30 2.30 2.30 2.30
2.30 2.30 2.30 2.30 2.30 2.30 2.30 2.30 2.30 2.30 2.30 2.30 2.30 2.30 2.30 2.30 2.30 2.30 2.30 2.30 2.30
2.30 2.30 2.30 2.30 2.30 2.30 2.30 2.30 2.30 2.30 2.30 2.30 2.30 2.30 2.30 2.30 2.30 2.30 2.30 2.30 2.30
2.30 2.30 2.30 2.30 2.30 2.30 2.30 2.30 2.30 2.30 2.30 2.30 2.30 2.30 2.30 2.30 2.30 2.30 2.30 2.30 2.30
2.30 2.30 2.30 2.30 2.30 2.30 2.30 2.30 2.30 2.30 2.30 2.30 2.30 2.30 2.30 2.30 2.30 2.30 2.30 2.30 2.30
2.30 2.30 2.30 2.30 2.30 2.30 2.30 2.30 2.30 2.30 2.30 2.30 2.30 2.30 2.30 2.30 2.30 2.30 2.30 2.30 2.30
2.30 2.30 2.30 2.30 2.30 2.30 2.30 2.30 2.30 2.30 2.30 2.30 2.30 2.30 2.30 2.30 2.30 2.30 2.30 2.30 2.30
2.30 2.30 2.30 2.30 2.30 2.30 2.30 2.30 2.30 2.30 2.30 2.30 2.30 2.30 2.30 2.30 2.30 2.30 2.30 2.30 2.30
2.30 2.30 2.30 2.30 2.30 2.30 2.30 2.30 2.30 2.30 2.30 2.30 2.30 2.30 2.30 2.30 2.30 2.30 2.30 2.30 2.30
2.30 2.30 2.30 2.30 2.30 2.30 2.30 2.30 2.30 2.30 2.30 2.30 2.30 2.30 2.30 2.30 2.30 2.30 2.30 2.30 2.30
2.30 2.30 2.30 2.30 2.30 2.30 2.30 2.30 2.30 2.30 2.30 2.30 2.30 2.30 2.30 2.30 2.30 2.30 2.30 2.30 2.30
2.30 2.30 2.30 2.30 2.30 2.30 2.30 2.30 2.30 2.30 2.30 2.30 2.30 2.30 2.30 2.30 2.30 2.30 2.30 2.30 2.30
2.30 2.30 2.30 2.30 2.30 2.30 2.30 2.30 2.30 2.30 2.30 2.30 2.30 2.30 2.30 2.30 2.30 2.30 2.30 2.30 2.30
2.30 2.30 2.30 2.30 2.30 2.30 2.30 2.30 2.30 2.30 2.30 2.30 2.30 2.30 2.30 2.30 2.30 2.30 2.30 2.30 2.30
2.30 2.30 2.30 2.30 2.30 2.30 2.30 2.30 2.30 2.30 2.30 2.30 2.30 2.30 2.30 2.30 2.30 2.30 2.30 2.30 2.30
2.30 2.30 2.30 2.30 2.30 2.30 2.30 2.30 2.30 2.30 2.30 2.30 2.30 2.30 2.30 2.30 2.30 2.30 2.30 2.30 2.30
2.30 2.30 2.30 2.30 2.30 2.30 2.30 2.30 2.30 2.30 2.30 2.30 2.30 2.30 2.30 2.30 2.30 2.30 2.30 2.30 2.30
2.30 2.30 2.30 2.30 2.30 2.30 2.30 2.30 2.30 2.30 2.30 2.30 2.30 2.30 2.30 2.30 2.30 2.30 2.30 2.30 2.30
2.30 2.30 2.30 2.30 2.30 2.30 2.30 2.30 2.30 2.30 2.30 2.30 2.30 2.30 2.30 2.30 2.30 2.30 2.30 2.30 2.30
2.30 2.30 2.30 2.30 2.30 2.30 2.30 2.30 2.30 2.30 2.30 2.30 2.30 2.30 2.30 2.30 2.30 2.30 2.30 2.30 2.30
2.30 2.30 2.30 2.30 2.30 2.30 2.30 2.30 2.30 2.30 2.30 2.30 2.30 2.30 2.30 2.30 2.30 2.30 2.30 2.30 2.30
2.30 2.30 2.30 2.30 2.30 2.30 2.30 2.30 2.30 2.30 2.30 2.30 2.30 2.30 2.30 2.30 2.30 2.30 2.30 2.30 2.30
2.30 2.30 2.30 2.30 2.30 2.30 2.30 2.30 2.30 2.30 2.30 2.30 2.30 2.30 2.30 2.30 2.30 2.30 2.30 2.30 2.30
2.30 2.30 2.30 2.30 2.30 2.30 2.30 2.30 2.30 2.30 2.30 2.30 2.30 2.30 2.30 2.30 2.30 2.30 2.30 2.30 2.30
2.30 2.30 2.30 2.30 2.30 2.30 2.30 2.30 2.30 2.30 2.30 2.30 2.30 2.30 2.30 2.30 2.30 2.30 2.30 2.30 2.30
2.30 2.30 2.30 2.30 2.30 2.30 2.30 2.30 2.30 2.30 2.30 2.30 2.30 2.30 2.30 2.30 2.30 2.30 2.30 2.30 2.30
2.30 2.30 2.30 2.30 2.30 2.30 2.30 2.30 2.30 2.30 2.30 2.30 2.30 2.30 2.30 2.30 2.30 2.30 2.30 2.30 2.30
2.30 2.30 2.30 2.30 2.30 2.30 2.30 2.30 2.30 2.30 2.30 2.30 2.30 2.30 2.30 2.30 2.30 2.30 2.30 2.30 2.30
2.30 2.30 2.30 2.30 2.30 2.30 2.30 2.30 2.30 2.30 2.30 2.30 2.30 2.30 2.30 2.30 2.30 2.30 2.30 2.30 2.30
2.30 2.30 2.30 2.30 2.30 2.30 2.30 2.30 2.30 2.30 2.30 2.30 2.30 2.30 2.30 2.30 2.30 2.30 2.30 2.30 2.30
2.30 2.30 2.30 2.30 2.30 2.30 2.30 2.30 2.30 2.30 2.30 2.30 2.30 2.30 2.30 2.30 2.30 2.30 2.30 2.30 2.30
2.30 2.30 2.30 2.30 2.30 2.30 2.30 2.30 2.30 2.30 2.30 2.30 2.30 2.30 2.30 2.30 2.30 2.30 2.30 2.30 2.30
2.30 2.30 2.30 2.30 2.30 2.30 2.30 2.30 2.30 2.30 2.30 2.30 2.30 2.30 2.30 2.30 2.30 2.30 2.30 2.30 2.30

Events.dat file for Berea Sandstone used in TomoDD

20100627	08120059	0.0984853532033750	0.7642838296864253	144.09000000	0.00	0	0	0	5	0
20100627	08210054	0.2431837601137514	1.1707721736639016	132.92000000	0.00	0	0	0	9	0
20100627	08500027	0.4615879180441009	0.9482653674350886	128.78000000	0.00	0	0	0	16	0
20100627	08520009	0.6935575516222982	-0.0155410723831313	171.40000000	0.00	0	0	0	17	0
20100627	09200041	0.0802171793309399	0.6663677425095893	160.87000000	0.00	0	0	0	23	0
20100627	09240043	0.4444049822234936	1.3273551415635081	202.13000000	0.00	0	0	0	24	0
20100627	10020041	0.5757187864946602	1.3785662233289682	165.37000000	0.00	0	0	0	29	0
20100627	10270032	0.4584226403929364	1.0682806475748126	41.05000000	0.00	0	0	0	35	0
20100627	11050058	0.6646178702402228	0.3069581844848320	199.44000000	0.00	0	0	0	39	0
20100627	11250029	0.3951170873696467	0.1968212367462213	160.31000000	0.00	0	0	0	43	0
20100627	12110041	0.5338466849949701	0.1943068901573038	142.88000000	0.00	0	0	0	93	0
20100627	12130030	0.3412169307955315	0.2402095857190553	119.09000000	0.00	0	0	0	99	0
20100627	12580042	0.9299585739121257	1.2515684538198362	122.25000000	0.00	0	0	0	895	0
20100627	13010045	0.9573608347207782	1.0462097713147689	112.31000000	0.00	0	0	0	1010	0
20100627	13050058	0.0034365871641214	1.1115708352780080	59.47000000	0.00	0	0	0	1211	0
20100627	13060031	0.3313593518247621	0.3904976847533127	125.23000000	0.00	0	0	0	1235	0
20100627	13060041	0.3376899071270911	0.9390990213922943	45.22000000	0.00	0	0	0	1245	0
20100627	13070023	0.1603439221575609	0.9302924425434956	14.68000000	0.00	0	0	0	1290	0

20100627	13080036	0.2664259417237306	0.5746514944849059	31.52000000	0.00	0	0	0	1329	0
20100627	13080050	0.3318115343463570	1.1564912008630317	31.28000000	0.00	0	0	0	1331	0
20100627	13090020	0.3074841146845500	0.7128128256128765	3.99000000	0.00	0	0	0	1340	0
20100627	13090035	0.2526795930672449	1.2098490312478023	17.00000000	0.00	0	0	0	1346	0
20100627	13090042	0.6204848561325580	0.9136859941388866	15.09000000	0.00	0	0	0	1348	0
20100627	13090052	0.4143800627895906	0.9927306077159430	41.17000000	0.00	0	0	0	1351	0
20100627	13090054	0.2477055853297007	0.8316588419916610	80.56000000	0.00	0	0	0	1352	0
20100627	13100009	0.1620622157396216	0.7338315103617747	18.27000000	0.00	0	0	0	1358	0
20100627	13100021	0.2178615389044355	0.6793044804786307	10.80000000	0.00	0	0	0	1362	0
20100627	13110009	0.1814156276638844	0.8550140849502596	57.64000000	0.00	0	0	0	1382	0
20100627	13120000	0.0557993231648139	0.4472694224815900	82.04000000	0.00	0	0	0	1398	0
20100627	13120039	0.2481577678512957	0.9515837316298647	42.47000000	0.00	0	0	0	1404	0
20100627	13150023	0.2405611014885009	0.0917178187934735	43.28000000	0.00	0	0	0	1443	0
20100627	13150056	1.1558689617009508	0.3481132370158801	31.30000000	0.00	0	0	0	1454	0
20100627	13170004	0.3730505803158143	0.9466457653968509	46.04000000	0.00	0	0	0	1474	0
20100627	13170025	0.1483158670831359	0.7829690805579773	51.54000000	0.00	0	0	0	1481	0
20100627	13180001	0.8499222675898237	0.5958662879435686	53.46000000	0.00	0	0	0	1495	0
20100627	13180044	0.1023741228890913	1.0638709051000430	94.83000000	0.00	0	0	0	1515	0
20100627	13190012	0.3183364952028283	0.8109090130598765	87.24000000	0.00	0	0	0	1526	0
20100627	13190014	0.4303873240540510	0.9335319623954389	37.80000000	0.00	0	0	0	1527	0
20100627	13200038	0.6477062439325727	0.7934013534941529	45.95000000	0.00	0	0	0	1561	0
20100627	13210012	0.2654311401762218	1.0080880010824298	53.16000000	0.00	0	0	0	1578	0
20100627	13210021	0.0955009485608485	0.8628286347522588	107.59000000	0.00	0	0	0	1582	0
20100627	13210024	0.0133846026392098	0.9844597430414344	74.95000000	0.00	0	0	0	1586	0
20100627	13220016	0.6933766786136602	1.0792511089667862	74.10000000	0.00	0	0	0	1601	0
20100627	13220034	0.0900747583017094	1.0552470160326275	90.35000000	0.00	0	0	0	1605	0
20100627	13230012	0.0419625380040092	0.9480781773398539	44.55000000	0.00	0	0	0	1619	0
20100627	13240007	0.2800818538758974	0.7668909151028295	44.30000000	0.00	0	0	0	1643	0
20100627	13260030	0.1438844783715056	1.1205548228271220	53.86000000	0.00	0	0	0	1676	0
20100627	13260056	0.2951847500971680	0.9615559370603498	68.43000000	0.00	0	0	0	1688	0
20100627	13260059	0.1357451929827969	0.8198896098635922	74.25000000	0.00	0	0	0	1690	0
20100627	13280000	0.1691162630765025	0.8251001363991748	62.16000000	0.00	0	0	0	1706	0
20100627	13280006	0.3367855420839012	0.9613772237064424	46.86000000	0.00	0	0	0	1708	0
20100627	13280024	0.7690720327286509	0.5632539201538840	127.34000000	0.00	0	0	0	1715	0
20100627	13280032	0.2466203472778729	0.9192444111664698	63.49000000	0.00	0	0	0	1717	0
20100627	13280037	0.3970162539603453	0.8015682312858135	130.98000000	0.00	0	0	0	1720	0
20100627	13290015	0.3972875634733023	0.9671280564710607	30.42000000	0.00	0	0	0	1736	0
20100627	13290056	0.0347276176584903	0.9435865991272716	66.87000000	0.00	0	0	0	1753	0
20100627	13300007	0.6133403722913581	0.9650698440951135	42.08000000	0.00	0	0	0	1758	0
20100627	13300036	0.1486776131004118	1.2432643550551634	29.14000000	0.00	0	0	0	1769	0
20100627	13330048	0.3920422462228012	0.7541369841331506	77.89000000	0.00	0	0	0	1842	0
20100627	13350033	0.6726667191246124	1.0688293695895543	27.20000000	0.00	0	0	0	1894	0
20100627	13350036	0.7234920345518822	0.8570061665502933	35.36000000	0.00	0	0	0	1898	0
20100627	13350046	0.8325584587605786	1.1265121437588554	49.55000000	0.00	0	0	0	1902	0
20100627	13360039	0.3552345889649742	1.0009934163785552	70.22000000	0.00	0	0	0	1923	0
20100627	13370022	0.0460321806983635	1.1250455990857340	159.05000000	0.00	0	0	0	1945	0
20100627	13370046	0.3611129617457082	0.8578019963363845	55.53000000	0.00	0	0	0	1958	0
20100627	13380039	0.4282168479503953	0.9789867796280479	65.30000000	0.00	0	0	0	1983	0
20100627	13380059	0.6248258083398693	0.7763323139316294	20.77000000	0.00	0	0	0	1992	0
20100627	13390034	0.1446984069103764	1.0628831794684002	82.52000000	0.00	0	0	0	2010	0
20100627	13400034	0.7385949307731529	1.1833701884333390	123.69000000	0.00	0	0	0	2038	0
20100627	13430038	0.7392279863033856	0.8192770437897249	119.09000000	0.00	0	0	0	2137	0
20100627	13440038	0.0994801547508838	1.0114094619306639	93.12000000	0.00	0	0	0	2169	0
20100627	13450012	0.0534479740525203	0.9832022056270906	55.57000000	0.00	0	0	0	2186	0
20100627	13450045	0.3576763745815867	0.8866378592652170	42.59000000	0.00	0	0	0	2197	0
20100627	13450047	0.3146285985257498	0.7480268922522512	16.22000000	0.00	0	0	0	2198	0
20100627	13450049	0.0310197209814120	0.9686494864053412	78.90000000	0.00	0	0	0	2199	0
20100627	13460022	0.6440887837598132	0.6034053391978703	32.37000000	0.00	0	0	0	2206	0
20100627	13460033	0.0855529330857601	0.9880532547074570	32.43000000	0.00	0	0	0	2214	0
20100627	13460038	0.6745658857153113	0.6148150032477039	2.00000000	0.00	0	0	0	2218	0
20100627	13460042	0.2949134405842110	0.6831682415321281	-7.04000000	0.00	0	0	0	2220	0
20100627	13460046	0.0911599963535372	1.1179491965238080	36.77000000	0.00	0	0	0	2224	0
20100627	13460056	0.1366495580259867	1.2535947859688250	75.58000000	0.00	0	0	0	2234	0
20100627	13470003	0.0472078552545103	0.9817648836669902	49.45000000	0.00	0	0	0	2241	0
20100627	13470012	0.8416021091924770	0.9229499480431865	24.92000000	0.00	0	0	0	2249	0
20100627	13470013	0.5779796991026349	0.5902879930407248	19.70000000	0.00	0	0	0	2250	0
20100627	13470016	0.4440432362062177	1.0519307336241643	93.10000000	0.00	0	0	0	2253	0
20100627	13470018	0.2978978452267375	0.8011169997282950	93.18000000	0.00	0	0	0	2254	0
20100627	13470028	0.5585358506740531	0.7827081134380572	60.36000000	0.00	0	0	0	2263	0
20100627	13470031	1.1678065802710569	0.6396306659741439	40.18000000	0.00	0	0	0	2265	0

20100627	13470032	0.2695007828705762	1.0523749686838857	48.19000000	0.00	0	0	0	2267	0
20100627	13470032	0.5768944610508071	0.6216394338006321	62.75000000	0.00	0	0	0	2268	0
20100627	13470033	0.5106949398893099	0.9442246263890746	81.50000000	0.00	0	0	0	2270	0
20100627	13470035	0.8709939730961473	0.7578373064110584	65.65000000	0.00	0	0	0	2274	0
20100627	13470035	0.5766231515378502	0.5445633241895624	14.62000000	0.00	0	0	0	2275	0
20100627	13470035	0.1219084078219922	1.0299148809101710	33.33000000	0.00	0	0	0	2276	0
20100627	13470037	0.6922010040575134	0.9619294296275799	33.43000000	0.00	0	0	0	2279	0
20100627	13470038	0.6394765220395449	1.1223678176490861	89.26000000	0.00	0	0	0	2283	0
20100627	13470039	1.0295291651673284	0.9420969412799299	63.25000000	0.00	0	0	0	2287	0
20100627	13470044	0.3128198684393702	0.5371923411727720	60.40000000	0.00	0	0	0	2301	0
20100627	13470045	0.7988256426495969	0.7273803803436868	14.70000000	0.00	0	0	0	2305	0
20100627	13470047	0.5331231929604182	0.6082533125747697	61.43000000	0.00	0	0	0	2310	0
20100627	13470049	0.3816420482261179	0.6895477951476718	13.81000000	0.00	0	0	0	2316	0
20100627	13470051	0.5211855743903122	1.0902021431058364	54.05000000	0.00	0	0	0	2319	0
20100627	13470051	0.7811000878030758	0.7603484082575990	22.66000000	0.00	0	0	0	2320	0
20100627	13470051	0.4078686344786237	0.9678470198291966	117.34000000	0.00	0	0	0	2321	0
20100627	13470052	0.6628995766581621	0.8263705288522175	80.48000000	0.00	0	0	0	2322	0
20100627	13470052	0.5122323604627327	0.7587214980186807	78.72000000	0.00	0	0	0	2324	0
20100627	13470054	0.5175681142175528	0.8002240705162669	60.95000000	0.00	0	0	0	2327	0
20100627	13470055	0.8371707204808467	0.8116459460695550	87.85000000	0.00	0	0	0	2329	0
20100627	13470057	0.7704285802934355	0.4879737694313102	10.97000000	0.00	0	0	0	2332	0
20100627	13470057	0.7022394560369207	0.6270331480984054	75.73000000	0.00	0	0	0	2333	0
20100627	13470058	0.4478415693876151	0.8445989766262959	37.59000000	0.00	0	0	0	2334	0
20100627	13470058	0.0262265862525057	0.9081032696957515	61.89000000	0.00	0	0	0	2335	0
20100627	13470059	0.4092251820434084	0.8815187675037930	73.32000000	0.00	0	0	0	2336	0
20100627	13470059	0.3169799476380434	0.8572620428790038	47.24000000	0.00	0	0	0	2337	0
20100627	13470059	0.7972882220761742	0.9538500884843100	17.00000000	0.00	0	0	0	2338	0
20100627	13480000	0.4816648220029156	0.9383845278311255	25.18000000	0.00	0	0	0	2340	0
20100627	13480002	0.7872497700967668	1.0149361329481181	-3.33000000	0.00	0	0	0	2345	0
20100627	13480003	0.9268837327652800	0.9394846455931559	48.85000000	0.00	0	0	0	2347	0
20100627	13480009	0.3534258588785945	1.0058442738454156	30.14000000	0.00	0	0	0	2356	0
20100627	13480010	0.2291661019443087	1.0256044334912433	40.31000000	0.00	0	0	0	2357	0
20100627	13480011	0.3804663736699711	1.1473298779533847	80.57000000	0.00	0	0	0	2358	0
20100627	13480012	0.1748137628485985	1.0114102471005044	45.66000000	0.00	0	0	0	2360	0
20100627	13480013	1.0361310299826143	1.0238470812376856	48.40000000	0.00	0	0	0	2361	0
20100627	13480015	0.6169578324641176	0.7300683174506057	76.93000000	0.00	0	0	0	2362	0
20100627	13480019	0.7431167559891020	0.9979551151910633	94.36000000	0.00	0	0	0	2365	0
20100627	13480022	0.8527257992237123	0.6472512248705090	6.06000000	0.00	0	0	0	2368	0
20100627	13480031	0.2165954278439698	0.7446118384453605	52.38000000	0.00	0	0	0	2374	0
20100627	13480049	0.4428675616500709	0.6905372529973151	78.30000000	0.00	0	0	0	2384	0
20100627	13480050	0.9938067459613292	0.8854986491181180	30.80000000	0.00	0	0	0	2386	0
20100627	13480054	0.6541272357392205	0.5937037128592544	28.90000000	0.00	0	0	0	2388	0
20100627	13490000	0.1260684870206655	0.9623618444665819	65.05000000	0.00	0	0	0	2389	0
20100627	13490008	0.4575182753497466	0.9026306435236257	2.40000000	0.00	0	0	0	2391	0
20100627	13490017	0.2128875311668913	0.9830241115467365	19.59000000	0.00	0	0	0	2395	0
20100627	13490029	0.9577225807380542	1.0629189710102127	1.60000000	0.00	0	0	0	2404	0
20100627	13490033	0.5824110878142652	0.8384049464845724	95.43000000	0.00	0	0	0	2405	0
20100627	13490050	0.4972199007457810	0.7466835781426194	-5.22000000	0.00	0	0	0	2411	0
20100627	13500000	0.6938288611352551	1.1040449843337010	72.04000000	0.00	0	0	0	2413	0
20100627	13500017	0.3065797496413601	0.8152207003748924	2.15000000	0.00	0	0	0	2418	0
20100627	13500040	0.8131146103319966	0.5622672273927557	-7.55000000	0.00	0	0	0	2426	0
20100627	13510001	0.1679405885203557	1.0433002549240447	126.11000000	0.00	0	0	0	2433	0
20100627	13510003	0.0508253154272697	0.9770038445441335	64.05000000	0.00	0	0	0	2435	0
20100627	13510004	0.2818001474579582	1.0054832287806239	34.15000000	0.00	0	0	0	2436	0
20100627	13510007	0.1753563818745124	0.2927601047011548	91.70000000	0.00	0	0	0	2439	0
20100627	13510009	0.0956818215694864	0.7259258934400038	96.29000000	0.00	0	0	0	2441	0
20100627	13510010	0.2001359840579144	1.0866892373607742	158.58000000	0.00	0	0	0	2443	0
20100627	13510018	0.3334895491977797	1.1395130842446055	142.25000000	0.00	0	0	0	2453	0
20100627	13510018	0.0488357123322521	0.7167629291601234	117.30000000	0.00	0	0	0	2454	0
20100627	13510020	0.6034827933205889	0.4644334771968680	159.99000000	0.00	0	0	0	2459	0
20100627	13510020	0.2364914587941465	0.4844604903775981	120.44000000	0.00	0	0	0	2460	0
20100627	13510021	0.8315636572130696	0.6459028556510335	56.58000000	0.00	0	0	0	2463	0
20100627	13510023	0.7400419148422566	0.8420946662151977	30.02000000	0.00	0	0	0	2467	0
20100627	13510024	0.3690713741257790	0.7918657711310765	112.06000000	0.00	0	0	0	2469	0
20100627	13510025	0.7223163599957355	0.7076139562698965	33.70000000	0.00	0	0	0	2471	0
20100627	13510026	0.4779569253258372	0.5474358173617006	114.86000000	0.00	0	0	0	2472	0
20100627	13510026	0.9731872229766005	0.8166841790160025	76.79000000	0.00	0	0	0	2473	0
20100627	13510032	0.4274029194115244	0.7836924611872481	46.05000000	0.00	0	0	0	2477	0
20100627	13510034	0.6045680313724166	0.5804071264926669	40.42000000	0.00	0	0	0	2479	0
20100627	13510036	0.3394986372134707	0.6301683506997466	117.75000000	0.00	0	0	0	2480	0

20100627	13510036	0.4691845844068956	0.7256621516671790	35.01000000	0.00	0	0	0	2481	0
20100627	13510037	0.1924488811908007	0.4723329223959397	198.67000000	0.00	0	0	0	2482	0
20100627	13510041	0.9739107150111525	0.8740883821788933	46.17000000	0.00	0	0	0	2485	0
20100627	13510042	0.7582196522103727	0.4502435231080216	39.44000000	0.00	0	0	0	2486	0
20100627	13510044	0.3167086381250865	0.3307595956714531	120.02000000	0.00	0	0	0	2487	0
20100627	13510050	1.0373067045387612	0.7540732813022403	1.31000000	0.00	0	0	0	2490	0
20100627	13510052	0.5778892625983159	0.7695932455516432	86.44000000	0.00	0	0	0	2492	0
20100627	13510057	0.6526802516701168	0.3709188161968215	31.73000000	0.00	0	0	0	2495	0
20100627	13510058	0.3891482780845937	0.6388828797636502	93.93000000	0.00	0	0	0	2496	0
20100627	13520001	0.2019447141442941	0.9513134940958707	28.70000000	0.00	0	0	0	2497	0
20100627	13520004	0.5637811679245544	0.7082373615453419	33.89000000	0.00	0	0	0	2499	0
20100627	13520015	0.4009050236460617	0.5731262929248666	124.46000000	0.00	0	0	0	2501	0
20100627	13520016	0.3019674879210919	0.6104946882135117	86.85000000	0.00	0	0	0	2502	0
20100627	13520032	0.5990514046089585	0.7907944064310697	68.74000000	0.00	0	0	0	2506	0
20100627	13520041	0.2067378488732003	0.7231420388152642	38.33000000	0.00	0	0	0	2509	0
20100627	13520042	0.7148101301372597	0.4898587456802240	32.05000000	0.00	0	0	0	2511	0
20100627	13520059	0.3999102220985529	0.6055555211559448	86.78000000	0.00	0	0	0	2515	0
20100627	13530009	0.3258427250613040	0.9425123419302227	87.51000000	0.00	0	0	0	2517	0
20100627	13530011	0.6750180682369061	0.5686410081509910	45.86000000	0.00	0	0	0	2518	0
20100627	13530020	0.0950487660392535	0.8975034733893287	41.54000000	0.00	0	0	0	2521	0
20100627	13530026	0.7392279863033856	0.6614404466473404	21.88000000	0.00	0	0	0	2522	0
20100627	13530027	0.2356775302552756	0.3368675714232472	126.59000000	0.00	0	0	0	2523	0
20100627	13530052	0.6652509257704558	0.5955006933888424	41.10000000	0.00	0	0	0	2529	0
20100627	13540001	0.2670589972539635	1.0555190160809058	84.95000000	0.00	0	0	0	2530	0
20100627	13540059	0.6192187450720923	0.1056429717574698	125.50000000	0.00	0	0	0	2538	0
20100627	13550002	0.6256397368787403	0.3588807813873668	19.19000000	0.00	0	0	0	2539	0
20100627	13550007	0.8661104018629220	0.6680932019306110	55.42000000	0.00	0	0	0	2540	0
20100627	13550035	0.5528383509019571	0.7309645821115258	47.65000000	0.00	0	0	0	2543	0
20100627	13550044	0.0421434110126471	0.7005933019991829	56.34000000	0.00	0	0	0	2545	0
20100627	13550049	0.6068289439803911	0.8912273168923309	1.09000000	0.00	0	0	0	2546	0
20100627	13560019	0.9556425411387175	0.9549380470242972	5.50000000	0.00	0	0	0	2547	0
20100627	13560039	0.2969030436792287	0.9790731089863034	87.32000000	0.00	0	0	0	2549	0
20100627	13560044	0.8933317896629366	0.6959429001616244	17.20000000	0.00	0	0	0	2552	0
20100627	13570031	1.0373971410430802	1.0507976213449552	36.59000000	0.00	0	0	0	2558	0
20100627	13570043	0.5561845015617595	0.5848076801008517	-3.14000000	0.00	0	0	0	2559	0
20100627	13570057	0.8389794505672265	0.8245820683500947	7.24000000	0.00	0	0	0	2561	0
20100627	13580042	0.3968353809517075	0.7955495033031194	78.20000000	0.00	0	0	0	2567	0
20100627	13590001	0.2296182844659036	0.9829345536240249	67.70000000	0.00	0	0	0	2569	0
20100627	13590022	0.8447673868436414	0.7400489776862319	37.86000000	0.00	0	0	0	2571	0
20100627	13590036	0.6139734278215910	1.1000880252967020	30.00000000	0.00	0	0	0	2575	0
20100627	13590047	0.2480673313469766	0.2191885491609775	87.39000000	0.00	0	0	0	2576	0
20100627	14000003	0.3595755411722855	0.9397283809967775	71.86000000	0.00	0	0	0	2580	0
20100627	14000020	0.7139057650940698	0.8015788328484614	56.32000000	0.00	0	0	0	2582	0
20100627	14000026	0.1607056681748368	1.3405517748793103	64.11000000	0.00	0	0	0	2583	0
20100627	14000051	0.6356781888581475	0.5215676615568111	36.53000000	0.00	0	0	0	2586	0
20100627	14000055	0.9329429785546520	1.0548320308914045	22.00000000	0.00	0	0	0	2587	0
20100627	14010004	0.3323541533722709	0.9180783154302186	102.34000000	0.00	0	0	0	2592	0
20100627	14010010	0.9144034951692601	0.8488413417591971	46.69000000	0.00	0	0	0	2594	0
20100627	14010024	0.6429131092036664	0.7611512800935036	60.38000000	0.00	0	0	0	2595	0
20100627	14010032	0.5797884291890145	0.7555794704115593	38.11000000	0.00	0	0	0	2598	0
20100627	14010035	0.3422117323430403	0.9722469755580597	13.43000000	0.00	0	0	0	2601	0
20100627	14010039	0.2058334838300105	0.1846931690637333	81.63000000	0.00	0	0	0	2606	0
20100627	14010049	0.3278323281563216	1.0484237590678396	66.19000000	0.00	0	0	0	2615	0
20100627	14010051	0.0046122617202682	0.7999465242985042	101.65000000	0.00	0	0	0	2617	0
20100627	14010053	0.3354289945191164	0.9272412038061790	66.59000000	0.00	0	0	0	2619	0
20100627	14020000	0.6253684273657832	0.9131472080813159	151.68000000	0.00	0	0	0	2624	0
20100627	14020002	1.0373067045387612	0.7989008447249015	29.36000000	0.00	0	0	0	2627	0

Station.dat file for Berea Sandstone used in TomoDD

a1	0.0000000000000000	0.6845134767302599	-30000
a2	0.4686419653809817	1.3416395181912253	-30000
a3	1.2404270932392021	1.0952848763814211	-30000
a4	1.2404270932392021	0.2738212190953553	-30000
a5	0.4686419653809817	0.0273987313725024	-30000
a6	0.1378252325821336	1.0952223443799660	-70000
a7	0.9096103604403539	1.3416701529349535	-70000
a8	1.3782523258213357	0.6845623303907085	-70000
a9	0.9096103604403539	0.0273993569899672	-70000

a10	0.1378252325821336	0.2738055860949915	-70000
a11	0.0000000000000000	0.6845134767302599	-110000
a12	0.4686419653809817	1.3416395181912253	-110000
a13	1.2404270932392021	1.0952848763814211	-110000
a14	1.2404270932392021	0.2738212190953553	-110000
a15	0.4686419653809817	0.0273987313725024	-110000

Phase.dat file for Berea Sandstone used in TomoDD

```
# 2010  6 27  8 12 59   0.0984853532033750   0.7642838296864253 144.090000  0.00 0 0 0     5
a1    76.73911 1 P
a2    97.23911 1 P
a6    52.73911 1 P
a7    70.73911 1 P
a9    77.73911 1 P
a10   59.23911 1 P
a11   25.23911 1 P
a12   49.73911 1 P
a13   90.23911 1 P
a14   74.23911 1 P
a15   59.23911 1 P
# 2010  6 27  8 21 54   0.2431837601137514   1.1707721736639016 132.920000  0.00 0 0 0     9
a1    54.80044 1 P
a2    67.80044 1 P
a4    82.30044 1 P
a6    39.30044 1 P
a7    40.80044 1 P
a9    70.80044 1 P
a10   57.30044 1 P
a11   35.30044 1 P
a12    9.80044 1 P
a13   56.30044 1 P
a14   85.30044 1 P
# 2010  6 27  8 50 27   0.4615879180441009   0.9482653674350886 128.780000  0.00 0 0 0    16
a1    49.05775 1 P
a2    48.55775 1 P
a3    55.05775 1 P
a6    33.05775 1 P
a7    27.05775 1 P
a9    43.55775 1 P
a10   45.55775 1 P
a12   17.55775 1 P
# 2010  6 27  8 52  9   0.6935575516222982  -0.0155410723831313 171.400000  0.00 0 0 0    17
a2    80.43445 1 P
a4    66.43445 1 P
a7    78.93445 1 P
a8    58.93445 1 P
a9    45.93445 1 P
a10   52.93445 1 P
a11   69.93445 1 P
a12   66.93445 1 P
a14   27.43445 1 P
a15   27.93445 1 P
# 2010  6 27  9 20 41   0.0802171793309399   0.6663677425095893 160.870000  0.00 0 0 0    23
a1    49.33021 1 P
a2    80.83021 1 P
a3    98.33021 1 P
a5    85.83021 1 P
a6    40.33021 1 P
a8    52.83021 1 P
a9    73.33021 1 P
a10   61.83021 1 P
a11   40.83021 1 P
a14   59.83021 1 P
a15   64.33021 1 P
# 2010  6 27  9 24 43   0.4444049822234936   1.3273551415635081 202.130000  0.00 0 0 0    24
a1    80.68659 1 P
a2    91.18659 1 P
a3   103.68659 1 P
```

a7 62.18659 1 P
a8 79.18659 1 P
a9 98.68659 1 P
a11 70.18659 1 P
a12 37.68659 1 P
a13 68.18659 1 P
2010 6 27 10 2 41 0.5757187864946602 1.3785662233289682 165.370000 0.00 0 0 0 29
a7 46.54414 1 P
a9 76.04414 1 P
a10 73.04414 1 P
a11 51.54414 1 P
a13 41.54414 1 P
a14 67.54414 1 P
2010 6 27 10 27 32 0.4584226403929364 1.0682806475748126 41.050000 0.00 0 0 0 35
a2 15.20490 1 P
a4 40.70490 1 P
a6 16.70490 1 P
a7 16.70490 1 P
a8 31.70490 1 P
a9 38.70490 1 P
a10 33.20490 1 P
a12 28.20490 1 P
a13 38.20490 1 P
a14 47.70490 1 P
a15 49.20490 1 P
2010 6 27 11 5 58 0.6646178702402228 0.3069581844848320 199.440000 0.00 0 0 0 39
a2 108.93705 1 P
a3 95.93705 1 P
a4 84.43705 1 P
a5 111.43705 1 P
a6 81.43705 1 P
a7 100.43705 1 P
a8 94.43705 1 P
a9 73.43705 1 P
a10 61.93705 1 P
a11 70.43705 1 P
a12 87.93705 1 P
a14 70.93705 1 P
a15 41.93705 1 P
2010 6 27 11 25 29 0.3951170873696467 0.1968212367462213 160.310000 0.00 0 0 0 43
a2 70.47568 1 P
a3 63.47568 1 P
a4 53.47568 1 P
a6 47.47568 1 P
a7 59.97568 1 P
a8 57.97568 1 P
a9 43.97568 1 P
a10 33.47568 1 P
a11 32.47568 1 P
a12 45.47568 1 P
a13 55.47568 1 P
a14 42.47568 1 P
a15 15.47568 1 P
2010 6 27 12 11 41 0.5338466849949701 0.1943068901573038 142.880000 0.00 0 0 0 93
a2 62.63173 1 P
a4 45.13173 1 P
a6 45.63173 1 P
a7 52.63173 1 P
a8 50.63173 1 P
a9 34.63173 1 P
a10 27.13173 1 P
a11 31.13173 1 P
a12 46.63173 1 P
a13 47.63173 1 P
a14 32.13173 1 P
a15 11.13173 1 P
2010 6 27 12 13 30 0.3412169307955315 0.2402095857190553 119.090000 0.00 0 0 0 99
a3 56.94423 1 P
a4 44.94423 1 P
a7 47.94423 1 P

a8 46.94423 1 P
a9 32.94423 1 P
a10 18.94423 1 P
a11 19.44423 1 P
a12 48.44423 1 P
a14 35.94423 1 P
a15 10.44423 1 P
2010 6 27 12 58 42 0.9299585739121257 1.2515684538198362 122.250000 0.00 0 0 0 895
a2 45.05578 1 P
a6 44.55578 1 P
a7 23.55578 1 P
a8 38.05578 1 P
a9 62.55578 1 P
a10 65.05578 1 P
a12 26.05578 1 P
a13 16.05578 1 P
a14 46.55578 1 P
2010 6 27 13 1 45 0.9573608347207782 1.0462097713147689 112.310000 0.00 0 0 0 1010
a2 63.43127 1 P
a7 46.43127 1 P
a8 51.93127 1 P
a12 48.43127 1 P
a13 11.93127 1 P
a14 59.93127 1 P
2010 6 27 13 5 58 0.0034365871641214 1.1115708352780080 59.470000 0.00 0 0 0 1211
a1 29.72041 1 P
a4 66.72041 1 P
a5 46.72041 1 P
a6 11.72041 1 P
a11 28.22041 1 P
a12 22.22041 1 P
a13 59.72041 1 P
a14 87.22041 1 P
a15 63.72041 1 P
2010 6 27 13 6 31 0.3313593518247621 0.3904976847533127 125.230000 0.00 0 0 0 1235
a2 46.87231 1 P
a6 29.87231 1 P
a8 45.87231 1 P
a9 34.37231 1 P
a10 24.37231 1 P
a12 41.87231 1 P
a15 11.87231 1 P
2010 6 27 13 6 41 0.3376899071270911 0.9390990213922943 45.220000 0.00 0 0 0 1245
a1 9.19064 1 P
a4 54.19064 1 P
a6 8.69064 1 P
a7 24.19064 1 P
a8 38.69064 1 P
a9 42.69064 1 P
a11 27.19064 1 P
a12 33.69064 1 P
a13 40.19064 1 P
a14 49.19064 1 P
2010 6 27 13 7 23 0.1603439221575609 0.9302924425434956 14.680000 0.00 0 0 0 1290
a4 30.43033 1 P
a6 12.93033 1 P
a7 21.93033 1 P
a8 38.43033 1 P
a10 31.93033 1 P
a12 22.43033 1 P
a13 38.43033 1 P
a14 53.93033 1 P
2010 6 27 13 8 36 0.2664259417237306 0.5746514944849059 31.520000 0.00 0 0 0 1329
a1 25.13373 1 P
a2 62.63373 1 P
a4 48.13373 1 P
a5 32.13373 1 P
a6 24.13373 1 P
a8 67.13373 1 P
a12 63.63373 1 P

a15 57.63373 1 P
2010 6 27 13 8 50 0.3318115343463570 1.1564912008630317 31.280000 0.00 0 0 0 1331
a1 19.45709 1 P
a5 51.95709 1 P
a6 17.45709 1 P
a8 47.45709 1 P
a9 47.45709 1 P
2010 6 27 13 9 20 0.3074841146845500 0.7128128256128765 3.990000 0.00 0 0 0 1340
a4 77.47284 1 P
a6 45.47284 1 P
a10 61.47284 1 P
a11 81.97284 1 P
a12 84.47284 1 P
a14 95.97284 1 P
a15 86.97284 1 P
2010 6 27 13 9 35 0.2526795930672449 1.2098490312478023 17.000000 0.00 0 0 0 1346
a1 31.77739 1 P
a6 28.27739 1 P
a7 45.27739 1 P
a11 56.27739 1 P
a15 81.27739 1 P
2010 6 27 13 9 42 0.6204848561325580 0.9136859941388866 15.090000 0.00 0 0 0 1348
a1 27.67459 1 P
a5 39.17459 1 P
a9 44.67459 1 P
a10 38.67459 1 P
a14 50.17459 1 P
2010 6 27 13 9 52 0.4143800627895906 0.9927306077159430 41.170000 0.00 0 0 0 1351
a1 11.31278 1 P
a3 37.81278 1 P
a4 37.81278 1 P
a5 34.31278 1 P
a6 6.81278 1 P
a7 27.81278 1 P
a8 38.81278 1 P
a9 41.81278 1 P
a11 37.81278 1 P
a12 22.31278 1 P
a14 48.81278 1 P
2010 6 27 13 9 54 0.2477055853297007 0.8316588419916610 80.560000 0.00 0 0 0 1352
a1 13.86933 1 P
a2 38.36933 1 P
a5 35.86933 1 P
a6 10.36933 1 P
a7 25.86933 1 P
a10 27.86933 1 P
2010 6 27 13 10 9 0.1620622157396216 0.7338315103617747 18.270000 0.00 0 0 0 1358
a1 9.37313 1 P
a2 37.87313 1 P
a4 46.37313 1 P
a5 19.37313 1 P
a6 11.37313 1 P
a7 38.37313 1 P
a8 39.87313 1 P
a10 26.87313 1 P
a12 52.87313 1 P
a14 51.37313 1 P
a15 46.87313 1 P
2010 6 27 13 10 21 0.2178615389044355 0.6793044804786307 10.800000 0.00 0 0 0 1362
a1 6.81547 1 P
a4 50.31547 1 P
a5 17.81547 1 P
a6 30.31547 1 P
a10 32.31547 1 P
a12 44.31547 1 P
a13 49.81547 1 P
a14 67.81547 1 P
a15 51.81547 1 P
2010 6 27 13 11 9 0.1814156276638844 0.8550140849502596 57.640000 0.00 0 0 0 1382
a4 38.64465 1 P

a5 35.64465 1 P
a8 38.64465 1 P
a10 32.14465 1 P
a15 41.64465 1 P
2010 6 27 13 12 0 0.0557993231648139 0.4472694224815900 82.040000 0.00 0 0 0 1398
a1 21.07723 1 P
a4 49.57723 1 P
a5 30.57723 1 P
a6 25.57723 1 P
a7 50.57723 1 P
2010 6 27 13 12 39 0.2481577678512957 0.9515837316298647 42.470000 0.00 0 0 0 1404
a1 7.90589 1 P
a2 28.40589 1 P
a3 46.90589 1 P
a4 36.40589 1 P
a5 25.90589 1 P
a8 37.40589 1 P
a11 20.90589 1 P
a12 28.40589 1 P
a14 50.90589 1 P
a15 57.40589 1 P
2010 6 27 13 15 23 0.2405611014885009 0.0917178187934735 43.280000 0.00 0 0 0 1443
a11 23.86285 1 P
a15 16.36285 1 P
2010 6 27 13 15 56 1.1558689617009508 0.3481132370158801 31.300000 0.00 0 0 0 1454
a3 10.23034 1 P
a4 1.73034 1 P
a5 46.73034 1 P
a8 18.23034 1 P
a9 13.23034 1 P
2010 6 27 13 17 4 0.3730505803158143 0.9466457653968509 46.040000 0.00 0 0 0 1474
a1 17.87892 1 P
a5 38.87892 1 P
a6 13.87892 1 P
a7 28.87892 1 P
2010 6 27 13 17 25 0.1483158670831359 0.7829690805579773 51.540000 0.00 0 0 0 1481
a1 5.68467 1 P
a4 46.18467 1 P
a5 28.68467 1 P
a6 6.68467 1 P
a7 34.18467 1 P
a10 27.68467 1 P
a14 45.18467 1 P
a15 45.18467 1 P
2010 6 27 13 18 1 0.8499222675898237 0.5958662879435686 53.460000 0.00 0 0 0 1495
a3 23.71211 1 P
a4 15.21211 1 P
a6 39.71211 1 P
a8 30.71211 1 P
a9 23.21211 1 P
2010 6 27 13 18 44 0.1023741228890913 1.0638709051000430 94.830000 0.00 0 0 0 1515
a6 8.23801 1 P
a7 40.23801 1 P
a11 20.23801 1 P
a12 16.73801 1 P
2010 6 27 13 19 12 0.3183364952028283 0.8109090130598765 87.240000 0.00 0 0 0 1526
a1 40.28668 1 P
a2 91.28668 1 P
a4 105.78668 1 P
a5 92.28668 1 P
a6 38.28668 1 P
a7 80.78668 1 P
a11 72.78668 1 P
a13 100.28668 1 P
a14 147.78668 1 P
2010 6 27 13 19 14 0.4303873240540510 0.9335319623954389 37.800000 0.00 0 0 0 1527
a1 19.28632 1 P
a6 16.28632 1 P
a7 30.28632 1 P
a8 40.78632 1 P

a10 30.28632 1 P
2010 6 27 13 20 38 0.6477062439325727 0.7934013534941529 45.950000 0.00 0 0 0 1561
a1 25.73304 1 P
a3 37.73304 1 P
a5 44.23304 1 P
a6 26.23304 1 P
a10 36.73304 1 P
2010 6 27 13 21 12 0.2654311401762218 1.0080880010824298 53.160000 0.00 0 0 0 1578
a1 11.23106 1 P
a4 53.73106 1 P
a5 37.23106 1 P
a6 5.23106 1 P
a7 27.73106 1 P
a9 40.73106 1 P
a10 36.23106 1 P
a11 23.23106 1 P
a14 48.73106 1 P
2010 6 27 13 21 21 0.0955009485608485 0.8628286347522588 107.590000 0.00 0 0 0 1582
a1 13.79065 1 P
a3 66.79065 1 P
a4 76.29065 1 P
a5 58.29065 1 P
a7 28.79065 1 P
a8 64.29065 1 P
a11 30.79065 1 P
a12 38.79065 1 P
2010 6 27 13 21 24 0.0133846026392098 0.9844597430414344 74.950000 0.00 0 0 0 1586
a1 16.37812 1 P
a4 61.87812 1 P
a11 24.87812 1 P
a12 25.37812 1 P
a15 43.37812 1 P
2010 6 27 13 22 16 0.6933766786136602 1.0792511089667862 74.100000 0.00 0 0 0 1601
a2 47.79254 1 P
a8 65.29254 1 P
a9 63.29254 1 P
a10 71.79254 1 P
a11 10.29254 1 P
a12 7.29254 1 P
a13 51.79254 1 P
a15 37.79254 1 P
2010 6 27 13 22 34 0.0900747583017094 1.0552470160326275 90.350000 0.00 0 0 0 1605
a1 27.18340 1 P
a2 48.18340 1 P
a4 71.68340 1 P
a6 9.18340 1 P
a7 36.68340 1 P
a10 43.18340 1 P
a11 26.68340 1 P
a12 30.68340 1 P
a13 51.68340 1 P
a15 56.68340 1 P
2010 6 27 13 23 12 0.0419625380040092 0.9480781773398539 44.550000 0.00 0 0 0 1619
a1 11.37115 1 P
a5 42.87115 1 P
a6 10.87115 1 P
a7 40.37115 1 P
2010 6 27 13 24 7 0.2800818538758974 0.7668909151028295 44.300000 0.00 0 0 0 1643
a1 6.34248 1 P
a4 30.34248 1 P
a5 26.34248 1 P
a10 25.34248 1 P
a12 25.84248 1 P
a14 39.84248 1 P
2010 6 27 13 26 30 0.1438844783715056 1.1205548228271220 53.860000 0.00 0 0 0 1676
a1 14.51724 1 P
a2 30.01724 1 P
a3 59.51724 1 P
a4 43.01724 1 P
a5 44.51724 1 P

a6 2.51724 1 P
a7 27.51724 1 P
a8 37.01724 1 P
a9 70.01724 1 P
a15 72.01724 1 P
2010 6 27 13 26 56 0.2951847500971680 0.9615559370603498 68.430000 0.00 0 0 0 1688
a1 13.32043 1 P
a2 26.82043 1 P
a5 49.82043 1 P
a6 8.32043 1 P
a8 37.32043 1 P
a11 23.82043 1 P
2010 6 27 13 26 59 0.1357451929827969 0.8198896098635922 74.250000 0.00 0 0 0 1690
a1 14.32569 1 P
a2 34.82569 1 P
a3 42.32569 1 P
a5 40.82569 1 P
a6 9.82569 1 P
2010 6 27 13 28 0 0.1691162630765025 0.8251001363991748 62.160000 0.00 0 0 0 1706
a2 51.37732 1 P
a4 63.87732 1 P
a5 59.37732 1 P
a6 9.87732 1 P
a9 79.87732 1 P
a15 56.37732 1 P
2010 6 27 13 28 6 0.3367855420839012 0.9613772237064424 46.860000 0.00 0 0 0 1708
a1 16.26777 1 P
a5 55.76777 1 P
a6 23.76777 1 P
a7 26.76777 1 P
a10 22.26777 1 P
2010 6 27 13 28 24 0.7690720327286509 0.5632539201538840 127.340000 0.00 0 0 0 1715
a2 76.46263 1 P
a3 71.96263 1 P
a4 74.96263 1 P
a8 60.46263 1 P
a9 53.46263 1 P
a14 31.96263 1 P
a15 55.46263 1 P
2010 6 27 13 28 32 0.2466203472778729 0.9192444111664698 63.490000 0.00 0 0 0 1717
a1 10.51555 1 P
a2 27.01555 1 P
a4 47.51555 1 P
a5 43.51555 1 P
a6 7.51555 1 P
a8 38.51555 1 P
a10 29.01555 1 P
2010 6 27 13 28 37 0.3970162539603453 0.8015682312858135 130.980000 0.00 0 0 0 1720
a2 128.29908 1 P
a5 123.79908 1 P
a6 75.29908 1 P
a7 111.79908 1 P
a8 131.29908 1 P
a10 115.79908 1 P
2010 6 27 13 29 15 0.3972875634733023 0.9671280564710607 30.420000 0.00 0 0 0 1736
a1 16.73563 1 P
a5 41.23563 1 P
a6 18.23563 1 P
a7 31.23563 1 P
2010 6 27 13 29 56 0.0347276176584903 0.9435865991272716 66.870000 0.00 0 0 0 1753
a1 10.87582 1 P
a2 34.87582 1 P
a4 48.37582 1 P
a8 48.87582 1 P
a9 52.37582 1 P
a10 35.37582 1 P
a11 18.37582 1 P
a12 28.37582 1 P
a13 40.87582 1 P
a14 54.37582 1 P

2010 6 27 13 30 7 0.6133403722913581 0.9650698440951135 42.080000 0.00 0 0 0 1758
a2 32.15710 1 P
a3 39.15710 1 P
a5 49.15710 1 P
a7 27.15710 1 P
a8 34.15710 1 P
a13 53.65710 1 P
2010 6 27 13 30 36 0.1486776131004118 1.2432643550551634 29.140000 0.00 0 0 0 1769
a1 22.58065 1 P
a4 57.08065 1 P
a6 16.08065 1 P
a10 40.08065 1 P
2010 6 27 13 33 48 0.3920422462228012 0.7541369841331506 77.890000 0.00 0 0 0 1842
a1 19.98907 1 P
a2 32.98907 1 P
a6 16.98907 1 P
a7 28.48907 1 P
a10 23.48907 1 P
2010 6 27 13 35 33 0.6726667191246124 1.0688293695895543 27.200000 0.00 0 0 0 1894
a2 34.84958 1 P
a3 46.34958 1 P
a5 51.84958 1 P
a6 18.34958 1 P
a7 32.34958 1 P
a8 53.34958 1 P
a14 88.34958 1 P
a15 79.84958 1 P
2010 6 27 13 35 36 0.7234920345518822 0.8570061665502933 35.360000 0.00 0 0 0 1898
a1 23.84677 1 P
a3 30.34677 1 P
a4 23.84677 1 P
a5 50.84677 1 P
a9 34.34677 1 P
a10 40.34677 1 P
a14 44.34677 1 P
2010 6 27 13 35 46 0.8325584587605786 1.1265121437588554 49.550000 0.00 0 0 0 1902
a3 8.27868 1 P
a4 17.77868 1 P
a7 10.77868 1 P
a8 13.27868 1 P
a9 19.77868 1 P
a14 27.27868 1 P
2010 6 27 13 36 39 0.3552345889649742 1.0009934163785552 70.220000 0.00 0 0 0 1923
a1 24.45969 1 P
a2 16.45969 1 P
a3 41.45969 1 P
a7 27.45969 1 P
a8 37.45969 1 P
2010 6 27 13 37 22 0.0460321806983635 1.1250455990857340 159.050000 0.00 0 0 0 1945
a3 66.47847 1 P
a5 64.97847 1 P
a6 31.97847 1 P
a7 46.97847 1 P
a10 46.97847 1 P
2010 6 27 13 37 46 0.3611129617457082 0.8578019963363845 55.530000 0.00 0 0 0 1958
a1 14.69686 1 P
a4 37.19686 1 P
a5 41.69686 1 P
a6 8.69686 1 P
a7 26.69686 1 P
a8 39.19686 1 P
a10 26.19686 1 P
a12 32.69686 1 P
a14 46.19686 1 P
a15 42.69686 1 P
2010 6 27 13 38 39 0.4282168479503953 0.9789867796280479 65.300000 0.00 0 0 0 1983
a1 21.52261 1 P
a3 41.02261 1 P
a4 39.52261 1 P
a5 34.52261 1 P

a7 19.02261 1 P
a8 33.52261 1 P
a9 40.02261 1 P
a11 20.02261 1 P
a12 28.02261 1 P
a13 32.52261 1 P
2010 6 27 13 38 59 0.6248258083398693 0.7763323139316294 20.770000 0.00 0 0 0 1992
a1 24.89864 1 P
a4 28.39864 1 P
a5 38.89864 1 P
a6 31.89864 1 P
a7 33.89864 1 P
a9 39.89864 1 P
a10 29.39864 1 P
2010 6 27 13 39 34 0.1446984069103764 1.0628831794684002 82.520000 0.00 0 0 0 2010
a1 21.75306 1 P
a6 4.75306 1 P
a7 34.75306 1 P
a11 18.75306 1 P
a14 56.75306 1 P
2010 6 27 13 40 34 0.7385949307731529 1.1833701884333390 123.690000 0.00 0 0 0 2038
a2 50.12776 1 P
a7 29.62776 1 P
a8 47.62776 1 P
a9 68.12776 1 P
a10 39.62776 1 P
a12 11.12776 1 P
a13 37.12776 1 P
a14 49.62776 1 P
a15 57.62776 1 P
2010 6 27 13 43 38 0.7392279863033856 0.8192770437897249 119.090000 0.00 0 0 0 2137
a1 28.87161 1 P
a3 38.37161 1 P
a4 29.87161 1 P
a6 32.87161 1 P
a10 27.37161 1 P
2010 6 27 13 44 38 0.0994801547508838 1.0114094619306639 93.120000 0.00 0 0 0 2169
a2 40.27044 1 P
a3 63.77044 1 P
a5 44.77044 1 P
a6 6.77044 1 P
a7 26.77044 1 P
a11 20.27044 1 P
2010 6 27 13 45 12 0.0534479740525203 0.9832022056270906 55.570000 0.00 0 0 0 2186
a1 14.92725 1 P
a2 24.92725 1 P
a6 6.42725 1 P
a9 51.92725 1 P
2010 6 27 13 45 45 0.3576763745815867 0.8866378592652170 42.590000 0.00 0 0 0 2197
a1 15.05228 1 P
a3 33.55228 1 P
a6 20.05228 1 P
a10 21.55228 1 P
2010 6 27 13 45 47 0.3146285985257498 0.7480268922522512 16.220000 0.00 0 0 0 2198
a2 44.85487 1 P
a3 53.35487 1 P
a4 62.85487 1 P
a5 28.85487 1 P
a6 27.85487 1 P
a7 43.85487 1 P
a8 53.85487 1 P
a9 56.85487 1 P
a10 44.35487 1 P
a11 40.85487 1 P
a12 65.35487 1 P
a15 71.35487 1 P
2010 6 27 13 45 49 0.0310197209814120 0.9686494864053412 78.900000 0.00 0 0 0 2199
a1 23.65689 1 P
a6 12.15689 1 P
a10 44.65689 1 P

a11 21.15689 1 P
a13 60.65689 1 P
a14 57.15689 1 P
a15 45.15689 1 P
2010 6 27 13 46 22 0.6440887837598132 0.6034053391978703 32.370000 0.00 0 0 0 2206
a1 29.65177 1 P
a3 40.65177 1 P
a4 28.65177 1 P
a6 46.65177 1 P
a9 37.15177 1 P
a10 27.15177 1 P
a14 50.65177 1 P
2010 6 27 13 46 33 0.0855529330857601 0.9880532547074570 32.430000 0.00 0 0 0 2214
a1 17.91640 1 P
a2 30.41640 1 P
a3 43.91640 1 P
a5 36.41640 1 P
a6 12.41640 1 P
a8 59.91640 1 P
a10 26.91640 1 P
a11 36.91640 1 P
2010 6 27 13 46 38 0.6745658857153113 0.6148150032477039 2.000000 0.00 0 0 0 2218
a1 34.98522 1 P
a2 43.48522 1 P
a3 45.98522 1 P
a4 34.98522 1 P
a7 46.48522 1 P
a8 51.98522 1 P
a9 42.48522 1 P
a10 35.48522 1 P
a11 68.48522 1 P
a14 58.48522 1 P
a15 50.48522 1 P
2010 6 27 13 46 42 0.2949134405842110 0.6831682415321281 -7.040000 0.00 0 0 0 2220
a1 18.09889 1 P
a2 46.09889 1 P
a3 53.09889 1 P
a4 52.09889 1 P
a5 27.59889 1 P
a7 47.59889 1 P
a8 46.59889 1 P
a9 50.59889 1 P
a10 35.59889 1 P
a14 55.09889 1 P
2010 6 27 13 46 46 0.0911599963535372 1.1179491965238080 36.770000 0.00 0 0 0 2224
a1 17.21492 1 P
a2 32.21492 1 P
a3 52.21492 1 P
a5 46.71492 1 P
a6 6.71492 1 P
a7 37.21492 1 P
a9 50.21492 1 P
a14 78.21492 1 P
2010 6 27 13 46 56 0.1366495580259867 1.2535947859688250 75.580000 0.00 0 0 0 2234
a7 34.29315 1 P
a8 47.79315 1 P
a9 46.79315 1 P
a10 42.29315 1 P
a14 55.29315 1 P
2010 6 27 13 47 3 0.0472078552545103 0.9817648836669902 49.450000 0.00 0 0 0 2241
a1 10.14624 1 P
a5 29.64624 1 P
a6 4.14624 1 P
a7 20.14624 1 P
a8 30.14624 1 P
a10 15.64624 1 P
a11 12.64624 1 P
2010 6 27 13 47 12 0.8416021091924770 0.9229499480431865 24.920000 0.00 0 0 0 2249
a2 42.04330 1 P
a3 41.04330 1 P

a4 33.54330 1 P
a5 75.54330 1 P
a6 41.04330 1 P
a8 46.54330 1 P
a9 44.54330 1 P
a14 58.54330 1 P
a15 93.04330 1 P
2010 6 27 13 47 13 0.5779796991026349 0.5902879930407248 19.700000 0.00 0 0 0 2250
a1 27.66200 1 P
a4 30.66200 1 P
a6 36.66200 1 P
a10 30.16200 1 P
a15 46.66200 1 P
2010 6 27 13 47 16 0.4440432362062177 1.0519307336241643 93.100000 0.00 0 0 0 2253
a2 19.30652 1 P
a3 27.30652 1 P
a6 8.80652 1 P
a7 17.30652 1 P
a8 25.80652 1 P
a11 14.30652 1 P
2010 6 27 13 47 18 0.2978978452267375 0.8011169997282950 93.180000 0.00 0 0 0 2254
a1 21.48962 1 P
a2 36.98962 1 P
a3 48.98962 1 P
a4 44.48962 1 P
a6 14.98962 1 P
a7 28.48962 1 P
a8 44.48962 1 P
a10 26.98962 1 P
2010 6 27 13 47 28 0.5585358506740531 0.7827081134380572 60.360000 0.00 0 0 0 2263
a2 27.37184 1 P
a3 33.87184 1 P
a6 24.37184 1 P
a7 28.37184 1 P
a8 34.37184 1 P
a14 39.87184 1 P
a15 37.37184 1 P
2010 6 27 13 47 31 1.1678065802710569 0.6396306659741439 40.180000 0.00 0 0 0 2265
a3 20.14461 1 P
a4 14.64461 1 P
a5 53.14461 1 P
a9 21.14461 1 P
a10 39.14461 1 P
a14 38.14461 1 P
2010 6 27 13 47 32 0.2695007828705762 1.0523749686838857 48.190000 0.00 0 0 0 2267
a1 19.16055 1 P
a2 27.66055 1 P
a3 35.66055 1 P
a5 58.66055 1 P
a6 15.16055 1 P
a7 25.66055 1 P
a8 34.16055 1 P
a10 20.16055 1 P
2010 6 27 13 47 32 0.5768944610508071 0.6216394338006321 62.750000 0.00 0 0 0 2268
a1 25.34088 1 P
a3 34.84088 1 P
a6 26.34088 1 P
a7 30.84088 1 P
a10 22.34088 1 P
2010 6 27 13 47 33 0.5106949398893099 0.9442246263890746 81.500000 0.00 0 0 0 2270
a1 15.34665 1 P
a2 33.84665 1 P
a4 33.34665 1 P
a7 23.34665 1 P
a8 35.34665 1 P
a9 37.84665 1 P
a14 44.84665 1 P
2010 6 27 13 47 35 0.8709939730961473 0.7578373064110584 65.650000 0.00 0 0 0 2274
a2 29.83341 1 P
a3 20.33341 1 P

a6 32.33341 1 P
a9 22.83341 1 P
a10 21.83341 1 P
a11 37.33341 1 P
2010 6 27 13 47 35 0.5766231515378502 0.5445633241895624 14.620000 0.00 0 0 0 2275
a1 25.94922 1 P
a4 27.44922 1 P
a7 39.94922 1 P
a9 34.94922 1 P
a10 25.94922 1 P
2010 6 27 13 47 35 0.1219084078219922 1.0299148809101710 33.330000 0.00 0 0 0 2276
a1 9.33030 1 P
a2 19.83030 1 P
a3 33.33030 1 P
a5 26.33030 1 P
a7 15.33030 1 P
a8 28.83030 1 P
a10 17.33030 1 P
2010 6 27 13 47 37 0.6922010040575134 0.9619294296275799 33.430000 0.00 0 0 0 2279
a2 30.76546 1 P
a4 34.76546 1 P
a7 18.26546 1 P
a8 31.26546 1 P
a12 48.26546 1 P
a14 41.76546 1 P
2010 6 27 13 47 38 0.6394765220395449 1.1223678176490861 89.260000 0.00 0 0 0 2283
a2 26.01098 1 P
a3 37.01098 1 P
a5 55.01098 1 P
a7 21.51098 1 P
a8 36.01098 1 P
a9 38.51098 1 P
a10 24.51098 1 P
2010 6 27 13 47 39 1.0295291651673284 0.9420969412799299 63.250000 0.00 0 0 0 2287
a2 26.12425 1 P
a3 19.12425 1 P
a4 16.62425 1 P
a6 36.12425 1 P
a8 30.12425 1 P
a9 21.12425 1 P
a10 45.62425 1 P
2010 6 27 13 47 44 0.3128198684393702 0.5371923411727720 60.400000 0.00 0 0 0 2301
a6 24.43425 1 P
a8 45.43425 1 P
a9 27.93425 1 P
a13 41.43425 1 P
a14 46.43425 1 P
2010 6 27 13 47 45 0.7988256426495969 0.7273803803436868 14.700000 0.00 0 0 0 2305
a1 34.01270 1 P
a2 34.51270 1 P
a3 33.51270 1 P
a4 29.51270 1 P
a6 41.01270 1 P
a7 39.01270 1 P
a8 37.51270 1 P
a9 32.01270 1 P
a10 32.01270 1 P
a11 45.51270 1 P
a13 61.51270 1 P
a14 38.51270 1 P
a15 72.51270 1 P
2010 6 27 13 47 47 0.5331231929604182 0.6082533125747697 61.430000 0.00 0 0 0 2310
a1 26.04186 1 P
a2 28.54186 1 P
a7 34.54186 1 P
a8 33.54186 1 P
a10 19.54186 1 P
2010 6 27 13 47 49 0.3816420482261179 0.6895477951476718 13.810000 0.00 0 0 0 2316
a2 30.50471 1 P
a4 23.00471 1 P

a8 24.00471 1 P
a9 26.00471 1 P
a14 55.50471 1 P
2010 6 27 13 47 51 0.5211855743903122 1.0902021431058364 54.050000 0.00 0 0 0 2319
a2 23.41087 1 P
a7 12.41087 1 P
a12 36.91087 1 P
a14 39.41087 1 P
2010 6 27 13 47 51 0.7811000878030758 0.7603484082575990 22.660000 0.00 0 0 0 2320
a2 21.31778 1 P
a3 21.81778 1 P
a4 28.31778 1 P
a9 29.81778 1 P
a10 34.31778 1 P
a14 38.81778 1 P
2010 6 27 13 47 51 0.4078686344786237 0.9678470198291966 117.340000 0.00 0 0 0 2321
a2 55.38686 1 P
a5 62.38686 1 P
a6 15.88686 1 P
a8 46.38686 1 P
a10 37.88686 1 P
a11 33.88686 1 P
2010 6 27 13 47 52 0.6628995766581621 0.8263705288522175 80.480000 0.00 0 0 0 2322
a1 46.11518 1 P
a3 57.61518 1 P
a4 41.61518 1 P
a6 46.11518 1 P
a9 46.11518 1 P
a10 33.61518 1 P
a15 65.11518 1 P
2010 6 27 13 47 52 0.5122323604627327 0.7587214980186807 78.720000 0.00 0 0 0 2324
a1 19.77235 1 P
a3 31.27235 1 P
a7 27.27235 1 P
a8 27.77235 1 P
a9 30.77235 1 P
a11 19.77235 1 P
a15 28.27235 1 P
2010 6 27 13 47 54 0.5175681142175528 0.8002240705162669 60.950000 0.00 0 0 0 2327
a4 38.90113 1 P
a7 26.40113 1 P
a8 38.90113 1 P
a9 41.90113 1 P
a12 35.90113 1 P
a14 48.40113 1 P
a15 61.40113 1 P
2010 6 27 13 47 55 0.8371707204808467 0.8116459460695550 87.850000 0.00 0 0 0 2329
a3 83.56285 1 P
a4 71.06285 1 P
a5 113.56285 1 P
a9 76.56285 1 P
a10 63.56285 1 P
a15 97.56285 1 P
2010 6 27 13 47 57 0.7704285802934355 0.4879737694313102 10.970000 0.00 0 0 0 2332
a1 34.30599 1 P
a2 34.80599 1 P
a3 29.80599 1 P
a4 23.80599 1 P
a6 41.30599 1 P
a7 44.30599 1 P
a8 34.80599 1 P
a9 27.80599 1 P
2010 6 27 13 47 57 0.7022394560369207 0.6270331480984054 75.730000 0.00 0 0 0 2333
a1 33.02443 1 P
a2 32.02443 1 P
a3 34.02443 1 P
a4 29.02443 1 P
a9 25.02443 1 P
2010 6 27 13 47 58 0.4478415693876151 0.8445989766262959 37.590000 0.00 0 0 0 2334
a2 37.22662 1 P

a4 26.22662 1 P
a7 17.22662 1 P
a8 27.22662 1 P
a12 35.22662 1 P
a14 37.22662 1 P
2010 6 27 13 47 58 0.0262265862525057 0.9081032696957515 61.890000 0.00 0 0 0 2335
a1 13.29423 1 P
a3 54.29423 1 P
a5 45.29423 1 P
a6 8.79423 1 P
a7 38.79423 1 P
2010 6 27 13 47 59 0.4092251820434084 0.8815187675037930 73.320000 0.00 0 0 0 2336
a1 20.39998 1 P
a2 30.39998 1 P
a3 38.89998 1 P
a6 9.39998 1 P
a7 29.89998 1 P
a8 36.39998 1 P
a9 43.39998 1 P
a10 25.89998 1 P
a11 24.89998 1 P
2010 6 27 13 47 59 0.3169799476380434 0.8572620428790038 47.240000 0.00 0 0 0 2337
a1 10.04723 1 P
a4 40.04723 1 P
a7 23.54723 1 P
a8 39.54723 1 P
a12 32.04723 1 P
a13 42.04723 1 P
a14 49.04723 1 P
2010 6 27 13 47 59 0.7972882220761742 0.9538500884843100 17.000000 0.00 0 0 0 2338
a2 24.35942 1 P
a8 36.35942 1 P
a10 40.85942 1 P
a12 45.85942 1 P
a14 48.35942 1 P
2010 6 27 13 48 0 0.4816648220029156 0.9383845278311255 25.180000 0.00 0 0 0 2340
a2 21.13805 1 P
a4 34.63805 1 P
a7 20.63805 1 P
a8 40.63805 1 P
a9 37.63805 1 P
a14 43.63805 1 P
2010 6 27 13 48 2 0.7872497700967668 1.0149361329481181 -3.330000 0.00 0 0 0 2345
a2 6.54118 1 P
a3 17.54118 1 P
a6 14.54118 1 P
a7 25.54118 1 P
2010 6 27 13 48 3 0.9268837327652800 0.9394846455931559 48.850000 0.00 0 0 0 2347
a1 22.04576 1 P
a2 12.04576 1 P
a3 11.04576 1 P
a4 14.04576 1 P
a6 25.04576 1 P
a10 28.54576 1 P
2010 6 27 13 48 9 0.3534258588785945 1.0058442738454156 30.140000 0.00 0 0 0 2356
a1 18.55321 1 P
a7 29.55321 1 P
a8 44.05321 1 P
a14 53.05321 1 P
2010 6 27 13 48 10 0.2291661019443087 1.0256044334912433 40.310000 0.00 0 0 0 2357
a1 17.20567 1 P
a2 30.20567 1 P
a3 38.70567 1 P
a4 40.20567 1 P
a5 58.70567 1 P
a6 9.70567 1 P
a7 24.70567 1 P
a8 36.70567 1 P
a10 29.70567 1 P
a11 32.70567 1 P

a13 64.70567 1 P
a14 76.20567 1 P
2010 6 27 13 48 11 0.3804663736699711 1.1473298779533847 80.570000 0.00 0 0 0 2358
a1 12.88459 1 P
a2 37.88459 1 P
a3 46.38459 1 P
a4 49.88459 1 P
a7 19.88459 1 P
a8 32.88459 1 P
a10 36.38459 1 P
a11 44.88459 1 P
a13 30.88459 1 P
a14 37.38459 1 P
2010 6 27 13 48 12 0.1748137628485985 1.0114102471005044 45.660000 0.00 0 0 0 2360
a1 17.34920 1 P
a3 39.34920 1 P
a5 44.84920 1 P
a6 3.34920 1 P
a7 31.34920 1 P
a11 32.84920 1 P
a13 55.84920 1 P
a14 65.84920 1 P
2010 6 27 13 48 13 1.0361310299826143 1.0238470812376856 48.400000 0.00 0 0 0 2361
a3 6.36179 1 P
a4 14.86179 1 P
a7 9.86179 1 P
a8 11.36179 1 P
a9 14.36179 1 P
a10 26.36179 1 P
a14 21.86179 1 P
a15 27.86179 1 P
2010 6 27 13 48 15 0.6169578324641176 0.7300683174506057 76.930000 0.00 0 0 0 2362
a1 18.84189 1 P
a3 28.34189 1 P
a4 19.84189 1 P
a7 33.84189 1 P
a9 26.34189 1 P
a10 16.84189 1 P
2010 6 27 13 48 19 0.7431167559891020 0.9979551151910633 94.360000 0.00 0 0 0 2365
a3 65.93870 1 P
a4 52.43870 1 P
a5 99.93870 1 P
a10 46.43870 1 P
a15 79.93870 1 P
2010 6 27 13 48 22 0.8527257992237123 0.6472512248705090 6.060000 0.00 0 0 0 2368
a1 46.34350 1 P
a2 41.84350 1 P
a3 38.84350 1 P
a4 35.34350 1 P
a6 54.84350 1 P
a8 40.84350 1 P
a9 45.34350 1 P
2010 6 27 13 48 31 0.2165954278439698 0.7446118384453605 52.380000 0.00 0 0 0 2374
a2 42.62852 1 P
a7 57.12852 1 P
a10 29.62852 1 P
a11 33.12852 1 P
a14 77.62852 1 P
a15 56.62852 1 P
2010 6 27 13 48 49 0.4428675616500709 0.6905372529973151 78.300000 0.00 0 0 0 2384
a1 27.98614 1 P
a3 39.98614 1 P
a5 29.98614 1 P
a7 32.98614 1 P
a8 36.98614 1 P
a9 32.48614 1 P
a10 20.48614 1 P
a11 22.48614 1 P
a15 32.48614 1 P
2010 6 27 13 48 50 0.9938067459613292 0.8854986491181180 30.800000 0.00 0 0 0 2386

a2 9.05129 1 P
a3 6.05129 1 P
a4 8.05129 1 P
a6 21.55129 1 P
a7 16.55129 1 P
a8 11.05129 1 P
a9 10.55129 1 P
a10 25.55129 1 P
a14 20.05129 1 P
2010 6 27 13 48 54 0.6541272357392205 0.5937037128592544 28.900000 0.00 0 0 0 2388
a1 25.76651 1 P
a2 30.26651 1 P
a3 31.76651 1 P
a4 24.76651 1 P
a7 33.26651 1 P
a9 29.26651 1 P
2010 6 27 13 49 0 0.1260684870206655 0.9623618444665819 65.050000 0.00 0 0 0 2389
a1 14.98124 1 P
a2 24.48124 1 P
a3 38.98124 1 P
a6 8.98124 1 P
a7 36.48124 1 P
a10 18.98124 1 P
2010 6 27 13 49 8 0.4575182753497466 0.9026306435236257 2.400000 0.00 0 0 0 2391
a2 21.93991 1 P
a3 37.43991 1 P
a7 30.93991 1 P
a8 36.93991 1 P
a9 45.93991 1 P
a14 47.43991 1 P
a15 54.43991 1 P
2010 6 27 13 49 17 0.2128875311668913 0.9830241115467365 19.590000 0.00 0 0 0 2395
a1 19.22138 1 P
a2 28.72138 1 P
a3 41.72138 1 P
a5 52.72138 1 P
a6 18.72138 1 P
a7 27.72138 1 P
a10 22.72138 1 P
2010 6 27 13 49 29 0.9577225807380542 1.0629189710102127 1.600000 0.00 0 0 0 2404
a2 22.64050 1 P
a3 20.64050 1 P
a4 26.14050 1 P
a6 38.64050 1 P
a7 31.64050 1 P
a8 28.14050 1 P
a10 51.14050 1 P
2010 6 27 13 49 33 0.5824110878142652 0.8384049464845724 95.430000 0.00 0 0 0 2405
a3 34.81179 1 P
a5 42.31179 1 P
a7 28.31179 1 P
a8 34.81179 1 P
a11 28.81179 1 P
2010 6 27 13 49 50 0.4972199007457810 0.7466835781426194 -5.220000 0.00 0 0 0 2411
a1 26.75761 1 P
a2 32.75761 1 P
a3 37.25761 1 P
a4 30.75761 1 P
a5 26.25761 1 P
a6 36.75761 1 P
a7 33.75761 1 P
a8 36.25761 1 P
a12 45.75761 1 P
a14 56.75761 1 P
2010 6 27 13 50 0 0.6938288611352551 1.1040449843337010 72.040000 0.00 0 0 0 2413
a2 28.55722 1 P
a4 42.55722 1 P
a5 56.05722 1 P
a6 10.05722 1 P
a7 18.05722 1 P

a8 30.55722 1 P
a10 39.55722 1 P
a11 50.05722 1 P
2010 6 27 13 50 17 0.3065797496413601 0.8152207003748924 2.150000 0.00 0 0 0 2418
a3 58.81576 1 P
a5 48.31576 1 P
a7 48.31576 1 P
a10 43.31576 1 P
a11 61.81576 1 P
2010 6 27 13 50 40 0.8131146103319966 0.5622672273927557 -7.550000 0.00 0 0 0 2426
a1 35.80625 1 P
a2 34.30625 1 P
a3 31.30625 1 P
a4 23.30625 1 P
a9 34.80625 1 P
2010 6 27 13 51 1 0.1679405885203557 1.0433002549240447 126.110000 0.00 0 0 0 2433
a2 89.02544 1 P
a4 144.02544 1 P
a6 44.02544 1 P
a7 67.02544 1 P
a8 102.02544 1 P
a9 121.52544 1 P
a10 72.52544 1 P
a11 45.02544 1 P
a12 42.52544 1 P
a13 89.52544 1 P
a15 90.52544 1 P
2010 6 27 13 51 3 0.0508253154272697 0.9770038445441335 64.050000 0.00 0 0 0 2435
a2 29.99229 1 P
a4 44.99229 1 P
a5 33.49229 1 P
a6 3.49229 1 P
a7 22.99229 1 P
a10 33.49229 1 P
a11 15.99229 1 P
a15 39.49229 1 P
2010 6 27 13 51 4 0.2818001474579582 1.0054832287806239 34.150000 0.00 0 0 0 2436
a1 19.17047 1 P
a3 44.67047 1 P
a5 50.17047 1 P
a6 11.17047 1 P
a7 26.17047 1 P
a10 27.17047 1 P
a11 41.17047 1 P
a14 65.67047 1 P
2010 6 27 13 51 7 0.1753563818745124 0.2927601047011548 91.700000 0.00 0 0 0 2439
a4 59.87390 1 P
a7 33.87390 1 P
a8 64.87390 1 P
a9 46.87390 1 P
a10 21.87390 1 P
a13 34.87390 1 P
a14 25.87390 1 P
a15 30.37390 1 P
2010 6 27 13 51 9 0.0956818215694864 0.7259258934400038 96.290000 0.00 0 0 0 2441
a6 17.11101 1 P
a10 21.61101 1 P
a11 7.11101 1 P
a14 50.61101 1 P
2010 6 27 13 51 10 0.2001359840579144 1.0866892373607742 158.580000 0.00 0 0 0 2443
a6 31.85828 1 P
a9 62.85828 1 P
a10 44.35828 1 P
a11 22.35828 1 P
a12 24.85828 1 P
a13 43.35828 1 P
a14 54.35828 1 P
a15 48.85828 1 P
2010 6 27 13 51 18 0.3333489549197797 1.1395130842446055 142.250000 0.00 0 0 0 2453
a1 73.48756 1 P

a6 36.98756 1 P
a7 44.98756 1 P
a8 61.98756 1 P
a10 53.48756 1 P
a11 26.98756 1 P
a12 24.98756 1 P
a13 62.48756 1 P
2010 6 27 13 51 18 0.0488357123322521 0.7167629291601234 117.300000 0.00 0 0 0 2454
a1 38.11514 1 P
a4 81.61514 1 P
a6 32.11514 1 P
a9 52.11514 1 P
a10 33.61514 1 P
a11 9.11514 1 P
a13 55.61514 1 P
a14 44.11514 1 P
a15 39.11514 1 P
2010 6 27 13 51 20 0.6034827933205889 0.4644334771968680 159.990000 0.00 0 0 0 2459
a1 41.94054 1 P
a2 42.44054 1 P
a3 44.44054 1 P
a4 38.44054 1 P
a7 47.44054 1 P
a9 35.44054 1 P
a15 16.94054 1 P
2010 6 27 13 51 20 0.2364914587941465 0.4844604903775981 120.440000 0.00 0 0 0 2460
a8 49.86314 1 P
a9 37.86314 1 P
a10 22.36314 1 P
a11 10.86314 1 P
a13 47.36314 1 P
a15 22.36314 1 P
2010 6 27 13 51 21 0.8315636572130696 0.6459028556510335 56.580000 0.00 0 0 0 2463
a1 34.79982 1 P
a2 35.79982 1 P
a3 33.79982 1 P
a4 23.79982 1 P
a6 42.29982 1 P
a7 38.29982 1 P
a8 35.29982 1 P
a9 23.79982 1 P
a12 54.79982 1 P
2010 6 27 13 51 23 0.7400419148422566 0.8420946662151977 30.020000 0.00 0 0 0 2467
a2 20.82336 1 P
a3 24.82336 1 P
a4 25.32336 1 P
a7 25.32336 1 P
a8 28.82336 1 P
a10 32.32336 1 P
a11 42.82336 1 P
a12 38.32336 1 P
a15 39.82336 1 P
2010 6 27 13 51 24 0.3690713741257790 0.7918657711310765 112.060000 0.00 0 0 0 2469
a2 37.40571 1 P
a6 25.90571 1 P
a7 26.40571 1 P
a8 37.90571 1 P
a9 46.40571 1 P
a10 26.40571 1 P
a11 17.40571 1 P
a12 22.90571 1 P
a13 35.40571 1 P
a14 37.90571 1 P
a15 29.90571 1 P
2010 6 27 13 51 25 0.7223163599957355 0.7076139562698965 33.700000 0.00 0 0 0 2471
a2 7.94667 1 P
a3 13.94667 1 P
a14 15.94667 1 P
2010 6 27 13 51 26 0.4779569253258372 0.5474358173617006 114.860000 0.00 0 0 0 2472
a1 36.31369 1 P

a3 54.31369 1 P
a6 29.81369 1 P
a8 42.81369 1 P
a9 30.81369 1 P
a11 25.81369 1 P
a14 40.31369 1 P
a15 26.81369 1 P
2010 6 27 13 51 26 0.9731872229766005 0.8166841790160025 76.790000 0.00 0 0 0 2473
a1 16.29139 1 P
a10 15.79139 1 P
2010 6 27 13 51 32 0.4274029194115244 0.7836924611872481 46.050000 0.00 0 0 0 2477
a1 17.55769 1 P
a2 22.55769 1 P
a3 50.55769 1 P
a5 41.55769 1 P
a6 30.55769 1 P
a7 24.05769 1 P
a9 49.05769 1 P
a10 13.55769 1 P
a12 29.05769 1 P
a15 44.05769 1 P
2010 6 27 13 51 34 0.6045680313724166 0.5804071264926669 40.420000 0.00 0 0 0 2479
a1 24.95339 1 P
a2 32.95339 1 P
a4 29.95339 1 P
a9 28.45339 1 P
a10 26.45339 1 P
a14 38.45339 1 P
a15 35.45339 1 P
2010 6 27 13 51 36 0.3394986372134707 0.6301683506997466 117.750000 0.00 0 0 0 2480
a8 44.45175 1 P
a11 13.45175 1 P
a13 40.95175 1 P
a15 25.45175 1 P
2010 6 27 13 51 36 0.4691845844068956 0.7256621516671790 35.010000 0.00 0 0 0 2481
a1 17.74803 1 P
a2 25.24803 1 P
a4 35.74803 1 P
a6 24.24803 1 P
a8 38.24803 1 P
2010 6 27 13 51 37 0.1924488811908007 0.4723329223959397 198.670000 0.00 0 0 0 2482
a1 80.30956 1 P
a2 125.30956 1 P
a3 128.80956 1 P
a7 86.80956 1 P
a8 123.80956 1 P
a9 111.30956 1 P
a12 68.80956 1 P
a13 97.80956 1 P
a14 105.80956 1 P
2010 6 27 13 51 41 0.9739107150111525 0.8740883821788933 46.170000 0.00 0 0 0 2485
a1 35.67576 1 P
a3 17.17576 1 P
a4 21.17576 1 P
a6 33.67576 1 P
a7 25.17576 1 P
a8 18.67576 1 P
a10 31.67576 1 P
a11 48.17576 1 P
a12 40.17576 1 P
2010 6 27 13 51 42 0.7582196522103727 0.4502435231080216 39.440000 0.00 0 0 0 2486
a1 40.12345 1 P
a2 41.12345 1 P
a3 36.12345 1 P
a4 26.62345 1 P
a9 22.62345 1 P
a14 36.12345 1 P
2010 6 27 13 51 44 0.3167086381250865 0.3307595956714531 120.020000 0.00 0 0 0 2487
a8 48.11963 1 P
a10 19.61963 1 P

a11 19.61963 1 P
a15 13.61963 1 P
2010 6 27 13 51 50 1.0373067045387612 0.7540732813022403 1.310000 0.00 0 0 0 2490
a2 44.82915 1 P
a3 38.32915 1 P
a4 47.32915 1 P
a6 68.82915 1 P
a7 62.32915 1 P
a8 45.82915 1 P
a10 67.82915 1 P
a14 56.32915 1 P
2010 6 27 13 51 52 0.5778892625983159 0.7695932455516432 86.440000 0.00 0 0 0 2492
a1 23.13783 1 P
a4 21.63783 1 P
a7 36.13783 1 P
a10 20.13783 1 P
2010 6 27 13 51 57 0.6526802516701168 0.3709188161968215 31.730000 0.00 0 0 0 2495
a1 28.39637 1 P
a3 35.89637 1 P
a4 22.89637 1 P
a6 38.89637 1 P
a7 40.39637 1 P
a9 24.39637 1 P
a10 22.89637 1 P
2010 6 27 13 51 58 0.3891482780845937 0.6388828797636502 93.930000 0.00 0 0 0 2496
a1 15.74935 1 P
a3 27.74935 1 P
a9 20.24935 1 P
a10 11.74935 1 P
a11 9.74935 1 P
2010 6 27 13 52 1 0.2019447141442941 0.9513134940958707 28.700000 0.00 0 0 0 2497
a2 27.89422 1 P
a3 48.39422 1 P
a4 49.89422 1 P
a8 39.39422 1 P
a9 48.39422 1 P
a10 42.89422 1 P
a12 36.39422 1 P
a13 49.39422 1 P
a15 49.39422 1 P
2010 6 27 13 52 4 0.5637811679245544 0.7082373615453419 33.890000 0.00 0 0 0 2499
a1 18.76684 1 P
a2 25.26684 1 P
a5 29.76684 1 P
a6 22.76684 1 P
a7 25.26684 1 P
a8 31.26684 1 P
a9 24.26684 1 P
a11 36.76684 1 P
a12 29.76684 1 P
a13 39.26684 1 P
a14 33.76684 1 P
2010 6 27 13 52 15 0.4009050236460617 0.5731262929248666 124.460000 0.00 0 0 0 2501
a1 64.21155 1 P
a6 40.21155 1 P
a7 57.21155 1 P
a9 48.21155 1 P
a10 39.21155 1 P
a11 34.21155 1 P
a13 60.71155 1 P
a14 52.21155 1 P
a15 41.21155 1 P
2010 6 27 13 52 16 0.3019674879210919 0.6104946882135117 86.850000 0.00 0 0 0 2502
a1 26.74015 1 P
a2 43.74015 1 P
a10 17.74015 1 P
a11 20.24015 1 P
a14 42.24015 1 P
a15 26.74015 1 P
2010 6 27 13 52 32 0.5990514046089585 0.7907944064310697 68.740000 0.00 0 0 0 2506

a1 20.90815 1 P
a2 26.90815 1 P
a3 44.90815 1 P
a6 25.40815 1 P
a7 28.90815 1 P
a8 35.90815 1 P
a9 26.40815 1 P
a10 17.40815 1 P
a11 39.40815 1 P
a15 39.40815 1 P
2010 6 27 13 52 41 0.2067378488732003 0.7231420388152642 38.330000 0.00 0 0 0 2509
a1 2.57601 1 P
a2 25.07601 1 P
a4 39.07601 1 P
a8 34.07601 1 P
a9 38.57601 1 P
a11 34.07601 1 P
a14 44.57601 1 P
a15 43.07601 1 P
2010 6 27 13 52 42 0.7148101301372597 0.4898587456802240 32.050000 0.00 0 0 0 2511
a1 29.26075 1 P
a2 34.76075 1 P
a3 31.76075 1 P
a4 22.76075 1 P
a6 36.26075 1 P
a9 23.76075 1 P
2010 6 27 13 52 59 0.3999102220985529 0.6055555211559448 86.780000 0.00 0 0 0 2515
a6 23.06587 1 P
a9 30.56587 1 P
a11 17.56587 1 P
a14 36.56587 1 P
a15 25.06587 1 P
2010 6 27 13 53 9 0.3258427250613040 0.9425123419302227 87.510000 0.00 0 0 0 2517
a1 14.79359 1 P
a2 38.29359 1 P
a3 48.29359 1 P
a4 62.29359 1 P
a7 28.29359 1 P
a8 37.29359 1 P
a9 38.29359 1 P
a12 9.29359 1 P
a13 47.79359 1 P
a14 42.29359 1 P
a15 39.79359 1 P
2010 6 27 13 53 11 0.6750180682369061 0.5686410081509910 45.860000 0.00 0 0 0 2518
a2 32.22619 1 P
a3 31.72619 1 P
a4 25.22619 1 P
a7 32.72619 1 P
a9 25.22619 1 P
2010 6 27 13 53 20 0.0950487660392535 0.8975034733893287 41.540000 0.00 0 0 0 2521
a1 12.88506 1 P
a3 56.88506 1 P
a7 29.38506 1 P
a8 45.38506 1 P
a9 49.88506 1 P
a13 66.88506 1 P
a14 59.38506 1 P
2010 6 27 13 53 26 0.7392279863033856 0.6614404466473404 21.880000 0.00 0 0 0 2522
a1 29.25318 1 P
a2 29.25318 1 P
a3 26.25318 1 P
a4 25.25318 1 P
a7 32.75318 1 P
a12 42.75318 1 P
2010 6 27 13 53 27 0.2356775302552756 0.3368675714232472 126.590000 0.00 0 0 0 2523
a7 44.65189 1 P
a8 50.65189 1 P
a10 24.15189 1 P
a11 10.65189 1 P

a14 38.15189 1 P
a15 16.65189 1 P
2010 6 27 13 53 52 0.6652509257704558 0.5955006933888424 41.100000 0.00 0 0 0 2529
a1 25.96723 1 P
a2 29.96723 1 P
a4 25.96723 1 P
a7 31.96723 1 P
a8 29.96723 1 P
2010 6 27 13 54 1 0.2670589972539635 1.0555190160809058 84.950000 0.00 0 0 0 2530
a1 23.54638 1 P
a6 8.54638 1 P
a7 27.54638 1 P
a10 34.04638 1 P
a11 18.54638 1 P
2010 6 27 13 54 59 0.6192187450720923 0.1056429717574698 125.500000 0.00 0 0 0 2538
a2 66.74663 1 P
a3 58.24663 1 P
a4 47.24663 1 P
a6 57.74663 1 P
a7 54.74663 1 P
a8 52.74663 1 P
a9 29.24663 1 P
a10 26.74663 1 P
a11 38.74663 1 P
a14 33.24663 1 P
a15 4.24663 1 P
2010 6 27 13 55 2 0.6256397368787403 0.3588807813873668 19.190000 0.00 0 0 0 2539
a1 29.39377 1 P
a2 36.39377 1 P
a4 25.39377 1 P
a6 42.39377 1 P
a10 24.39377 1 P
2010 6 27 13 55 7 0.8661104018629220 0.6680932019306110 55.420000 0.00 0 0 0 2540
a1 22.99790 1 P
a2 24.99790 1 P
a4 18.99790 1 P
a9 18.99790 1 P
a10 22.99790 1 P
a15 28.99790 1 P
2010 6 27 13 55 35 0.5528383509019571 0.7309645821115258 47.650000 0.00 0 0 0 2543
a1 19.62220 1 P
a2 26.62220 1 P
a3 33.62220 1 P
a6 28.12220 1 P
a7 33.62220 1 P
a9 29.62220 1 P
a10 19.62220 1 P
a12 32.62220 1 P
a13 41.12220 1 P
a15 33.12220 1 P
2010 6 27 13 55 44 0.0421434110126471 0.7005933019991829 56.340000 0.00 0 0 0 2545
a1 11.14893 1 P
a2 28.14893 1 P
a3 68.64893 1 P
a8 60.14893 1 P
a12 49.64893 1 P
a14 46.64893 1 P
2010 6 27 13 55 49 0.6068289439803911 0.8912273168923309 1.090000 0.00 0 0 0 2546
a1 23.91399 1 P
a2 31.91399 1 P
a6 38.91399 1 P
a7 36.91399 1 P
a8 47.91399 1 P
a9 44.91399 1 P
a11 46.41399 1 P
2010 6 27 13 56 19 0.9556425411387175 0.9549380470242972 5.500000 0.00 0 0 0 2547
a1 46.48091 1 P
a2 38.48091 1 P
a4 36.98091 1 P
a6 53.98091 1 P

a7 50.48091 1 P
a8 42.98091 1 P
a15 86.98091 1 P
2010 6 27 13 56 39 0.2969030436792287 0.9790731089863034 87.320000 0.00 0 0 0 2549
a6 10.28558 1 P
a11 17.28558 1 P
a12 20.28558 1 P
a15 39.78558 1 P
2010 6 27 13 56 44 0.8933317896629366 0.6959429001616244 17.200000 0.00 0 0 0 2552
a1 32.73026 1 P
a3 20.73026 1 P
a4 19.73026 1 P
a7 30.23026 1 P
a8 26.73026 1 P
a10 38.73026 1 P
2010 6 27 13 57 31 1.0373971410430802 1.0507976213449552 36.590000 0.00 0 0 0 2558
a2 17.02105 1 P
a3 17.02105 1 P
a4 26.52105 1 P
a7 23.02105 1 P
a10 63.52105 1 P
a11 54.02105 1 P
a12 44.52105 1 P
a14 29.02105 1 P
a15 64.02105 1 P
2010 6 27 13 57 43 0.5561845015617595 0.5848076801008517 -3.140000 0.00 0 0 0 2559
a1 40.88283 1 P
a2 56.38283 1 P
a3 51.38283 1 P
a6 58.88283 1 P
a7 45.38283 1 P
a10 30.88283 1 P
a15 79.38283 1 P
2010 6 27 13 57 57 0.8389794505672265 0.8245820683500947 7.240000 0.00 0 0 0 2561
a1 27.22490 1 P
a2 30.22490 1 P
a3 33.22490 1 P
a4 26.22490 1 P
a6 54.72490 1 P
a7 34.72490 1 P
a8 36.22490 1 P
a9 30.72490 1 P
a10 31.22490 1 P
a15 71.72490 1 P
2010 6 27 13 58 42 0.3968353809517075 0.7955495033031194 78.200000 0.00 0 0 0 2567
a1 16.74889 1 P
a2 31.24889 1 P
a3 35.24889 1 P
a6 25.24889 1 P
a7 29.74889 1 P
a10 16.24889 1 P
2010 6 27 13 59 1 0.2296182844659036 0.9829345536240249 67.700000 0.00 0 0 0 2569
a1 17.40912 1 P
a2 33.90912 1 P
a3 49.40912 1 P
a6 5.40912 1 P
a7 22.40912 1 P
a8 37.40912 1 P
a10 19.90912 1 P
a11 24.40912 1 P
a13 50.90912 1 P
a14 60.90912 1 P
a15 49.90912 1 P
2010 6 27 13 59 22 0.8447673868436414 0.7400489776862319 37.860000 0.00 0 0 0 2571
a1 27.34706 1 P
a2 29.84706 1 P
a3 27.84706 1 P
a4 23.84706 1 P
a6 39.84706 1 P
a7 34.34706 1 P

a8 30.34706 1 P
a9 24.84706 1 P
a11 56.84706 1 P
a12 43.34706 1 P
2010 6 27 13 59 36 0.6139734278215910 1.1000880252967020 30.000000 0.00 0 0 0 2575
a1 14.66871 1 P
a2 12.16871 1 P
a3 38.66871 1 P
2010 6 27 13 59 47 0.2480673313469766 0.2191885491609775 87.390000 0.00 0 0 0 2576
a4 43.08113 1 P
a6 31.08113 1 P
a9 33.08113 1 P
a10 5.08113 1 P
a11 29.58113 1 P
a13 44.58113 1 P
a14 46.08113 1 P
a15 6.08113 1 P
2010 6 27 14 0 3 0.3595755411722855 0.9397283809967775 71.860000 0.00 0 0 0 2580
a1 12.53464 1 P
a2 33.03464 1 P
a3 50.03464 1 P
a6 10.03464 1 P
a7 23.03464 1 P
a8 37.53464 1 P
a11 35.53464 1 P
a12 16.03464 1 P
a13 37.03464 1 P
2010 6 27 14 0 20 0.7139057650940698 0.8015788328484614 56.320000 0.00 0 0 0 2582
a1 53.50237 1 P
a2 54.50237 1 P
a3 56.50237 1 P
a6 40.00237 1 P
a7 49.00237 1 P
a8 47.00237 1 P
a11 67.00237 1 P
a13 54.00237 1 P
a15 75.50237 1 P
2010 6 27 14 0 26 0.1607056681748368 1.3405517748793103 64.110000 0.00 0 0 0 2583
a1 29.92957 1 P
a7 36.42957 1 P
a9 60.92957 1 P
a12 17.92957 1 P
a15 54.92957 1 P
2010 6 27 14 0 51 0.6356781888581475 0.5215676615568111 36.530000 0.00 0 0 0 2586
a1 20.57608 1 P
a3 27.07608 1 P
a4 21.57608 1 P
a7 29.07608 1 P
a9 19.57608 1 P
a14 29.57608 1 P
a15 26.07608 1 P
2010 6 27 14 0 55 0.9329429785546520 1.0548320308914045 22.000000 0.00 0 0 0 2587
a7 13.58025 1 P
a8 14.58025 1 P
2010 6 27 14 1 4 0.3323541533722709 0.9180783154302186 102.340000 0.00 0 0 0 2592
a2 56.55007 1 P
a6 25.05007 1 P
a7 46.05007 1 P
a10 47.05007 1 P
a11 37.55007 1 P
a15 50.05007 1 P
2010 6 27 14 1 10 0.9144034951692601 0.8488413417591971 46.690000 0.00 0 0 0 2594
a7 9.04015 1 P
2010 6 27 14 1 24 0.6429131092036664 0.7611512800935036 60.380000 0.00 0 0 0 2595
a1 28.59021 1 P
a2 34.09021 1 P
a3 42.59021 1 P
a6 33.59021 1 P
a7 36.09021 1 P
a8 39.59021 1 P

a9 34.09021 1 P
a10 26.59021 1 P
a11 47.09021 1 P
2010 6 27 14 1 32 0.5797884291890145 0.7555794704115593 38.110000 0.00 0 0 0 2598
a1 23.46235 1 P
a2 21.46235 1 P
a3 30.46235 1 P
a7 29.96235 1 P
a8 31.46235 1 P
2010 6 27 14 1 35 0.3422117323430403 0.9722469755580597 13.430000 0.00 0 0 0 2601
a1 18.57047 1 P
a2 18.57047 1 P
a3 41.07047 1 P
a4 52.57047 1 P
a8 48.57047 1 P
a15 54.57047 1 P
2010 6 27 14 1 39 0.2058334838300105 0.1846931690637333 81.630000 0.00 0 0 0 2606
a9 27.55375 1 P
a10 4.05375 1 P
a11 16.55375 1 P
a14 36.55375 1 P
a15 22.05375 1 P
2010 6 27 14 1 49 0.3278323281563216 1.0484237590678396 66.190000 0.00 0 0 0 2615
a1 24.03813 1 P
a7 25.53813 1 P
a12 19.03813 1 P
a14 49.53813 1 P
2010 6 27 14 1 51 0.0046122617202682 0.7999465242985042 101.650000 0.00 0 0 0 2617
a1 30.09791 1 P
a2 51.09791 1 P
a7 31.59791 1 P
a8 43.59791 1 P
a12 20.59791 1 P
a14 53.09791 1 P
2010 6 27 14 1 53 0.3354289945191164 0.9272412038061790 66.590000 0.00 0 0 0 2619
a3 45.71658 1 P
a4 33.21658 1 P
a5 64.71658 1 P
a6 12.21658 1 P
a10 8.21658 1 P
a11 30.21658 1 P
a15 49.21658 1 P
2010 6 27 14 2 0 0.6253684273657832 0.9131472080813159 151.680000 0.00 0 0 0 2624
a2 48.27464 1 P
a3 70.27464 1 P
a8 34.77464 1 P
a9 40.27464 1 P
a11 48.77464 1 P
a13 44.27464 1 P
a14 40.77464 1 P
a15 39.27464 1 P
2010 6 27 14 2 2 1.0373067045387612 0.7989008447249015 29.360000 0.00 0 0 0 2627
a1 27.38793 1 P
a2 22.38793 1 P
a3 24.38793 1 P
a4 19.38793 1 P
a6 61.38793 1 P
a7 27.88793 1 P
a8 24.38793 1 P
a9 23.38793 1 P
a12 37.38793 1 P
2010 6 27 14 2 6 0.1576308270279913 0.2941973397628274 110.940000 0.00 0 0 0 2635
a3 56.95937 1 P
a8 63.95937 1 P
a9 34.95937 1 P
a11 13.95937 1 P
a13 59.95937 1 P
a14 43.45937 1 P

Tt.dat file for Berea Sandstone used in TomoDD

```
#   5
a1    76.73911 1 P
a2    97.23911 1 P
a6    52.73911 1 P
a7    70.73911 1 P
a9    77.73911 1 P
a10   59.23911 1 P
a11   25.23911 1 P
a12   49.73911 1 P
a13   90.23911 1 P
a14   74.23911 1 P
a15   59.23911 1 P
#   9
a1    54.80044 1 P
a2    67.80044 1 P
a4    82.30044 1 P
a6    39.30044 1 P
a7    40.80044 1 P
a9    70.80044 1 P
a10   57.30044 1 P
a11   35.30044 1 P
a12    9.80044 1 P
a13   56.30044 1 P
a14   85.30044 1 P
#   16
a1    49.05775 1 P
a2    48.55775 1 P
a3    55.05775 1 P
a6    33.05775 1 P
a7    27.05775 1 P
a9    43.55775 1 P
a10   45.55775 1 P
a12   17.55775 1 P
#   17
a2    80.43445 1 P
a4    66.43445 1 P
a7    78.93445 1 P
a8    58.93445 1 P
a9    45.93445 1 P
a10   52.93445 1 P
a11   69.93445 1 P
a12   66.93445 1 P
a14   27.43445 1 P
a15   27.93445 1 P
#   23
a1    49.33021 1 P
a2    80.83021 1 P
a3    98.33021 1 P
a5    85.83021 1 P
a6    40.33021 1 P
a8    52.83021 1 P
a9    73.33021 1 P
a10   61.83021 1 P
a11   40.83021 1 P
a14   59.83021 1 P
a15   64.33021 1 P
#   24
a1    80.68659 1 P
a2    91.18659 1 P
a3   103.68659 1 P
a7    62.18659 1 P
a8    79.18659 1 P
a9    98.68659 1 P
a11   70.18659 1 P
a12   37.68659 1 P
a13   68.18659 1 P
#   29
```

a7 46.54414 1 P
a9 76.04414 1 P
a10 73.04414 1 P
a11 51.54414 1 P
a13 41.54414 1 P
a14 67.54414 1 P
35
a2 15.20490 1 P
a4 40.70490 1 P
a6 16.70490 1 P
a7 16.70490 1 P
a8 31.70490 1 P
a9 38.70490 1 P
a10 33.20490 1 P
a12 28.20490 1 P
a13 38.20490 1 P
a14 47.70490 1 P
a15 49.20490 1 P
39
a2 108.93705 1 P
a3 95.93705 1 P
a4 84.43705 1 P
a5 111.43705 1 P
a6 81.43705 1 P
a7 100.43705 1 P
a8 94.43705 1 P
a9 73.43705 1 P
a10 61.93705 1 P
a11 70.43705 1 P
a12 87.93705 1 P
a14 70.93705 1 P
a15 41.93705 1 P
43
a2 70.47568 1 P
a3 63.47568 1 P
a4 53.47568 1 P
a6 47.47568 1 P
a7 59.97568 1 P
a8 57.97568 1 P
a9 43.97568 1 P
a10 33.47568 1 P
a11 32.47568 1 P
a12 45.47568 1 P
a13 55.47568 1 P
a14 42.47568 1 P
a15 15.47568 1 P
93
a2 62.63173 1 P
a4 45.13173 1 P
a6 45.63173 1 P
a7 52.63173 1 P
a8 50.63173 1 P
a9 34.63173 1 P
a10 27.13173 1 P
a11 31.13173 1 P
a12 46.63173 1 P
a13 47.63173 1 P
a14 32.13173 1 P
a15 11.13173 1 P
99
a3 56.94423 1 P
a4 44.94423 1 P
a7 47.94423 1 P
a8 46.94423 1 P
a9 32.94423 1 P
a10 18.94423 1 P
a11 19.44423 1 P
a12 48.44423 1 P
a14 35.94423 1 P
a15 10.44423 1 P

```
#  895
a2    45.05578 1 P
a6    44.55578 1 P
a7    23.55578 1 P
a8    38.05578 1 P
a9    62.55578 1 P
a10   65.05578 1 P
a12   26.05578 1 P
a13   16.05578 1 P
a14   46.55578 1 P
# 1010
a2    63.43127 1 P
a7    46.43127 1 P
a8    51.93127 1 P
a12   48.43127 1 P
a13   11.93127 1 P
a14   59.93127 1 P
# 1211
a1    29.72041 1 P
a4    66.72041 1 P
a5    46.72041 1 P
a6    11.72041 1 P
a11   28.22041 1 P
a12   22.22041 1 P
a13   59.72041 1 P
a14   87.22041 1 P
a15   63.72041 1 P
# 1235
a2    46.87231 1 P
a6    29.87231 1 P
a8    45.87231 1 P
a9    34.37231 1 P
a10   24.37231 1 P
a12   41.87231 1 P
a15   11.87231 1 P
# 1245
a1     9.19064 1 P
a4    54.19064 1 P
a6     8.69064 1 P
a7    24.19064 1 P
a8    38.69064 1 P
a9    42.69064 1 P
a11   27.19064 1 P
a12   33.69064 1 P
a13   40.19064 1 P
a14   49.19064 1 P
# 1290
a4    30.43033 1 P
a6    12.93033 1 P
a7    21.93033 1 P
a8    38.43033 1 P
a10   31.93033 1 P
a12   22.43033 1 P
a13   38.43033 1 P
a14   53.93033 1 P
# 1329
a1    25.13373 1 P
a2    62.63373 1 P
a4    48.13373 1 P
a5    32.13373 1 P
a6    24.13373 1 P
a8    67.13373 1 P
a12   63.63373 1 P
a15   57.63373 1 P
# 1331
a1    19.45709 1 P
a5    51.95709 1 P
a6    17.45709 1 P
a8    47.45709 1 P
a9    47.45709 1 P
```

1340
a4 77.47284 1 P
a6 45.47284 1 P
a10 61.47284 1 P
a11 81.97284 1 P
a12 84.47284 1 P
a14 95.97284 1 P
a15 86.97284 1 P
1346
a1 31.77739 1 P
a6 28.27739 1 P
a7 45.27739 1 P
a11 56.27739 1 P
a15 81.27739 1 P
1348
a1 27.67459 1 P
a5 39.17459 1 P
a9 44.67459 1 P
a10 38.67459 1 P
a14 50.17459 1 P
1351
a1 11.31278 1 P
a3 37.81278 1 P
a4 37.81278 1 P
a5 34.31278 1 P
a6 6.81278 1 P
a7 27.81278 1 P
a8 38.81278 1 P
a9 41.81278 1 P
a11 37.81278 1 P
a12 22.31278 1 P
a14 48.81278 1 P
1352
a1 13.86933 1 P
a2 38.36933 1 P
a5 35.86933 1 P
a6 10.36933 1 P
a7 25.86933 1 P
a10 27.86933 1 P
1358
a1 9.37313 1 P
a2 37.87313 1 P
a4 46.37313 1 P
a5 19.37313 1 P
a6 11.37313 1 P
a7 38.37313 1 P
a8 39.87313 1 P
a10 26.87313 1 P
a12 52.87313 1 P
a14 51.37313 1 P
a15 46.87313 1 P
1362
a1 6.81547 1 P
a4 50.31547 1 P
a5 17.81547 1 P
a6 30.31547 1 P
a10 32.31547 1 P
a12 44.31547 1 P
a13 49.81547 1 P
a14 67.81547 1 P
a15 51.81547 1 P
1382
a4 38.64465 1 P
a5 35.64465 1 P
a8 38.64465 1 P
a10 32.14465 1 P
a15 41.64465 1 P
1398
a1 21.07723 1 P
a4 49.57723 1 P

a5 30.57723 1 P
a6 25.57723 1 P
a7 50.57723 1 P
1404
a1 7.90589 1 P
a2 28.40589 1 P
a3 46.90589 1 P
a4 36.40589 1 P
a5 25.90589 1 P
a8 37.40589 1 P
a11 20.90589 1 P
a12 28.40589 1 P
a14 50.90589 1 P
a15 57.40589 1 P
1443
a11 23.86285 1 P
a15 16.36285 1 P
1454
a3 10.23034 1 P
a4 1.73034 1 P
a5 46.73034 1 P
a8 18.23034 1 P
a9 13.23034 1 P
1474
a1 17.87892 1 P
a5 38.87892 1 P
a6 13.87892 1 P
a7 28.87892 1 P
1481
a1 5.68467 1 P
a4 46.18467 1 P
a5 28.68467 1 P
a6 6.68467 1 P
a7 34.18467 1 P
a10 27.68467 1 P
a14 45.18467 1 P
a15 45.18467 1 P
1495
a3 23.71211 1 P
a4 15.21211 1 P
a6 39.71211 1 P
a8 30.71211 1 P
a9 23.21211 1 P
1515
a6 8.23801 1 P
a7 40.23801 1 P
a11 20.23801 1 P
a12 16.73801 1 P
1526
a1 40.28668 1 P
a2 91.28668 1 P
a4 105.78668 1 P
a5 92.28668 1 P
a6 38.28668 1 P
a7 80.78668 1 P
a11 72.78668 1 P
a13 100.28668 1 P
a14 147.78668 1 P
1527
a1 19.28632 1 P
a6 16.28632 1 P
a7 30.28632 1 P
a8 40.78632 1 P
a10 30.28632 1 P
1561
a1 25.73304 1 P
a3 37.73304 1 P
a5 44.23304 1 P
a6 26.23304 1 P
a10 36.73304 1 P

1578
a1 11.23106 1 P
a4 53.73106 1 P
a5 37.23106 1 P
a6 5.23106 1 P
a7 27.73106 1 P
a9 40.73106 1 P
a10 36.23106 1 P
a11 23.23106 1 P
a14 48.73106 1 P
1582
a1 13.79065 1 P
a3 66.79065 1 P
a4 76.29065 1 P
a5 58.29065 1 P
a7 28.79065 1 P
a8 64.29065 1 P
a11 30.79065 1 P
a12 38.79065 1 P
1586
a1 16.37812 1 P
a4 61.87812 1 P
a11 24.87812 1 P
a12 25.37812 1 P
a15 43.37812 1 P
1601
a2 47.79254 1 P
a8 65.29254 1 P
a9 63.29254 1 P
a10 71.79254 1 P
a11 10.29254 1 P
a12 7.29254 1 P
a13 51.79254 1 P
a15 37.79254 1 P
1605
a1 27.18340 1 P
a2 48.18340 1 P
a4 71.68340 1 P
a6 9.18340 1 P
a7 36.68340 1 P
a10 43.18340 1 P
a11 26.68340 1 P
a12 30.68340 1 P
a13 51.68340 1 P
a15 56.68340 1 P
1619
a1 11.37115 1 P
a5 42.87115 1 P
a6 10.87115 1 P
a7 40.37115 1 P
1643
a1 6.34248 1 P
a4 30.34248 1 P
a5 26.34248 1 P
a10 25.34248 1 P
a12 25.84248 1 P
a14 39.84248 1 P
1676
a1 14.51724 1 P
a2 30.01724 1 P
a3 59.51724 1 P
a4 43.01724 1 P
a5 44.51724 1 P
a6 2.51724 1 P
a7 27.51724 1 P
a8 37.01724 1 P
a9 70.01724 1 P
a15 72.01724 1 P
1688
a1 13.32043 1 P

a2 26.82043 1 P
a5 49.82043 1 P
a6 8.32043 1 P
a8 37.32043 1 P
a11 23.82043 1 P
1690
a1 14.32569 1 P
a2 34.82569 1 P
a3 42.32569 1 P
a5 40.82569 1 P
a6 9.82569 1 P
1706
a2 51.37732 1 P
a4 63.87732 1 P
a5 59.37732 1 P
a6 9.87732 1 P
a9 79.87732 1 P
a15 56.37732 1 P
1708
a1 16.26777 1 P
a5 55.76777 1 P
a6 23.76777 1 P
a7 26.76777 1 P
a10 22.26777 1 P
1715
a2 76.46263 1 P
a3 71.96263 1 P
a4 74.96263 1 P
a8 60.46263 1 P
a9 53.46263 1 P
a14 31.96263 1 P
a15 55.46263 1 P
1717
a1 10.51555 1 P
a2 27.01555 1 P
a4 47.51555 1 P
a5 43.51555 1 P
a6 7.51555 1 P
a8 38.51555 1 P
a10 29.01555 1 P
1720
a2 128.29908 1 P
a5 123.79908 1 P
a6 75.29908 1 P
a7 111.79908 1 P
a8 131.29908 1 P
a10 115.79908 1 P
1736
a1 16.73563 1 P
a5 41.23563 1 P
a6 18.23563 1 P
a7 31.23563 1 P
1753
a1 10.87582 1 P
a2 34.87582 1 P
a4 48.37582 1 P
a8 48.87582 1 P
a9 52.37582 1 P
a10 35.37582 1 P
a11 18.37582 1 P
a12 28.37582 1 P
a13 40.87582 1 P
a14 54.37582 1 P
1758
a2 32.15710 1 P
a3 39.15710 1 P
a5 49.15710 1 P
a7 27.15710 1 P
a8 34.15710 1 P
a13 53.65710 1 P

1769
a1 22.58065 1 P
a4 57.08065 1 P
a6 16.08065 1 P
a10 40.08065 1 P
1842
a1 19.98907 1 P
a2 32.98907 1 P
a6 16.98907 1 P
a7 28.48907 1 P
a10 23.48907 1 P
1894
a2 34.84958 1 P
a3 46.34958 1 P
a5 51.84958 1 P
a6 18.34958 1 P
a7 32.34958 1 P
a8 53.34958 1 P
a14 88.34958 1 P
a15 79.84958 1 P
1898
a1 23.84677 1 P
a3 30.34677 1 P
a4 23.84677 1 P
a5 50.84677 1 P
a9 34.34677 1 P
a10 40.34677 1 P
a14 44.34677 1 P
1902
a3 8.27868 1 P
a4 17.77868 1 P
a7 10.77868 1 P
a8 13.27868 1 P
a9 19.77868 1 P
a14 27.27868 1 P
1923
a1 24.45969 1 P
a2 16.45969 1 P
a3 41.45969 1 P
a7 27.45969 1 P
a8 37.45969 1 P
1945
a3 66.47847 1 P
a5 64.97847 1 P
a6 31.97847 1 P
a7 46.97847 1 P
a10 46.97847 1 P
1958
a1 14.69686 1 P
a4 37.19686 1 P
a5 41.69686 1 P
a6 8.69686 1 P
a7 26.69686 1 P
a8 39.19686 1 P
a10 26.19686 1 P
a12 32.69686 1 P
a14 46.19686 1 P
a15 42.69686 1 P
1983
a1 21.52261 1 P
a3 41.02261 1 P
a4 39.52261 1 P
a5 34.52261 1 P
a7 19.02261 1 P
a8 33.52261 1 P
a9 40.02261 1 P
a11 20.02261 1 P
a12 28.02261 1 P
a13 32.52261 1 P
1992

a1 24.89864 1 P
a4 28.39864 1 P
a5 38.89864 1 P
a6 31.89864 1 P
a7 33.89864 1 P
a9 39.89864 1 P
a10 29.39864 1 P
2010
a1 21.75306 1 P
a6 4.75306 1 P
a7 34.75306 1 P
a11 18.75306 1 P
a14 56.75306 1 P
2038
a2 50.12776 1 P
a7 29.62776 1 P
a8 47.62776 1 P
a9 68.12776 1 P
a10 39.62776 1 P
a12 11.12776 1 P
a13 37.12776 1 P
a14 49.62776 1 P
a15 57.62776 1 P
2137
a1 28.87161 1 P
a3 38.37161 1 P
a4 29.87161 1 P
a6 32.87161 1 P
a10 27.37161 1 P
2169
a2 40.27044 1 P
a3 63.77044 1 P
a5 44.77044 1 P
a6 6.77044 1 P
a7 26.77044 1 P
a11 20.27044 1 P
2186
a1 14.92725 1 P
a2 24.92725 1 P
a6 6.42725 1 P
a9 51.92725 1 P
2197
a1 15.05228 1 P
a3 33.55228 1 P
a6 20.05228 1 P
a10 21.55228 1 P
2198
a2 44.85487 1 P
a3 53.35487 1 P
a4 62.85487 1 P
a5 28.85487 1 P
a6 27.85487 1 P
a7 43.85487 1 P
a8 53.85487 1 P
a9 56.85487 1 P
a10 44.35487 1 P
a11 40.85487 1 P
a12 65.35487 1 P
a15 71.35487 1 P
2199
a1 23.65689 1 P
a6 12.15689 1 P
a10 44.65689 1 P
a11 21.15689 1 P
a13 60.65689 1 P
a14 57.15689 1 P
a15 45.15689 1 P
2206
a1 29.65177 1 P
a3 40.65177 1 P

a4 28.65177 1 P
a6 46.65177 1 P
a9 37.15177 1 P
a10 27.15177 1 P
a14 50.65177 1 P
2214
a1 17.91640 1 P
a2 30.41640 1 P
a3 43.91640 1 P
a5 36.41640 1 P
a6 12.41640 1 P
a8 59.91640 1 P
a10 26.91640 1 P
a11 36.91640 1 P
2218
a1 34.98522 1 P
a2 43.48522 1 P
a3 45.98522 1 P
a4 34.98522 1 P
a7 46.48522 1 P
a8 51.98522 1 P
a9 42.48522 1 P
a10 35.48522 1 P
a11 68.48522 1 P
a14 58.48522 1 P
a15 50.48522 1 P
2220
a1 18.09889 1 P
a2 46.09889 1 P
a3 53.09889 1 P
a4 52.09889 1 P
a5 27.59889 1 P
a7 47.59889 1 P
a8 46.59889 1 P
a9 50.59889 1 P
a10 35.59889 1 P
a14 55.09889 1 P
2224
a1 17.21492 1 P
a2 32.21492 1 P
a3 52.21492 1 P
a5 46.71492 1 P
a6 6.71492 1 P
a7 37.21492 1 P
a9 50.21492 1 P
a14 78.21492 1 P
2234
a7 34.29315 1 P
a8 47.79315 1 P
a9 46.79315 1 P
a10 42.29315 1 P
a14 55.29315 1 P
2241
a1 10.14624 1 P
a5 29.64624 1 P
a6 4.14624 1 P
a7 20.14624 1 P
a8 30.14624 1 P
a10 15.64624 1 P
a11 12.64624 1 P
2249
a2 42.04330 1 P
a3 41.04330 1 P
a4 33.54330 1 P
a5 75.54330 1 P
a6 41.04330 1 P
a8 46.54330 1 P
a9 44.54330 1 P
a14 58.54330 1 P
a15 93.04330 1 P

2250
a1 27.66200 1 P
a4 30.66200 1 P
a6 36.66200 1 P
a10 30.16200 1 P
a15 46.66200 1 P
2253
a2 19.30652 1 P
a3 27.30652 1 P
a6 8.80652 1 P
a7 17.30652 1 P
a8 25.80652 1 P
a11 14.30652 1 P
2254
a1 21.48962 1 P
a2 36.98962 1 P
a3 48.98962 1 P
a4 44.48962 1 P
a6 14.98962 1 P
a7 28.48962 1 P
a8 44.48962 1 P
a10 26.98962 1 P
2263
a2 27.37184 1 P
a3 33.87184 1 P
a6 24.37184 1 P
a7 28.37184 1 P
a8 34.37184 1 P
a14 39.87184 1 P
a15 37.37184 1 P
2265
a3 20.14461 1 P
a4 14.64461 1 P
a5 53.14461 1 P
a9 21.14461 1 P
a10 39.14461 1 P
a14 38.14461 1 P
2267
a1 19.16055 1 P
a2 27.66055 1 P
a3 35.66055 1 P
a5 58.66055 1 P
a6 15.16055 1 P
a7 25.66055 1 P
a8 34.16055 1 P
a10 20.16055 1 P
2268
a1 25.34088 1 P
a3 34.84088 1 P
a6 26.34088 1 P
a7 30.84088 1 P
a10 22.34088 1 P
2270
a1 15.34665 1 P
a2 33.84665 1 P
a4 33.34665 1 P
a7 23.34665 1 P
a8 35.34665 1 P
a9 37.84665 1 P
a14 44.84665 1 P
2274
a2 29.83341 1 P
a3 20.33341 1 P
a6 32.33341 1 P
a9 22.83341 1 P
a10 21.83341 1 P
a11 37.33341 1 P
2275
a1 25.94922 1 P
a4 27.44922 1 P

a7 39.94922 1 P
a9 34.94922 1 P
a10 25.94922 1 P
2276
a1 9.33030 1 P
a2 19.83030 1 P
a3 33.33030 1 P
a5 26.33030 1 P
a7 15.33030 1 P
a8 28.83030 1 P
a10 17.33030 1 P
2279
a2 30.76546 1 P
a4 34.76546 1 P
a7 18.26546 1 P
a8 31.26546 1 P
a12 48.26546 1 P
a14 41.76546 1 P
2283
a2 26.01098 1 P
a3 37.01098 1 P
a5 55.01098 1 P
a7 21.51098 1 P
a8 36.01098 1 P
a9 38.51098 1 P
a10 24.51098 1 P
2287
a2 26.12425 1 P
a3 19.12425 1 P
a4 16.62425 1 P
a6 36.12425 1 P
a8 30.12425 1 P
a9 21.12425 1 P
a10 45.62425 1 P
2301
a6 24.43425 1 P
a8 45.43425 1 P
a9 27.93425 1 P
a13 41.43425 1 P
a14 46.43425 1 P
2305
a1 34.01270 1 P
a2 34.51270 1 P
a3 33.51270 1 P
a4 29.51270 1 P
a6 41.01270 1 P
a7 39.01270 1 P
a8 37.51270 1 P
a9 32.01270 1 P
a10 32.01270 1 P
a11 45.51270 1 P
a13 61.51270 1 P
a14 38.51270 1 P
a15 72.51270 1 P
2310
a1 26.04186 1 P
a2 28.54186 1 P
a7 34.54186 1 P
a8 33.54186 1 P
a10 19.54186 1 P
2316
a2 30.50471 1 P
a4 23.00471 1 P
a8 24.00471 1 P
a9 26.00471 1 P
a14 55.50471 1 P
2319
a2 23.41087 1 P
a7 12.41087 1 P
a12 36.91087 1 P

a14 39.41087 1 P
2320
a2 21.31778 1 P
a3 21.81778 1 P
a4 28.31778 1 P
a9 29.81778 1 P
a10 34.31778 1 P
a14 38.81778 1 P
2321
a2 55.38686 1 P
a5 62.38686 1 P
a6 15.88686 1 P
a8 46.38686 1 P
a10 37.88686 1 P
a11 33.88686 1 P
2322
a1 46.11518 1 P
a3 57.61518 1 P
a4 41.61518 1 P
a6 46.11518 1 P
a9 46.11518 1 P
a10 33.61518 1 P
a15 65.11518 1 P
2324
a1 19.77235 1 P
a3 31.27235 1 P
a7 27.27235 1 P
a8 27.77235 1 P
a9 30.77235 1 P
a11 19.77235 1 P
a15 28.27235 1 P
2327
a4 38.90113 1 P
a7 26.40113 1 P
a8 38.90113 1 P
a9 41.90113 1 P
a12 35.90113 1 P
a14 48.40113 1 P
a15 61.40113 1 P
2329
a3 83.56285 1 P
a4 71.06285 1 P
a5 113.56285 1 P
a9 76.56285 1 P
a10 63.56285 1 P
a15 97.56285 1 P
2332
a1 34.30599 1 P
a2 34.80599 1 P
a3 29.80599 1 P
a4 23.80599 1 P
a6 41.30599 1 P
a7 44.30599 1 P
a8 34.80599 1 P
a9 27.80599 1 P
2333
a1 33.02443 1 P
a2 32.02443 1 P
a3 34.02443 1 P
a4 29.02443 1 P
a9 25.02443 1 P
2334
a2 37.22662 1 P
a4 26.22662 1 P
a7 17.22662 1 P
a8 27.22662 1 P
a12 35.22662 1 P
a14 37.22662 1 P
2335
a1 13.29423 1 P

a3 54.29423 1 P
a5 45.29423 1 P
a6 8.79423 1 P
a7 38.79423 1 P
2336
a1 20.39998 1 P
a2 30.39998 1 P
a3 38.89998 1 P
a6 9.39998 1 P
a7 29.89998 1 P
a8 36.39998 1 P
a9 43.39998 1 P
a10 25.89998 1 P
a11 24.89998 1 P
2337
a1 10.04723 1 P
a4 40.04723 1 P
a7 23.54723 1 P
a8 39.54723 1 P
a12 32.04723 1 P
a13 42.04723 1 P
a14 49.04723 1 P
2338
a2 24.35942 1 P
a8 36.35942 1 P
a10 40.85942 1 P
a12 45.85942 1 P
a14 48.35942 1 P
2340
a2 21.13805 1 P
a4 34.63805 1 P
a7 20.63805 1 P
a8 40.63805 1 P
a9 37.63805 1 P
a14 43.63805 1 P
2345
a2 6.54118 1 P
a3 17.54118 1 P
a6 14.54118 1 P
a7 25.54118 1 P
2347
a1 22.04576 1 P
a2 12.04576 1 P
a3 11.04576 1 P
a4 14.04576 1 P
a6 25.04576 1 P
a10 28.54576 1 P
2356
a1 18.55321 1 P
a7 29.55321 1 P
a8 44.05321 1 P
a14 53.05321 1 P
2357
a1 17.20567 1 P
a2 30.20567 1 P
a3 38.70567 1 P
a4 40.20567 1 P
a5 58.70567 1 P
a6 9.70567 1 P
a7 24.70567 1 P
a8 36.70567 1 P
a10 29.70567 1 P
a11 32.70567 1 P
a13 64.70567 1 P
a14 76.20567 1 P
2358
a1 12.88459 1 P
a2 37.88459 1 P
a3 46.38459 1 P
a4 49.88459 1 P

a7 19.88459 1 P
a8 32.88459 1 P
a10 36.38459 1 P
a11 44.88459 1 P
a13 30.88459 1 P
a14 37.38459 1 P
2360
a1 17.34920 1 P
a3 39.34920 1 P
a5 44.84920 1 P
a6 3.34920 1 P
a7 31.34920 1 P
a11 32.84920 1 P
a13 55.84920 1 P
a14 65.84920 1 P
2361
a3 6.36179 1 P
a4 14.86179 1 P
a7 9.86179 1 P
a8 11.36179 1 P
a9 14.36179 1 P
a10 26.36179 1 P
a14 21.86179 1 P
a15 27.86179 1 P
2362
a1 18.84189 1 P
a3 28.34189 1 P
a4 19.84189 1 P
a7 33.84189 1 P
a9 26.34189 1 P
a10 16.84189 1 P
2365
a3 65.93870 1 P
a4 52.43870 1 P
a5 99.93870 1 P
a10 46.43870 1 P
a15 79.93870 1 P
2368
a1 46.34350 1 P
a2 41.84350 1 P
a3 38.84350 1 P
a4 35.34350 1 P
a6 54.84350 1 P
a8 40.84350 1 P
a9 45.34350 1 P
2374
a2 42.62852 1 P
a7 57.12852 1 P
a10 29.62852 1 P
a11 33.12852 1 P
a14 77.62852 1 P
a15 56.62852 1 P
2384
a1 27.98614 1 P
a3 39.98614 1 P
a5 29.98614 1 P
a7 32.98614 1 P
a8 36.98614 1 P
a9 32.48614 1 P
a10 20.48614 1 P
a11 22.48614 1 P
a15 32.48614 1 P
2386
a2 9.05129 1 P
a3 6.05129 1 P
a4 8.05129 1 P
a6 21.55129 1 P
a7 16.55129 1 P
a8 11.05129 1 P
a9 10.55129 1 P

a10 25.55129 1 P
a14 20.05129 1 P
2388
a1 25.76651 1 P
a2 30.26651 1 P
a3 31.76651 1 P
a4 24.76651 1 P
a7 33.26651 1 P
a9 29.26651 1 P
2389
a1 14.98124 1 P
a2 24.48124 1 P
a3 38.98124 1 P
a6 8.98124 1 P
a7 36.48124 1 P
a10 18.98124 1 P
2391
a2 21.93991 1 P
a3 37.43991 1 P
a7 30.93991 1 P
a8 36.93991 1 P
a9 45.93991 1 P
a14 47.43991 1 P
a15 54.43991 1 P
2395
a1 19.22138 1 P
a2 28.72138 1 P
a3 41.72138 1 P
a5 52.72138 1 P
a6 18.72138 1 P
a7 27.72138 1 P
a10 22.72138 1 P
2404
a2 22.64050 1 P
a3 20.64050 1 P
a4 26.14050 1 P
a6 38.64050 1 P
a7 31.64050 1 P
a8 28.14050 1 P
a10 51.14050 1 P
2405
a3 34.81179 1 P
a5 42.31179 1 P
a7 28.31179 1 P
a8 34.81179 1 P
a11 28.81179 1 P
2411
a1 26.75761 1 P
a2 32.75761 1 P
a3 37.25761 1 P
a4 30.75761 1 P
a5 26.25761 1 P
a6 36.75761 1 P
a7 33.75761 1 P
a8 36.25761 1 P
a12 45.75761 1 P
a14 56.75761 1 P
2413
a2 28.55722 1 P
a4 42.55722 1 P
a5 56.05722 1 P
a6 10.05722 1 P
a7 18.05722 1 P
a8 30.55722 1 P
a10 39.55722 1 P
a11 50.05722 1 P
2418
a3 58.81576 1 P
a5 48.31576 1 P
a7 48.31576 1 P

a10 43.31576 1 P
a11 61.81576 1 P
2426
a1 35.80625 1 P
a2 34.30625 1 P
a3 31.30625 1 P
a4 23.30625 1 P
a9 34.80625 1 P
2433
a2 89.02544 1 P
a4 144.02544 1 P
a6 44.02544 1 P
a7 67.02544 1 P
a8 102.02544 1 P
a9 121.52544 1 P
a10 72.52544 1 P
a11 45.02544 1 P
a12 42.52544 1 P
a13 89.52544 1 P
a15 90.52544 1 P
2435
a2 29.99229 1 P
a4 44.99229 1 P
a5 33.49229 1 P
a6 3.49229 1 P
a7 22.99229 1 P
a10 33.49229 1 P
a11 15.99229 1 P
a15 39.49229 1 P
2436
a1 19.17047 1 P
a3 44.67047 1 P
a5 50.17047 1 P
a6 11.17047 1 P
a7 26.17047 1 P
a10 27.17047 1 P
a11 41.17047 1 P
a14 65.67047 1 P
2439
a4 59.87390 1 P
a7 33.87390 1 P
a8 64.87390 1 P
a9 46.87390 1 P
a10 21.87390 1 P
a13 34.87390 1 P
a14 25.87390 1 P
a15 30.37390 1 P
2441
a6 17.11101 1 P
a10 21.61101 1 P
a11 7.11101 1 P
a14 50.61101 1 P
2443
a6 31.85828 1 P
a9 62.85828 1 P
a10 44.35828 1 P
a11 22.35828 1 P
a12 24.85828 1 P
a13 43.35828 1 P
a14 54.35828 1 P
a15 48.85828 1 P
2453
a1 73.48756 1 P
a6 36.98756 1 P
a7 44.98756 1 P
a8 61.98756 1 P
a10 53.48756 1 P
a11 26.98756 1 P
a12 24.98756 1 P
a13 62.48756 1 P

2454
a1 38.11514 1 P
a4 81.61514 1 P
a6 32.11514 1 P
a9 52.11514 1 P
a10 33.61514 1 P
a11 9.11514 1 P
a13 55.61514 1 P
a14 44.11514 1 P
a15 39.11514 1 P
2459
a1 41.94054 1 P
a2 42.44054 1 P
a3 44.44054 1 P
a4 38.44054 1 P
a7 47.44054 1 P
a9 35.44054 1 P
a15 16.94054 1 P
2460
a8 49.86314 1 P
a9 37.86314 1 P
a10 22.36314 1 P
a11 10.86314 1 P
a13 47.36314 1 P
a15 22.36314 1 P
2463
a1 34.79982 1 P
a2 35.79982 1 P
a3 33.79982 1 P
a4 23.79982 1 P
a6 42.29982 1 P
a7 38.29982 1 P
a8 35.29982 1 P
a9 23.79982 1 P
a12 54.79982 1 P
2467
a2 20.82336 1 P
a3 24.82336 1 P
a4 25.32336 1 P
a7 25.32336 1 P
a8 28.82336 1 P
a10 32.32336 1 P
a11 42.82336 1 P
a12 38.32336 1 P
a15 39.82336 1 P
2469
a2 37.40571 1 P
a6 25.90571 1 P
a7 26.40571 1 P
a8 37.90571 1 P
a9 46.40571 1 P
a10 26.40571 1 P
a11 17.40571 1 P
a12 22.90571 1 P
a13 35.40571 1 P
a14 37.90571 1 P
a15 29.90571 1 P
2471
a2 7.94667 1 P
a3 13.94667 1 P
a14 15.94667 1 P
2472
a1 36.31369 1 P
a3 54.31369 1 P
a6 29.81369 1 P
a8 42.81369 1 P
a9 30.81369 1 P
a11 25.81369 1 P
a14 40.31369 1 P
a15 26.81369 1 P

2473
a1 16.29139 1 P
a10 15.79139 1 P
2477
a1 17.55769 1 P
a2 22.55769 1 P
a3 50.55769 1 P
a5 41.55769 1 P
a6 30.55769 1 P
a7 24.05769 1 P
a9 49.05769 1 P
a10 13.55769 1 P
a12 29.05769 1 P
a15 44.05769 1 P
2479
a1 24.95339 1 P
a2 32.95339 1 P
a4 29.95339 1 P
a9 28.45339 1 P
a10 26.45339 1 P
a14 38.45339 1 P
a15 35.45339 1 P
2480
a8 44.45175 1 P
a11 13.45175 1 P
a13 40.95175 1 P
a15 25.45175 1 P
2481
a1 17.74803 1 P
a2 25.24803 1 P
a4 35.74803 1 P
a6 24.24803 1 P
a8 38.24803 1 P
2482
a1 80.30956 1 P
a2 125.30956 1 P
a3 128.80956 1 P
a7 86.80956 1 P
a8 123.80956 1 P
a9 111.30956 1 P
a12 68.80956 1 P
a13 97.80956 1 P
a14 105.80956 1 P
2485
a1 35.67576 1 P
a3 17.17576 1 P
a4 21.17576 1 P
a6 33.67576 1 P
a7 25.17576 1 P
a8 18.67576 1 P
a10 31.67576 1 P
a11 48.17576 1 P
a12 40.17576 1 P
2486
a1 40.12345 1 P
a2 41.12345 1 P
a3 36.12345 1 P
a4 26.62345 1 P
a9 22.62345 1 P
a14 36.12345 1 P
2487
a8 48.11963 1 P
a10 19.61963 1 P
a11 19.61963 1 P
a15 13.61963 1 P
2490
a2 44.82915 1 P
a3 38.32915 1 P
a4 47.32915 1 P
a6 68.82915 1 P

a7 62.32915 1 P
a8 45.82915 1 P
a10 67.82915 1 P
a14 56.32915 1 P
2492
a1 23.13783 1 P
a4 21.63783 1 P
a7 36.13783 1 P
a10 20.13783 1 P
2495
a1 28.39637 1 P
a3 35.89637 1 P
a4 22.89637 1 P
a6 38.89637 1 P
a7 40.39637 1 P
a9 24.39637 1 P
a10 22.89637 1 P
2496
a1 15.74935 1 P
a3 27.74935 1 P
a9 20.24935 1 P
a10 11.74935 1 P
a11 9.74935 1 P
2497
a2 27.89422 1 P
a3 48.39422 1 P
a4 49.89422 1 P
a8 39.39422 1 P
a9 48.39422 1 P
a10 42.89422 1 P
a12 36.39422 1 P
a13 49.39422 1 P
a15 49.39422 1 P
2499
a1 18.76684 1 P
a2 25.26684 1 P
a5 29.76684 1 P
a6 22.76684 1 P
a7 25.26684 1 P
a8 31.26684 1 P
a9 24.26684 1 P
a11 36.76684 1 P
a12 29.76684 1 P
a13 39.26684 1 P
a14 33.76684 1 P
2501
a1 64.21155 1 P
a6 40.21155 1 P
a7 57.21155 1 P
a9 48.21155 1 P
a10 39.21155 1 P
a11 34.21155 1 P
a13 60.71155 1 P
a14 52.21155 1 P
a15 41.21155 1 P
2502
a1 26.74015 1 P
a2 43.74015 1 P
a10 17.74015 1 P
a11 20.24015 1 P
a14 42.24015 1 P
a15 26.74015 1 P
2506
a1 20.90815 1 P
a2 26.90815 1 P
a3 44.90815 1 P
a6 25.40815 1 P
a7 28.90815 1 P
a8 35.90815 1 P
a9 26.40815 1 P

a10 17.40815 1 P
a11 39.40815 1 P
a15 39.40815 1 P
2509
a1 2.57601 1 P
a2 25.07601 1 P
a4 39.07601 1 P
a8 34.07601 1 P
a9 38.57601 1 P
a11 34.07601 1 P
a14 44.57601 1 P
a15 43.07601 1 P
2511
a1 29.26075 1 P
a2 34.76075 1 P
a3 31.76075 1 P
a4 22.76075 1 P
a6 36.26075 1 P
a9 23.76075 1 P
2515
a6 23.06587 1 P
a9 30.56587 1 P
a11 17.56587 1 P
a14 36.56587 1 P
a15 25.06587 1 P
2517
a1 14.79359 1 P
a2 38.29359 1 P
a3 48.29359 1 P
a4 62.29359 1 P
a7 28.29359 1 P
a8 37.29359 1 P
a9 38.29359 1 P
a12 9.29359 1 P
a13 47.79359 1 P
a14 42.29359 1 P
a15 39.79359 1 P
2518
a2 32.22619 1 P
a3 31.72619 1 P
a4 25.22619 1 P
a7 32.72619 1 P
a9 25.22619 1 P
2521
a1 12.88506 1 P
a3 56.88506 1 P
a7 29.38506 1 P
a8 45.38506 1 P
a9 49.88506 1 P
a13 66.88506 1 P
a14 59.38506 1 P
2522
a1 29.25318 1 P
a2 29.25318 1 P
a3 26.25318 1 P
a4 25.25318 1 P
a7 32.75318 1 P
a12 42.75318 1 P
2523
a7 44.65189 1 P
a8 50.65189 1 P
a10 24.15189 1 P
a11 10.65189 1 P
a14 38.15189 1 P
a15 16.65189 1 P
2529
a1 25.96723 1 P
a2 29.96723 1 P
a4 25.96723 1 P
a7 31.96723 1 P

a8 29.96723 1 P
2530
a1 23.54638 1 P
a6 8.54638 1 P
a7 27.54638 1 P
a10 34.04638 1 P
a11 18.54638 1 P
2538
a2 66.74663 1 P
a3 58.24663 1 P
a4 47.24663 1 P
a6 57.74663 1 P
a7 54.74663 1 P
a8 52.74663 1 P
a9 29.24663 1 P
a10 26.74663 1 P
a11 38.74663 1 P
a14 33.24663 1 P
a15 4.24663 1 P
2539
a1 29.39377 1 P
a2 36.39377 1 P
a4 25.39377 1 P
a6 42.39377 1 P
a10 24.39377 1 P
2540
a1 22.99790 1 P
a2 24.99790 1 P
a4 18.99790 1 P
a9 18.99790 1 P
a10 22.99790 1 P
a15 28.99790 1 P
2543
a1 19.62220 1 P
a2 26.62220 1 P
a3 33.62220 1 P
a6 28.12220 1 P
a7 33.62220 1 P
a9 29.62220 1 P
a10 19.62220 1 P
a12 32.62220 1 P
a13 41.12220 1 P
a15 33.12220 1 P
2545
a1 11.14893 1 P
a2 28.14893 1 P
a3 68.64893 1 P
a8 60.14893 1 P
a12 49.64893 1 P
a14 46.64893 1 P
2546
a1 23.91399 1 P
a2 31.91399 1 P
a6 38.91399 1 P
a7 36.91399 1 P
a8 47.91399 1 P
a9 44.91399 1 P
a11 46.41399 1 P
2547
a1 46.48091 1 P
a2 38.48091 1 P
a4 36.98091 1 P
a6 53.98091 1 P
a7 50.48091 1 P
a8 42.98091 1 P
a15 86.98091 1 P
2549
a6 10.28558 1 P
a11 17.28558 1 P
a12 20.28558 1 P

a15 39.78558 1 P
2552
a1 32.73026 1 P
a3 20.73026 1 P
a4 19.73026 1 P
a7 30.23026 1 P
a8 26.73026 1 P
a10 38.73026 1 P
2558
a2 17.02105 1 P
a3 17.02105 1 P
a4 26.52105 1 P
a7 23.02105 1 P
a10 63.52105 1 P
a11 54.02105 1 P
a12 44.52105 1 P
a14 29.02105 1 P
a15 64.02105 1 P
2559
a1 40.88283 1 P
a2 56.38283 1 P
a3 51.38283 1 P
a6 58.88283 1 P
a7 45.38283 1 P
a10 30.88283 1 P
a15 79.38283 1 P
2561
a1 27.22490 1 P
a2 30.22490 1 P
a3 33.22490 1 P
a4 26.22490 1 P
a6 54.72490 1 P
a7 34.72490 1 P
a8 36.22490 1 P
a9 30.72490 1 P
a10 31.22490 1 P
a15 71.72490 1 P
2567
a1 16.74889 1 P
a2 31.24889 1 P
a3 35.24889 1 P
a6 25.24889 1 P
a7 29.74889 1 P
a10 16.24889 1 P
2569
a1 17.40912 1 P
a2 33.90912 1 P
a3 49.40912 1 P
a6 5.40912 1 P
a7 22.40912 1 P
a8 37.40912 1 P
a10 19.90912 1 P
a11 24.40912 1 P
a13 50.90912 1 P
a14 60.90912 1 P
a15 49.90912 1 P
2571
a1 27.34706 1 P
a2 29.84706 1 P
a3 27.84706 1 P
a4 23.84706 1 P
a6 39.84706 1 P
a7 34.34706 1 P
a8 30.34706 1 P
a9 24.84706 1 P
a11 56.84706 1 P
a12 43.34706 1 P
2575
a1 14.66871 1 P
a2 12.16871 1 P

a3 38.66871 1 P
2576
a4 43.08113 1 P
a6 31.08113 1 P
a9 33.08113 1 P
a10 5.08113 1 P
a11 29.58113 1 P
a13 44.58113 1 P
a14 46.08113 1 P
a15 6.08113 1 P
2580
a1 12.53464 1 P
a2 33.03464 1 P
a3 50.03464 1 P
a6 10.03464 1 P
a7 23.03464 1 P
a8 37.53464 1 P
a11 35.53464 1 P
a12 16.03464 1 P
a13 37.03464 1 P
2582
a1 53.50237 1 P
a2 54.50237 1 P
a3 56.50237 1 P
a6 40.00237 1 P
a7 49.00237 1 P
a8 47.00237 1 P
a11 67.00237 1 P
a13 54.00237 1 P
a15 75.50237 1 P
2583
a1 29.92957 1 P
a7 36.42957 1 P
a9 60.92957 1 P
a12 17.92957 1 P
a15 54.92957 1 P
2586
a1 20.57608 1 P
a3 27.07608 1 P
a4 21.57608 1 P
a7 29.07608 1 P
a9 19.57608 1 P
a14 29.57608 1 P
a15 26.07608 1 P
2587
a7 13.58025 1 P
a8 14.58025 1 P
2592
a2 56.55007 1 P
a6 25.05007 1 P
a7 46.05007 1 P
a10 47.05007 1 P
a11 37.55007 1 P
a15 50.05007 1 P
2594
a7 9.04015 1 P
2595
a1 28.59021 1 P
a2 34.09021 1 P
a3 42.59021 1 P
a6 33.59021 1 P
a7 36.09021 1 P
a8 39.59021 1 P
a9 34.09021 1 P
a10 26.59021 1 P
a11 47.09021 1 P
2598
a1 23.46235 1 P
a2 21.46235 1 P
a3 30.46235 1 P

a7 29.96235 1 P
a8 31.46235 1 P
2601
a1 18.57047 1 P
a2 18.57047 1 P
a3 41.07047 1 P
a4 52.57047 1 P
a8 48.57047 1 P
a15 54.57047 1 P
2606
a9 27.55375 1 P
a10 4.05375 1 P
a11 16.55375 1 P
a14 36.55375 1 P
a15 22.05375 1 P
2615
a1 24.03813 1 P
a7 25.53813 1 P
a12 19.03813 1 P
a14 49.53813 1 P
2617
a1 30.09791 1 P
a2 51.09791 1 P
a7 31.59791 1 P
a8 43.59791 1 P
a12 20.59791 1 P
a14 53.09791 1 P
2619
a3 45.71658 1 P
a4 33.21658 1 P
a5 64.71658 1 P
a6 12.21658 1 P
a10 8.21658 1 P
a11 30.21658 1 P
a15 49.21658 1 P
2624
a2 48.27464 1 P
a3 70.27464 1 P
a8 34.77464 1 P
a9 40.27464 1 P
a11 48.77464 1 P
a13 44.27464 1 P
a14 40.77464 1 P
a15 39.27464 1 P
2627
a1 27.38793 1 P
a2 22.38793 1 P
a3 24.38793 1 P
a4 19.38793 1 P
a6 61.38793 1 P
a7 27.88793 1 P
a8 24.38793 1 P
a9 23.38793 1 P
a12 37.38793 1 P
2635
a3 56.95937 1 P
a8 63.95937 1 P
a9 34.95937 1 P
a11 13.95937 1 P
a13 59.95937 1 P
a14 43.45937 1 P

Figure A-6: Top view of the Marcellus Shale sample prior to testing.

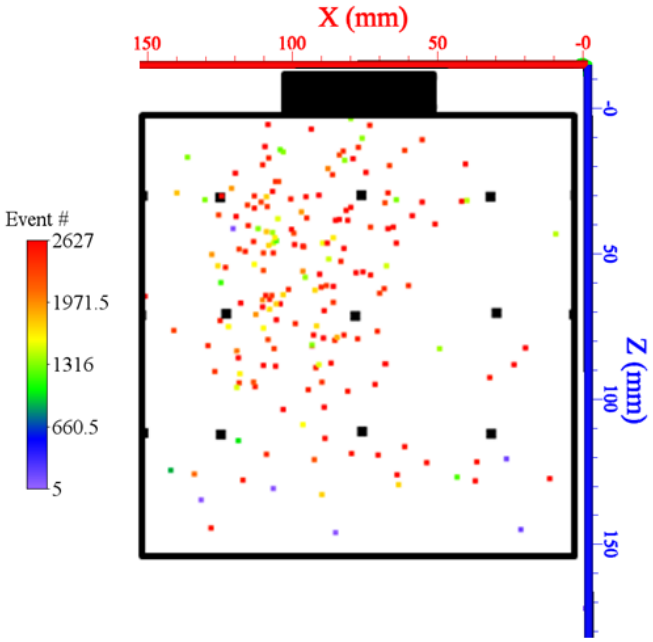

Figure A-7: The original event locations from ESG software for the Berea Sandstone sample in the XZ plane. Multicolored nodes represent events, the black outline is the extent of the sample, and the solid block is the indenter.

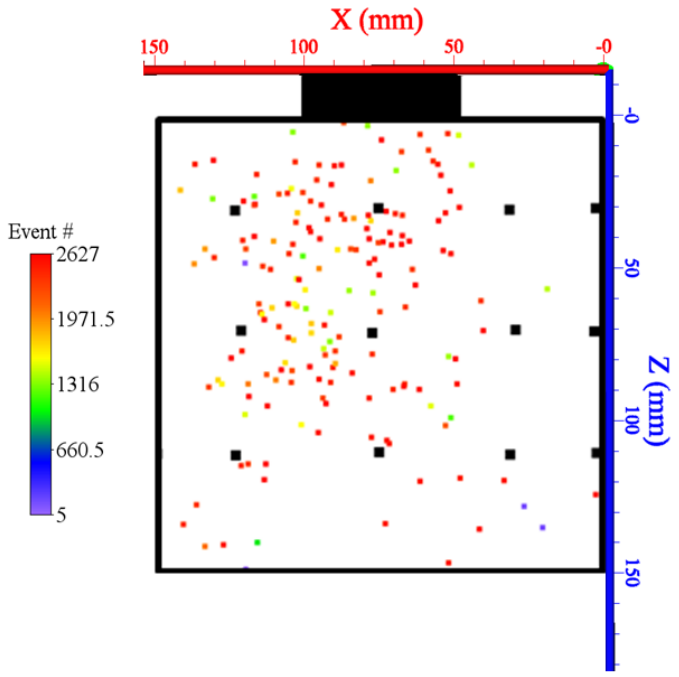

Figure A-8: The relocated event locations from TomoDD for the Berea Sandstone sample in the XZ plane. Multicolored nodes represent events, the black outline is the extent of the sample, and the solid block is the indenter.

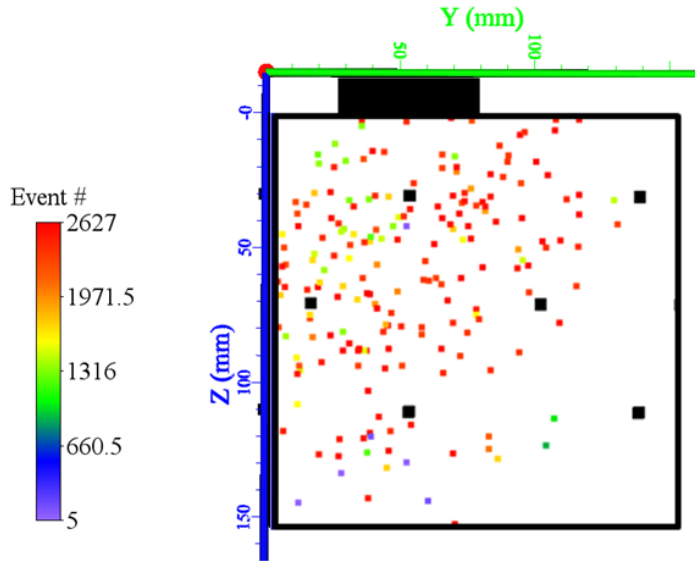

Figure A-9: The original event locations from ESG software for the Berea Sandstone sample in the YZ plane. Multicolored nodes represent events, the black outline is the extent of the sample, and the solid block is the indenter.

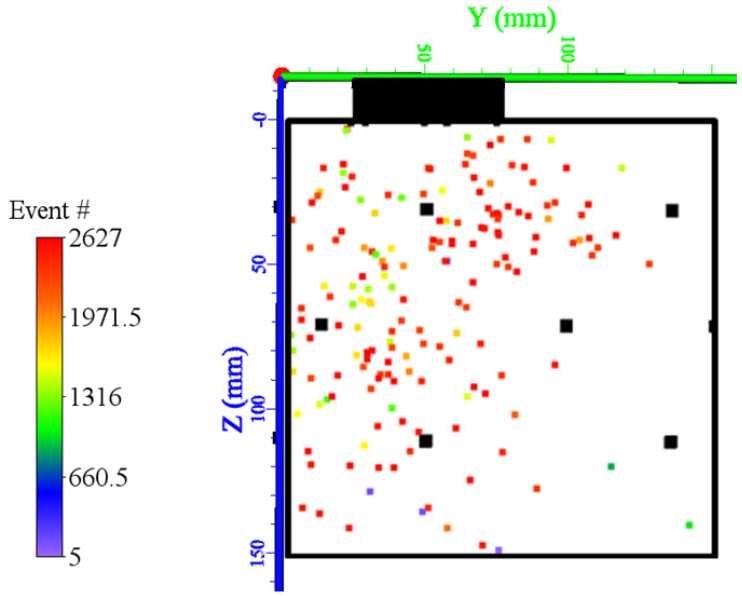

Figure A-10: The relocated event locations from TomoDD for the Berea Sandstone sample in the YZ plane. Multicolored nodes represent events the black outline is the extent of the sample, and the solid block is the indenter.

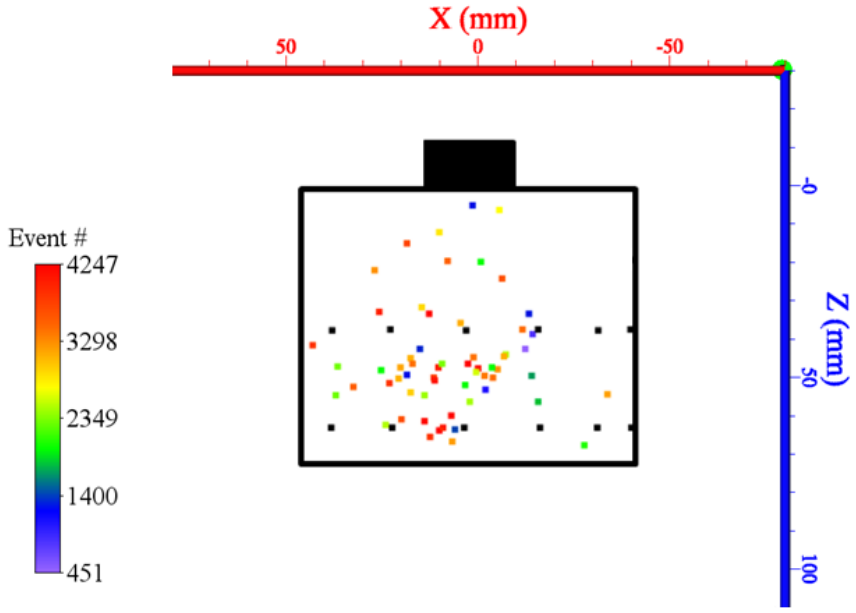

Figure A-11: The original event locations from ESG software for the Marcellus Shale sample in the XZ plane. Multicolored nodes represent events, the black outline is the extent of the sample, and the solid block is the indenter.

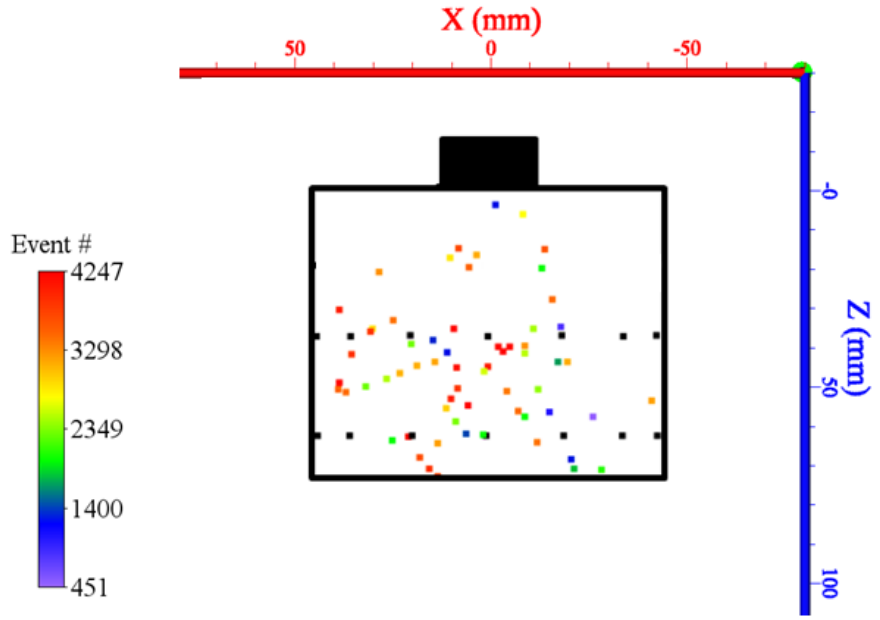

Figure A-12: The relocated event locations from TomoDD for the Marcellus Shale sample in the XZ plane. Multicolored nodes represent events, the black outline is the extent of the sample, and the solid block is the indenter.

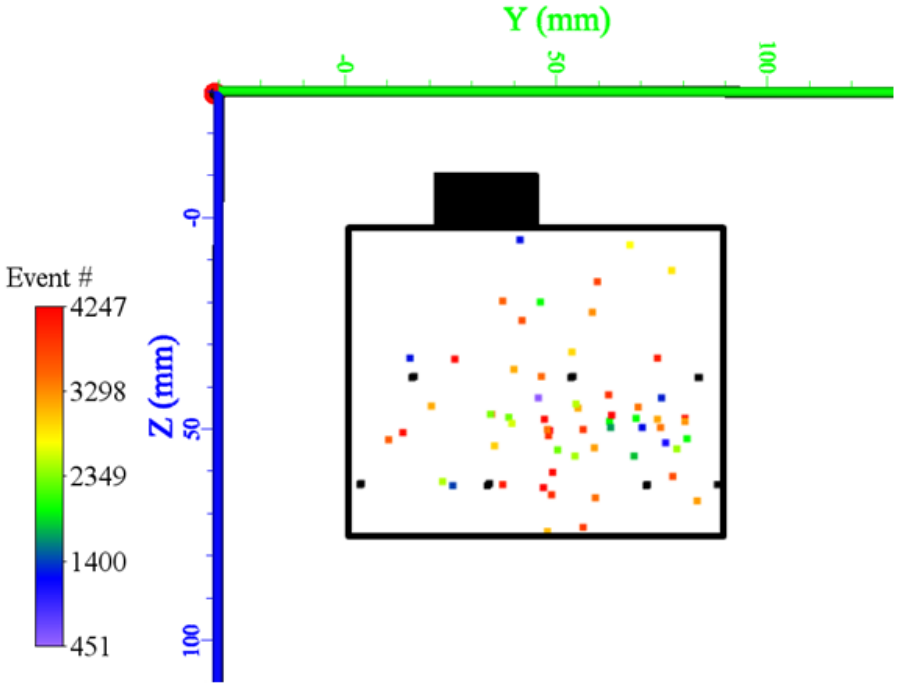

Figure A-13: The original event locations from ESG software for the Marcellus Shale sample in the YZ plane. Multicolored nodes represent events, the black outline is the extent of the sample, and the solid block is the indenter.

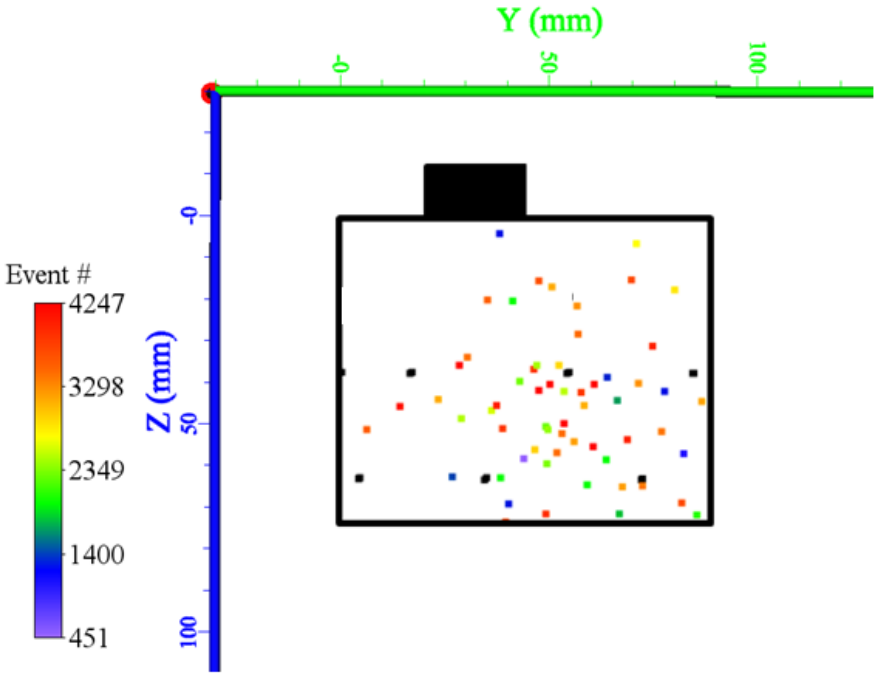

Figure A-14: The relocated event locations from TomoDD for the Marcellus Shale sample in the YZ plane. Multicolored nodes represent events, the black outline is the extent of the sample, and the solid block is the indenter.

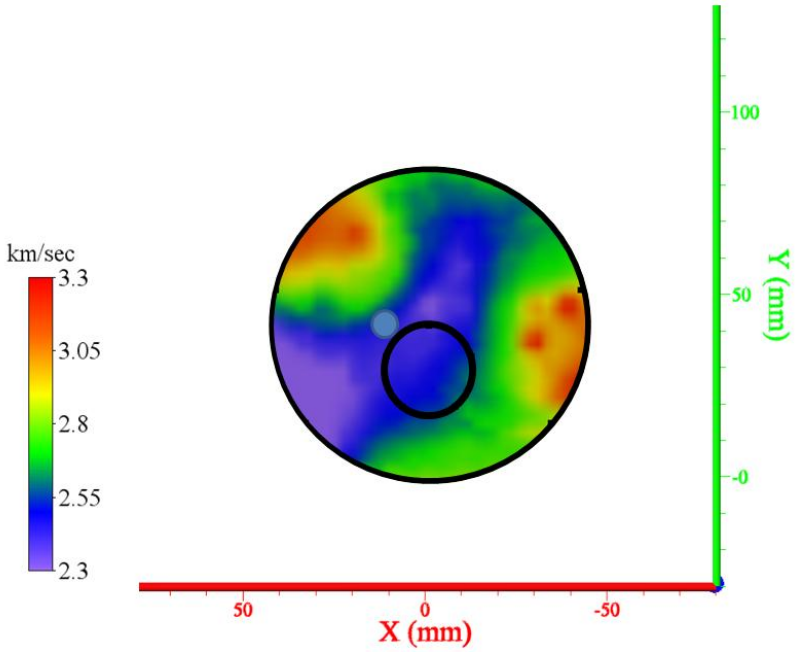

Figure A-15: Orthogonal image for the first regime of the Marcellus Shale sample. Point of interest located at 10 mm in the x direction and 40 mm in the y direction, at a depth of 50 mm represented by the blue point.

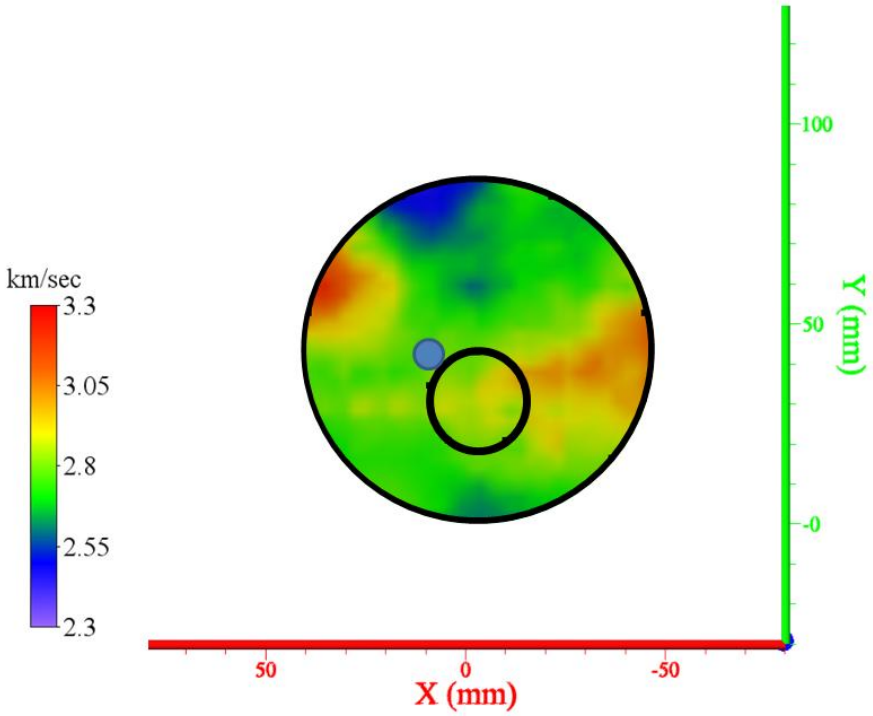

Figure A-16: Orthogonal image for the second regime of the Marcellus Shale sample. Point of interest located at 10 mm in the x direction and 40 mm in the y direction, at a depth of 50 mm represented by the blue point.

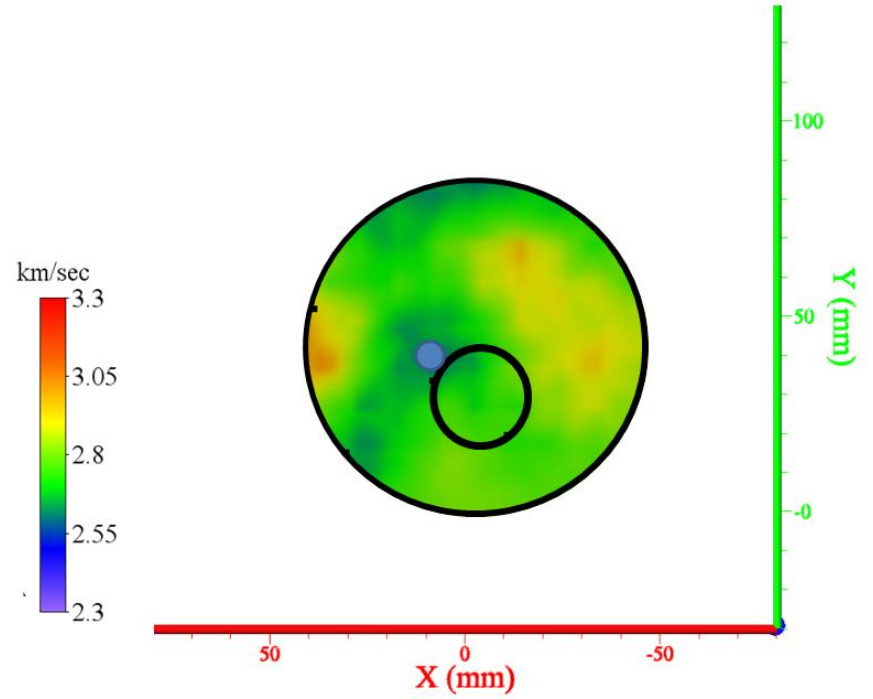

Figure A-17: Orthogonal image for the third regime of the Marcellus Shale sample. Point of interest located at 10 mm in the x direction and 40 mm in the y direction, at a depth of 50 mm represented by the blue point.

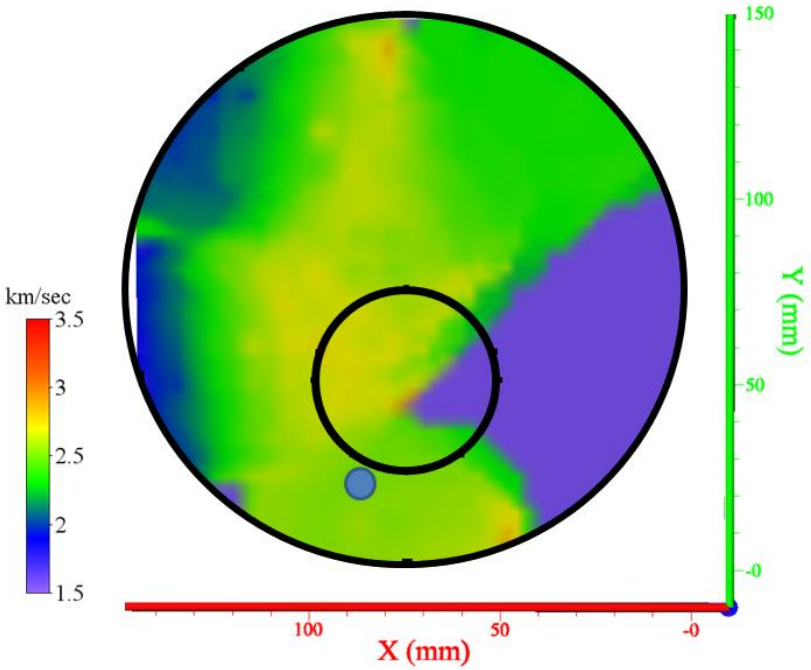

Figure A-18: Orthogonal image for the first regime of the Berea Sandstone sample. Point of interest located at 85 mm in the x direction and 20 mm in the y direction, at a depth of 50 mm represented by the blue point.

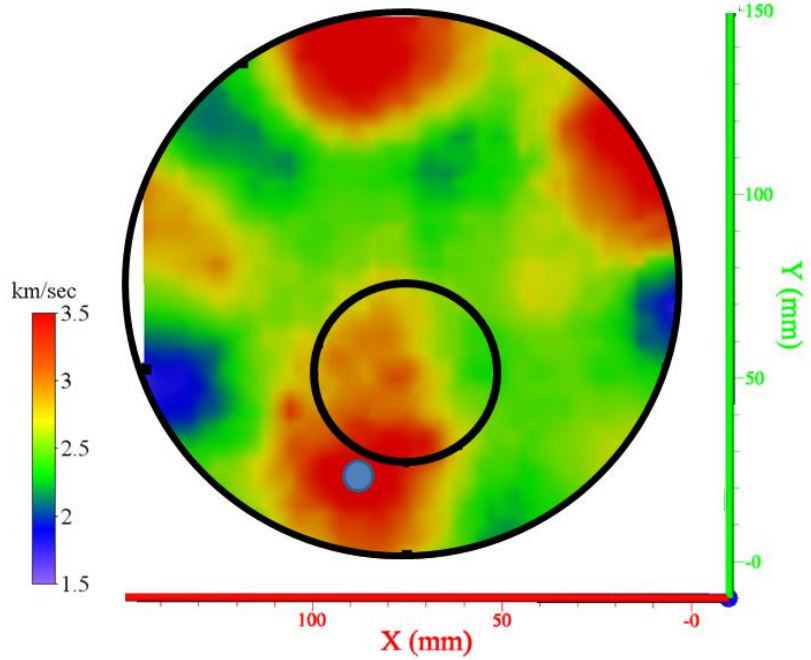

Figure A-19: Orthogonal image for the second regime of the Berea Sandstone sample. Point of interest located at 85 mm in the x direction and 20 mm in the y direction, at a depth of 50 mm represented by the blue point.

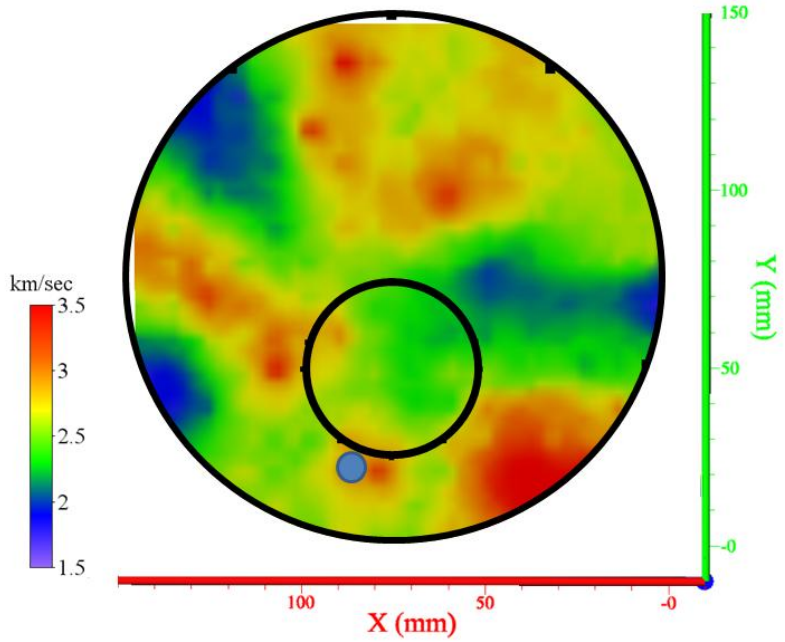

Figure A-20: Orthogonal image for the third regime of the Berea Sandstone sample. Point of interest located at 85 mm in the x direction and 20 mm in the y direction, at a depth of 50 mm represented by the blue point.

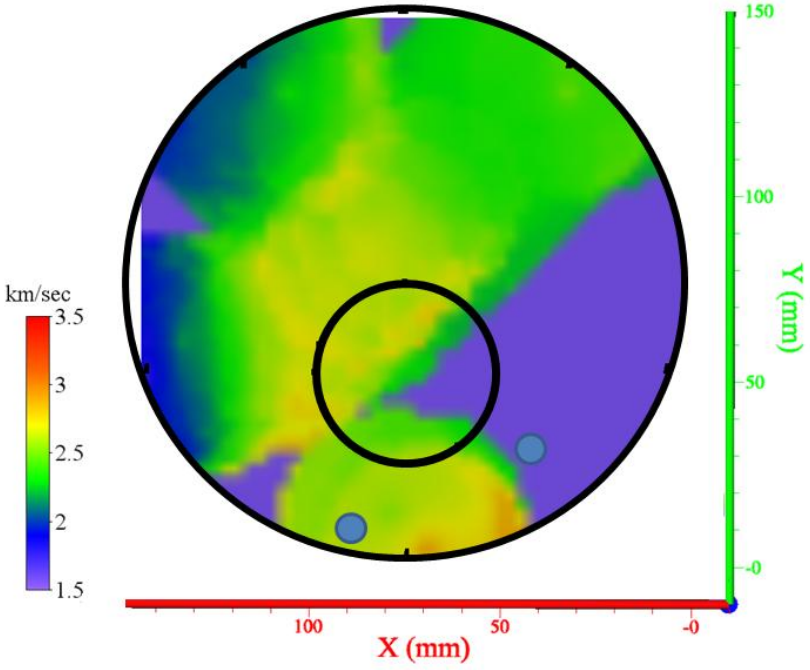

Figure A-21: Orthogonal image for the first regime of the Berea Sandstone sample. Points of interest: 90 mm in the x direction and 10 mm in the y direction, and 40 mm in the x direction and 30 mm in the y direction, at a depth of 30 mm represented by the blue points.

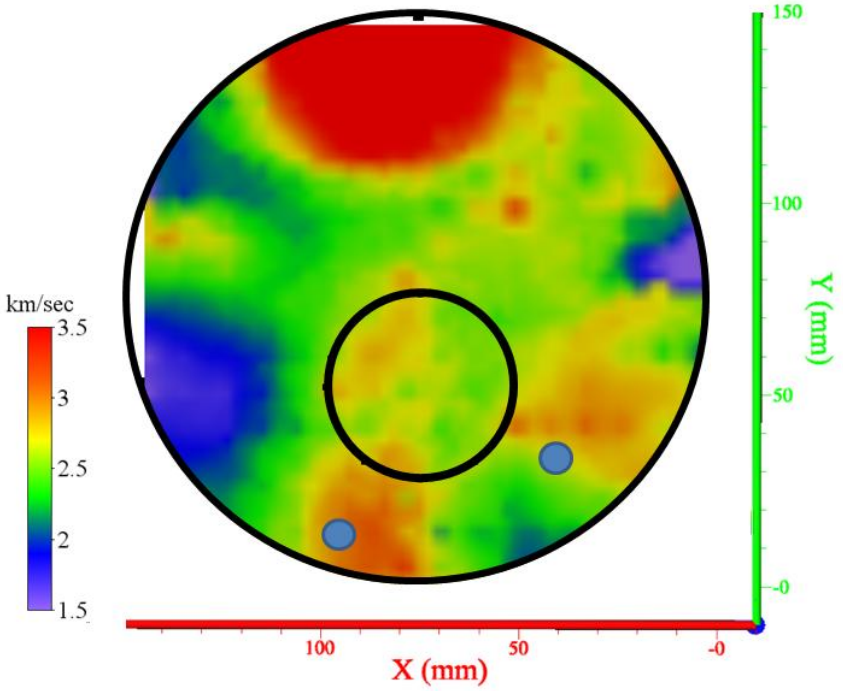

Figure A-22: Orthogonal image for the second regime of the Berea Sandstone sample. Points of interest: 90 mm in the x direction and 10 mm in the y direction, and 40 mm in the x direction and 30 mm in the y direction, at a depth of 30 mm represented by the blue points.

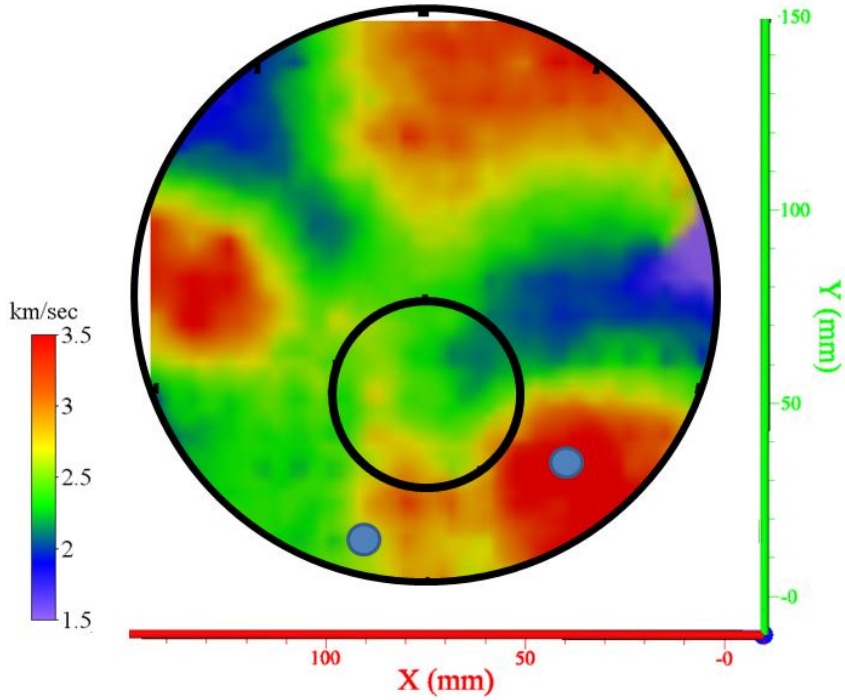

Figure A-23: Orthogonal image for the first regime of the Berea Sandstone sample. Points of interest: 90 mm in the x direction and 10 mm in the y direction, and 40 mm in the x direction and 30 mm in the y direction, at a depth of 30 mm represented by the blue points.

Appendix B – Secondary Testing

Appendix B will have information that is relevant to the understanding of the results of the secondary experiments. The photographic progression of the shear failure test will be presented in chronological order. A diagram of the caprock sample design followed by images of the testing apparatus will follow. Finally the cross sections of all six caprock samples will be included along with the seismic events located for each test.

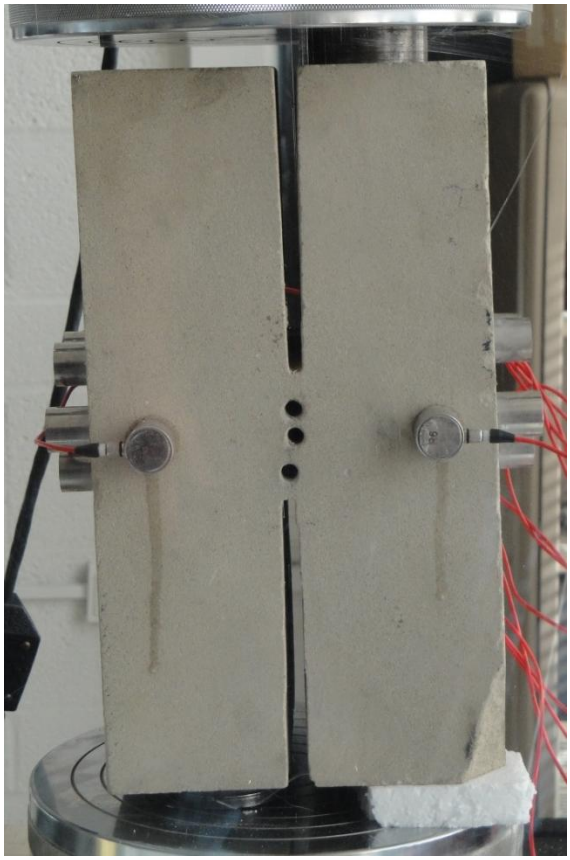

Figure B-1: Berea Sandstone shear sample prior to loading.

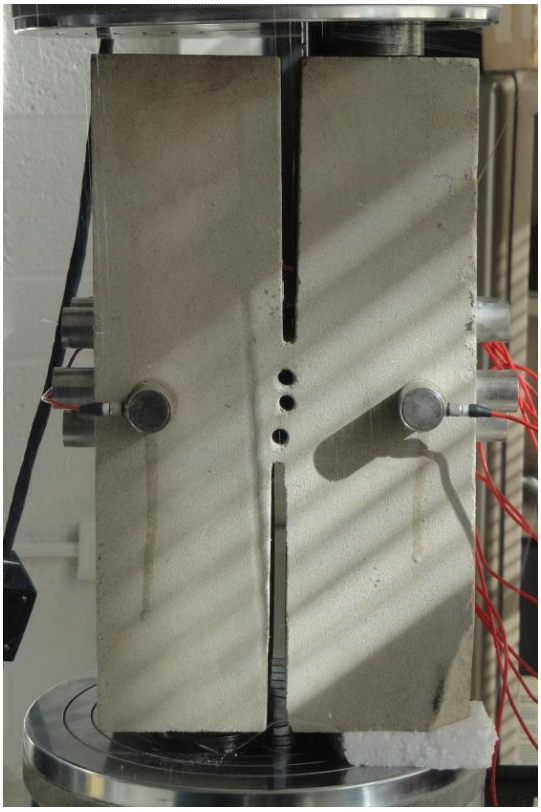

Figure B-2: Berea Sandstone shear sample prior to failure.

Figure B.3: Berea Sandstone shear sample post failure.

Figure B-4: Berea Sandstone shear sample after halves were separated post failure.

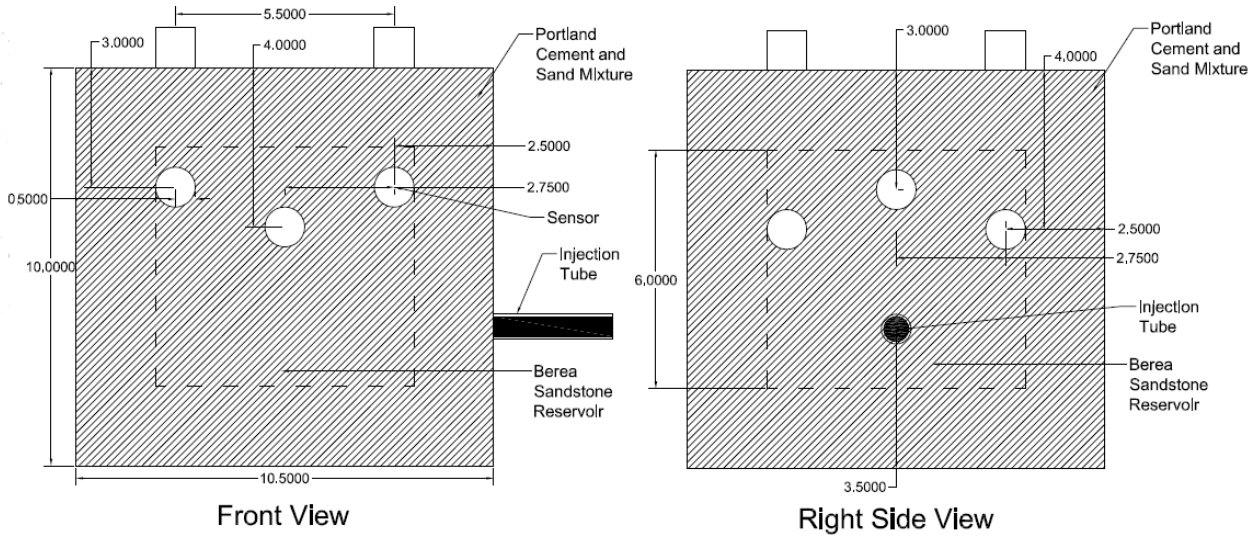

Figure B-5: Schematic for initial caprock design with sensor locations.

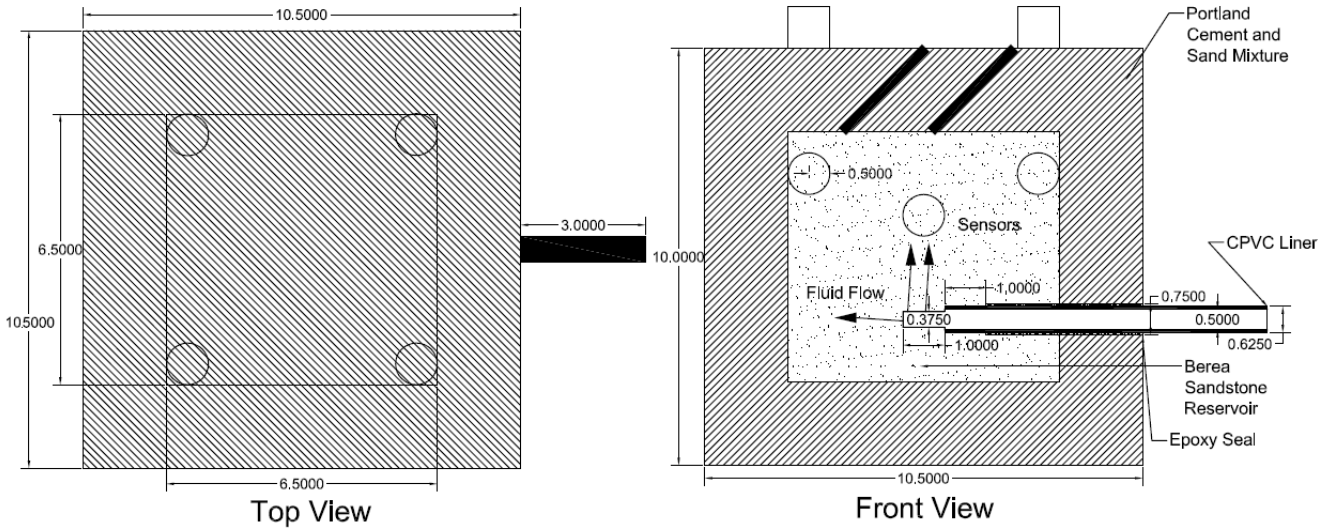

Figure B-6: Schematic for initial caprock design.

Figure B-7: Schematic Pressure tank with injection tube and air regulator.

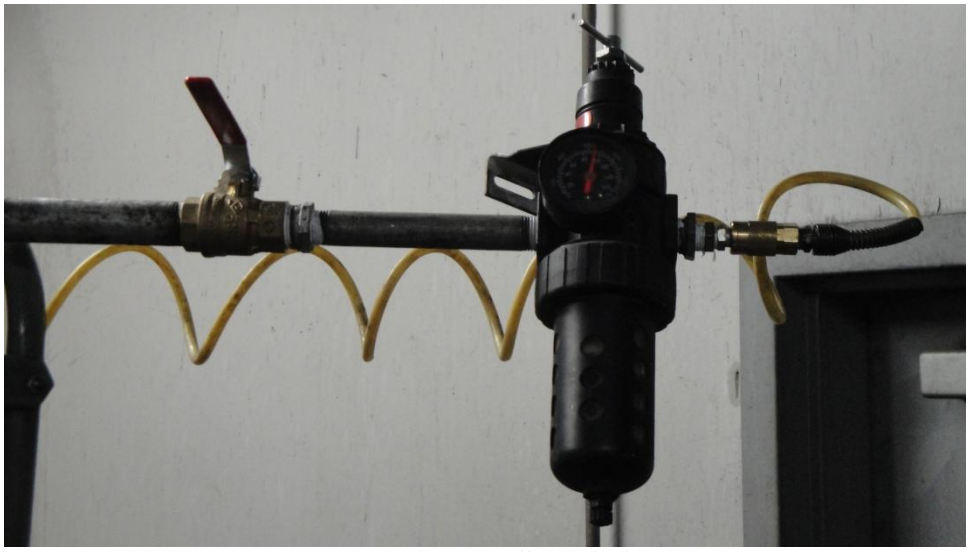

Figure B-8: Air regulator and air cutoff valve for fluid pressure tank.

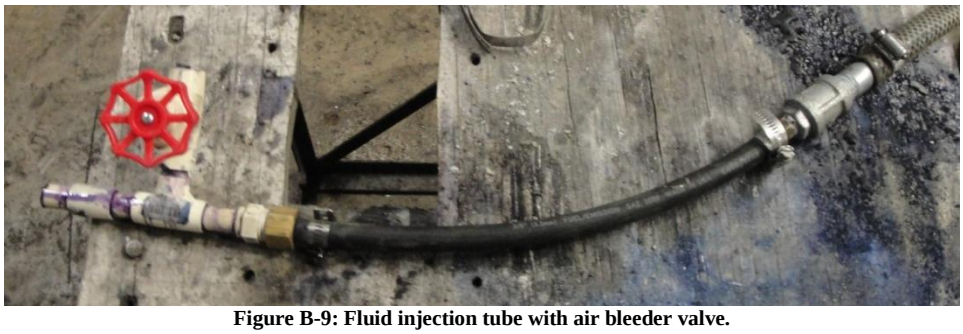

Figure B-9: Fluid injection tube with air bleeder valve.

Figure B-10: Fluid level indicator tube on the side of the fluid pressure tank.

Figure B-11: Caprock sample from test number one, post testing cut into quarters. With injection tube at the bottom, top left quadrant is displayed.

Figure B-12: Caprock sample from test number one, post testing cut into quarters. With injection tube at the bottom, top right quadrant is displayed.

Figure B-13: Caprock sample from test number one, post testing cut into quarters. With injection tube at the bottom, bottom right quadrant is displayed.

Figure B-14: Caprock sample from test number one, post testing cut into quarters. With injection tube at the bottom, bottom left quadrant is displayed.

Figure B-15: Caprock sample from test number two, post testing cut into quarters. With injection tube at the bottom, top left quadrant is displayed.

Figure B-16: Caprock sample from test number two, post testing cut into quarters. With injection tube at the bottom, top right quadrant is displayed.

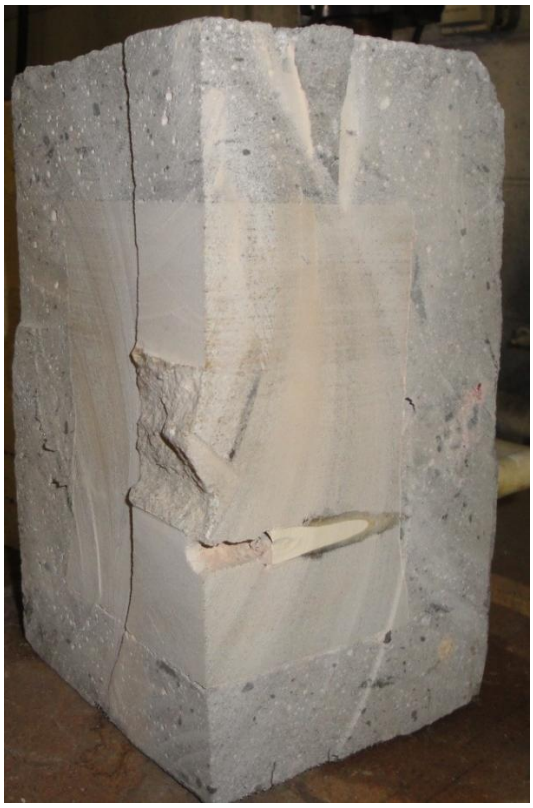

Figure B-17: Caprock sample from test number two, post testing cut into quarters. With injection tube at the bottom, bottom right quadrant is displayed.

Figure B-18: Caprock sample from test number two, post testing cut into quarters. With injection tube at the bottom, bottom left quadrant is displayed.

Figure B-19: Caprock sample from test number three, post testing cut into quarters. With injection tube at the bottom, top left quadrant is displayed.

Figure B-20: Caprock sample from test number three, post testing cut into quarters. With injection tube at the bottom, top right quadrant is displayed.

Figure B-21: Caprock sample from test number three, post testing cut into quarters. With injection tube at the bottom, bottom right quadrant is displayed.

Figure B-22: Caprock sample from test number three, post testing cut into quarters. With injection tube at the bottom, bottom left quadrant is displayed.

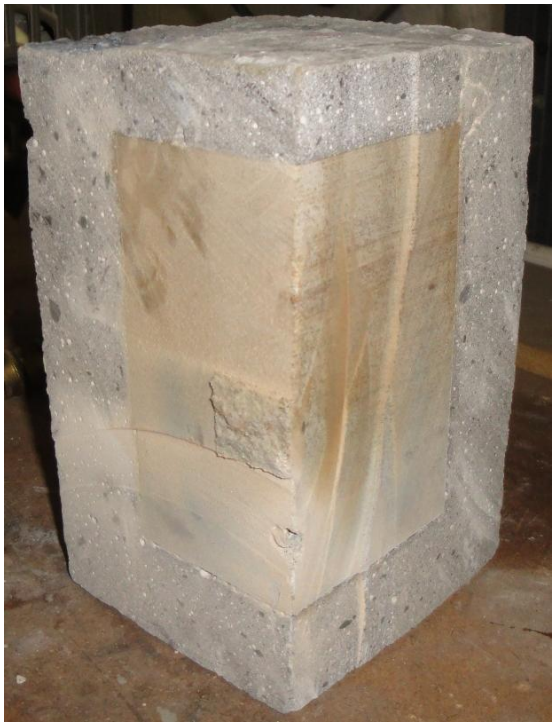

Figure B-23: Caprock sample from test number four, post testing cut into quarters. With injection tube at the bottom, top left quadrant is displayed.

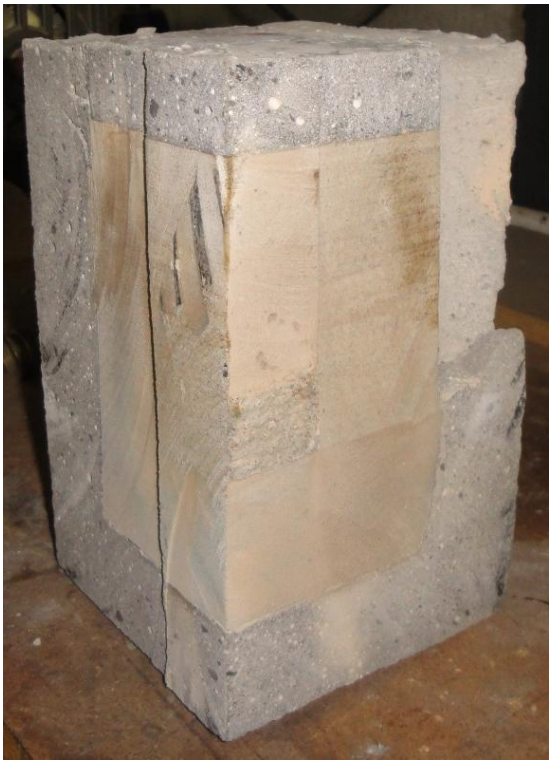

Figure B-24: Caprock sample from test number four, post testing cut into quarters. With injection tube at the bottom, top right quadrant is displayed.

Figure B-25: Caprock sample from test number four, post testing cut into quarters. With injection tube at the bottom, bottom right quadrant is displayed.

Figure B-26: Caprock sample from test number four, post testing cut into quarters. With injection tube at the bottom, bottom left quadrant is displayed.

Figure B-27: Caprock sample from test number five, post testing cut into quarters. With injection tube at the bottom, top left quadrant is displayed.

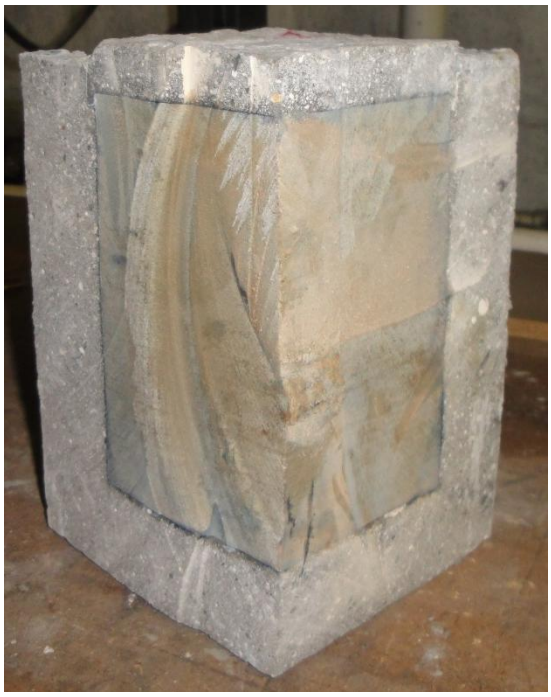

Figure B-28: Caprock sample from test number five, post testing cut into quarters. With injection tube at the bottom, top right quadrant is displayed.

Figure B-29: Caprock sample from test number five, post testing cut into quarters. With injection tube at the bottom, bottom right quadrant is displayed.

Figure B-30: Caprock sample from test number five, post testing cut into quarters. With injection tube at the bottom, bottom left quadrant is displayed.

Figure B-31: Caprock sample from test number six, post testing cut into quarters. With injection tube at the bottom, top left quadrant is displayed.

Figure B-32: Caprock sample from test number six, post testing cut into quarters. With injection tube at the bottom, top right quadrant is displayed.

Figure B-33: Caprock sample from test number six, post testing cut into quarters. With injection tube at the bottom, bottom right quadrant is displayed.

Figure B-34: Caprock sample from test number six, post testing cut into quarters. With injection tube at the bottom, bottom left quadrant is displayed.

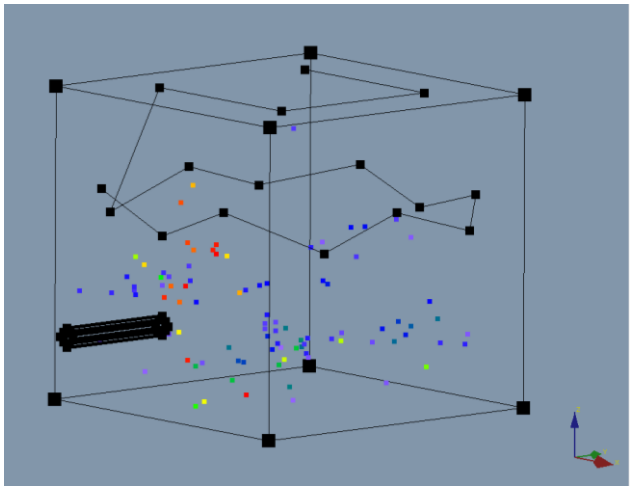

Figure B-35: Caprock sample from test number one, modeled in Voxler with event locations in color.

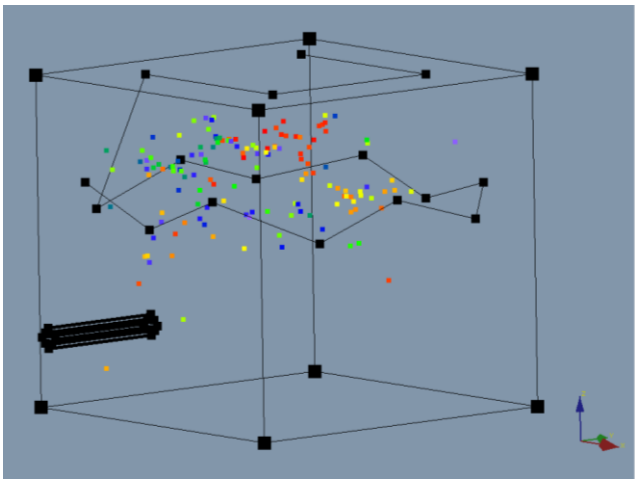

Figure B-36: Caprock sample from test number two, modeled in Voxler with event locations in color.

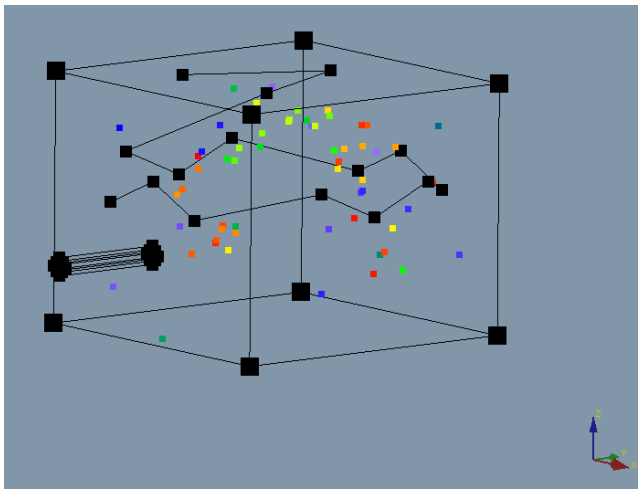

Figure B-37: Caprock sample from test number five, modeled in Voxler with event locations in color.

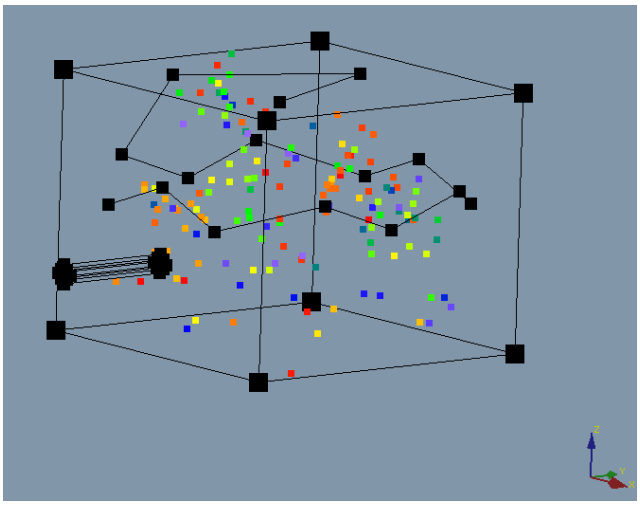

Figure B-38: Caprock sample from test number six, modeled in Voxler with event locations in color.

Appendix C – MTS Tutorial

Tutorial for MTS Million Ton and 100 Kip Presses in Rock Mechanics Laboratory

Room 129, Holden Hall

Prepared By:

Daniel Sadtler

4-11-2011

Prepared For:

Dr. Mario Karfakis and Dr. Erik Westman

This tutorial is only for use with the following equipment MTS million ton press and MTS 100 kip press.

****If one of the following machines are not being used, these directions probably will not work****

If the station is no longer using this equipment, find another tutorial, or it is time to make a new one.

The first step to using this equipment is to make sure all of the hydraulic hoses are hooked up to the presses and the data cable for the respective press, being used, is correctly connected to the console, or the computer monitor will not display and load values even when the press is applying one.

1. Open Station Manager. The program will prompt for which file to open. If the million ton press is being used, open "MILLION ftse.cfg" configuration file. If the 100 Kip press is being used, open the file which best fits the experiment, "100 Kip w extensometers.cfg" or "100 kip Axial.cfg"

   ****Remember when closing/saving, ONLY SAVE YOUR PROCEDURE, not the station itself. This would not make Mario happy if you lost his presets.****

2. Before any adjustments can be made, the box next to "Exclusive Control" must be selected to give access to the full setup.

3. After this, check to see if a procedure has been loaded. If a procedure is not on the screen, look on the left side of the screen for 3 or 4 buttons which can be depressed, in a column by themselves. If there is not a fourth button, go into the file directory and open a saved procedure (the path can be found in Mario's secret journal, ask before searching). Drag the cursor over these boxes and make sure they are labeled "Function Generator", "External Command", "Auto Tuning," and "MPT." Depress the "MPT" button if not already depressed and check again for the procedure to appear. Open the procedure management window by selecting the "Procedure Editor" button. At this point if there is still no procedure showing, one needs to be loaded and a copy needs to be saved in order to make changes. This can be accomplished by selecting the "Open Procedure," which also has the option to **SAVE AS** from the drop down menu. **Figure 1** following these instructions is color coded, and labeled to show where each of these buttons can be found on the main screen.

4. Now it is time to build a procedure. After saving the procedure as a new filename, to ensure no accidental saving over existing files, find the "Process Palette window. Inside this window there are different categories of processes that can be included in the procedure. These categories are Command, Data Acquisition, Event, External Control, Other. At the writing of this tutorial, all of the processes are not known exactly how they work, so in the future if

   The command section contains the actions which the machine is capable of doing. Ramp, Hold and Cycle are three of these which have been used. The Ramp command works by

setting a loading rate based on stroke (movement of piston in a unit of measure), force (movement of piston in a unit for pressure/load), and the displacement recorded by extensometers. This will tell the machine to load the sample, always increasing, by the rate which it has been set. The Hold command tells the machine to hold in place without moving for a set amount of time, or until another function begins. The Cycle command tells the machine to repeat a set type of load repeatedly until the desired completion time.

The Data Acquisition section has the functions necessary to record the data from the test into data files. The two that are used regularly in the current lab are Max/Min Acquisition and Timed Acquisition. Max/Min Acquisition records the maximum and minimum load etc. that is recorded during the test. Timed Acquisition records different set values, such as force and stroke, based on a set time interval. This data can be used after the program has been closed by accessing the data files.

The Event section has different functions that can be used while the procedure is running. The major functions are the Button function, and Failure Detection function. Failure Detection is set to lock the press whenever the piston travels a certain distance in a certain amount of time when the loading rate remains the same. The Button function is a very important tool because it is used to trigger other functions within the procedure. The Button function creates a button when the procedure is run that can be programmed to say and do whatever is necessary.

The Other section has functions that can do different things that were not classified under the previous sections. Most used is the Data Display function. This will display user determined variables on a continuously updating graph as the experiment is taking place.

To begin building the procedure, click on the desired function in the “Process Palette” window and drag it over to the procedure box. If the procedure window has undesired functions in it, right click on the image and select delete. When the function is brought over into the procedure window, three columns will appear: Name, Start and Interrupt. Fill in the name for process to be called and then continue to the next columns. In these columns pick which other process in the procedure will either start or end the current process. This means that if it is desired for “button 1” to start a ramping function and “button 2” to end the test, under the ramp command, “button 1” would be selected under the start column and “button 2” would be selected under the interrupt column. When programing, make sure to make a button that will stop the machine and all processes and end the procedure. This will make

sure that in case something goes wrong there will be a way to prevent further damage. A sample of a working procedure is shown in F**igure 2** on the pages following these directions.

Each function has a menu that has different options for the process. To get to this menu, right click on the function in the procedure window and select open. Since each function has different options, the following are some key settings that need to be check. Under the ramp command, the load rate can be changed with in this menu as well as the control mode. The control mode changes which variable is going to be adjusted i.e. force or stroke. For the Hold command, make sure to set the duration of the hold to a value greater than 0, which is the default. For the button command, make sure to set to trigger once or continuously, depending on the desired result. Trigger once causes the button to disappear after one use. For data acquisition, make sure to set the x and y axis to the appropriate signals, and adjust the data capture time accordingly.

****Test procedure on sample rocks before actual testing begins to make sure the procedure is programmed correctly, unless you are using an already proven procedure****

5. Now that the procedure is complete, name the specimen so that the data collected can be saved. Do this in the left window, below the test timer, where there is a drop down menu. Just click on the white area and type in the test name and date, i.e. Acoustic_Test_4-11-11.

6. Before continuing, all of the windows for testing should be opened. These windows are "Meters," "Auto Offset," "Manual Command" and "Detectors." "Meters" brings up a window with the load, stroke and displacement of extensometers for the press being used. The "Auto Offset" button brings up a menu that provides a way to zero the force, stroke and displacement values. "Detectors" is a menu which brings up added safety for the experiment. This menu provides the ability to set maximum values for the press which will cause it to shut down once these values are reached. This will prevent the press from causing too much damage if something should go wrong and the tester does not notice.

   Now it is time to prepare the press for the experiment. Make sure all hands are free of the machine and click the rest button highlighted in figure 4. Next turn the hydraulic pressure on by pressing "Power Low," allowing it to stop flashing, followed by the "Power High" button in the HSM-J28 box. The million pound press must be in "Power High" mode to operate, but the 100 kip press only requires "Power Low." Once the hydraulic pressure is ready to go, go

into the Manual Control dialog box and select the box at the bottom marked “Enable Manual Command.” Change the control mode to stroke and open up the press so that the sample will fit using the slider bar at the bottom on the window. If the press does not open far enough due to the slide not being able to travel far enough, go into the “Auto Offset” window and zero the stroke value and try again.

****At any point during the test, you can stop the press by pressing the Power Off button in the HSM-J28 box****

7. Now it is time to set the sample. The next step is VERY important. Make sure the sample is centered under the piston so that the surface which will be in contact with the press is not off centered. This means that if using a punch, center the punch on the press, not the sample. Slowly bring the sample into contact with the top plate by adjusting the stroke of the press in the manual command slide bar.

   ****Be careful not to crush the sample while doing this.****

   When the sample is within a 1/16” to contact, switch the control mode to force, and type into the window 50 lbf. The machine will automatically advance until it applies 50 lbf to the sample.

8. Now that the sample is set, unselect “Enable Manual Command,” and zero the stroke and force in the “Auto Offset” window. Double check everything. Press the play button, the test will begin. **Figure 3** show the commands in steps 5-8 highlighted on the main screen.

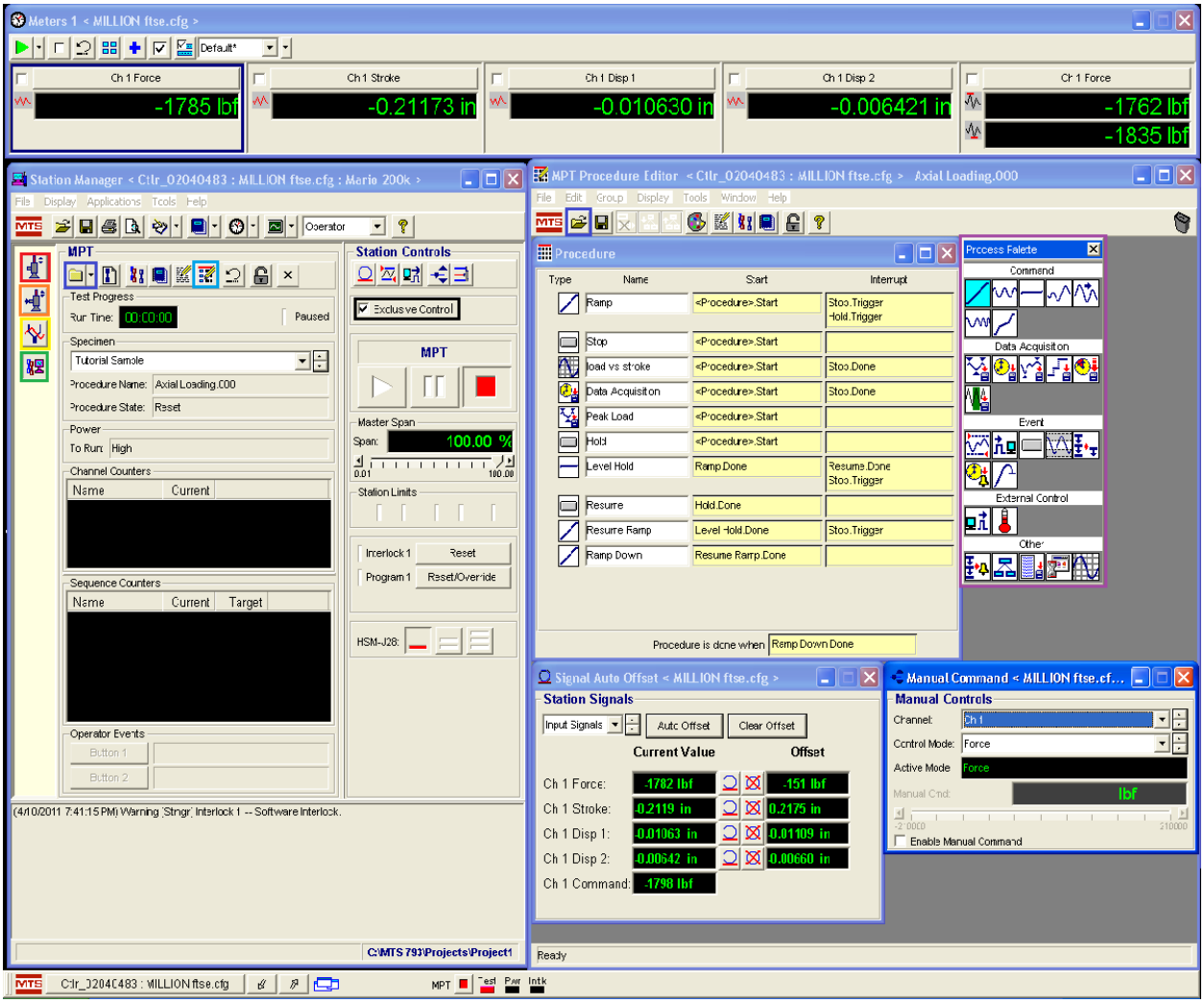

Legend

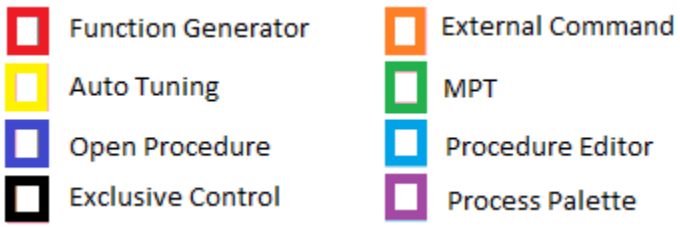

Figure 1: MTS station manager with certain functions highlighted.

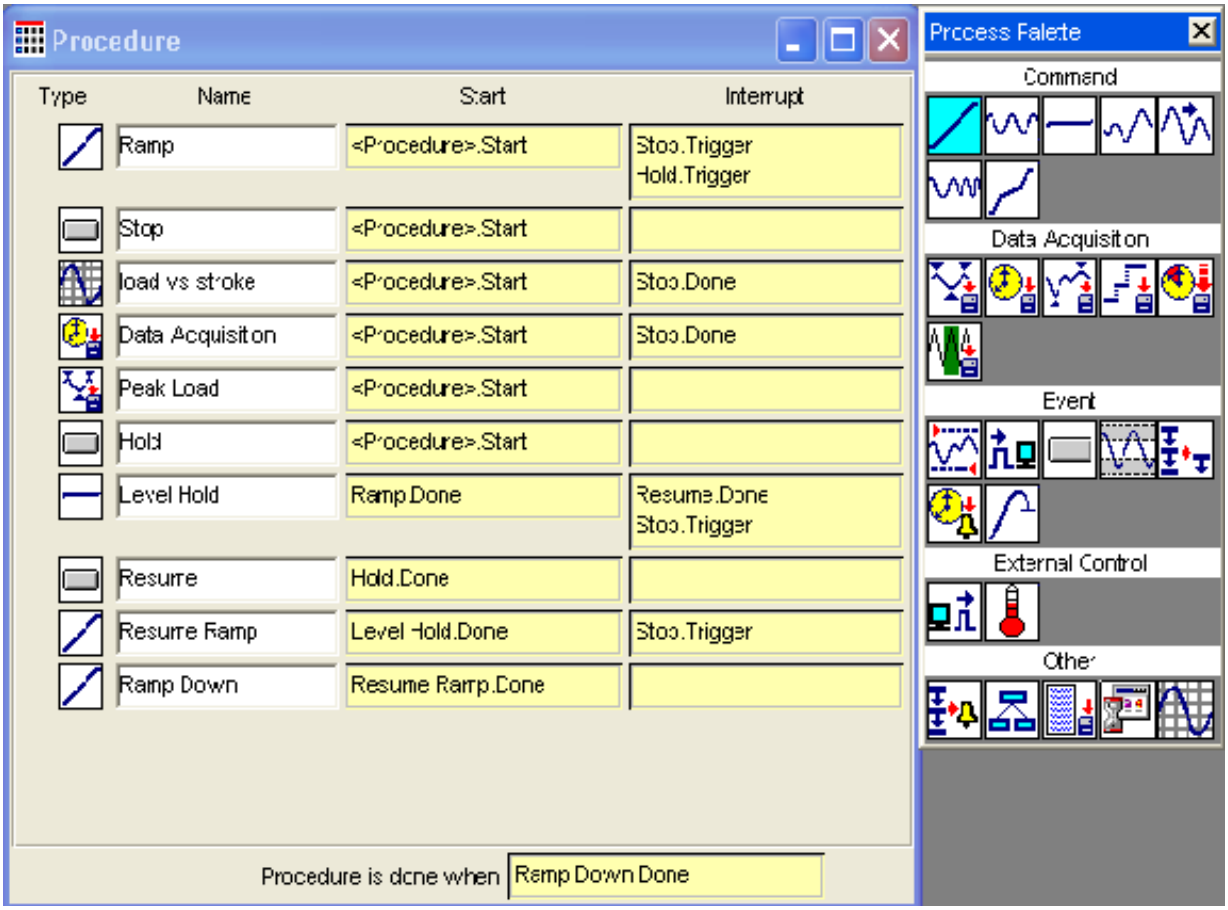

Figure 2: Functional procedure from rock mechanics lab.

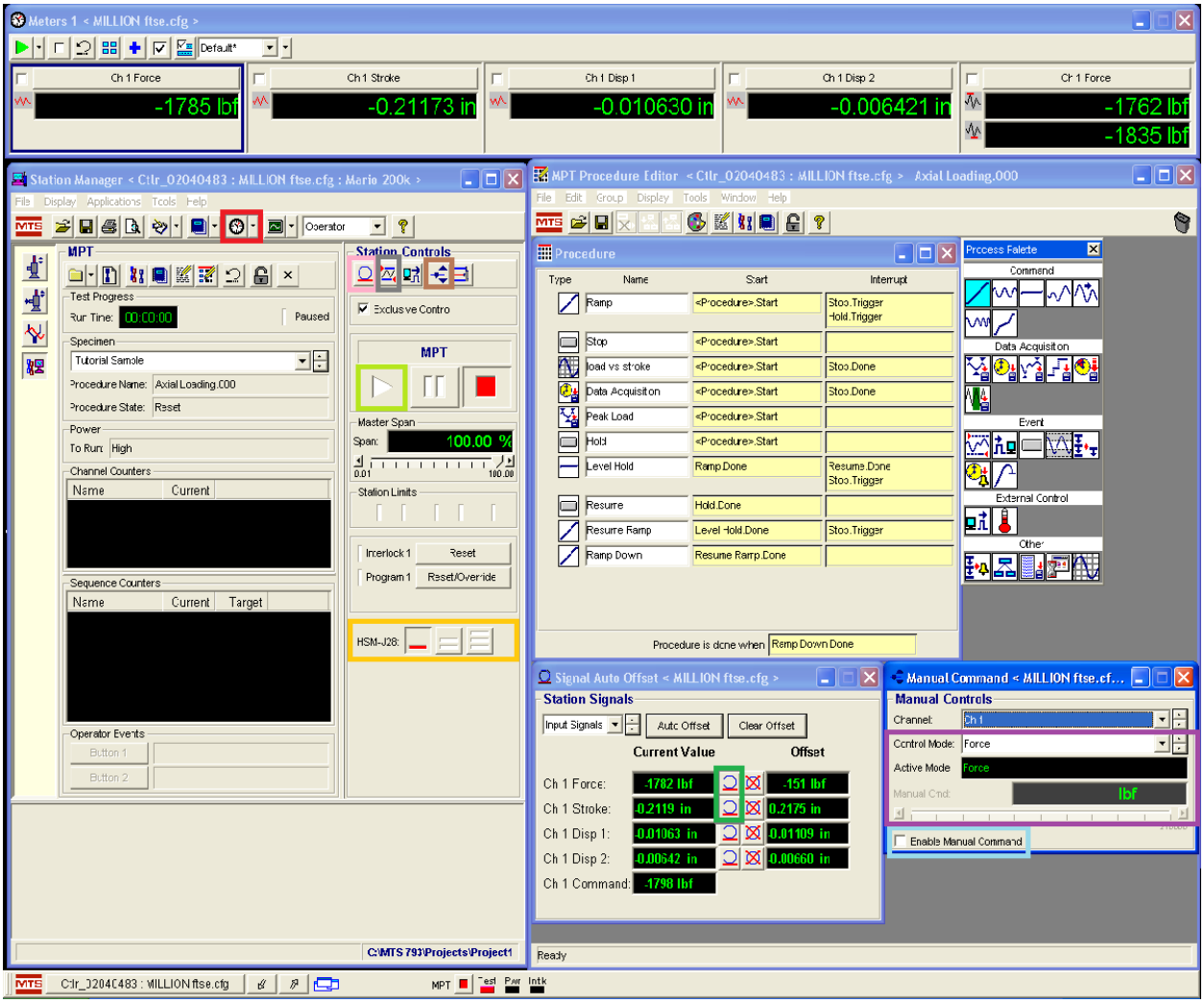

Legend

Figure 3: MTS station manager with selected functions highlighted

Appendix D – ESG Tomography System Tutorial

Tutorial for ESG Acoustic Emissions Equipment

Created By:

Daniel Sadtler

12-16-2011

This tutorial has been organized for use in cooperation with the ESG software. To prevent any confusion, please use the ESG software version 12.6.1 released in 2006 while working through this tutorial.

1.1 - Using ESG Computer

To turn on, make sure the surge protector is plugged in and powered on. Check that the computer is plugged into the surge protector and all 16 channels, which are labeled on the front of the blue amplifiers, have leads connected correctly to the back of the tower. If the switch on the front of the machine is not illuminated there is no power connected to the machine. Flip the switch to the on position and turn on the computer monitor. Once the system has booted up, the sensors will need to be tested to make sure both the channels and sensors are working before testing can begin.

1.2 - Testing Sensors

To test the sensors hook up eight sensors to the first eight channels leads, which are the red wires hooked into the light blue amplifier boxes. Only eight sensors should be connected because the monitoring program, UltrACQ, only displays eight channels at a time. Arrange the sensors in a position that the base is solidly on a countertop or solid surface and the sensors able to stand freely without being pulled off of the countertop. Setting each sensor on a drop or two of oil will ensure good contact with the surface so that the waves will be registered by the sensors. A method that has been used in the past is to place the sensors in a circle using a protective shield from the rock press to keep pressure on the tops of the sensors. The shield provides the required weight to keep the sensors in position. Next, double click on the ESG Ultrasonic shortcut on the desktop and open the UltraACQ inside of the folder that open up. The ESG Ultrasonic menu is shown in Figure 1.

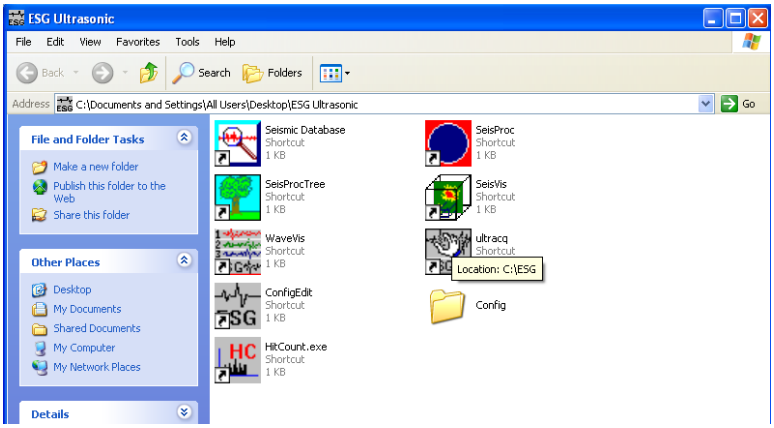

Figure 1: ESG Ultrasonic menu.

This program is used to record wave data picked up from the sensors. More in depth instructions of how to use this program can be found further into this tutorial. With a pen, pencil or screwdriver tap the countertop in between the sensors and watch the "hit count" for each sensor. If the sensors do not record any movement test them individually by tapping the top of the sensors. If there is no response still, the sensor most likely is not functioning correctly and needs to be set aside.

1.3 - Setting Up Sensors

Before data collection begins, the sensors must be programmed into the system using the ConfigEdit dialog in the ESG folder. Open the SENSOR file located in the bottom left most section of ConfigEdit, as seen in Figure 2, and input the orientation of the sensors on the sample using relative values of northing easting and depth. To open this file, select the edit command in the sensor section. When the sensor file is saved, make sure to reopen the new file before continuing. Do not save the ".sen file" as anything other than ULTRA.sen, case sensitive, or the program will not recognize the newly created sensor file and will use the default file located in the C:/ESG directory.

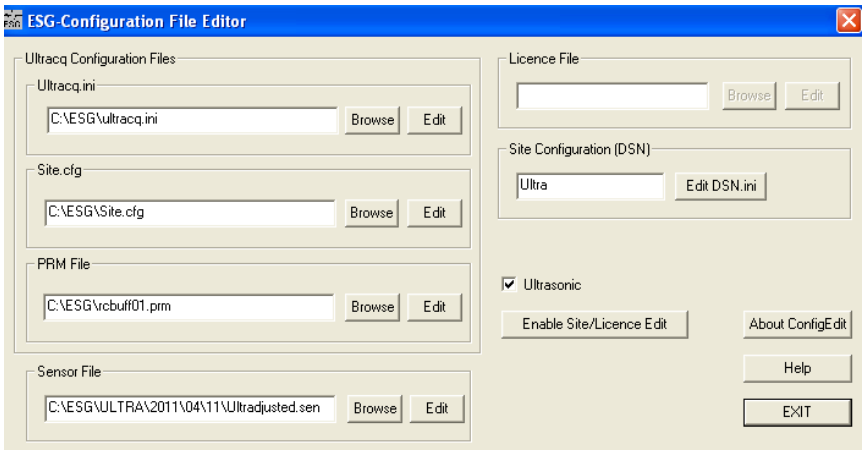

Figure 2: ESG ConfigEdit dialog box.

When collecting data, the ESG software will automatically create a directory that is in the following format: C:/ESG/ULTRA/YEAR/MONTH/ DATE. It is recommended that these subfolders are made and the sensor file for that specific test be saved in this folder. Make sure that the location for the sensor file is set correctly in ConfigEdit. Just because a new file is created, the program does not automatically set it as the file to be used. To set threshold values for the sensors open ConfigEdit and Ultracq.ini. Select the sensors that need to be adjusted on the left hand side of the screen and select the threshold button to adjust the values. In this menu there is also an option for triggering events. This option provides the adjustment to set how many sensors must be triggered by an event before the program will record the data.

1.4 - Using UltrAcq

UltrAcq is the section of the ESG software that records the signals picked up by the sensors. The layout of the UltraAcq window is basic with menus for *File, Channel, View* and *Special*. The *File* menu has only one option, EXIT. The *Channel* menu has an option for 1-8 and 9-16. This option determines which set of channels are displayed in the viewing window. When one set of channels is selected, there will be a check mark located to the left of the sensor numbers in the dropdown menu. The *View* menu adjusts the frequency and clarity of the plotted data, as the sensors collect data. The options include 10 mV/div, 100 mV/div, 1 V/div, 10 V/div, which adjust the scale for the frequencies plotted on the screen. The other options are 4k points, 2k points, 1k point and 512 points which adjust the number of points that are plotted per graph. The *Special* menu has four options, *Trigger Once*, *Trigger Always*, *Pulse* and *Zero*. *Trigger Once* records data for the first event that triggers the sensors. *Trigger Always* continuously records data once it is selected. To pause or stop this recording unselect trigger always. The sensors will still record data if enough sensors are triggered if the pause option is selected, but the program will no longer be collecting data continuously. *Pulse* gives the option to set the number of times the sensors record data. The function of *Zero* is not known. Ultracq saves files in the directory ESG/Ultra/ (year)/ (month)/ (day) when using *Trigger* options, and ESG/PULSE/ (year)/ (month)/ (day) when using the Pulse function.

1.5 - Using Wave Vis

To begin open the .inx file from the file directory created by the Ultracq program. This will open and display events recorded by the sensors. To process the wave data, first a processor must be set to each of the following: *Event Processor, Alternative Batch Processor*, and *Batch Processor*. To do this, under the *File* menu, select one of the processors. A menu will open; select the image of the tree, which will open the *Seistree* program. This will open a window providing the ability to build a processor. For more information into how to build a processor see section 1.6. At the top of the page there will be a button labeled Read PRC which is used to open processor files. In the base ESG directory there will be a number of files with .prc extensions. These files are the different processors that can be used. The recommended processor is ESGOffLine.prc. Repeat this step for all three of the processors in the file menu. Once the three processors are set, open the *Event* menu on the task bar and select Batch Process. This command will run the processor file that has been set and adjust the P and S wave picks. Also in the *Event* menu the command *Locate Event* will open a menu that will show the location of the event in a 2-D rendering of the sample, with the option to see the sample from any of the 3-D planes. To cycle through the different triggering events, select the drop down menu at the top of the screen containing the date of

the data recording and a number in parenthesis on the right hand side. If there is an asterisk (*) after one of the recordings, that particular recording has been marked by the program as an event. Once one of the events has been selected, the main screen will update to show the waves recorded. Each line represents one channel/sensor and its corresponding wave recording. The sensors that are not working correctly or the channels without a sensor connected will have waves with extremely high frequency making the wave representation lines look fuzzy. Based on prior tests finished before the completion of this tutorial, channels 8 and 12 consistently show more noise than the other sixteen channels. To zoom in on the waves, click and hold the mouse and drag it across the desired location. When the magnification is complete, double click the mouse in the viewing area and the scale will return to normal.

1.6 - Creating a Processor

To create a processor the program *Seistree* must me opened. If the left hand column is not blank, clear out the sub categories by selecting the text and dragging it out of the column. To start pull the Geomanager text into the left column. Select the new text in the left hand column and the right hand column will present new options. The top options will be Geiger, Simplex and Simplex_Ps. Geiger is a method utilizing the method of least squares, Simplex and Simplex_Ps us different methods than Geiger. The Simplex_Ps is recommended for use by ESG. Select the method which best suits the project and drag it into the left hand column. A menu will open. Make sure to set the P and S wave velocities before pressing OK. There is also an option for preventing an event from being located outside of a certain boundary called)()()()(). The area generated is a rectangular prism, so by entering coordinates into the specified areas, the program will filter out any events that are not within the boundaries. Once one of these methods has been selected, highlight your selection in the left hand column and the right hand column will open up new options. At this point it is time to add the Pickers and Filters. Pickers are the functions that will go through the data and select where the P and S waves begin. If these are not included in the processor procedure, no P or S waves arrival times will be selected. If not arrival times are picked, no events will be located. There are 6 P wave pickers available and one S wave picker. P_Picker is the recommended picker, but different tests require different pickers. The filters are used to take out excess noise from the recorded data. If the frequency of the noise is known there are a couple of filters that can be used to clean up the data.

Also the processor can be edited to print out the wave data in text format as well as a source file. The source file is a file that provides the location information for recorded events. QDB files, abbreviated from Quality Data Base file, provide the detail for each event, such as the wave arrival times. For more information see version 15, volume 1, Appendix C of the ESG software manual.

1.7 Created Files

When using the ESG software there are certain file extensions that are created that contain the information need for processing. These files can be found in the dated subfolder for the date the test was run. The .hdf file extension is for recorded wave information per recorded event. This means that a .hdf file is one that can only be read by WaveVIS and contains all sensor information for one event. The rcbuff files are used within the program itself, preventing files such as rcbuff.inx from opening outside the software. The rcbuff.dat file however, provides a file with wave information that can be opened in other applications. To create text files with the data from each event there is a Text_Out processor that can be created in the same fashion as depicted in previous sections and run.